Modified pigments and mechanisms of energy transfer in LH2 complexes from purple bacteria

by Niall Johnston Fraser

A thesis submitted for the degree of Doctor of philosophy

Division of Biochemistry and Molecular Biology
Institute of Biomedical and Life Sciences
University of Glasgow
December 1998

ProQuest LLC.
789 East Eisenhower Parkway
P.O. Box 1346
Ann Arbor, MI 48106 – 1346

Declaration

I declare that this thesis is less than 100, 000 words in length and that all the work described was performed by myself unless otherwise stated.

Niall Johnston Fraser

December 1998

Abstract

The energy transfer processes in the LH2 complex from *Rps. acidophila* 10050 were investigated using a pigment-exchange strategy. In this approach, the Bchl*a*-B800 molecules were selectively removed from their binding pockets and were replaced with modified pigments with altered spectral properties. Spectroscopic analysis of these modified complexes gave valuable insights into the mechanisms of energy transfer within the complex.

The Bchl*a*-B800 molecules can be released from their binding pockets by an acid treatment using buffer containing the novel Triton detergent TBG10. B850-only complexes can then be purified by ion-exchange chromatography. Later, the empty B800 sites can be reconstituted with native Bchl*a*. Maximal occupancy of the B800 sites can be obtained by incubating the B850-only complexes in buffer solution containing the detergent dodecyl-β-D-maltoside (LM) with a 3x fold excess of Bchl*a* for 2 h at pH 8 and at room temperature.

The Bchl*a*-B800 reconstituted complex was fully characterised to determine how similar it is to native LH2. The average occupancy of the B800 sites in the Bchl*a*-B800 reconstituted complex is ~ 80%. Resonance Raman spectroscopy showed that the reconstituted pigments are correctly bound within the complex and, as judged by CD spectroscopy, the structure of the LH complex is not affected by the pigment-exchange process. In addition, the reconstituted molecules participate in efficient B800→B850 energy transfer.

The pigment-exchange protocol was then used with a series of modified pigments. The B800 binding sites can be reconstitued with geranylgeraniol Bchl*a*, 13^2OH Bchl*a*, Zn-Bph*e*, 3^1vinyl Bchl*a*, 3^1OH Bchl*a*, acetyl Chl*a* and Chl*a*. The B800 pockets can not be reconstituted with either pyro-Bchl*a*, Cu-Bph*e* or Ni-Bph*e*. The 3^1vinyl Bchl*a*-, 3^1OH Bchl*a*-, acetyl Chl*a*- and Chl*a*-B800 reconstituted complexes are of particular interest as they have strongly blue-shifted "B800" Q_y absorptions with maxima at 765, 751, 693 and 669 nm. CD spectroscopy again showed that the reconstituted pigments are correctly bound within the respective complexes. The occupancies of the B800 sites in the 3^1vinyl Bchl*a*-, 3^1OH Bchl*a*-, acetyl Chl*a*- and Chl*a*-B800 reconstituted complexes have yet to be accurately determined. In all of the reconstituted complexes, those pigment molecules which are correctly bound within the B800 binding pockets participate in efficient B800→B850 energy transfer. The kinetics of B800→B850 energy transfer in native and selected reconstituted complexes were studied by fs transient absorption spectroscopy. In both the native and Bchl*a*-B800 reconstituted complexes, B800→B850 energy transfer takes approximately 0.9 ps. The time constants for B800→B850 energy transfer in the 3^1vinyl Bchl*a*-, 3^1OH Bchl*a*-, acetyl Chl*a*- and Chl*a*-B800 reconstituted complexes are 1.4, 1.8, 4.4 and 8.5 ps respectively. This shows that the rate of B800→B850 energy transfer decreases as the spectral separation between the "B800" and B850 Q_y absorption bands increases. This effect is rather small, however, given the apparent large decrease in spectral overlap. Model calculations show that B800→B850 energy transfer in these complexes can not be adequately

described by Förster's mechanism. In all of the reconstituted complexes, the efficiency of B800→B850 energy transfer is predicted to be 100%.

B800→B800 energy transfer in native LH2 and selected reconstituted complexes was studied by following the decay of anisotropy in the "B800" Q_y absorption band with time. The time constant for B800→B800 energy transfer in both native and Bchl*a*-B800 reconstituted complexes is 0.7 ps. The B800→B800 hopping times in the 3^1vinyl Bchl*a*-, 3^1OH Bchl*a*-, acetyl Chl*a*- and Chl*a*-B800 reconstituted complexes are 1.7, 2.0, 2.8 and 3.8 ps respectively. This shows that the rate of B800→B800 energy transfer decreases as the "B800" Q_y absorption band is blue-shifted. The underlying mechanism which gives rise to this trend is not fully understood.

Carotenoid to B850 energy transfer was studied using both steady-state and rapid kinetic techniques. The lifetimes of the carotenoid rhodopin glucoside S_2 state in native and B850-only complexes are significantly shorter than that in benzyl alcohol. This shows that excitation energy is transferred from the S_2 state of the carotenoid to both the Bchl*a*-B800 and -B850 molecules. Limited energy transfer from the S_1 state of the carotenoid to the Bchl*a*-B800 molecules also occurs. Approximately two-thirds of carotenoid→B850 energy transfer occurs directly. The remaining third occurs indirectly via the Bchl*a*-B800 molecules. The efficiency of carotenoid to B800 energy transfer in native, 3^1vinyl Bchl*a*-, 3^1OH Bchl*a*-, acetyl Chl*a*- and Chl*a*-B800 reconstituted complexes was investigated. In the native, 3^1vinyl Bchl*a*- and 3^1OH Bchl*a*-B800 reconstituted complexes, the acceptor state of the (B)Chl-B800 molecules is the Q_x state. In the acetyl Chl*a*- and Chl*a*-B800

reconstituted complexes, however, the acceptor state of the (B)ChI-B800 molecules is the Q_y state.

The Saviour dy'd, but rose again
triumphant from the grave;
And pleads our cause at God's right hand,
omnipotent to save.

Who then can e'er divide us more
from Jesus and His love,
Or break the sacred chain that binds
the earth to heav'n above?

Let troubles rise, and terrors frown,
and days of darkness fall;
Through Him all dangers we'll defy,
and more than conquer all.

Nor death nor life, nor earth nor hell
nor time's destroying sway,
Can e'er efface us from His heart,
or make His love decay.

Each future period that will bless,
as it has bless'd the past;
He lov'd us from the first of time,
He loves us to the last.

Paraphrase Romans 8 v 33-35.

A prayer of thanksgiving

Lord Jesus,

In truth, I have never experienced anything like the last three years. In the midst of many highs and lows, I have found you to be completely dependable. In each and every situation, I have found that "your grace is sufficient for me and that your power is made perfect in my weakness". I want to acknowledge that all that I have accomplished in the last three years has been in your strength and not mine...so thanks!

Light-harvesting complexes - how fascinating!.....what a privilege to study the protein with the most amazing structure I have ever seen. Ultra-fast, ultra-efficient - perfect? (who would argue)!

I would like to thank you for all the help I have received from my supervisor, Prof. Richard Cogdell. In particular, I am very grateful for all the opportunities I have had to travel - both to conferences in Rehovot, Blarney and Budapest and to work in labs in Munich, Lund and Leiden. I am also very grateful for the freedom that I have had to do my own research and for the speedy turn around of my scribbling.

Lord, I would like to thank you for the privilege of being a Gatsby student and for all the perks that I have received there-in.....the financial support, the training weekends, the opportunity to present and for the friends that I have made.

Lab B4a - what a lab! Lord Jesus, I want to thank you for the times shared with and the help received from everyone associated with the lab...Juan Arellano, Stuart Barrett, Peter Dominy (for all the time spent calibrating the fluorimeter), Paul Fyfe, Tina Howard (FPLC woman), Evelyn Johnston, Chris Law, Katherine McAuley-Hecht (chief decoder), Karen McClusky, Kimberly McKendrick, Joannie Mitchell and Steve Prince. I am also indebted to you for the many good friends I have made both here and abroad - the members of the Bond lab, the Arnott lab and lab C15, the footballing lads especially "the

Gizibos", Dave Hamilton (Wye College) and Thania Spathapolous (Leiden University).
Most of all, I want to thank you for placing me in a Dept. where there are so many Christians. I have really benefited from meeting to pray each day. For the encouragement, instruction and "fellowship" that I have shared and still do share with Jay, Chris, Gill, Ang, Geraldine, Heather, Hyo-Eun and Jason to name but a few, I want to say thanks. Without doubt, my deepest joy in the past three years has been seeing your hand upon Ang's life as you have dealt with her and brought her into everlasting life. Lord, my desire for Ang is that she "being rooted and established in love" would have the "eyes of her heart enlightened so that she may increasingly know the hope to which she is called and discover the incomparably great power of your Holy Spirit"
Finally Lord, I want to thank you for Mum, Dad, Fi and Lyndz, for the love and closeness that we share as a family and for Sunday afternoon walks.

With much love

Niall

Abbreviations

2D	two-dimensional
3D	three-dimensional
Å	angstrom (10^{-10} m)
A	absorbance
ΔA	change in absorbance
ATP	adenosine 5′ triphosphate
AU	absorbance units
B800→B850	energy transfer from the (B)Chl-B800 to the Bchl*a*-B850 molecules
Bchl*a*	bacteriochlorophyll *a*
Bchl*a*-B800, -B850	Bchl*a* molecule in the B800 and B850 binding pockets, respectively
Bchl*a*-B800*	Bchl*a*-B800 excited state
(B)Chl-B800	general reference to any (native or modified) pigment in the B800 sites
βOG	β-octyl glucoside
Bph*e*	bacteriopheophytin
CD	circular dichroism
CF	correction file
Chl*a*	chlorophyll *a*
CM	cytoplasmic membrane
cps	counts per second
DAD	diode-array-detector
DNase	deoxyribonuclease
ENDOR	electron nuclear double resonance
ESA	excited-state absorption
FPLC	fast protein liquid chromatography
fs	femtosecond (10^{-15} s)
fwhm	full-width, half-maximum
HITC	1,1′,3,3,3′,3′ - hexamethylindotricarbocyanine perchlorate
HPLC	high pressure liquid chromatography
ICM	intracytoplasmic membrane
IRF	instrument response function
LD	linear dichroism
LDAO	N-lauryl-N,N′-dimethyl-N-oxide
LDS	lithium dodecyl sulphate
LH	light-harvesting

LH1	light-harvesting complex 1
LH2	light-harvesting complex 2
LM	dodecyl-βD-maltoside
MCA	multi-channel analyser
MIA	microwave-induced absorption
$NADH_2$	nicotinamide adenine dinucleotide (reduced form)
NIR	near-infrared
ns	nanosecond (10^{-9}s)
OD	optical density
PMT	photomultiplier tube
ps	picosecond (10^{-12} s)
PSU	photosynthetic unit
QH_2	quinol
R	reference
Rb.	*Rhodobacter*
Rps.	*Rhodopseudomonas*
Rs.	*Rhodospirillum*
RC	reaction centre
RR	resonance Raman
S	signal
SD	silicon detector
S_1, S_2	first and second excited singlet states
TAC	time-to-amplitude converter
TLC	thin layer chromatography

Table of contents

Introduction

Chapter 1 : *Purple photosynthetic bacteria*

1.1 A general introduction to photosynthesis 1

1.2 A brief history of photosynthesis 1

1.3 Taxonomy of anoxygenic photosynthetic bacteria 2

1.4 Membrane structure 3

1.5 The photosynthetic unit (PSU) 4

1.5.1 An introduction to the PSU 4

1.5.2 An overview of energy trapping in the PSU 6

1.6 The structure of the components of the PSU 9

1.6.1 Introduction 9

1.6.2 Reaction Centres - structural features 9

1.6.3 LH1 structural features 14

1.6.4 Puf X :- an essential component in PSU function 17

1.6.5 LH2 18

1.6.5.1 Common structural features 18

1.6.5.2 Pigment-protein interactions in the LH2 complex from *Rps. acidophila* 10050 24

Chapter 2 : *Modified pigments and mechanisms of energy transfer*

2.1 Introduction 25

2.2 Mechanisms of excitation transfer 25

2.2.1 Introduction 25

2.2.2 Förster theory 26

2.2.3 Exciton theory 27

2.2.4 Dexter theory 28

2.3 The kinetics of energy transfer within LH2 complexes 28

2.3.1 Introduction 28

2.3.2 B800→B850 energy transfer 29

2.3.3 B800→B800 energy transfer 32

2.3.4 B850 - an excitonically coupled ring 34

2.3.5 Carotenoid→B850 energy transfer 35

2.3.5.1 The role of the carotenoid S_1 and S_2 excited states in singlet-singlet energy transfer 35
2.3.5.2 The dynamics of carotenoid to Bchl*a* energy transfer 36
2.3.5.3 Methods for exchange and reconstitution of carotenoids in LH2 37
2.4 The use of modified pigments to probe the photochemical reactions in RC and LH complexes 38
2.4.1 Modified (bacterio)chlorin molecules 39
2.4.2 Pigment-exchange expts. in RC 41
2.4.2.1 Pigment exchange protocol 41
2.4.2.2 Selectivity of the exchange 42
2.4.2.3 Insights into RC function 43
2.4.3 LH1 reconstitution experiments 44
2.4.3.1 The reversible dissociation of LH1 into its constituent parts 44
2.4.4 Reconstitution experiments with LH2 complexes 47

Materials and Methods

Chapter 3 : *Biochemical techniques*
3.1 Cell culture 48
3.2 Isolation and storage of the bacterial whole cells 48
3.3 Purification of LH2 complexes from *Rps. acidophila* 10050 49
3.3.1 Introduction 49
3.3.2 Membrane isolation 49
3.3.3 Membrane solubilisation 49
3.3.4 Sucrose gradient 50
3.3.5 Gel filtration chromatography 50
3.4 Purification of the detergent TBG10 51
3.5 Pigment purification and handling techniques 51
3.5.1 Purification of Bchl*a* 52
3.5.2 Purification of geranylgeraniol Bchl*a* 53
3.5.3 Modified pigments 53
3.5.4 Qualitative analysis of the Bchl*a* and Chl*a* pigments 53
3.5.5 Purification of rhodopin glucoside 54
3.5.6 Determination of the pigment extinction coefficients 55

3.6 Determination of the Bchl*a* concentration of a LH2 sample 57

Chapter 4 : *Optimising the pigment-exchange procedure*

4.1 Optimisation of the conditions for release of the Bchl*a*-B800 molecules 58

4.1.1 Introduction 58

4.1.2 Effects of protein concentration, the pH and temperature of incubation and the choice of detergent on Bchl*a*-B800 release 58

4.2 The time course of the reconstitution reaction 59

4.3 Optimising the conditions for the reconstitution reaction 60

4.3.1 Introduction 60

4.3.2 The effect of the Bchl*a* concentration, the temperature of incubation and the choice of detergent on the occupancy of the B800 sites in the reconstituted complexes 61

4.4 Protocol for pigment exchange 62

Chapter 5 : *Spectroscopic techniques*

5.1 Absorption spectroscopy 65

5.2 Steady-state fluorescence measurements 65

5.2.1 Excitation spectra 65

5.2.2 Emission spectra 66

5.3 Circular dichroism spectroscopy 66

5.4 Resonance Raman spectroscopy 68

5.5 Pigment analysis of the LH complexes 68

5.5.1 Pigment extraction 68

5.5.2 HPLC 68

5.6 Fs transient absorption measurements 69

5.7 Fluorescence up-conversion 70

5.8 Time-resolved photon counting 71

Results and Discussion

Chapter 6 : *Devising a pigment-exchange protocol*

6.1 Introduction 72

6.2 Release of the Bchl*a*-B800 molecules from their binding pockets 72

6.3 Optimising the conditions for pigment release 76

6.3.1 The effect of protein concentration on the rate of Bchl*a*-B800 release 76
6.3.2 The effect of pH of incubation on the rate of Bchla-B800 release 78
6.3.3 The effect of temperature of incubation on rate of Bchl*a*-B800 release 78
6.3.4 The effect of choice of detergent on Bchl*a*-B800 release 82
6.3.5 Summary 83
6.4 Purification of the B850-only complexes 83
6.5 Optimising the conditions for reconstitution 84
6.5.1 LM as the preferred detergent for reconstitution 87
6.5.2 Time course of reconstitution 88
6.5.3 The effect of Bchl*a* concentration on the occupancy of the B800 site 88
6.5.4 The effect of temperature of incubation on the occupancy of the B800 sites 91
6.5.5 Summary 92
6.6 Comparison of the absorption spectra of native LH2 and Bchl*a*-B800 reconstituted complexes 92

Chapter 7 : *Structural and functional studies on the Bchla-B800 reconstituted complex*

7.1 Introduction 93
7.2 Determination of the pigment composition of the native LH2, B850-only and Bchl*a*-B800 reconstituted complexes by HPLC 94
7.2.1 Introduction 94
7.2.2 The pigment composition of the native LH2, B850-only and Bchl*a*-B800 reconstituted complexes 95
7.3 Structural analysis of the native LH2, B850-only and Bchl*a*-B800 reconstituted complexes by circular dichroism spectroscopy 98
7.3.1 Introduction 99
7.3.2 CD spectra of the LH2, B850-only and Bchl*a*-B800 reconstituted complexes in the NIR 100
7.3.3 CD spectra of the LH2, B850-only and Bchl*a*-B800 reconstituted complexes in the visible region 102
7.4 A study of the protein-Bchl*a* interactions in the native, B850-only and Bchl*a*-B800 reconstituted complexes by resonance Raman spectroscopy 104
7.4.1 Introduction 104

7.4.2 The carbonyl stretching modes of Bchl*a* in native, B850-only and Bchl*a*-B800 reconstituted complexes 106
7.4.3 A comparison of all of the Bchl*a* vibrational modes in native and Bchl*a*-B800 reconstituted complexes 109
7.5 Fluorescence emission experiments as a simple probe of B800 to B850 energy transfer 111
7.5.1 Introduction 111
7.5.2 B800→B850 energy transfer in native LH2 and Bchl*a*-B800 reconstituted complexes 113
7.6 Summary 114

Chapter 8 : *Spectrally modified LH2 complexes*
8.1 Introduction 115
8.2 Creating spectrally modified complexes 115
8.3 Determination of the occupancy of the B800 sites in each of the modified complexes by HPLC 121
8.3.1 Introduction 121
8.3.2 Results 122
8.4 CD as a probe of the overall structure and binding of the (B)Chl-B800 pigments in the modified, reconstituted complexes 125
8.4.1 Introduction 125
8.4.2 CD spectra of the reconstituted complexes containing modified pigments 126
8.5 Investigating B800 to B850 energy transfer in the modified reconstituted complexes by fluorescence emission spectroscopy 128
8.5.1 Introduction 128
8.5.2 Fluorescence emission spectra of the reconstituted complexes 128
8.6 Summary 131

Chapter 9 : *B800 to B850 energy transfer*
9.1 Introduction 133
9.2 The kinetics of B800-B850 energy transfer 133
9.2.1 Introduction 133
9.2.2 Transient absorption spectroscopy 134
9.2.3 Isotropic kinetics in the (B)Chl-B800 band 135
9.2.4 B850 rise kinetics 140

9.3 Modelling the rate of B800→B850 energy transfer in native and selected reconstituted complexes by Förster theory 142

9.4 The effect of spectral overlap on the efficiency of B800→B850 energy transfer 146

Chapter 10 : *B800 to B800 energy transfer*

10.1 Introduction 148

10.2 Calculating anisotropy values and B800→B800 hopping times from isotropic kinetic data 148

10.3 B800→B800 energy transfer in native LH2 and selected reconstituted complexes 150

Chapter 11 : *Carotenoid to B850 energy transfer*

11.1 Introduction 158

11.2 A comparison of the S_2 and S_1 lifetimes of rhodopin glucoside in native LH2 and B850-only complexes with those in benzyl alcohol 159

11.2.1 Introduction 159

11.2.2 Fluorescence up-conversion 160

11.2.3 S_2 and S_1 lifetime data 162

11.3 A comparison of the kinetics of carotenoid→B850 energy transfer in the native and B850-only complexes 164

11.3.1 Introduction 164

11.3.2 The kinetics of carotenoid→B850 energy transfer in the LH2 and B850-only complexes 165

11.4 A comparison of the efficiencies of carotenoid→B850 energy transfer in the native and B850-only complexes 168

11.4.1 Introduction 168

11.4.2 Results 169

11.5 A comparison of the efficiency of carotenoid→B850 energy transfer in selected reconstituted complexes 170

11.5.1 Introduction 171

11.5.2 Results 172

Chapter 12 : *Discussion* 177

Appendices

Appendix A : *Fluorescence lifetimes of the modified pigments* 184

A.1 Introduction 184

A.2 Time-resolved single photon counting 187

A.3 The fluorescence lifetimes of the modified pigments

Appendix B : *Calibration of the fluorimeter for fluorescence excitation spectra* 190

B.1 Introduction 193

B.2 Correction of fluorescence excitation spectra in the visible region using rhodamine 6B as a quantum counter 194

B.3 Approaches to correcting fluorescence excitation spectra in the NIR region 197

B.3.1 Quantum counter approach 200

B.3.2 Direct approach

205

References

Table of figures

Figure 1a Cartoon representation of the four basic structures of the intracytoplasmic membrane which occur in purple photosynthetic bacteria 5

Figure 1b A schematic model of the photosynthetic membrane 7-8

Figure 1c The 3D structure of the RC complex from *Rb. sphaeroides* as viewed parallel to the membrane surface 11

Figure 1d The arrangement of the pigment co-factors in the RC complex from *Rb.sphaeroides* 13

Figure 1e Projection map for LH1 complexes from *Rs. rubrum* at a resolution of 8.5Å 16

Figure 1f The LH2 complex from *Rps. acidophila* 10050 as viewed from the cytoplasmic side of the membrane 19

Figure 1g Arrangement of the pigment molecules in the LH2 complex from *Rps. acidophila* 10050 as viewed parallel to the membrane surface 21-22

Figure 2a Chemical structure of a Bchl*a* molecule 40

Figure 6a A comparison of the absorption spectra of LH2 complexes from *Rps. acidophila* 10050 before and after the release of all of the Bchl*a*-B800 molecules from their binding pockets 73

Figure 6b Difference absorption spectrum which shows the changes in absorption which occur on the complete release of the Bchl*a*-B800 molecules from their binding pockets 74

Figure 6c The effect of pH of incubation on the initial rate of release of the Bchl*a*-B800 molecules from their binding pockets 79

Figure 6d The effect of temperature of incubation on the initial rate of release of the Bchl*a*-B800 molecules from their binding pockets 80

Figure 6e Absorption spectra of the (a) native LH2, (b) B850-only and (c) Bchl*a*-B800 reconstituted complexes 85

Figure 6f The time course of the reconstitution reaction 89

Figure 6g The effect of the concentration of exogenous Bchl*a* in the incubation mixture on the final occupancy of the B800 sites in the reconstituted complex 90

Figure 7a The elution profile of a pigment extract from the native complex 96

Figure 7b CD spectra of the (a) LH2, (b) B850-only and (c) Bchl*a*-B800 reconstituted complexes in the NIR 101

Figure 7c CD spectra of the (a) LH2, (b) B850-only and Bchl*a*-B800 reconstituted complexes in the visible region 103

Figure 7d The high frequency carbonyl stretching modes of the Bchl*a* molecules in the (a) native, (b) B850-only and (c) Bchl*a*-B800 reconstituted complexes 107-108

Figure 7e Comparison of the vibrational modes of the Bchl*a* molecules in the (a) native and (b) Bchl*a*-B800 reconstituted complexes over an extended frequency range (400 to 1740 cm^{-1}) 110

Figure 7f The fluorescence emission spectra of the (a) native and (b) Bchl*a*-B800 reconstituted complexes 113

Figure 8a Absorption spectra of the A) native LH2, B) Zn-Bphe-, C) 3^1vinyl Bchl*a*-, D) 3^1OH Bchl*a*-, E) acetyl Chl*a*- and F) Chl*a*-B800 reconstituted complexes 118-119

Figure 8b Elution profile of the pigments extracted from the Chl*a*-B800 reconstituted complex 123-124

Figure 8c The (a) absorption and (b) CD spectra of the acetyl Chl*a*-B800 reconstituted complexes 127

Figure 8d Fluorescence emission spectra of a) 3^1 vinyl Bchl*a*- and b) acetyl Chl*a*-B800 reconstituted complexes 130

Figure 9a Isotropic kinetic data showing the time-dependent bleaching and recovery of the "B800" Q_y absorption band in LH2 complexes reconstituted with 3^1OH Bchl*a* 136

Figure 9b Calculated isotropic kinetics for the bleaching and recovery of the "B800" Q_y absorption band in 3^1OH Bchl*a*-B800 reconstituted complexes from which the contribution of B850 ESA has been subtracted 137

Figure 9c The rise in bleaching of the Q_y absorption band of the Bchl*a*-B850 molecules with time in native LH2 and selected reconstituted complexes after Q_y excitation of their (B)Chl-B800 molecules 141

Figure 9d Dependence of the rate of B800→B850 energy transfer on the spectral separation between the (B)Chl-B800 and B850 Q_y absorption bands (energy gap) 144-145

Figure 10a The depolarisation of the Bchl*a*-B800 Q_y absorption band in native LH2 with time 151

Figure 10b The kinetics of depolarisation of the "B800" Q_y absorption band in LH2 complexes reconstituted with Chl*a* 152

Figure 11a Fluorescence up-conversion 161

Figure 11b A comparison of the decay kinetics of fluorescence emission from the rhodopin glucoside S_2 state in benzyl alcohol with that in the native LH2 and B850-only complexes 163

Figure 11c The time-dependent rise in fluorescence emission of the Bchl*a*-B850 molecules in the native LH2 complex after excitation of the rhodopin glucoside molecules at 499 nm 166

Figure 11d The time-dependent rise in fluorescence emission of the Bchl*a*-B850 molecules with time in the B850-only complex after excitation of the rhodopin glucoside molecules at 499 nm 167

Figure 11e The % restoration of carotenoid→B850 energy transfer via the (B)Chl-B800 molecules in the Bchl*a*-, 3^1vinyl Bchl*a*-, 3^1OH Bchl*a*-, acetyl Chl*a*- and Chl*a*-B800 reconstituted complexes 172

Figure 11f Spectral overlap between the hypothetical fluorescence emission spectra of the S_2 and S_1 states of rhodopin glucoside and the Q_x transition of the (B)Chl-B800 molecules in the 3^1vinyl Bchl*a*- and 3^1OH Bchl*a*-B800 reconstituted complexes and the $Q_y$transition of those in the acetyl Chl*a*- and Chl*a*-B800 reconstituted complexes 175

Figure A1 Time-resolved single photon counting 185-186

Figure A2 The time-dependent rise and decay in fluorescence emission of Bchl*a* molecules after excitation in their Soret absorption transition at 375 nm 188

Figure B1 Schematic diagram of the Spex Fluorolog2 fluorimeter 191-192

Figure B2 Correction file for fluorescence excitation spectra in the visible region using rhodamine 6B as a quantum counter 195

Figure B3 Action spectrum for B850-only complexes in the visible region 196

Figure B4 Correction file for fluorescence excitation spectra in the NIR region using HITC as a quantum counter 198

Figure B5 Action spectrum for LH2 complexes in the NIR region 199

Figure B6 The response curve of the SD as determined using a thermopile 201

Figure B7 Correction file for the light path in the region 580 to 1000 nm 202

Figure B8 Action spectrum for LH2 complexes in the NIR region 204

List of tables

Table 2i The functional side groups of a range of modified (bacterio)chlorophyll molecules 40

Table 3i The extinction coefficients of the Q_y transitions of modified pigments relative to that of Bchl*a* (Bandilla *et al.*, 1998) 56

Table 5i Excitation wavelengths and emission wavelength ranges used in the fluorescence emission experiments with the native LH2 and reconstituted complexes 67

Table 6i The effect of protein concentration on the incubation period necessary for release of all the Bchl*a*-B800 molecules from the LH2 complex 77

Table 6ii The effect of the pH of incubation on the length of time necessary for complete release of the Bchl*a*-B800 molecules from their binding pockets 77

Table 6iii The effect of temperature of incubation on the time required for all of the Bchl*a*-B800 molecules to be completely released from their binding sites 81

Table 6iv The wavelengths of the absorption maxima in the native, B850-only and Bchl*a*-B800 reconstituted complexes 86

Table 7i The pigment ratios in the native, B850-only and Bchl*a*-B800 reconstituted complexes as determined by HPLC 97

Table 8i The "B800" Q_y maxima for reconstituted complexes containing modified pigments 117

Table 9i Calculated isotropic kinetic data for the bleaching and recovery of the "B800" Q_y absorption band in native LH2 and selected reconstituted complexes 139

Table 9ii The time constants for B800→B850 energy transfer in native and reconstituted complexes as determined from the time-dependent rise in the bleaching of the B850 Q_y absorption band after excitation of their (B)Chl-B800 molecules 139

Table 10i The time constants for depolarisation of the (B)Chl-B800 Q_y absorption band and B800→B800 energy transfer in native LH2 and selected reconstituted complexes 154

Table 11i The efficiencies of carotenoid→B850 energy transfer in native, B850-only and selected reconstituted complexes 170

Table Ai The fluorescence lifetimes of the modified (bacterio)chlorin molecules as determined by time-resolved single photon counting 189

Introduction

1.1 A general introduction to photosynthesis

Photosynthesis is the process by which light energy is converted to useful chemical energy by a group of organisms called phototrophs. Photosynthesis is now known to consist of two sets of reactions, namely the light and dark reactions (Emerson & Arnold, 1932). In the light reactions, light energy is trapped by the photosynthetic organism and converted to chemical energy in the form of $NADH_2$ and ATP. In the dark reactions, these molecules are utilised to fix CO_2 as carbohydrate. The work presented in this thesis is concerned with the light reactions which occur in the photosynthetic membranes of purple bacteria.

1.2 A brief history of photosynthesis

In 1780, Joseph Priestly showed that plants can "restore air which had been injured by the burning of candles". The underlying explanation for this phenomenon is that plants can produce oxygen. In 1786, Jan Ingenhousz showed that this oxygen production is stimulated by sunlight. In 1782, Jean Senebier showed that CO_2 is consumed in photosynthesis. In 1804, Nichola de Suassure showed that the sum of the weights of organic matter produced and the oxygen gas evolved by the plants was much greater that the mass of CO_2 consumed. From the law of the conservation of mass, de Suassure concluded that another substance was being utilised in the photosynthetic process. That reactant is water. In 1842, Julius Mayer, who discovered the law of conservation of energy, proposed that plants absorb light energy and convert it to chemical energy. These key observations meant that by the

middle of the 19th century, plants were known to use light energy to convert CO_2 and H_2O to organic material and oxygen.

It is now known that photosynthesis is not just performed by plants but by a diverse range of organisms including algae, cyanobacteria and anoxygenic phototropic bacteria (Gest, 1993). In 1941, van Niel proposed a general formula for photosynthesis :-

$$CO_2 + 2\,H_2X \xrightarrow{h\upsilon} CH_2O + H_2O + 2X$$

where H_2X is an oxidisable substrate. In plants and algae this oxidisable substrate is water. Anoxygenic photosynthetic bacteria can use various different reductants. These include sulphide and certain other reduced sulphur compounds, hydrogen and a number of small organic molecules such as succinate.

1.3 Taxonomy of anoxygenic photosynthetic bacteria

Apart from their common ability to perform photosynthesis, anoxygenic phototropic bacteria are a very heterogeneous group and have a variety of morphological and physiological properties. According to their phenotypic properties, anoxygenic phototropic bacteria can be divided into three main groups. These are the green bacteria, purple bacteria and heliobacteria. Purple bacteria can be divided into 3 main sub-groups according to their ability to form globules of elemental sulphur. Historically, Molisch (1907) distinguished two types of purple bacteria. Those bacteria which can form globules of elemental sulphur inside their cells were called the

Thiorhodaceae. Those bacteria which can not were called the *Anthiorhodaceae*. These two main groups still remain although they have been renamed as the *Chromatiaceae* (Bavendamm, 1924) and the *Rhodospirillaceae* (Pfenning & Truper, 1971) respectively. The discovery of purple bacteria which accumulate elemental sulphur outside their cells led to a classification crisis. These bacteria were originally included in the *Chromatiaceae* family as the genus *Ectothiorhodospira* (Pfenning & Truper, 1974) but have since been re-classified as a distinct family known as the *Ectothiorhodospiraceae* (Imhoff, 1984).

The *Rhodospirillaceae* are a diverse group of bacteria. This diversity is reflected in greatly varying morphology, internal membrane structure, carotenoid composition and utilisation of carbon sources etc (Imhoff & Truper, 1989). Accordingly, the purple non-sulphur bacteria were sub-divided into further genera. These are the *Rhodospirillum, Rhodopila, Rhodomicrobium, Rhodobacter, Rhodopseudomonas, Rhodocyclus, Rhodoferax* and *Rubrivivax* genera. Certain of the bacteria of these genera have been used as model organisms for studying the light reactions of photosynthesis. These include *Rps. acidophila, Rps. viridis, Rb. sphaeroides, Rs. rubrum* and *Rs. molischianum*.

1.4 Membrane structure

Most purple bacteria have three membranes - a cytoplasmic membrane (CM) which encloses the protoplast, an intracytoplasmic membrane (ICM) and an outer membrane which is associated with the cell wall. The CM

contains the components of the respiratory chain whereas the ICM contains the photosynthetic machinery (Bowyer *et al.*, 1985). The ICM is formed by the invagination of the CM (Hickman & Frenkel, 1965). The ICM can adopt one of four different structures (see figure 1a) (Drews & Imhoff, 1991; Bachofen & Wiemken, 1986; Sprague & Varga, 1986; Oelze & Drews, 1972). Firstly, the ICM can adopt a vesicular structure such as that observed in *Rb. sphaeroides*, *Rs. rubrum* and *Chr. vinosum*. Secondly, the ICM can be arranged as a series of tubules such as that observed in *Th. pfennigii*. Thirdly, the ICM can exist as a network of thylakoid-like flat lamellae such as that observed in *Rs. molischianum*. Finally, the ICM can be arranged as a series of irregular, non-stacked membranes such as that observed in *Rps. acidophila* and *Rps. viridis*.

1.5 The photosynthetic unit (PSU)

1.5.1 An introduction to the PSU

The primary events of photosynthesis involve the capture and trapping of light energy in a chemical form. These events occur in the ICM within discrete units called photosynthetic units (PSU). Historically, PSUs were first proposed by Emerson and Arnold (1932) after their classical experiments with *Chlorella*. Emerson and Arnold found that the production of a single molecule of oxygen required the co-operative activity of approximately 2400 Chl*a*. This suggested that the majority of the chlorophyll molecules functioned in light-harvesting and only a limited number of chlorophyll molecules were directly involved in the photochemical reaction. Hence the

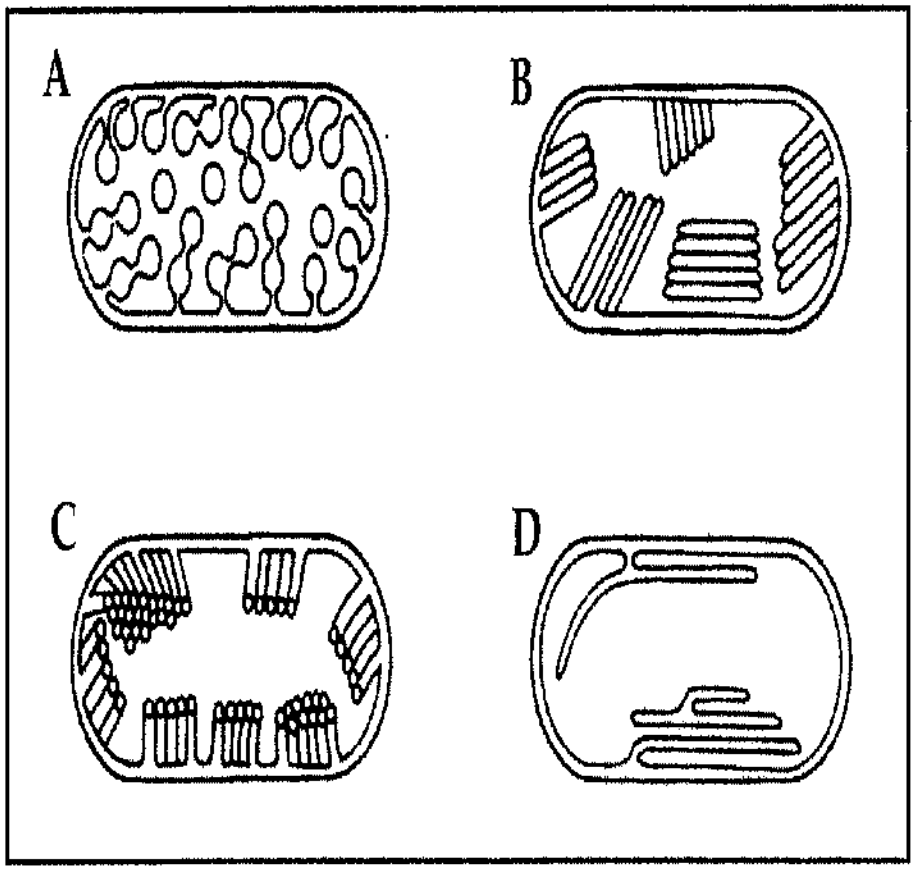

Figure 1a Cartoon representation of the four basic structures of the intracytoplasmic membrane which occur in purple photosynthetic bacteria. A) vesicular structure as found in *Rb. sphaeroides* B) a series of tubules such as that in *Th. pfennigi* C) a network of thylakoid-like flat lamellae as found in *Rs. molischianum* and D) a series of irregular, non-stacked membranes such as that in *Rps. acidophila*.

concept of a photosynthetic unit consisting of separate, antenna light-harvesting (LH) and reaction centre (RC) complexes was coined.

The size of the PSU is variable and is affected by the intensity of the illuminating light (Aagaard & Sistrom, 1972). For example, the size of the PSU in *Rb. sphaeroides* varies from 30 Bchl*a* molecules per RC (high light) to 200-250 Bchl*a* molecules per RC (low light). Implicit in this work was the suggestion that there are two distinct types of antenna complex - those which are associated with the RC in a fixed stoichiometry and those which are more peripheral in their location and variable in their amount. These complexes are now known as the LH1 and LH2 complexes respectively.

1.5.2 An overview of energy trapping in the PSU

Energy trapping in the PSU is summarised in figure 1b. Light energy absorbed by the LH1 and LH2 complexes is transferred to the RC where it is trapped. Photo-oxidation of the primary electron donor P, a Bchl*a* dimer, results in charge separation across the membrane (Parson & Warshel, 1987; Feher *et al.*, 1989). Two subsequent turnovers of the RC lead to the reduction of Q_B, a quinone (Q) molecule bound in the RC. A quinol (QH_2) molecule leaves the RC and enters a pool of Q/QH_2 molecules in the hydrophobic part of the membrane. The quinol molecule diffuses to a cytochrome bc_1 complex where it acts as an electron donor. The electrons are transferred to cytochrome c_2, which is located in the periplasm. This, in turn, re-reduces the photo-oxidized Bchl*a* dimer of the RC. Cyclical electron transfer is coupled to the generation of a proton gradient across the

Figure 1b A schematic model of the photosynthetic membrane. Photons of light energy absorbed by the LH1 and LH2 complexes are transferred to the RC where they are trapped. After two charge separation events, a quinol molecule (QH_2) is released from the RC into the membrane. The quinol diffuses to a cytochrome bc_1 complex where it donates its electrons. The electrons are then transferred to cytochrome c_2, which, in turn, re-reduces the RC. Cyclical electron transport is coupled to the generation of a proton gradient across the membrane. This is then utilised by the ATP synthase complexes to produce ATP.

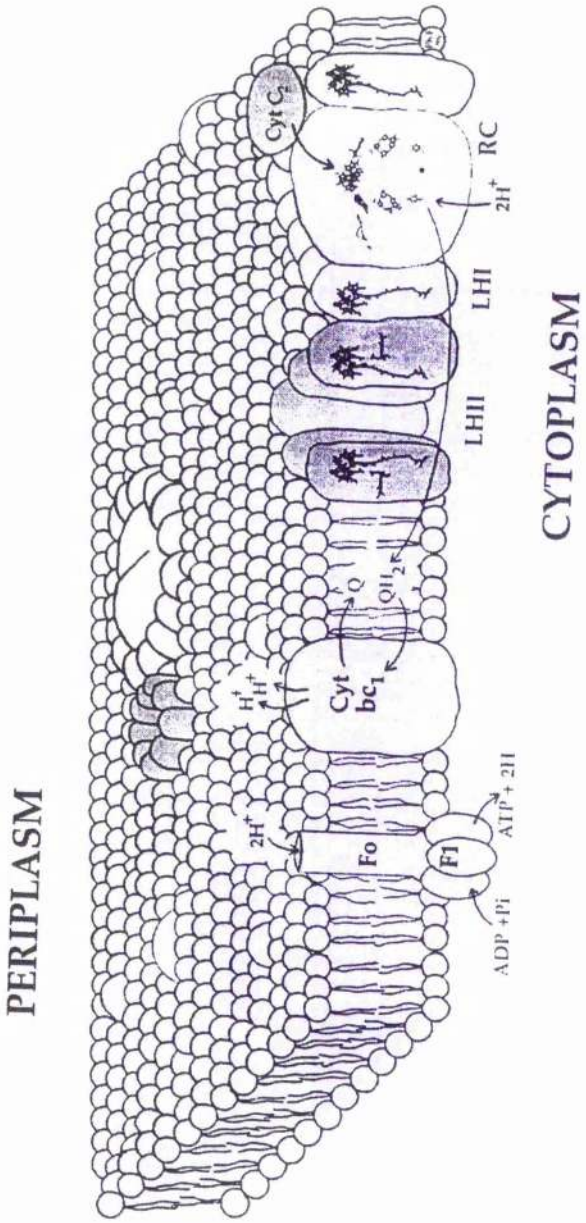
PERIPLASM
CYTOPLASM
Cyt C_2
RC
$2H^+$
LHII
LHIII
Q
QH_2
Cyt bc_1
H^+
H^+
$2H^+$
Fo
F1
$ATP + 2H$
ADP +Pi

membrane. This is then utilised by the ATP synthase complexes to produce ATP.

1.6 The structure of the components of the PSU

1.6.1 Introduction

Our understanding of PSU function has been greatly advanced by the structural determination of the individual components of the PSU. The 3D structures of the RC from *Rps. viridis* (Deisenhofer *et al.*, 1985) and *Rb. sphaeroides* (Allen *et al.*, 1987a,b) and the LH2 complexes from *Rps. acidophila* 10050 (McDermott *et al.*, 1995) and *Rs. molischianum* (Koepke *et al.*, 1996) are now known. In addition, an 8 Å projection map of the LH1 complex from *Rs. rubrum* has been presented (Karrasch *et al.*, 1995). These structures have been integrated to produce a 3D model of the complete PSU (Papiz *et al.*, 1996). In this Section, the structures of the RC, LH1 and LH2 complexes are described.

1.6.2 Reaction Centres - structural features

At the RC, photons of light energy are converted into chemical potential. RCs were first isolated from photosynthetic membranes by Reed and Clayton (1968). RCs consist of three different polypeptides which have been named the H (heavy), M (medium) and L (light) sub-units according to their apparent molecular weight as determined by gel electrophoresis (Feher, 1971). The RC also contains four bacteriochlorphyll, two

bacteriopheophytin, one carotenoid, one non-heme iron and two quinone molecules. These are non-covalently bound to the protein sub-units.

In 1985, the structure of the RC from *Rps. viridis* was solved by X-ray crystallography to a resolution of 3.0 Å (Deisenhofer *et al.*, 1985) This was the first occasion in which the structure of a membrane protein had been determined. This outstanding achievement was formally recognised when Johann Deisenhofer, Robert Huber and Hartmut Michel were awarded the Nobel Prize for Chemistry in 1988. Since then, the resolution of the crystal structure from *Rps. viridis* has been improved to 2.3 Å (Deisenhofer *et al.*, 1995). In addition, the structures of the RC from several different strains of *Rb. sphaeroides* have been determined (e.g. Allen *et al.*, 1987a,b; Ducruix *et al.*, 1987; Arnoux *et al.*, 1989; Ermler *et al.*, 1994; McAuley-Hecht *et al.*, 1998). To date, the best resolved RC structure from *Rb. sphaeroides* is that of Stowell *et al.* (1997) to a resolution of 2.2 Å.

The 3D structures of the RCs from *Rb. sphaeroides* and *Rps. viridis* are very similar (El-Kabbani *et al.*, 1991). In both structures, the L and M sub-units form the core of the RC and each cross the membrane five times. In contrast, the H sub-unit is essentially located on the cytoplasmic side of the membrane and crosses the membrane only once (see figure 1c). The most important domain of the protein for function is the hydrophobic transmembrane region, in which the pigment molecules are located. In this region, the transmembrane helices of the L and M sub-units follow approximate two-fold symmetry. All of the pigments with the exception of the carotenoid are arranged in two branches (A and B) and are related by an

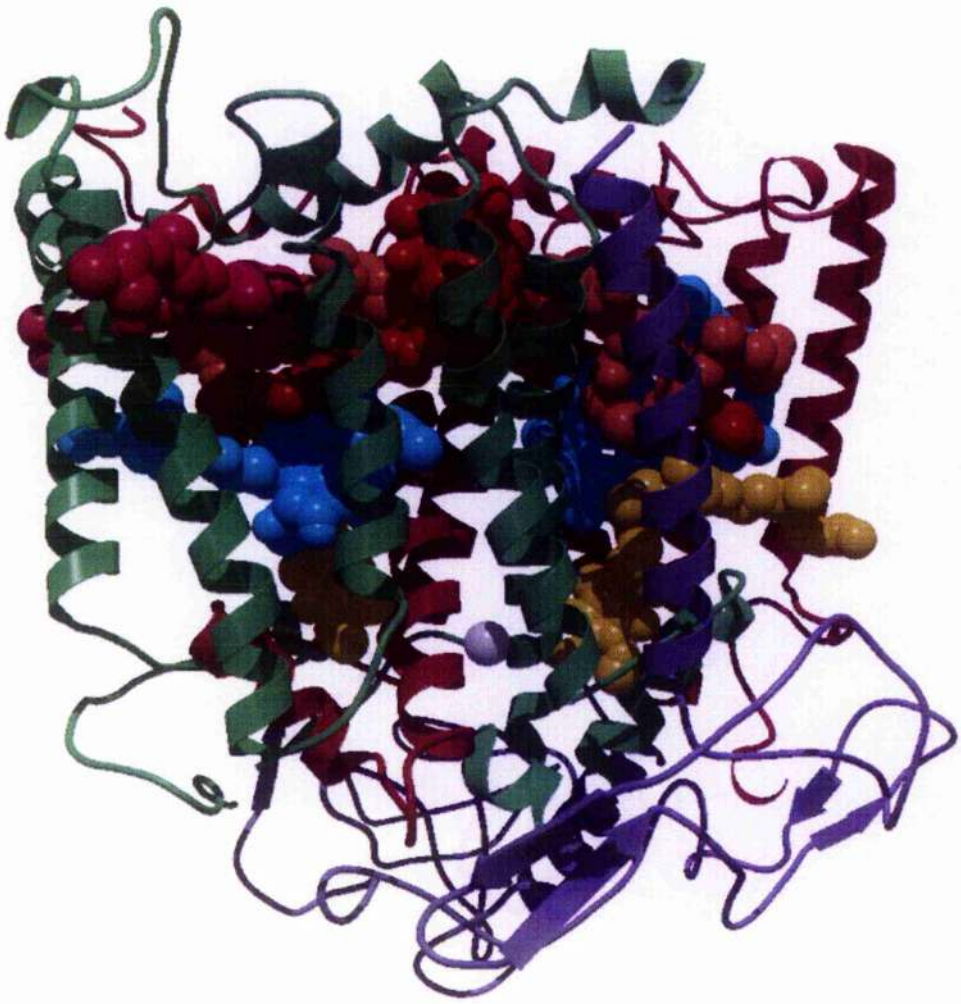

Figure 1c The 3D structure of the RC complex from *Rb. sphaeroides* as viewed parallel to the membrane surface. [**Key** Protein sub-units L - maroon, M - green, H - purple : Co-factors "special pair" Bchl*a* red, accessory Bchl*a* beige, Bph*e* cyan, quinone yellow, non-haem iron grey, carotenoid pink].

approximate two-fold symmetry (see figure 1d). These two branches diverge from the "special pair" Bchl*a* molecules (P). Each branch consists of an accessory Bchl*a* (B), a Bph*e* (H) and a quinone (Q). The carotenoid is located next to the B branch (see figure 1d). Although the two pigment arms are structurally very similar, only the A arm is involved in the charge transfer process.

The kinetics of charge separation have been adequately reviewed elsewhere (see Parson & Warshel, 1987; Fleming & van Grondelle, 1994 for a more full discussion). In short, photons of light energy absorbed by the RC either directly or from the LH1 complex are quickly transferred to the "special pair" (P). On absorption of a photon, P is promoted to its first excited singlet state, P^*. An electron is then released from P^* and is quickly transferred to the bacteriopheophytin molecule (H_A) via the accessory bacteriochlorophyll (B_A). Electron transfer from P to H_A takes approximately 3 ps (Zinth *et al.*, 1985; Breton *et al.*, 1986; Martin *et al.*, 1986; Fleming *et al.*, 1988). The electron then moves to Q_A in ~ 200 ps (Kirmaier & Holten, 1987) before it is finally transferred to Q_B. The time constant for electron transfer from Q_A to Q_B is 100 μs (Debus *et al.*, 1986). For complete reduction of a quinone molecule, two electrons are required. This is accomplished by a second round of charge separation and electron transfer. Prior to a second electron transfer event, P is re-reduced by cytochrome c_2. After P is re-reduced, a second excitation event occurs (Wraight 1979; Kleinfield *et al.*, 1984; Dracheva *et al.*, 1988) and the doubly reduced quinone Q_B^{2-} is formed. On acquiring two protons from the cytoplasm, the quinol is released from the

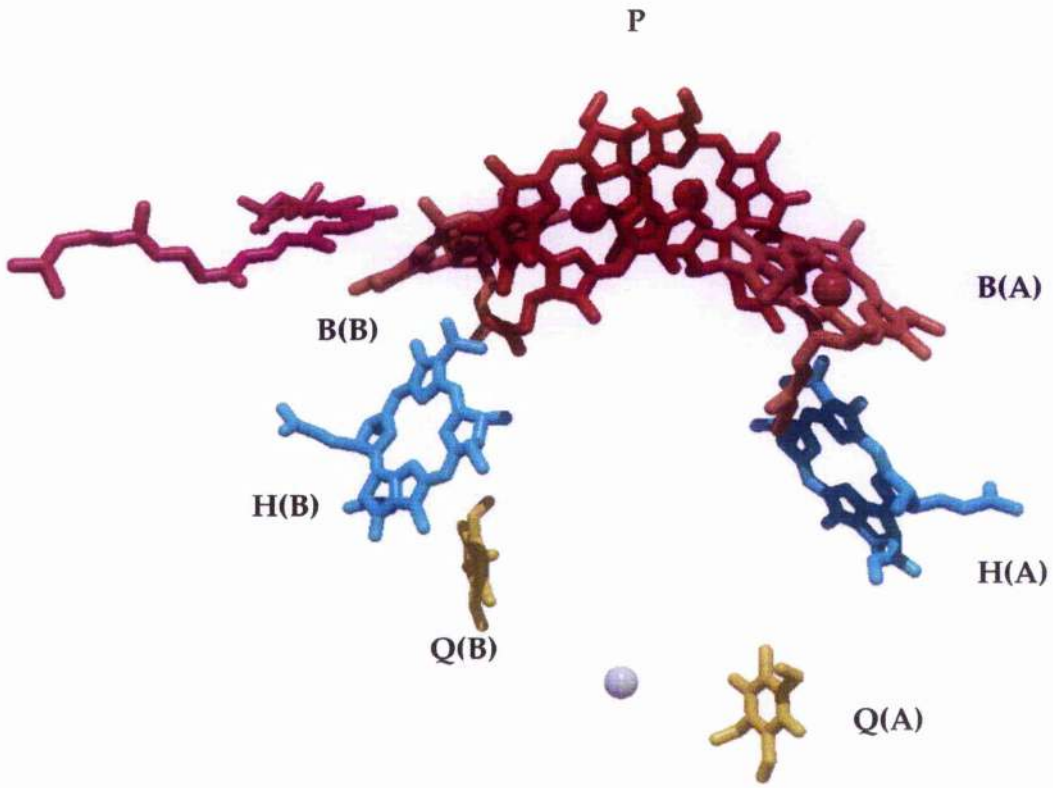

Figure 1d The arrangement of the pigment co-factors in the RC complex from *Rb. sphaeroides*. All of the pigments, with the exception of the carotenoid, are arranged in two branches (A and B) which are related by an approximate two-fold symmetry. These two branches diverge from the "special pair" Bchl*a* molecules (P). Each branch consists of an accessory Bchl*a* (B), a Bph*e* (H) and a quinone (Q). The carotenoid is located next to the B branch. Although the two pigment arms are structurally very similar, only the A arm is involved in the charge transfer process. [**Key** "special pair" Bchl*a* red, accessory Bchl*a* beige, Bph*e* cyan, quinone yellow, non-haem iron grey, carotenoid pink].

RC. It then diffuses through the membrane to the cytochrome bc_1 complex where it is oxidised (Gabbelini et al., 1982; Dutton 1986). The empty Q_B site in the RC is re-filled with a quinone molecule from the membrane pool (Crofts & Wraight, 1983).

1.6.3 LH1 structural features

The photosynthetic membranes of *Rps. viridis* contain an extensive, regular arrangement of core complexes. Structural analysis of this membrane by electron microscopy revealed a repeating pattern of structural units (Miller, 1982). The repeat structure was found to consist of a large central mass which protruded on both sides of the membrane and was surrounded by six smaller centres of mass. This structure was interpreted as a RC surrounded by a series of LH antenna complexes. This observation was confirmed by a later higher resolution analysis to 18 Å (Stark *et al.*, 1984). At this resolution, the core complex was found to have a diameter of 130 Å and that the LH1 ring consisted of 12 sub-units. The ratio of Bchl*a*/RC was found to be 24 : 1 (Jay *et al.*, 1984). This evidence suggested that the RC is surrounded by an $\alpha_{12}\beta_{12}\gamma_{12}$ LH1 ring. The first low-resolution structure of a Bchl*a* containing core complex was determined in *Rps. marina* (Meckenstock *et al.*, 1992b). These core complexes were also found to have ring-like structures with apparent 6-fold symmetry. In all of these studies, the resolution of the imaging was not sufficiently good to determine the actual size of the LH1 ring. In an attempt to determine the size of the LH1 ring, the number of Bchl*a* molecules/RC was determined for core complexes isolated from

several different types of bacteria. Separate studies have suggested ratios of approximately 32 : 1 (Dawkins *et al.*, 1988; Gall 1995) and 24 : 1 (Francke & Amesz, 1995). It was not possible to conclude if the observed variation in the Bchl*a* : RC ratio was due to different LH1 ring sizes in different bacteria or was merely an artefact of core complex isolation (Dawkins *et al.*, 1988). The usefulness of this technique in determining the size of the LH1 ring was, therefore, limited.

Our understanding of LH1 ring structure has been greatly advanced by a high resolution study of 2D crystals of reconstituted LH1 complexes from *Rs. rubrum* (Karrasch *et al.*, 1995). Image processing of electron micrographs of these crystals yielded a projection map to a resolution of 8.5 Å. The ring has 16 sub-units. Each sub-unit has three domains of electron density (see figure 1e). These were assigned to the α and β apoproteins and to the B870 molecules. The ring has a diameter of 120 Å. This is in good agreement with previous low resolution studies (Meckenstock *et al.*, 1992; Boonstra *et al.*, 1994). The hole at the centre of the ring has a diameter of 70 Å. This is sufficiently big to incorporate a RC *in vivo*.

A previous low resolution study of the same complex suggested that it had 6 fold symmetry (Ghosh *et al.*, 1993). In the high resolution structure, however, the core complexes were found to have 8 fold symmetry. This may suggest that the 6 fold symmetries which have been previously observed for core complexes from *Rps. viridis* (Stark *et al.*, 1984), *Rp. marinum* (Meckenstock *et al.*, 1992b) and *Rs. molischianum* (Boonstra *et al.*, 1994) are an artefact of low resolution. Further high resolution

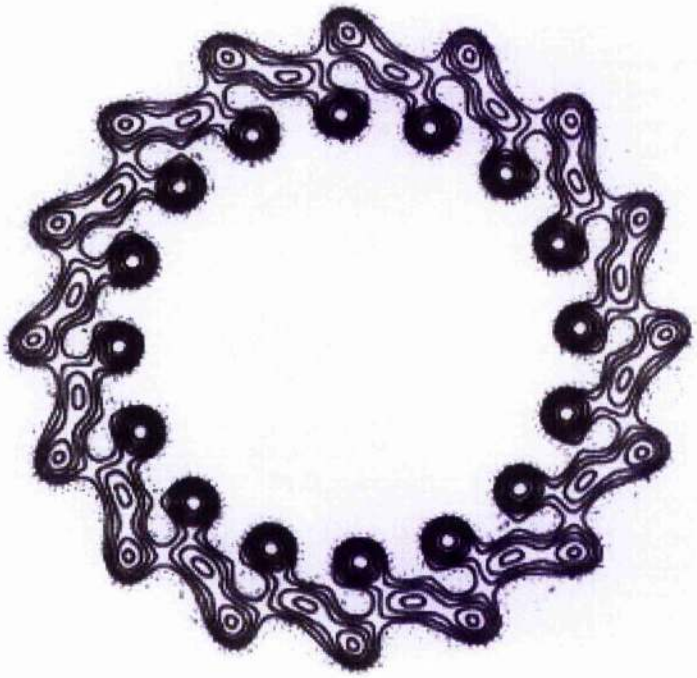

Figure 1e Projection map for LH1 complexes from *Rs. rubrum* at a resolution of 8.5Å. The inner and outer peaks represent the α and β apoproteins respectively. The density between the apoproteins corresponds to the B870 molecules.

structures from several different types of bacteria are required before it will be possible to conclude whether or not the $\alpha_{15}\beta_{16}$ ring structure observed in *Rs. rubrum* has a universal occurrence.

The structure of the reconstituted LH1 ring from *R. rubrum* has been confirmed by subsequent, high resolution crystallisation studies of the native complex (Walz & Ghosh, 1997). The size of the LH1 ring in the native complex is the same as that in the reconstituted complex. In the native complex, the LH1 ring has a central, diffuse, stain-excluding region. This is due to the RC. After averaging many unit cells, it was not possible to see a defined RC shape. This suggests that the RC have a different orientation in neighbouring LH1 rings. The resolution of this structure was not sufficiently good to determine whether or not the LH1 ring contains a PufX type channel (see Section 1.6.4)

1.6.4 Puf X :- an essential component in PSU function

Electron transfer between the RC and the cytochrome bc_1 complex is mediated by membrane-bound quinone molecules. For function, the quinones must have access to the Q_B site of the RC. This could occur in one of two ways. The quinones may access the RC either through the temporary opening of the LH1 ring or via a protein channel situated in the LH1 ring. In *Rb. sphaeroides*, the pufx gene is expressed as a 9 kDa membrane protein which is closely associated with the LH1-RC complex (Lee *et al.*, 1989; Farchaus *et al.*, 1992). The PufX protein is thought to form a channel within the LH1 ring where it facilitates quinone movement. This hypothesis is

supported by several lines of evidence. PufX is essential for anaerobic photosynthetic growth (Farchaus *et al.*, 1992; Westerhuis *et al.*, 1993; McGlynn *et al.*, 1994). Rapid Q/QH_2 exchange only occurs in the presence of PufX (Barz *et al.*, 1995a,b). Mutations which significantly affect the tertiary structure of the LH1 ring restore photosynthetic competence to pufx deletion mutants (Barz & Oesterhelt, 1994). The ability of several *Rb. sphaeroides* pufx deletion mutants to grow photosynthetically depends on the size of the LH1 ring. These mutants can grow photosynthetically in the absence of Puf X if the size of the LH1 ring is smaller than 21 Bchl*a*/RC (McGlynn *et al.*, 1996). In addition, it was shown that for any given ring size, the absence of Puf X results in an increase in ring size of between 1-2 Bchl*a* molecules/RC (McGlynn *et al.*, 1996). This suggests that the PufX protein can replace an αβ pair within the LH1 ring.

In short, the current evidence suggests that quinone molecules are able to access the Q_B site of the RC via a PufX channel situated in the LH1 ring.

1.6.5 LH2

1.6.5.1 Common structural features

The crystal structure of the LH2 complex from *Rps. acidophila* 10050 has recently been determined to a resolution of 2.5Å (McDermott *et al.*, 1995) (see figure 1f). The complex is an $\alpha_9\beta_9$ oligomer. Each monomeric unit consists of an α and β apoprotein, three Bchl*a* molecules and one carotenoid (rhodopin glucoside) molecule. The nine α apoproteins form a hollow cylinder with the nine β apoproteins arranged radially outside. The complex

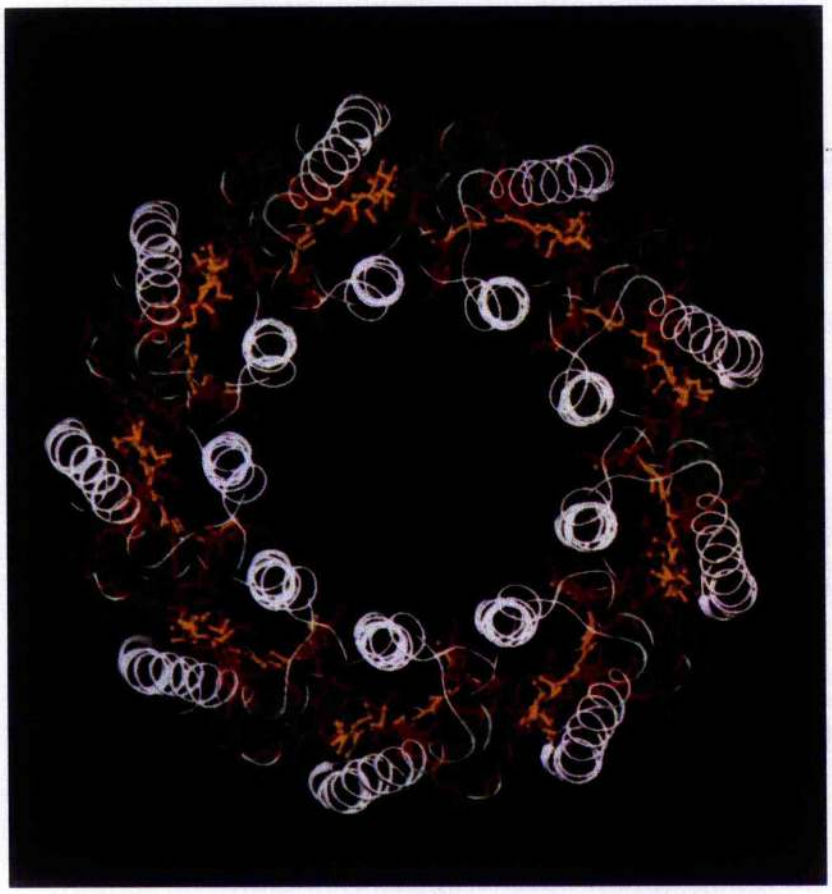

Figure 1f The LH2 complex from *Rps. acidophila* 10050 as viewed from the cytoplasmic side of the membrane. The nine α apoproteins form a hollow cylinder with the nine β apoproteins arranged radially outside. The Bchl*a*-B850 molecules form a continuous overlapping ring and are sandwiched between the α and β apoproteins. The Bchl*a*-B800 molecules are located in pockets between the β apoproteins. The carotenoids interact closely with both the Bchl*a*-B800 and -B850 molecules. [**Key** protein sub-units white, Bchl*a*-B800 green, Bchl*a*-B850 red and carotenoid yellow].

contains twenty-seven Bchl*a* molecules which are divided into two discrete pools. Eighteen molecules of Bchl*a* are sandwiched between the α and β apoproteins and form a continuous overlapping ring. The remaining nine Bchl*a* are located between the β apoproteins. Previously, CD studies had predicted that the Bchl*a*-B850 molecules were excitonically coupled (i.e. interacted with each other) whereas the Bchl*a*-B800 molecules were predicted to be monomeric (Cogdell & Scheer, 1985). On this basis, the overlapping ring of Bchl*a* molecules were identified as the Bchl*a*-B850 molecules and the peripherally located Bchl*a* molecules were identified as the Bchl*a*-B800 molecules. The Bchl*a*-B850 molecules are co-ordinated to a conserved histidine residue on either the α or β apoproteins. The Bchl*a*-B800 molecules are liganded to the N-terminal residue of the α apoprotein. In the original structure, this residue was thought to be a formyl-methionine (McDermott *et al.*, 1995). In subsequent higher resolution models, however, electron density previously attributed to a formyl group has been suggested to belong to an acetyl group instead (Steve Prince, personal communication). The bacteriochlorin rings of the Bchl*a*-B850 molecules are perpendicular to the membrane surface whereas those of the Bchl*a*-B800 molecules are parallel to it (see figure 1g). In the original crystal structure, nine carotenoid molecules were identified. The carotenoids span the membrane in an extended conformation and make van der Waals contact with both the Bchl*a*-B800 and -B850 molecules. The sugar headgroups of these carotenoid molecules are located at the cytoplasmic surface of the membrane. Further crystallisation studies using a different

Figure 1g Arrangement of the pigment molecules in the LH2 complex from *Rps. acidophila* 10050 as viewed parallel to the membrane surface. The relative orientations of the Q_y transition dipoles of the Bchl*a*-B800 and -B850 molecules are also shown. [**Key** Bchl*a*-B800 cyan, Bchl*a*-B850 green, carotenoid white, Q_y transition dipole - red/yellow bar].

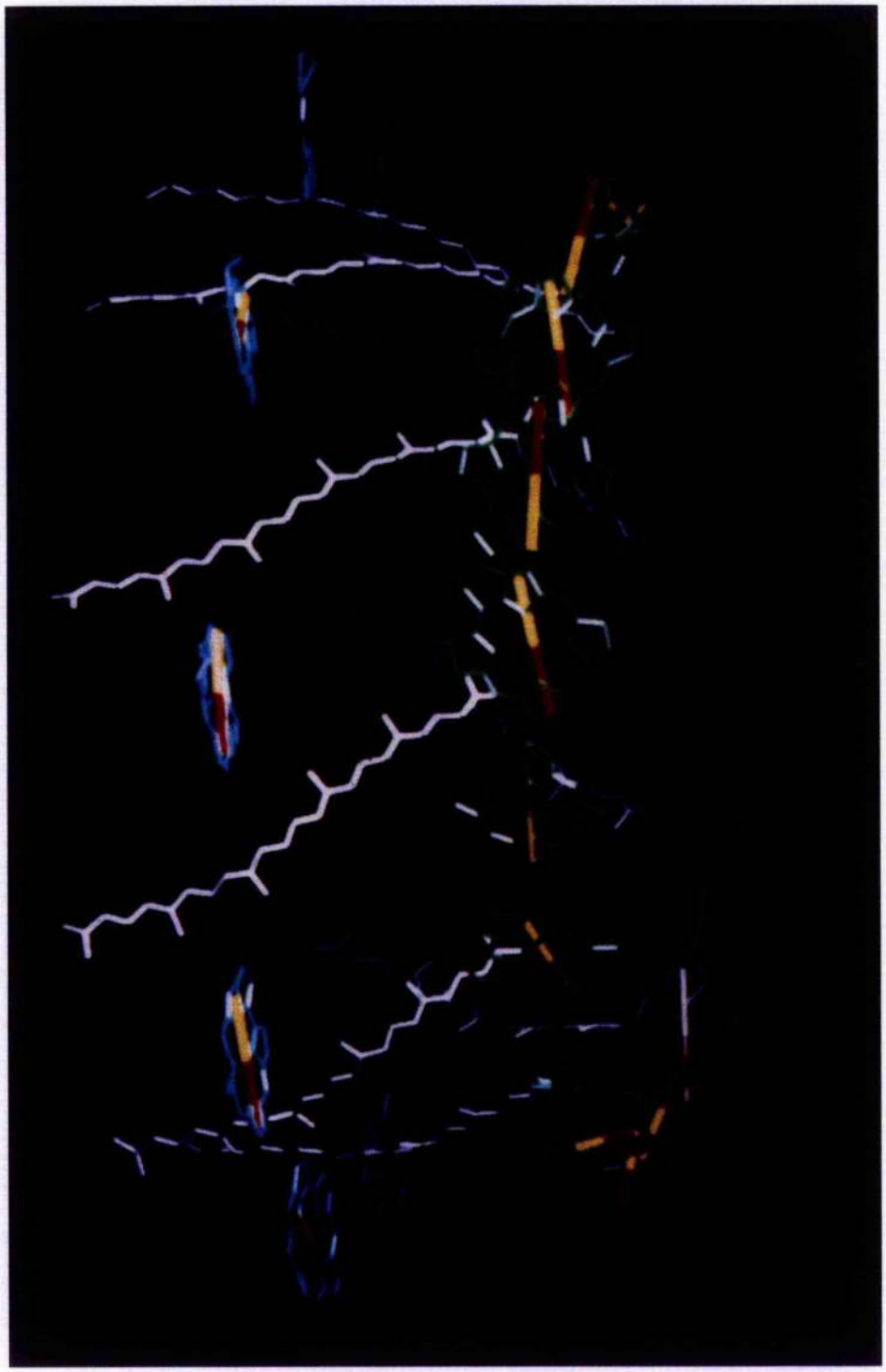

detergent resulted in the tentative identification of a further 9 carotenoid molecules (Freer *et al.*, 1996). Similar to the first pool of carotenoids, these molecules are thought to span the membrane in an extended conformation. The putative sugar head groups of these molecules, however, are thought to be located on the extra-cytoplasmic surface of the membrane.

Similar ring-like assemblies have also been observed in *Rs. molischianum* (Koepke *et al.*, 1996) and *Rv. sulfidophilum* (Savage *et al.*, 1996). The crystal structure of the LH2 complex from *Rs. molischianum* has been determined to a resolution of 2.4 Å. This structure is essentially the same as that for *Rps. acidophila* in that the Bchl*a*-B800 molecules occupy a peripheral binding pocket, the Bchl*a*-B850 molecules form an overlapping ring and that the carotenoid molecules span the complex interacting with both the Bchl*a*-B800 and -B850 molecules. The structure of the LH2 complex from *Rs. molischianum* differs from *Rps. acidophila* in that the complex is an octamer, the Bchl*a*-B800 molecules are liganded to an Asp residue at position 6 on the α apoprotein and the Bchl*a*-B800 molecules are tilted by 20° with respect to those in *Rps. acidophila*. The 2D structure of the LH2 complex from *Rv. sulfidophilum* has been determined to a resolution of 7Å by electron microscopy. This complex is a nonamer. From the projection maps, it was possible to allocate electron density to the α and β apoproteins and the pigment molecules. It is likely that all LH2 complexes have similar ring-like structures. More structural information is required, however, before the extent of variability in sub-unit oligomerization is fully appreciated.

1.6.5.2 Pigment-protein interactions in the LH2 complex from *Rps. acidophila* 10050

In this Section, the pigment-protein interactions in the LH2 complex of *Rps. acidophila* 10050 are described in more detail (for an extensive discussion see Prince *et al.*, 1997). In brief, all of the Bchl*a* molecules make two specific interactions with the protein. The primary contact between the Bchl*a* molecules and the protein is via its central Mg^{2+} ion. The Mg^{2+} ions of the Bchl*a*-B850 molecules are co-ordinated to conserved His residues on the α and β apoproteins whereas those of the Bchl*a*-B800 molecules are liganded to the N-terminal residue of the α apoprotein (see Section 1.5.5.1 for a more in-depth discussion). The C3 acetyl groups of both the Bchl*a*-B800 and -B850 molecules are hydrogen bonded. In contrast, the keto groups at position C13 on ring E of the Bchl*a* molecules are not. The Bchl*a*-B800, -B850 and carotenoid molecules interact extensively and form a large pigment ring which is enclosed by the apoproteins. This ring is only penetrated by one residue, βPhe22. βPhe22 is highly conserved and interacts with the ether oxygen atoms of the Bchl*a* phytol chains and with the methoxycarbonyl groups at position C13 of both the Bchl*a*-B850 molecules (Freer *et al.*, 1996). The remaining pigment-protein interactions which occur have van der Waal's character.

2.1 Introduction

In the LH2 complex, there are five discrete energy transfer events which occur. These are the B800→B800, B800→B850, B850→B850, carotenoid→B800 and carotenoid→B850 energy transfer processes. In this Chapter, the theoretical models which have been proposed to explain these energy transfer events are discussed (see Section 2.2). The kinetics of each energy transfer process are described (see Section 2.3). Finally, the use of modified pigments as a tool to probe the mechanisms of energy transfer within the RC and antenna complexes is detailed (see Section 2.4)

2.2 Mechanisms of excitation transfer

2.2.1 Introduction

In the LH2 complex, the mechanism by which excitation energy is transferred between donor and acceptor pigments primarily depends upon two factors - the spectral properties of the pigments involved and the strength of the interaction between them. As the distance between two molecules increases, the strength of the coupling between them decreases. Pigments which are separated by relatively long distances (> 20 Å) interact rather weakly. In this situation, energy transfer between donor and acceptor molecules can be thought of as occurring in discrete jumps. This type of energy transfer is well described by Förster's dipole-dipole, weak interaction mechanism (Förster, 1948). Molecules which are separated by short distances (<10 Å) are thought to be strongly coupled. In such a situation, the donor and acceptor pigments can be considered as an excitonically coupled super-

molecule. In such a scenario, energy transfer does not occur in discrete jumps. Rather, it occurs by relaxation of the excited state between the molecules. This type of energy transfer is described by exciton theory (Davydov, 1962). Thirdly, if the molecular orbitals of the donor and acceptor pigments overlap, energy transfer can occur by an electron exchange mechanism (Dexter, 1953).

In this Section, the Förster, exciton and Dexter theories of energy transfer are discussed.

2.2.2 Förster theory

Förster theory applies to energy transfer between donor and acceptor molecules which share a weak dipole-dipole interaction. The rate of energy transfer between donor (D) and acceptor (A) molecules, k_{DA}, can be expressed as

$$k_{DA} = \frac{R_O^6}{\tau_D \, R_{DA}^6}$$

where R_O^6 is the Förster radius , τ_D is the fluorescence lifetime of the donor excited state and R_{DA} is the distance between the chromophores. The Förster radius can be expressed as

$$R_o^6 = C \kappa^2 \eta^{-2} J$$

where C is a constant, κ is the geometric factor, η is the refractive index of the medium and J is the overlap integral between the fluorescence emission spectrum of the donor and the absorption spectrum of the acceptor

pigments. The geometric factor, κ, depends upon the mutual orientation of the donor and acceptor transition dipole moments and is described by the equation

$$\kappa = \cos\gamma - 3\cos\theta_1\cos\theta_2$$

where γ is the angle between the dipoles and θ_1 and θ_2 are the angles between the dipoles of the donor and acceptor pigments and the vector which connects them.

2.2.3 Exciton theory

If two pigment molecules are in close proximity (< 10 Å), the dipole-dipole interactions are so strong that the excited states of the donor and acceptor pigments become mixed. In this situation, the energy of interaction between the donor and the acceptor pigments is given by the formula :-

$$E_{DA} = \frac{C\,\mu_D\,\mu_A\,\kappa}{R^3}$$

where R is the distance between the donor and acceptor molecules, $\mu_D\,\mu_A$ are the transition dipole moments of the donor and acceptor pigments, κ is the geometric factor and C is a constant. According to exciton theory, the rate of energy transfer between the two molecules is proportional to their interaction energy. This is primarily influenced by the inverse cube of the molecular separation, R.

2.2.4 Dexter theory

If the donor and acceptor pigments are sufficiently close that their molecular orbitals overlap (< 5 Å), energy transfer can occur by an electron exchange mechanism (Dexter, 1953). In such a mechanism, the rate of energy transfer K_{DA} is given by

$$k_{DA} = K J \exp(-2R_{DA}/L)$$

where K is the specific orbital interactions between the donor and acceptor pigments, J is the spectral overlap function, R_{DA} is the D-A centre to centre separation and L is the sum of the van der Waals radii for the D-A pair. According to Dexter's theory, the rate of energy transfer is proportional to both the distance separating and the spectral overlap function between the donor and acceptor molecules. In contrast to Förster's theory, however, energy transfer from electronic states which are symmetry forbidden from the ground state can occur by Dexter's mechanism e.g. the carotenoid S_1 state.

2.3 The kinetics of energy transfer within LH2 complexes

2.3.1 Introduction

Historically, the bacteria which have been preferred for studying the energy transfer processes within the LH2 complex are *Rb. sphaeroides*. The popularity of *Rb. sphaeroides* is due to their ease of growth and to the available genetics systems which have been used to create a series of diverse, spectroscopically interesting complexes. Accurate interpretation of any

kinetic data, however, requires a high resolution crystal structure. At present, all LH2 complexes are thought to have ring-like structures. Between species, however, local differences in structure such as pigment-pigment distances and dipole-dipole orientations are known to occur. One consequence of local structural variation is that the time constants for analogous energy transfer processes in LH2 complexes from different bacteria differ slightly. For the same reason, caution must be exercised when spectroscopic data obtained in one type of bacteria is explained in terms of the absolute pigment geometry of a known LH2 structure from another species. The most desirable solution to these problems is to obtain kinetic data in a species of bacteria which has a known LH2 structure. For this reason, the LH2 complexes from *Rps. acidophila* 10050 and *Rs. molischianum* have been extensively studied by spectroscopists in recent years.

In this Section, the kinetics and mechanisms of energy transfer within the LH2 complex are described.

2.3.2 B800→B850 energy transfer

B800→B850 energy transfer has been extensively studied in *Rb. sphaeroides*. B800→B850 energy transfer was first correctly time resolved in a fs transient absorption study. The time constant of energy transfer at room temperature was found to be 0.7 ps (Shreve *et al.*, 1991b). This result has been confirmed in further transient absorption studies (Hess *et al.*, 1995; Monshouwer *et al.*, 1995; Kennis *et al.*, 1997; Pullerits *et al.*, 1997) and a rapid kinetic fluorescence

study (Jimenez *et al.*, 1996). In *Rps. acidophila* 10050, the time constant for B800 to B850 energy transfer is 0.9 ps (Kennis *et al.*, 1997; Ma *et al.*, 1997). In the LH2 complex from *Rps. acidophila* 10050, the centre-to-centre distances between each Bchl*a*-B800 molecule and its nearest -B850 molecules are 17.6 Å (α apoprotein associated) and 18.3 Å (β apoprotein associated) (McDermott *et al.*, 1995). In addition, the Bchl*a*-B800 Q_y transition dipole is well aligned with that of the closest α Bchl*a*-B850 molecule ($\kappa^2 = 0.61$) (Freer *et al.*, 1996). These observations suggest that B800→B850 energy transfer should be well described by Förster's weakly interacting, dipole-dipole mechanism of energy transfer (see Section 2.2.2).

The effect of spectral overlap on the rate of B800→B850 energy transfer has been investigated. The Q_y absorption band of the Bchl*a*-B850 molecules can be blue-shifted by mutation of a TyrTyr motif at positions 44 and 45 of the α apoprotein. Mutation of this motif to either PheTyr, TyrPhe or PheLeu gives "B850" Q_y absorption bands at 838, 838 and 826 nm respectively (Fowler *et al.*, 1992). The blue shift from 850 to 838 and then to 826 nm is due to the breakage of a hydrogen bond between the protein and the 3acetyl group of one of the Bchl*a*-B850 molecules (Fowler *et al.*, 1994). In these mutants, the rate of energy transfer increases with increasing spectral overlap (Hess *et al.*, 1994). In a complementary study, the rate of B800→B850 energy transfer was studied in a series of mutants in which their B800 Q_y absorption maximum was blue-shifted. In these mutants, the rate of B800→B850 energy transfer decreases as the separation between the Bchl*a*-B800 and -B850 Q_y absorption bands increases (Fowler *et al.*, 1997). In both

studies, it was concluded that the changes in the rates of energy transfer were in qualitative agreement with that predicted by Förster. Using this technique, however, it was not possible to conduct a more thorough investigation of the effect of spectral overlap on the rate of B800→B850 energy transfer. The reason for this is quite simple. Site-directed mutagenesis can only be used to change the environment of the protein so much. This meant that the changes in the wavelength of the Bchl*a*-B800 and -B850 Q_y absorption maxima were limited also.

At low temperatures, the Q_y absorption bands of the Bchl*a*-B800 and -B850 molecules sharpen. As a consequence, the spectral overlap between the pigments decreases. At 300, 77 and 4.2 K, the time constants of B800→B850 energy transfer in the LH2 complex from *Rb. sphaeroides* are 0.7, 1.2 and 1.5 ps respectively (Pullerits *et al.*, 1997). In this study, the measured kinetics were found to be significantly faster than that predicted in model calculations based solely upon simple Förster theory. Two possible explanations were given for this anomaly. Firstly, the Bchl*a*-B800 molecules transfer excitation energy into the upper exciton absorption component associated with the Bchl*a*-B850 molecules. This absorption component arises from the mixing of the excited states of the Bchl*a*-B850 molecules and is thought to be located in the same spectral region as the Bchl*a*-B800 Q_y absorption band (Sauer *et al.*, 1996). If this were true, the actual spectral overlap between the Bchl*a*-B800 and -B850 molecules would be greater than that which was predicted and would explain the observed discrepancy. Alternatively, the carotenoids were suggested to act as "molecular wires"

connecting the Bchla-B800 and -B850 molecules and, by some unknown mechanism, enhance the rate of B800→B850 energy transfer.

2.3.3 B800→B800 energy transfer

Local site variations in the interactions between the Bchl*a*-B800 molecules and the protein causes them to have slightly different energies. This phenomenon is known as inhomogenous broadening. Hopping between Bchl*a*-B800 molecules which have slightly different energies can be time-resolved in isotropic kinetic measurements by pumping the blue and probing the red side of the Bchl*a*-B800 Q_y absorption band (Sündstrom *et al.*, 1986). In addition, the transition dipole moments of the Bchl*a*-B800 molecules have different orientations in the LH2 complex. This means that B800→B800 energy transfer can be followed by time-resolved anisotropic measurements.

In 1984, a steady-state fluorescence polarisation study indicated that fast excitation transfer among the Bchl*a*-B800 molecules occurs (Kramer *et al.*, 1984). Subsequent fs pump-probe measurements have shown that the transient absorption anisotropy in the Q_y transition of the Bchl*a*-B800 molecules decays with a time constant of between 0.8 - 1.6 ps at room temperature. This was interpreted as energy transfer within their inhomogenously broadened Q_y absorption band (Hess *et al.*, 1993). In addition, a 300 fs decay component was observed in the isotropic kinetics (Hess *et al.*, 1993). This was suggested to be due to either vibrational relaxation of or excitation transfer among the Bchl*a*-B800 molecules. This

fast component was also observed at 77 K (Hess *et al.*, 1995). The possibility that this fast component was due to the vibrational motions of the Bchl*a*-B800 molecules themselves was investigated by studying the intramolecular relaxation processes of Bchl*a* molecules in solution at room temperature and in glasses at 77 K. The vibrational motions of the Bchl*a* molecules were significantly slower than the previously measured isotropic decay components. From this, it was concluded that the decay kinetics did actually reflect B800→B800 energy transfer (Hess *et al.*, 1995). Further direct evidence for B800→B800 energy transfer came from the observation that bleaching at the red edge of the Bchl*a*-B800 Q_y absorption band has a rise component of 400 fs after exciting at its blue-edge (Monshouwer & van Grondelle, 1996). In contrast to these studies, a three-pulse photon echo experiment by Fleming and co-workers suggested that no significant B800→B800 energy transfer takes place at room temperature (Joo *et al.*, 1996). In more recent work based on fluorescence up-conversion measurements and Förster calculations, however, Fleming's group concluded that B800→B800 energy transfer does occur and takes approximately 1 ps at room temperature (Jiminez *et al.*, 1996).

In *Rps. acidophila* 10050, the centre-to-centre distance between neighbouring Bchl*a*-B800 molecules is 21 Å (McDermott *et al.*, 1995). In addition, the Q_y transition dipoles of neighbouring Bchl*a*-B800 molecules are optimally aligned for energy transfer (κ^2= 1.54) (Freer *et al.*, 1996). These structural observations suggest that B800→B800 energy transfer is likely to occur by

Förster's mechanism. In addition, all of the kinetic data obtained thus far has been adequately modelled using Förster's theory.

2.3.4 B850 - an excitonically coupled ring

In the B850 ring, the edges of neighbouring tetrapyrolle rings essentially touch one another. Consequently, the ring can be viewed as a single supermolecule. Alternatively, at the other extreme, the ring can be viewed as nine sèparate dimers. Since the structure of the LH2 complex from *Rps. acidophila* 10050 has been determined, there have been several attempts to calculate its spectral properties from first principles (Sauer *et al.*, 1996; Alden *et al.*, 1997; Koolhaas *et al.*, 1997). In the calculations, the only way to get a good fit for both the absorption and circular dichroism spectra was to assume that the excited state was completely delocalized over the B850 ring. In contrast to this, transient absorption experiments which have looked at the energy transfer properties of the B850 ring have suggested that the excited state is more localised (Chachisvilis *et al.*, 1997; Pullerits *et al.*, 1996; Meier *et al.*, 1997). In this case, the best fits to the kinetic data suggest that the exciton has a coherence length of 4 ± 2 Bchl*a*. This means that the exciton is delocalized over approximately 4 Bchl*a* molecules. This model is supported by superradiance measurements in the LH2 complex from *Rb. sphaeroides* (Monshouwer *et al.*, 1997).

The actual delocalization length has important implications for the energy transfer mechanism which applies. If the exciton is delocalized over the entire ring, nearest neighbour energy transfer will occur via relaxation

between different excited states. As the coherence length decreases, energy transfer around the B850 ring will have a more Förster-like, "hopping" character.

2.3.5 Carotenoid→B850 energy transfer

2.3.5.1 The role of the carotenoid S_1 and S_2 excited states in singlet-singlet energy transfer

Carotenoids have two low-lying excited states which are involved in singlet-singlet energy transfer. The first excited singlet state is denoted S_1 and the second S_2. The ground state, S_0, and the S_1 state both possess A_g symmetry. In contrast, the S_2 state has B_u symmetry. One photon electronic transitions between the S_0 and S_1 states are symmetry forbidden whereas those between S_0 and S_2 are strongly allowed. The S_2 state has a typical lifetime of several hundred fs. For example, β-carotene has a S_2 lifetime of 150-250 fs (Shreve *et al.*, 1991a; Andersson *et al.*, 1995; MacPherson & Gillbro, 1998) and spheroidene 340fs (Shreve *et al.*, 1991b; Ricci *et al.*, 1996). This very short lifetime is due to rapid internal conversion from the S_2 to the S_1 states. In contrast, the S_1 state has a lifetime on the ps time-scale. For example, β-carotene has a S_1 lifetime of 10 ps (Wasielewski & Kispert, 1986), spheroidene of 10 ps (Kuki *et al.*, 1990; Frank *et al.*, 1993a), spheroidenone of 15 ps (Gillbro & Cogdell, 1989) and okenone 8 ps (Andersson *et al.*, 1996). As the lifetime of the S_1 state is significantly longer than that of the S_2 state, it has been traditionally thought that the S_1 state would be the primary carotenoid donor state. How much energy proceeds via the S_2 compared to

the S_1 state depends upon several different factors. These include i) the lifetimes of the S_2 and S_1 states ii) the extent of spectral overlap between the fluorescence emission spectrum of the S_2 and S_1 states and the absorption profiles of the Bchl*a*-B800 and -B850 molecules iii) the distance between the donor and acceptor molecules and iv) the orientation of the donor and acceptor transition dipole moments. Which carotenoid excited state participates as donor in the energy transfer process determines the mechanism of energy transfer which takes place. The S_2 state has a strong transition dipole. It is likely then that energy transfer from this state occurs by either a Förster-type (Förster, 1948) or a coulombic coupling (Nagae *et al.*, 1993) mechanism. In contrast, the S_1 state has a very small transition dipole moment. This means that energy transfer from this state is unlikely to occur by a dipole-dipole resonance mechanism. Rather, energy transfer from the S_1 state is thought to occur by either an electron exchange (Dexter, 1953) or a coulombic coupling mechanism (Nagae *et al.*, 1993).

2.3.5.2 The dynamics of carotenoid→Bchl*a* energy transfer

Accurate kinetic data concerning carotenoid to Bchl*a* energy transfer in LH2 complexes is rather limited. In LH2 complexes from *Rb. sphaeroides*, spheroidene transfers most of its excitation energy to the Bchl*a*-B850 molecules directly in 300-400 fs (Shreve *et al.*, 1991b). The remainder of the energy is transferred to the Bchl*a*-B850 molecules via the -B800 molecules in approximately 1 ps. The best fit of the dynamics data required energy transfer from both S_2 and S_1 to be considered. More recently, the

fluorescence lifetime of the S_2 state of spheroidene in the LH2 complex has been shown to be significantly shorter than that in organic solvents. This reduced lifetime shows that energy transfer occurs from the S_2 state in the LH2 complex (Ricci *et al.*, 1996). In the B800-830 complexes of *Chr. purpuratum* energy transfer occurs from both the S_2 and S_1 states of the carotenoid okenone to both the Bchl*a*-B800 and -B830 molecules (Andersson *et al.*, 1996).

2.3.5.3 Methods for exchange and reconstitution of carotenoids in LH2

The factors which affect the efficiency of carotenoid→Bchl*a* energy transfer in the LH2 complex can be systematically investigated as follows. Technologies have been developed which allow the carotenoid composition of certain LH2 complexes to be varied. The efficiency of carotenoid→B850 energy transfer in these complexes can then be determined from their action spectra. By comparing the efficiencies of energy transfer between complexes, it is possible to study the effects of varying certain properties of the carotenoid.

The carotenoid content of LH2 complexes can be manipulated either genetically or using reconstitution techniques. The genes for the carotenoid biosynthetic pathways from *Rb. capsulatus*, *Rb. sphaeroides* and *Erwinia (Er.) herbicola* have been cloned and sequenced (Armstrong *et al.*, 1989; Lang *et al.*, 1993; Hundle *et al.*, 1995). *Er. herbicola* can synthesise plant-type carotenoids including β-carotene, lycopene and zeaxanthin. Genetically

modified strains of *Rb. sphaeroides* which are capable of manufacturing and inserting these carotenoids into their antenna complexes have been created by splicing the carotenoid biosynthetic genes of *Er. Herbicola* into the host genome (Hunter *et al.*, 1994). For example, *Rb. sphaeroides* strain TC40 (pRERIA) produces a LH2 complex in which the major carotenoid is β-carotene.

Alternatively, the carotenoidless LH2 complex from *Rb. sphaeroides* strain R26.1 can be reconstituted biochemically *in vitro* (Davidson & Cogdell, 1981; Frank *et al.*, 1993b). This system has been used to study the effect of the length of the carotenoid conjugated system on the efficiency of carotenoid→ B850 energy transfer (Frank *et al.*, 1993; Desamero *et al.*, 1998).

2.4 The use of modified pigments to probe the photochemical reactions in RC and LH complexes

The photochemical reactions of the RC and LH complexes can be probed in an unique way using modified pigments. In this approach, techniques have been developed which allow the creation of complexes with altered spectroscopic properties by selective exchange of the native pigments with modified pigments. The various modified pigments and their properties are described in Section 2.4.1. In addition, the pigment-exchange strategies which exist for the RC, LH1 and LH2 complexes and the insights into function which have been gained from this approach are detailed in Sections 2.4.2-4.

2.4.1 Modified (bacterio)chlorin molecules

The structure of a Bchl*a* molecule is shown in figure 2a. The key features of this molecule are as follows. The central Mg^{2+} ion is surrounded by a tetrapyrrole ring. The Bchl*a* molecule has an acetyl group at position C3, a methoxycarbonyl group at position $C13^2$ and an esterifying alcohol at position $C17^4$. The bond between the C7 and C8 atoms is fully saturated. At each of these positions, the Bchl*a* molecules can be modified. A summary of possible modifications is recorded in table 2i. Bchl*a* can be demetalated to give Bph*e*. A variety of metal ions including Ni^{2-}, Zn^{2+}, Pd^{2+} and Cu^{2+} can then be incorporated into the Bph*e* ring. This modification can result in a drastic shortening of the fluorescence lifetime of the pigment. For example, the lifetime of Ni-Bph*e* is 1 ps compared to 3 ns for Mg-Bph*e* (Teuchner *et al.*, 1997). Consequently, Ni-Bph*e* has a very low fluorescence quantum yield and essentially quenches all of the excitation energy which it receives. Certain groups around the tetrapyrrole ring can also be modified. The acetyl group at position C3 can be replaced with either a vinyl or a hydroxyethyl group. These changes cause a blue-shift in the Q_y absorption maximum of the Bchl*a* molecule. The methoxycarbonyl group at position $C13^2$ can be removed as in pyro-Bchl*a* or replaced with a OH group as in 13^2OH Bchl*a*. The esterifying alcohol attached at position $C17^4$ can also be altered. In purple bacteria, there are two types of esterifying alcohol which occur naturally. In most strains of purple bacteria, including *Rb. sphaeroides*, the esterifying alcohol is a phytol. In *Rs. rubrum*, however, the esterifying

Figure 2a Chemical structure of a Bchl*a* molecule. Ellipses indicate those functional groups which can be modified (see table 2i)

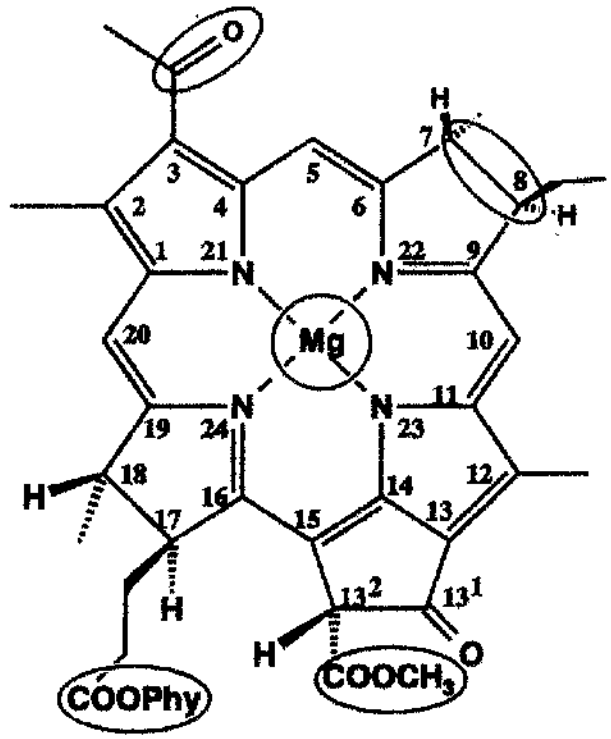

Table 2i The functional side groups of a range of modified (bacterio)chlorophyll molecules.

Pigment	Central ion	C17	$C13^2$	C3	C7/8
Bchl*a*	Mg^{2+}	p	$COOCH_3$/H	acetyl	dihydro
geranylgeraniol Bchl*a*	Mg^{2+}	gg	$COOCH_3$/H	acetyl	dihydro
13^2OH Bchl*a*	Mg^{2+}	p	$COOCH_3$/OH	acetyl	dihydro
pyro-Bchl*a*	Mg^{2+}	p	H/H	acetyl	dihydro
3^1vinyl Bchl*a*	Mg^{2+}	p	$COOCH_3$/H	vinyl	dihydro
3^1OH Bchl*a*	Mg^{2+}	p	$COOCH_3$/H	α-hydroxyethyl	dihydro
Chl*a*	Mg^{2+}	p	$COOCH_3$/H	vinyl	double bond
acetyl Chl*a*	Mg^{2+}	p	$COOCH_3$/H	acetyl	double bond
Zn-Bphe	Zn^{2+}	p	$COOCH_3$/H	acetyl	dihydro
Ni-Bphe	Ni^{2+}	p	$COOCH_3$/H	acetyl	dihydro
Cu-Bphe	Cu^{2+}	p	$COOCH_3$/H	acetyl	dihydro

alcohol is a geranylgeraniol. Shorter alcohol chains (e.g. ethyl) can also be attached.

The structure of Chl*a* is essentially the same as that of Bchl*a*. The primary difference between the two molecules is the type of bond between the C7 and C8 atoms on the tetrapyrrole ring. In Chl*a*, there is a double bond whereas in Bchl*a*, there is a single bond. In addition, Chl*a* has a vinyl group at position C3 whereas Bchl*a* has an acetyl group. These variations cause a dramatic blue-shift of the Q_y absorption maximum by 110 nm. The vinyl group at position C3 can be replaced with an acetyl group. This causes the Q_y absorption maximum to be red-shifted by approximately 20 nm.

2.4.2 Pigment-exchange expts. in RC

In the late 1980s, the group of Hugo Scheer developed a method for creating RCs with altered spectral properties by exchange of modified pigment molecules into both the $B_{A,B}$ and the $H_{A,B}$ sites (see review by Scheer & Hartwich, 1995). These complexes have been used to probe the photochemical reactions which occur in the RC. This Section describes the pigment-exchange strategy which was adopted by the Scheer group, the selectivity of the exchange process and some of the insights gained into RC function using this approach.

2.4.2.1 Pigment exchange protocol

The native pigments in either the $B_{A,B}$ or the $H_{A,B}$ sites can be completely exchanged with modified pigments by incubating RCs from the

carotenoidless mutant R26.1 of *Rb. sphaeroides* with a 20x fold excess of modified pigment at 42°C for 90 min. At this temperature, the RC proteins "breathe", allowing access of the modified pigments to the protein interior. Equilibration between the excess, exogenous pigments and the native ones results in a complete exchange. In addition, modified pigments can be selectively exchanged into either the B_A or the B_B sites by using the RC carotenoid as a physical barrier which prevents exchange at the B_B site. The reconstituted pigments have been shown to be correctly bound within the RC in an identical fashion to those in the native complex by circular dichroism (CD), linear dichroism (LD) (Meyer *et al.*, 1996), and ENDOR spectroscopies.

2.4.2.2 Selectivity of the exchange

Using this technique, a wide variety of modified (bacterio)chlorophyll and (bacterio)pheophytin molecules can be incorporated into the $B_{A,B}$ and $H_{A,B}$ sites of the RC respectively. The pigment modifications which are tolerated are as follows. The influence of the central metal ion is very distinct. Irrespective of the substituents at the periphery, whenever a pigment can undergo exchange, the presence of a metal ion in the tetrapyrrole ring directs the pigment to the $B_{A,B}$ sites. In its absence, the modified (B)phes bind in the $H_{A,B}$ sites. For example, both Zn-Bphe and Ni-Bphe can undergo exchange whereas Cu-Bphe can not (Hartwich *et al.*, 1994).

The ability of pigments modified around their tetrapyrrole ring to undergo reconstitution depends upon the particular modification which has been

made. For example, Bchl*a* molecules with either acetyl, vinyl or hydroxyethyl groups at position C3 can all bind in the monomeric Bchl*a* sites (Struck *et al.*, 1990a). Modifications at the $C13^2$ position other than hydroxylation, however, are not tolerated (Struck & Scheer, 1990b). Phytol, geranylgeraniol and various short chain aliphatic alcohols at position $C17^4$ are all tolerated. Neither Chl*a* nor acetyl Chl*a* undergo exchange. In contrast, the $H_{A,B}$ sites accommodate both modified bacteriopheophytin and pheophytin molecules (Meyer & Scheer, 1995).

2.4.2.3 Insights into RC function

To illustrate the usefulness of this approach in understanding the photochemical reactions which occur in the RC, a number of examples are given.

In RCs containing 3^1vinyl, 13^2OH Bchl*a* in either their B_A or B_B sites the wavelength of maximum absorption of the Q_y absorption band of the other accessory molecule was assigned (Hartwich *et al.*, 1995a). Similarly, in RCs fully exchanged with 3^1vinyl, 13^2OH Bchl*a*, the wavelength of maximum absorption of the upper exciton component of the primary donor P^+ was determined (Hartwich *et al.*, 1995a).

Incorporation of Ni-Bph*e* into the $B_{A,B}$ sites prevents energy transfer between the $H_{A,B}$ molecules and the primary donor. This shows that excitation energy absorbed by the Bph*e* molecules in the native complex is transferred to P via $B_{A,B}$. (Hartwich *et al.*, 1995b).

In RCs containing 3^1vinyl,13^2OH Bchl*a* the carotenoid triplet state was shown to interact with the B_B pigment by microwave induced absorption (MIA) (Hartwich *et al.*, 1995a). In addition, the transfer of triplet energy from the primary donor to the carotenoid in RCs containing modified pigments in the $B_{A,B}$ sites is strongly dependent upon the triplet state energy of the accessory B_B molecule (Frank *et al.*, 1996). Together, these results show that B_B is a real intermediate in the transfer of triplet energy from P to the carotenoid.

Finally, in RC fully exchanged with 3^1vinyl, 13^2OH Bchl*a* in its $B_{A,B}$ sites, the rate of electron transfer from P to H_A is ten times slower than that in the native complex (Finkele *et al.*, 1992). This shows that B_A is a real electron transfer intermediate between P and H_A.

2.4.3 LH1 reconstitution experiments

The group of Paul Loach have developed a reconstitution technique which allows the reversible dissociation of the LH1 complex into its constituent polypeptides and pigments. In this Section, the strategy adopted by Loach is described. In addition, the usefulness of this technique to create modified LH1 complexes is discussed.

2.4.3.1 The reversible dissociation of LH1 into its constituent parts.

The LH1 complex can be dissociated into structural sub-units using a suitable detergent. This has been demonstrated in several different types of

purple bacteria including *Rs. rubrum* (Parkes-Loach *et al.*, 1988, Loach *et al.*, 1994), *Rb. sphaeroides* (Loach *et al.*, 1994), *Rb. capsulatus* (Loach *et al.*, 1994), *Rps. viridis* (Parkes-Loach *et al.*, 1994) and *Rps. marina* (Meckenstock *et al.*, 1992a). These structural sub-units are smaller in size than the native LH1 complex and their Bchl*a* Q_y absorption maximum is blue-shifted relative to that in the LH1 complex. Upon further addition of detergent, the sub-units can be dissociated into its constituent polypeptides and Bchl*a*. By later decreasing the concentration of detergent, sub-unit and LH1-type complexes consisting of α and β apoproteins and Bchl*a* can be formed (Parkes-Loach *et al.*, 1988; Heller & Loach, 1990; Chang, 1990). Since then, it has been shown that sub-unit and LH1-type complexes can be reconstituted from separately isolated polypeptides and Bchl*a*. The ability to reconstitute the LH1 complex from its individual component is a uniquely powerful tool for evaluating structural relationships within the complex (Parkes-Loach *et al.*, 1990; Loach *et al.*, 1994). The requirements for sub-unit and LH1 formation have been probed using both modified polypeptides and (bacterio)chlorin molecules. The α and β polypeptides can be modified in one of three ways. Firstly, charged amino acids can be chemically modified (e.g. Lys residues can be acetylated and the carboxyl groups of Asp and Glu residues can be esterified) (Heller, 1992). Secondly, polypeptides can be truncated using proteolytic enzymes (Meadows *et al.*, 1995). Thirdly, small polypeptides can be synthesised *in vitro* which allows amino acids and even atoms on amino acids to be changed (Meadows *et al.*, 1998; Kehoe *et al.*, 1998).

Using the reconstitution assay, the abilities of several modified (bacterio)chlorin molecules to form sub-unit and LH1-type complexes with the α and β polypeptides from *Rs. rubrum* and *Rb. sphaeroides* have been determined (Parkes-Loach *et al.*, 1990; Davis *et al.*, 1996). Pigments which lack a central metal ion are unable to form either sub-unit or LH1-type complexes. Sub-unit and LH1-type complexes can be formed with both Zn-Bph*e* and Ni-Bph*e*. Pigments modified around their tetrapyrrole ring have a varied ability to undergo reconstitution. Using 3^1vinyl Bchl*a*, a sub-unit type complex can be formed in *Rs. rubrum* but not in *Rb. sphaeroides*. LH1-type complexes can not formed in either species. Using 13^2OH Bchl*a*, both sub-unit and LH1 complexes can be formed with polypeptides from *Rb. sphaeroides* but not from *Rs. rubrum*. Changing the esterifying alcohol at position $C17^4$ does not affect either sub-unit or LH1 complex formation. Bchl*b* can be successfully reconstituted whereas Chl*a* and acetyl Chl*a* can not. This shows that the bacteriochlorin ring structure is an absolute requirement for reconstitution.

By modifying this technique, it was possible to form LH1 complexes containing carotenoid molecules (Davis *et al.*, 1995). In *Rs. rubrum* , the carotenoids spirilloxanthin (the native carotenoid of *Rs. rubrum*) and spheroidene (the native carotenoid of *Rb. sphaeroides*) can both be successfully reconstituted. The reconstituted carotenoids can efficiently transfer excitation energy to the B875 molecules and protect the Bchl*a* molecules against photo-oxidation.

2.4.4 Reconstitution experiments with LH2 complexes

At present, techniques which allow the creation of spectrally modified LH2 complexes are rather limited. Existing work has focused upon the reversible binding of the Bchl*a*-B800 molecules in the complex. In 1981, it was shown that the 800 nm absorption peak can be attenuated by treating the LH2 complex with lithium dodecyl sulphate (LDS) (Clayton & Clayton, 1981). On dialysis of this complex into buffer containing LDAO, the absorption peak was re-instated. Originally, this effect was interpreted as the reversible binding of the Bchl*a*-B800 molecules to the complex. It was later shown that the absorption changes are actually due to changes in the conformation of the protein (Chadwick *et al.*, 1987; Robert, 1988b). Recently, a method which allows the reversible binding of the Bchl*a*-B800 molecules in the LH2 complex from *Rb. sphaeroides* has been reported (Bandilla *et al.*, 1998). In this approach, the Bchl*a*-B800 molecules can be released from their binding pockets by an acid treatment using buffer containing the novel Triton detergent TBG10. B850-only complexes can then be purified by ion-exchange chromatography. The B800 sites can later be reconstituted with a limited number of modified pigments including Bchl*a* (an estimated occupancy of 50%), 3^{1}OH Bchl*a* (50%), 3^{1}vinyl Bchl*a* (7%) and acetyl Chl*a* (7%).

In my work, the approach of Bandilla *et al.* has been adopted and optimised for complexes from *Rps. acidophila* 10050. The modified LH2 complexes have been analysed using both steady-state and rapid kinetic spectroscopic techniques. The insights gained into the mechanisms of energy transfer within the LH2 complex are discussed.

Materials & Methods

3.1 Cell culture

All cultures were maintained in agar stabs at room temperature. Bacterial stocks were kept in 30% glycerol at -70°C. Liquid cultures of *Rps. acidophila* strain 10050 were grown anaerobically at 30°C in Pfenning's medium (Pfenning, 1969) and illuminated with light of intensity 40 W cm^{-2}.

Initial liquid cultures were prepared by the addition of Pfenning's medium to the cells stored in agar. After 2-3 days growth, these cells were used to inoculate a 100 ml flat sided bottle of the same medium. After 2 days growth, these cells were used to inoculate several 500 ml flat sided bottles. Finally, a 10 litre flask was inoculated using several of the 500 ml cultures. *Rs. rubrum* and the carotenoidless *Rb. sphaeroides* strain R26.1 were grown on media using succinate as the sole carbon source (Bose, 1963). The bottles containing R26.1 were wrapped in foil overnight before they were exposed to the light. During this period, the bacteria respired away any remaining oxygen. This ensured that when the bacteria were exposed to the light, the growth conditions were completely anaerobic.

3.2 Isolation and storage of the bacterial whole cells

Cells in the stationary phase of their growth curve were harvested by centrifugation at 2500 x g in a Mistral 6000 Coolspin centrifuge for 20 minutes at 4°C. Pelleted cells were resuspended in 20 mM Tris-HCl pH 8.0. Whole cells were stored at -20°C and used on a "needs" basis.

3.3 Purification of LH2 complexes from *Rps. acidophila* 10050

3.3.1 Introduction

Before purification was possible, it was first necessary to rupture the whole cells. The membranes were then solubilised with LDAO. After solubilisation, LH2 complexes were purified in a 2 step procedure. This consisted of a sucrose gradient step followed by gel filtration chromatography. The purity of an LH2 containing sample was determined by measuring the ratio of the absorbance at 859 nm (i.e. that which was specifically due to the LH2 complexes) to the absorbance by the aromatic amino acids at 270 nm (i.e. that attributable to all proteins). All samples with an A_{859}:A_{270} ratio > 3 were "pure". The individual steps are now described in greater detail.

3.3.2 Membrane isolation

A small amount of both DNase and magnesium chloride were added to the resuspended cells, before they were homogenised. Membranes were then isolated by rupturing the whole cells in a French press at a pressure of 15000 psi.

3.3.3 Membrane solubilisation

The membranes were diluted with 20 mM Tris-HCl pH 8.0 such that they had an OD_{859} of 75 cm^{-1}. Solubilisation was achieved by adding 2% (v/v) LDAO and stirring the sample at 4°C for 4 h. After solubilisation was complete, the sample was centrifuged at 10,500 x g in a Sigma 3K20 bench

top centrifuge for 10 min at 4°C. The supernatant, which contains solubilised proteins, was removed and kept for future purification. The pellet, which contains unsolubilised material, was discarded.

3.3.4 Sucrose gradient

A sucrose gradient consisting of 4 discrete sucrose concentrations was prepared by slowly layering equal volumes of 0.8, 0.6, 0.4 and 0.2 M sucrose solution in 20 mM Tris-HCl pH 8.0, 0.2% (v/v) LDAO into polycarbonate centrifuge tubes. Approximately 5 ml of solubilised membranes were layered on top of each sucrose gradient. The sucrose gradients were spun in either a Sorvall OTD 65B or a Beckman 27-55 ultracentrifuge at 150,000 x g for 16 h overnight. After centrifugation was complete, the sucrose gradients had two discrete bands. The upper band contains LH2 complexes whereas the lower band contains LH1-RC complexes. The LH2 containing band was removed with a pasteur pipette.

3.3.5 Gel filtration chromatography

The LH2 complexes were further purified by gel filtration chromatography using a Superdex 200 column. This technique allows proteins to be separated according to their native molecular weight. The Superdex 200 column was equilibrated in 20 mM Tris-HCl pH 8.0, 0.2% (v/v) LDAO overnight. The LH2 sample was concentrated under nitrogen using an Amicon ultrafiltration stirred cell before it was passed through a 22 μm nylon filter. 2 ml aliquots were then injected onto the column. The proteins were separated by pumping the column with 20 mM Tris-HCl pH 8.0, 0.2%

(v/v) LDAO at a flow rate of 0.75 ml/min. As the LH2 complexes emerged from the column, 1 ml fractions were collected. Those fractions with an A_{859} : A_{280} ratio greater than 3 were retained for future experiments. The purified sample was stored in a freezer at -20°C unless it was going to be used immediately.

3.4 Purification of the detergent TBG10

The novel Triton detergent TBG10 was bought from the industrial chemical firm Surfachem. As supplied, TBG10 is very viscous and is unusable with any biological sample. Before it was used in the experiments described in this thesis, TBG10 was first purified (Hugo Scheer, personal communication). TBG10 was diluted 10 fold with distilled water. The detergent solution was treated with the anion exchange chromatography media DE52. After stirring for 4 h, the "dirty" DE52 material was removed by filtration using a Buchner funnel. This process was repeated four times. During purification, some of the detergent molecules were removed along with the impurities. It was essential that the concentration of the purified detergent was the same between batches. This was achieved by defining a detergent solution with an A_{262} of 3 to have a concentration of 10%.

3.5 Pigment purification and handling techniques

To prevent photo-oxidation of the pigments, they were always handled in the dark.

3.5.1 Purification of Bchl*a*

Bchl*a* was purified from whole cells of the carotenoidless *Rb. sphaeroides* strain R26.1. Cells were harvested as previously described (see Section 3.2). The pigments were extracted by incubation with an acetone/methanol 7 : 2 (v/v) mixture for 30 min. Particulate matter was removed by centrifugation at 10,500 x g in a Sigma 3K20 bench top centrifuge for 10 min. The supernatant containing the pigments was retained whereas the pellet was discarded. The pigment extract was then mixed with a small volume of light petroleum ether (40-60°C). Phase separation was achieved by adding approximately 50 ml of 1 M NaCl. The upper, non-polar layer containing the pigments was retained. Residual water was removed from the pigment sample by saturating it with NaCl salt. After 15 min, the extract was filtered through a glass funnel containing cotton wool. The pigments were then dried down using a rotary evaporator. Bchl*a* was purified by column chromatography using Sepharose CL6B as the adsorbant. The Sepharose CL6B column was equilibrated using a hexane/isopropanol 19 : 1 (v/v) mixture. The pigment extract was redissolved in the equilibration buffer and was loaded onto the column. The column was washed with several different hexane/isopropanol mixtures containing a progressively greater proportion of isopropanol (i.e. 19:1, 18:2, 17:3 etc). At 10% isopropanol, bacteriopheophytin was eluted from the column. At 25% isopropanol, Bchl*a* was eluted from the column. The Bchl*a* was collected, dried down using a rotary evaporator and stored at -20 °C. Bchl*a* oxidation products were later removed from the column by washing with methanol. The column material was recovered and stored in acetone between usages.

3.5.2 Purification of geranylgeraniol Bchl*a*

Geranylgeraniol Bchl*a* was purified from whole cells of *R. rubrum* S1 using the same protocol as that for Bchl*a*. Purification of geranylgeraniol Bchl*a* is slightly more complicated than that for Bchl*a* as incubation of the whole cells with acetone/methanol 7 : 2 (v/v) results in extraction of both carotenoid and Bchl*a* molecules. The carotenoids did not bind to the Sepharose CL6B column, however, and were easily removed by washing the column with several column volumes of hexane/isopropanol 19 : 1 (v/v).

3.5.3 Modified pigments

All modified bacteriochlorophyll and chlorophyll molecules were kindly supplied by Ingrid Katheder and Hugo Scheer from the Botanisches-Institut der Universität München. Chl*a* was purified from spinach as described in (Omata & Murata, 1983). 13^2OH Bchl*a*, 3^1vinyl Bchl*a*, 3^1OH Bchl*a*, pyro-Bchl*a*, acetyl Chl*a*, Zn-Bph*e*, Ni-Bph*e* and Cu-Bph*e* were all prepared as described by Scheer & Struck (1993).

3.5.4 Qualitative analysis of the Bchl*a* and Chl*a* pigments

The purities of all pigments were checked by thin layer chromatography (TLC) before reconstitution experiments were performed. The purities of the Zn-Bph*e*, Ni-Bph*e* and Cu-Bph*e* were checked as follows. The pigment of interest was redissolved in diethylether. Aliquots were then spotted onto a silica TLC plate. The plates were developed using a 90% toluene, 5% acetone, 4% methanol and 1% isopropanol (v/v) solvent mixture. Under

these conditions, both bacteriochlorin epimers are observed. Pigments which gave rise to two narrowly separated bands were pure. The purities of all the other (bacterio)chlorin molecules were checked by spotting aliquots of the redissolved pigments onto a reverse-phase TLC plate. These plates were developed using methanol. Pigments which gave rise to a single band were pure.

3.5.5 Purification of rhodopin glucoside

Rhodopin glucoside was purified from whole cells of *Rps. acidophila* strain 10050 (Juan Arellano, personal communication). Cells were harvested as previously described (see Section 3.2) and the carotenoids extracted by incubation with an acetone/methanol 7 : 2 (v/v) mixture for 30 min. Particulate matter was removed by centrifugation at 10,500 x g in a Sigma 3K20 bench top centrifuge for 10 min. The supernatant containing the carotenoids was retained. The carotenoids were transferred to light petroleum ether (40-60°C) before they were dried down in a rotary evaporator as described in 3.5.1. Rhodopin glucoside was purified from the other carotenoids by stepwise elution silicagel column chromatography. The pigment extract was redissolved in a diethylether/dichloromethane 9 : 1 (v/v) mixture and loaded onto a silicagel column equilibrated with the same solvent mixture. The column was washed with several column volumes of diethylether/dichloromethane 9 : 1 (v/v). This resulted in the elution of the non-polar carotenoids from the column. The column was then washed with a diethylether/dichloromethane 9 : 1 (v/v) mixture containing an increasing % of ethanol (1,2....5%). As the % ethanol was

increased, the polar carotenoids were eluted from the column. Rhodopin glucoside was eluted from the column using 5% ethanol. Fractions were collected and their purity checked by recording their absorption spectra. The pure fractions were pooled, dried down using a rotary evaporator and stored at -20°C.

3.5.6 Determination of the pigment extinction coefficients

The extinction coefficient of the Q_y transition of Bchl*a* in methanol is 42 mM^{-1} cm^{-1} (Clayton, 1966). The extinction coefficients of Bchl*a* in hexane and isopropanol were determined as follows. Bchl*a* was re-dissolved in a small volume of diethylether. 10 µl aliquots were then transferred to a series of small glass vials before they were dried down using nitrogen. The aliquots were then redissolved in 1 ml of either methanol, isopropanol or a hexane / isopropanol 9 : 1 (v/v) mixture. The maximum absorption values of the Q_y transition of Bchl*a* in each of the solvents were noted. These measurements were repeated a further four times. The extinction coefficients of Bchl*a* in isopropanol and hexane relative to that in methanol were determined by comparing the absorption of Bchl*a* in isopropanol and hexane with that in methanol. The extinction coefficients of the modified pigments relative to that of Bchl*a* were taken from the literature (Bandilla *et al.*, 1988) (see table 3i).

Table 3i The extinction coefficients of the Q_y transitions of modified pigments relative to that of Bchl*a* (Bandilla *et al.*, 1998).

Pigment	$\varepsilon_{relative}$
Bchl*a*	1.00
geranylgeraniol Bchl*a*	1.00
13^2OH Bchl*a*	1.00
pyro-Bchl*a*	1.00
3^1vinyl Bchl*a*	0.75
3^1OH Bchl*a*	0.60
3acetyl Chl*a*	0.82
Chl*a*	0.94
Zn-Bph*e*	0.82
Ni-Bph*e*	0.70

The extinction coefficient of rhodopin glucoside in methanol is 150 mM^{-1} cm^{-1} (Davies, 1965). The extinction coefficients of rhodopin glucoside in isopropanol and hexane were determined using a similar approach to that for Bchl*a*.

3.6 Determination of the Bchl*a* concentration of a LH2 sample

20 µl of an LH2 containing sample were added to 980 µl of an acetone /methanol 7 : 2 (v/v) mixture in a plastic eppendorf. The eppendorf was spun in a bench top microfuge for 2 min. The A_{772} of the extracted sample was then measured and its Bchl*a* concentration calculated according to the Beer-Lambert law. The ε_{772} value of Bchl*a* in acetone/methanol 7 : 2 (v/v) is 76 mM^{-1} cm^{-1}. The concentration of LH2 complexes could then be calculated by dividing the Bchl*a* concentration by 27 (the number of Bchl*a* molecules / LH2 complex (McDermott *et al.*, 1995)).

4.1 Optimisation of the conditions for release of the Bchl*a*-B800 molecules

4.1.1 Introduction

The conditions for release of the Bchl*a*-B800 molecules from their binding pockets were optimised with respect to protein concentration, the pH and temperature of incubation and the choice of detergent. For each set of conditions, the pigment release reaction was started by reducing the pH of the solution to below 5.5 with acetic acid. At regular time intervals, the absorption spectrum of the sample was recorded. With time, the absorption peak at 800 nm (corresponding to bound Bchl*a*-B800) decreased and the absorption peak at 770 nm (corresponding to free Bchl*a*) increased. Once the A_{800} had reached its minimum value, the reaction was said to be complete. From this, the length of time which was necessary for complete release of the Bchl*a*-B800 molecules was determined. A graph of A_{800} v time was also plotted. The initial rate of reaction was given by measuring the tangent to this curve at time t=0.

4.1.2 Effects of protein concentration, the pH and temperature of incubation and the choice of detergent on Bchl*a*-B800 release

Protein concentration For each set of conditions, 1 ml of purified LH2 was added to 9 ml of 20 mM Tris-HCl pH 8.0, 1% (v/v) TBG10 such that the diluted sample had the desired protein concentration. The pH of the incubation mixture was reduced to pH 5.3 with acetic acid. On doing this, the solution turned cloudy. By gradually adding TBG10, however, the

solution became clear again. The length of time necessary for complete release of the Bchl*a*-B800 molecules was determined as described in Section 4.1.1.

pH of incubation At each different pH of incubation, the release of the Bchl*a*-B800 molecules was investigated as described in Section 4.1.1. The concentration of LH2 complexes in each incubation mixture was 0.7 μM. All reactions were performed at room temperature.

Temperature of incubation At each different temperature of incubation, the kinetics of Bchl*a*-B800 release were investigated as outlined in Section 4.1.1. The samples all had a LH2 concentration of 0.7 μM. The reaction cocktails were incubated at a pH of 4.75.

Effect of choice of detergent 1 ml of a LH2 sample in 20 mM Tris-HCl pH 8.0, 0.1% (v/v) LDAO with a concentration of 7.4 μM was added to 9 ml of 20 mM Tris HCl pH 8.0 containing the detergent of interest. The % concentration of the various detergents used were 0.05 % (v/v) Triton X100, 1 % (w/v) βOG, 0.1 % (w/v) LM, 0.5 % (w/v) Chaps and 0.05 % (w/v) Brij 98. The reaction was started by reducing the pH of the incubation mixture to 4.75 with acetic acid. The release reaction was characterised as described in Section 4.1.1.

4.2 The time course of the reconstitution reaction

The reconstitution reaction was followed by determining the occupancy of the B800 site every 10 s during a 2 h period. At each time point, the occupancy of the B800 site was determined by measuring the fluorescence

emission from the Bchl*a*-B850 molecules after exciting the incubation mixture at 800 nm. Both the Bchl*a* molecules in the B800 binding pockets and those in solution were able to absorb the excitation light. Only those Bchl*a* molecules which were properly bound within the complex, however, were able to transfer the excitation energy to the Bchl*a*-B850 molecules. The yield of fluorescence from the Bchl*a*-B850 molecules was, therefore, an indirect measure of the amount of Bchl*a* correctly bound within the B800 binding sites. The reconstitution cocktail contained purified B850-only complexes with a Bchl*a* concentration of 0.5 μM (this is equivalent to a B850-only sample with an A_{859} of 0.1 cm^{-1}) and a 3 fold excess of Bchl*a*. The reconstitution reaction was started by adjusting the pH to 8 with KOH. The excitation and emission wavelengths were 800 and 875 nm respectively. The excitation and emission slit widths were both 10 nm.

4.3 Optimising the conditions for the reconstitution reaction

4.3.1 Introduction

The effects of the concentration of exogenous Bchl*a* in the reaction mixture, the temperature of incubation and the choice of detergent on the occupancy of the B800 sites in the reconstituted complexes was investigated (see Section 6.5). The % occupancy of the B800 sites in each of the reconstituted complexes was determined from its absorption spectrum as follows. The A_{800}/A_{859} ratios in the LH2 and B850-only complexes were measured. The difference between these two ratios was defined as 100 % occupancy of the B800 sites. For each reconstituted complex, the A_{800}/A_{859} ratio was measured.

From this, the ratio in the B850-only complex was subtracted. This value was then expressed as a % occupancy relative to the defined maximum.

4.3.2 The effect of the Bchl*a* concentration, the temperature of incubation and the choice of detergent on the occupancy of the B800 sites in the reconstituted complexes

Concentration of exogenous Bchl*a* in the reaction cocktail For each concentration of exogenous Bchl*a*, a reconstitution reaction was performed, the sample purified and the % occupancy of the B800 sites determined. The method used is outlined below. The B850-only complexes were diluted with 20 mM potassium phosphate pH 4.75, 0.1% (w/v) LM such that they had a Bchl*a* concentration of 9 μM. Bchl*a* was re-suspended in methanol and its concentration determined. An aliquout of the Bchl*a* solution was then added to 10 ml of the B850-only sample. The reaction was started by adjusting the pH of the solution to 8 with KOH. The sample was gently shaken on a Luckham R100TW Rotatest shaker for 2 h at room temperature. After incubation was complete, the reconstituted complexes were purified by ion-exchange column chromatography. The incubation mixture was loaded onto a DE52 column equilibrated in 20 mM Tris-HCl pH 8.0. The excess, unbound Bchl*a* was removed by washing the column with 20 mM Tris-HCl pH 8.0, 0.05 % (w/v) LM. The reconstituted complexes were eluted with 300 mM NaCl in 20 mM Tris-HCl pH 8.0, 0.05 % (w/v) LM. The % occupancy of the B800 sites was then determined as described in Section 4.3.1.

Temperature of incubation The effect of temperature of incubation on the % occupancy of the B800 sites was determined as follows. B850-only samples with a Bchl*a* concentration of 9 μM were incubated with either a 3 fold excess or no exogenous Bchl*a* at 30°C for 2 h. After this period, the reconstituted complexes were purified as previously described. The % occupancy of the B800 sites in both complexes was determined as described in Section 4.3.1.

Choice of detergent The effect of choice of detergent on the % occupancy of the B800 sites was investigated as follows. 1 ml of B850-only complexes with a Bchl*a* concentration of 0.09 mM was added to 9 ml of 20 mM potassium phosphate pH 4.75 containing either 0.1 % (w/v) LM, 1 % (w/v) βOG or 0.05 % (v/v) Triton X100. A 3-fold excess of Bchl*a* was added to each sample, and a reconstitution reaction performed. The % occupancy of the B800 sites in each reconstituted complex was determined as described in Section 4.3.1.

4.4 Protocol for pigment exchange

Pigment removal Purified LH2 was loaded onto a DE52 ion exchange column in 20 mM Tris-HCl pH 8.0. Detergent exchange was performed in a two step procedure. LDAO was removed by washing with 5 column volumes of 20 mM Tris-HCl pH 8.0. The sample was then washed with 5 column volumes of 20 mM Tris-HCl pH 8.0, 1% (v/v) TBG10. The sample was eluted from the column using 300 mM NaCl in 100 mM sodium acetate pH 4.75, 1% (v/v) TBG10. The LH2 complexes were diluted with 100 mM

sodium acetate pH 4.75, 1% (v/v) TBG10 such that they had a Bchl*a* concentration of 0.02 mM (this is equivalent to a protein concentration of 0.74 μM). TBG10 was added until the protein solution became clear. The Bchl*a*-B800 molecules were released from their binding pockets by incubation in a water bath at 30°C for 1 h. The sample was then loaded onto a phosphocellulose column, which had been equilibrated with 20 mM potassium phosphate pH 4.75. The "free" Bchl*a* molecules were removed by washing the column with 20 mM potassium phosphate 4.75, 1% (v/v) TBG10. The absorption spectra of the eluant was recorded at regular time intervals. The column was washed until the eluant had an A_{770} <0.01. At this point, it was decided that the majority of all of the "free" Bchl*a* molecules had been removed. The B850-only complexes were exchanged into the detergent dodecyl maltoside (LM) on the column. TBG10 was removed by washing with 5 column volumes of 20 mM potassium phosphate pH 4.75. The column was then washed with 20 mM potassium phosphate pH 4.75, 0.1% (w/v) LM until the eluant had an A_{770}< 0.01 cm^{-1}. Finally, the B850-only complexes were eluted with 500 mM potassium phosphate pH 4.75, 0.1% (w/v) LM. Ultra-pure B850 complexes were made by applying a concentrated B850-only sample to a Sephadex 200 column which had been equilibrated in 500 mM potassium phosphate pH 4.75, 0.1% (w/v) LM. The B850-only complexes came off first from the column. Any residual, "free" Bchl*a* emerged later. 1 ml fractions were collected, their absorption spectra checked and the best fractions pooled. Samples were stored at 4°C, prior to use in reconstitution experiments.

Reconstitution of the B800 site The Bchl*a* concentration of the B850-only sample was measured as described in Section 3.6. The B850-only complexes were diluted with 20 mM potassium phosphate pH 4.75, 0.1% (w/v) LM such that they had a Bchl*a* concentration of 9 µM. The pigment which was to be reconstituted was resuspended in methanol and its concentration determined. An appropriate volume of the resuspended pigment was added to the B850-only sample such that its concentration was 15 µM (this concentration was 3x greater than that which was required to fill all of the available binding sites). The pH of the reconstitution cocktail was adjusted to 8 with KOH. The sample was shaken gently for 2 h at room temperature on a Luckham R100TW Rotatest shaker. After incubation, the sample was concentrated in an Amicon ultrafiltration stirred cell under nitrogen. The concentrated sample was then loaded onto a Sephadex 200 column which had been equilibrated in 500 mM NaCl in 20 mM Tris-HCl pH 8.0, 0.05% (w/v) LM. The reconstituted sample and the excess, unbound modified pigment were seperated on the column. The reconstituted complexes emerged first. The excess pigments were eluted later. 1 ml fractions were collected and their absorption spectra recorded. The best fractions were pooled and concentrated using Amicon centricon concentrators (50 kDa cut off) in a Sigma 3K20 benchtop centrifuge. The reconstituted complexes were stored at 4°C.

5.1 Absorption spectroscopy

Absorption spectra were routinely measured using a Shimadzu Corporation UV-160A spectrophotometer. More accurate spectra were recorded using a Shimadzu UV-PC2101 spectrophotometer. All of the samples had an OD_{859} of 0.5 cm^{-1}. A baseline correction was made prior to all measurements using an appropriate buffer solution.

5.2 Steady-state fluorescence measurements

All steady-state fluorescence measurements were made using a Spex Fluorolog 2. A schematic diagram of the fluorimeter is shown in figure B1. All of the samples had an OD_{859} of 0.1 cm^{-1}. In both fluorescence excitation and emission experiments, fluorescence from the sample was measured at right angles to the excitation beam.

5.2.1 Excitation spectra

The efficiencies of carotenoid to B850 energy transfer in the native, B850-only and reconstituted complexes were determined from their action spectra (see Appendix B). Signal (S) and reference (R) values were measured at 0.5 nm intervals in the range 350 - 600 nm. The calculated S/R ratio was then corrected for instrument function as described in Appendix B. Emission from the Bchl*a*-B850 molecules was measured at 875 nm. The excitation and emission slit widths were both 5 nm.

The correction file for the visible region was generated by recording the R/S ratio at 0.5 nm intervals in the range 350 - 600 nm with a 5 g l^{-1} solution of

rhodamine 6B in the sample position. This ratio was then scaled such that it had a maximum value of 1 (see figure B2).

5.2.2 Emission spectra

B800→B850 energy transfer in the native LH2 and reconstituted complexes was probed in a series of simple fluorescence emission experiments (see Sections 6.5 and 7.4). The (B)Chl-B800 molecules were excited on the blue side of their Q_y absorption band. The excitation wavelengths for each complex are recorded in table 5i. After excitation, an emission spectrum was recorded. The wavelength range over which fluorescence was recorded was different for each of the reconstituted complexes (see table 5i). The excitation and emission slit widths were both 5 nm.

5.3 Circular dichroism spectroscopy

All circular dichroism measurements were made using a JASCO J-600 spectropolarimeter at the Scottish Circular Dichroism Facility, University of Stirling. All samples had an OD_{859} of 0.6 cm^{-1}. Spectra in the visible region were recorded in the wavelength region 300 to 650 nm and those in the NIR region between 630 and 950 nm. Baseline corrections were made using an appropriate buffer solution. The curves were smoothed by averaging the signal over 10 nm in the visible region and 20 nm in the NIR region. After smoothing, the spectra were compared with the original spectra to check that no spectral resolution had been lost.

Table 5i Excitation wavelengths and emission wavelength ranges used in the fluorescence emission experiments with the native LH2 and reconstituted complexes.

Complex	Excitation wavelength (nm)	Wavelength range of emission spectrum (nm)
native LH2	785	800 - 950
Reconstituted complexes		
Bchl*a*-B800	785	800 - 950
geranylgeraniol Bchl*a*-B800	785	800 - 950
13^2OH Bchl*a*-B800	785	800 - 950
Zn-Bph*e*-B800	778	793 - 950
3^1vinyl Bchl*a*-B800	750	765 - 950
3^1OH Bchl*a*-B800	735	750 - 950
acetyl Chl*a*-B800	675	690 - 950
Chl*a*-B800	650	665 - 950

5.4 Resonance Raman spectroscopy

The resonance Raman measurements were performed by Dr. Andrew Gall in the laboratory of Dr. Bruno Robert in the CEN laboratories at Saclay, France. The Bchl*a* molecules were selectively excited at 364 nm using a Coherent Innova 100 Argon laser. Spectra were recorded at right angles to the excitation beam using a Jobin Yvon U1000 spectrometer equipped with a back-thinned charge-coupled device detector (Jobin Yvon Spectrum ONE). Samples were maintained at 10 K in a flow cryostat cooled with liquid helium.

5.5 Pigment analysis of the LH complexes

5.5.1 Pigment extraction

Pigments were extracted by adding a small volume (approximately 100 µl) of the LH complex to 25 ml of an acetone/methanol 7 : 2 (v/v) mixture. The sample was filtered through a 0.2 µm nylon filter into a round-bottomed flask. The sample was dried down using a rotary evaporator. The extracted pigments were taken up in approximately 500 µl of HPLC grade dichloromethane. Finally, the sample was filtered through a 0.2 µm nylon filter into a sample vial ready for HPLC analysis.

5.5.2 HPLC

Analytical HPLC determinations were carried out using a Hewlett Packard 1100 series. The HP ChemStations software was used for data analysis. The pigments were separated on a Spherisorb ODS-2 silica column (dimensions

250 x 5 mm). The mobile phase consisted of a hexane / isopropanol 85 : 15 (v/v) mixture unless otherwise indicated.

5.6 Fs transient absorption measurements

All fs transient absorption measurements were made in the Dept. of Chemical Physics at Lund University, Sweden with the help of Drs. Jennifer Herek and Thomas Polívka. The principles of transient absorption spectroscopy are described in Section 10.2. Pulses of approximately 100 fs were generated using a Ti : Sa laser system. The initial pulses were then amplified in a Ti : Sa regenerative amplifier. These pulses were split into two beams - one to excite the Q_y absorption band of the (B)Chl-B800 molecules and the other to generate white probe light. The wavelength of the probe beam was selected using a single-grating monochromater. The probe beam was then split into a further two beams. One series of pulses was used to probe the region which had been excited. The other was used to probe a region which had not been excited. Both beams were detected using NIR photodiodes. The difference in absorption between these two beams is ΔA. After the sample had been excited, ΔA was measured at different time delays. All samples were diluted with the appropriate buffer solution such that the sample had an OD of 1 cm^{-1} at the excitation wavelength. In order to minimise excitation annihilation and sample degradation, the excitation intensity was kept below 1×10^{14} photons cm^{-2} $pulse^{-1}$. Time-resolved changes in anisotropy in the Q_y absorption band of the (B)Chl-B800 molecules in the reconstituted complexes were determined from two

independent kinetic measurements with the polarization of the probe light either parallel or perpendicular to that of the excitation light. Anisotropy values were then calculated as described in Section 10.2. The kinetic data was fitted using the Spectra Solve software.

5.7 Fluorescence up-conversion

The fluorescence up-conversion measurements were performed by Dr. Alisdair MacPherson at the University of Umea, Sweden. The principles of fluorescence up-conversion are described in Section 11.2. The carotenoid molecules were excited at 82 Mhz in the region of 490 to 500 nm by frequency doubling the approximate 60 fs IR pulses which were produced by a Ti : Sapphire laser. The fluorescence up-conversion spectrometer had a response function of approximately 170 fs. Fluorescence from the sample was detected using a cooled Peltier element, low-noise photon counting photomultiplier (Hamamatsu R4220P) and counted using a gated photon counter (Stanford Researcg Systems SR400). Fluorescence emission from the S_2 state of the rhodopin glucoside molecules was probed at 570 nm and from the Bchl*a*-B850 molecules was probed at 870 nm. The kinetic data was fitted using the SPECTRA program. The errors associated with the fitting were estimated to be better than 10 fs on the basis of fits made using different instrument response functions.

5.8 Time-resolved photon counting

The time-resolved photon counting experiments were made in the Dept. of Chemical Physics at the University of Lund, Sweden with the help of Dr. Arkady Yartsev. The apparatus used in these experiments is described in Appendix A. This technique was used to measure the fluorescence lifetimes of the modified (bacterio)chlorin molecules. The modified pigments were all excited in their Soret transition at 375 nm. Fluorescence was detected using a cooled microchannel plate photomultiplier (Hamamatsu R 2809U-05) and was time resolved as described in Appendix A. The wavelength of fluorescence emission was selected using an appropriate narrow band interference filter.

Results

6.1 Introduction

Previously, Bandilla *et al.* (1998) have reported a method which allows the Bchl*a*-B800 molecules from the LH2 complex of *Rb. sphaeroides* to be exchanged with several different modified (bacterio)chlorin molecules in a 3 step procedure. Firstly, the Bchl*a*-B800 molecules can be released from their binding pockets by an acid treatment using buffer containing the novel Triton detergent TBG10. Secondly, the "free" pigments can be removed by ion-exchange chromatography to give purified, B850-only complexes. Finally, this protocol also allows limited reconstitution of the B800 binding sites with a variety of modified (bacterio)chlorin molecules including Bchl*a*, 3^1OH Bchl*a*, 3^1vinyl Bchl*a* and acetyl Chl*a*.

This chapter describes the adaptation and optimisation of this protocol for LH2 complexes from *Rps. acidophila* 10050.

6.2 Release of the Bchl*a*-B800 molecules from their binding pockets

Acidification of the LH2 complex from *Rps. acidophila* 10050 to pH 5.3 in buffer containing TBG10 results in a decrease in A_{800} (corresponding to bound Bchl*a*) with a concurrent increase in A_{770} (corresponding to free Bchl*a*) (see figure 6a). This shows that the Bchl*a*-B800 molecules can be released from their binding pockets by an acid treatment similar to those in *Rb. sphaeroides*. The changes in absorption which occur on release of the Bchl*a*-B800 molecules were visualised by plotting a difference absorption spectrum (see figure 6b). Bchl*a*-B800 release affects the intensities and the wavelengths of maximum absorption of both the carotenoid and Bchl*a*

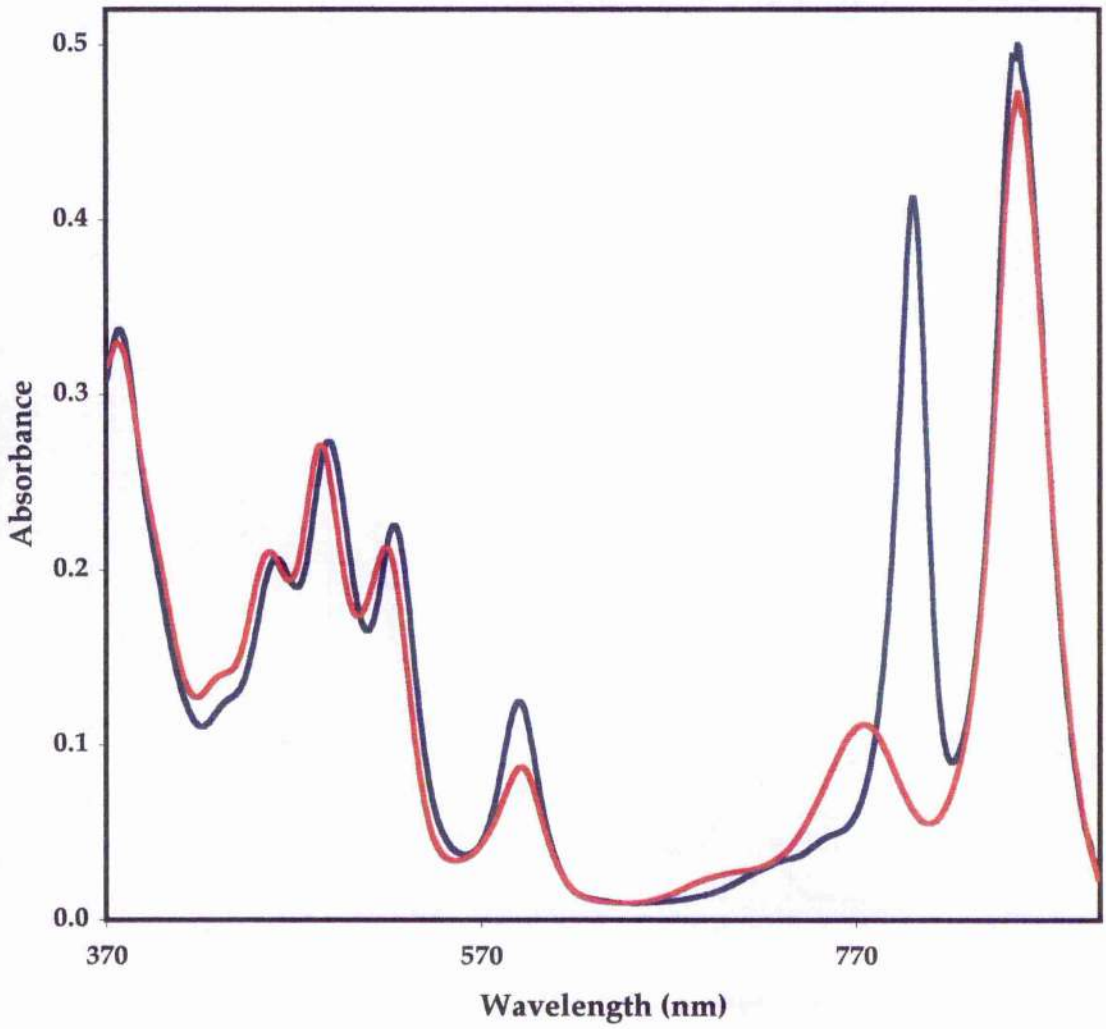

Figure 6a A comparison of the absorption spectra of LH2 complexes from *Rps. acidophila* 10050 before and after the release of all of the Bchl*a*-B800 molecules from their binding pockets. The Bchl*a* molecules were released from the complex by incubating the LH2 sample in buffer containing the Triton detergent TBG10 at a pH of 5.3. [**Key** Blue before pigment release, Red after pigment release].

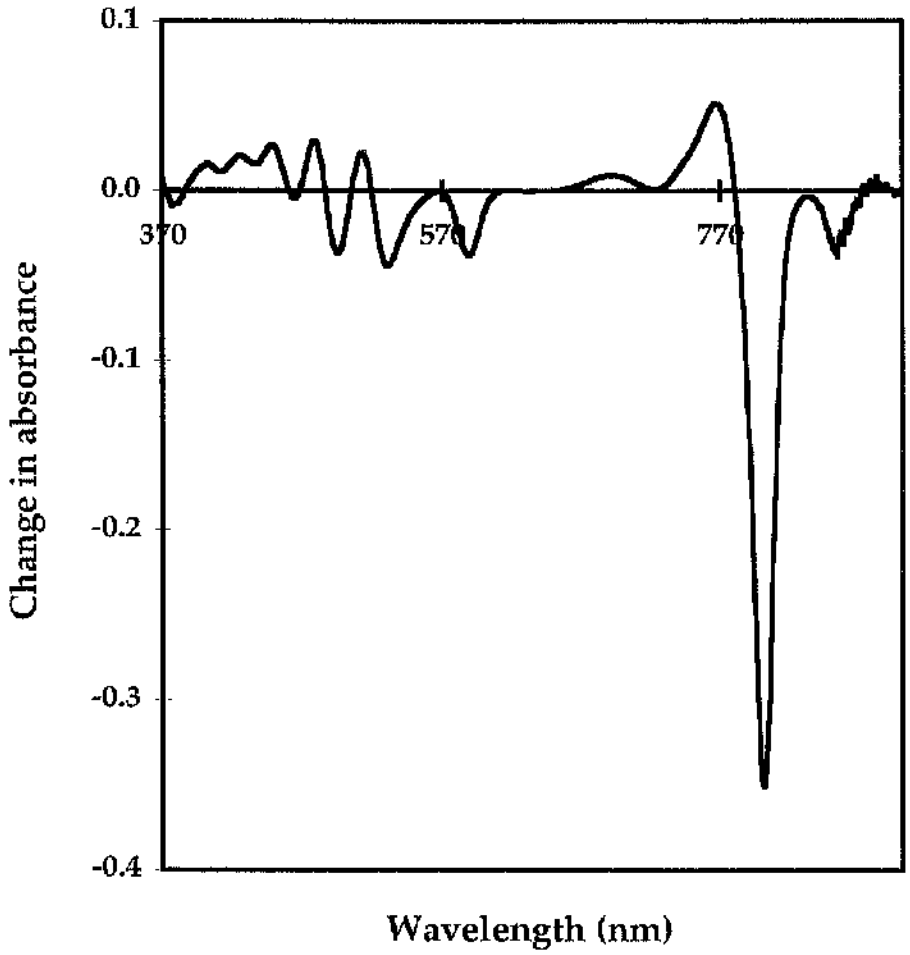

Figure 6b Difference absorption spectrum which shows the changes in absorption which occur on the complete release of the Bchl*a*-B800 molecules from their binding pockets. This spectrum was obtained by subtracting the absorption spectrum of native complexes from the absorption spectrum after all of the Bchl*a*-B800 molecules had been released (see figure 6a).

molecules. The difference spectrum has a small negative peak at 377 nm, a series of related maxima and minima at 449, 479 and 513 and at 464, 495 and 531 nm respectively, a negative peak at 590 nm, 2 positive peaks at 692 and 768 nm, a large negative peak at 801 nm and a small negative peak at 858 nm. These changes in absorption can be explained as follows. The negative peak at 370 nm is caused by a small decrease in the absorption intensity of and 2 nm red shift in the Bchl*a* Soret absorption band. The series of maxima at 449, 479 and 513 nm and minima at 464, 495 and 531 nm are due to a 4 nm blue shift in absorption by the carotenoid. The negative peak at 594 nm is due to a significant decrease in the absorption intensity of the Bchl*a* Q_x transition and red-shift by 4 nm. The sharp negative peak at 800 nm is due to the release of the Bchl*a*-B800 molecules from their binding pockets. The two positive peaks at 770 and 680 nm correspond to free and oxidised, free Bchl*a*. The small negative peak at 860 nm is due to a decrease in absorption intensity and 2 nm red shift by the Bchl*a*-B850 molecules in their Q_y transition.

The observation that the absorptions of the carotenoid and Bchl*a*-B850 molecules are affected by the release of the Bchl*a*-B800 molecules from their binding pockets suggests that the Bchl*a*-B800 molecules interact with both the carotenoid and the Bchl*a*-B850 molecules in the native complex fine tuning their absorption properties.

6.3 Optimising the conditions for pigment release

In order to optimise the conditions for rapid Bchl*a*-B800 release, the effects of protein concentration, the pH and temperature of incubation and the choice of detergent on Bchl*a*-B800 release were investigated.

6.3.1 The effect of protein concentration on the rate of Bchl*a*-B800 release

The effect of protein concentration on the rate of Bchl*a*-B800 release was investigated as described in Section 4.1.2. The length of time taken for complete release of the Bchl*a*-B800 molecules was recorded at several different protein concentrations (see table 6i). The length of time necessary for release of all of the Bchl*a*-B800 molecules is very dependent on protein concentration. If the protein sample had a concentration of either 3.7 or 1.5 μM then all of the Bchl*a*-B800 molecules were not released from their binding sites within 5 h. Samples with a protein concentration of either 0.7 or 0.3 μM, however, had significantly shorter incubation periods in which complete Bchl*a*-B800 release took 90 and 60 min respectively.

The optimal concentration for Bchl*a*-B800 release is 0.7 μM. This concentration allows rapid Bchl*a*-B800 release without having excessively large sample volumes.

Table 6i The effect of protein concentration on the incubation period necessary for release of all the Bchl*a*-B800 molecules from the LH2 complex. The Bchl*a*-B800 molecules were released by incubating the LH2 sample at a pH of 5.3 in buffer containing the Triton detergent TBG10. The protein concentration of each LH2 sample was determined as described in Section 3.6.

Concentration of protein (μM)	Length of time for all Bchl*a*-B800 molecules to be released
0.4	60 min
0.7	90 min
1.5	75% released after 5 h
3.7	50% released after 6 h

Table 6ii The effect of the pH of incubation on the length of time necessary for complete release of the Bchl*a*-B800 molecules from their binding pockets. All samples had a protein concentration of 0.7 μM and were incubated at room temperature.

pH	Length of time for all Bchl*a*-B800 molecules to be released
3.75	30 min
4	45 min
4.25	60 min
4.5	90 min
4.75	90 min
5	90 min
5.5	75% are released after 5 h
8	no reaction

6.3.2 The effect of pH of incubation on the rate of Bchl*a*-B800 release

The effect of the pH of incubation on the kinetics of Bchl*a*-B800 release were investigated as described in Section 4.1.2. At each different pH of incubation, the length of time taken for complete release of the Bchl*a*-B800 molecules and the initial rate of Bchl*a*-B800 release were determined (see table 6i and figure 6c). Release of the Bchl*a*-B800 molecules from their binding pockets is very sensitive to pH. Above pH 5.5, the Bchl*a*-B800 molecules are released very slowly, if at all. Below pH 5.5, however, the Bchl*a*-B800 molecules are released rapidly. On reducing the pH of incubation from 5.5 to 3.75, the initial rate of pigment release increases by a factor of 4 and the length of time for complete Bchl*a*-B800 release decreases from an estimated 8 h to 30 min.

The optimal pH of incubation is 4.75. At this pH, rapid pigment release occurs without exposing the protein to unnecessarily extreme acidic conditions.

6.3.3 The effect of temperature of incubation on rate of Bchl*a*-B800 release

The effect of temperature of incubation on the rate of Bchl*a*-B800 release was investigated as described in Section 4.1.2. The lengths of time taken for complete release of the Bchl*a*-B800 molecules and the initial rate of Bchl*a*-B800 release were measured at several different temperatures (see table 6iii and figure 6d).

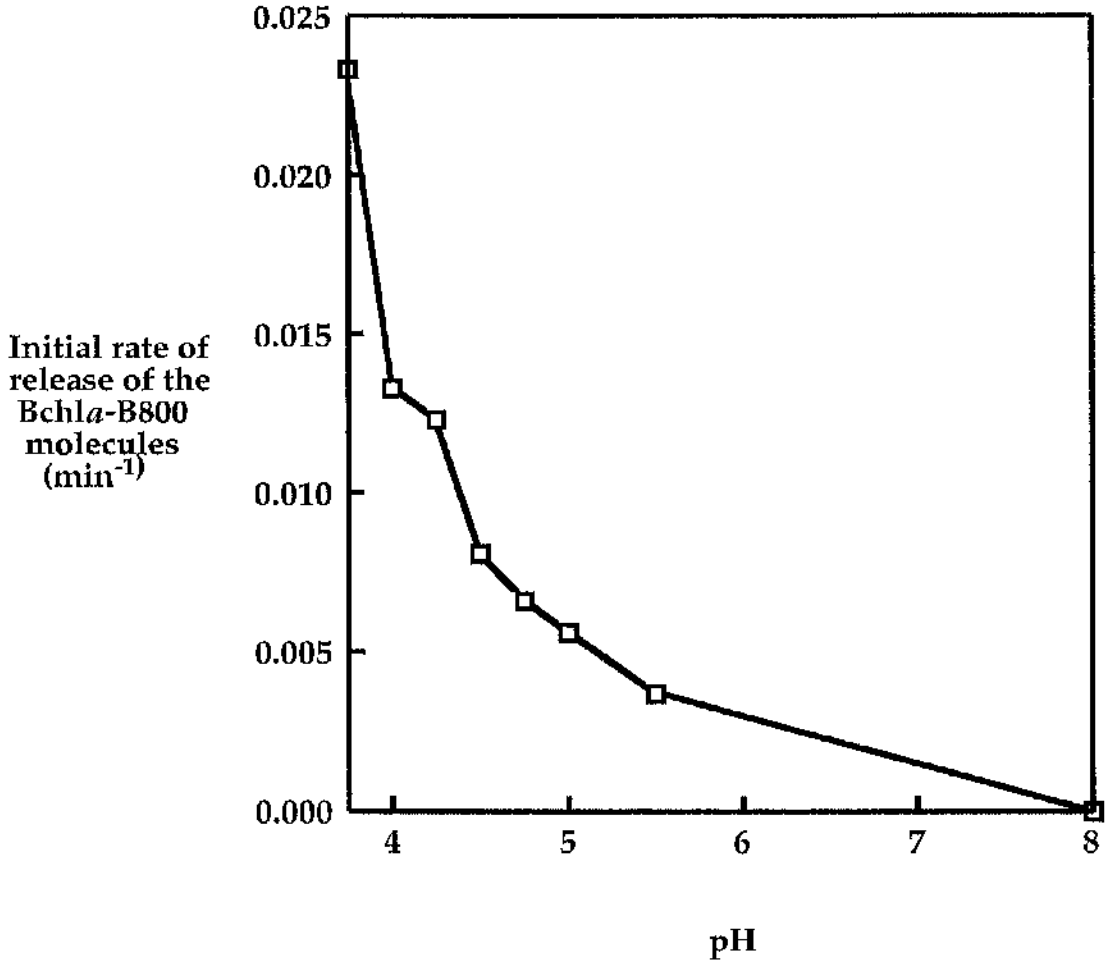

Figure 6c The effect of pH of incubation on the initial rate of release of the Bchl*a*-B800 molecules from their binding pockets. At each pH of incubation, the initial rate of release of the Bchl*a*-B800 molecules was determined as described in Section 4.1.1. The length of time necessary for complete release of the Bchl*a*-B800 molecules is recorded in table 6ii. All the samples had a protein concentration of 0.7 μM and were incubated at room temperature.

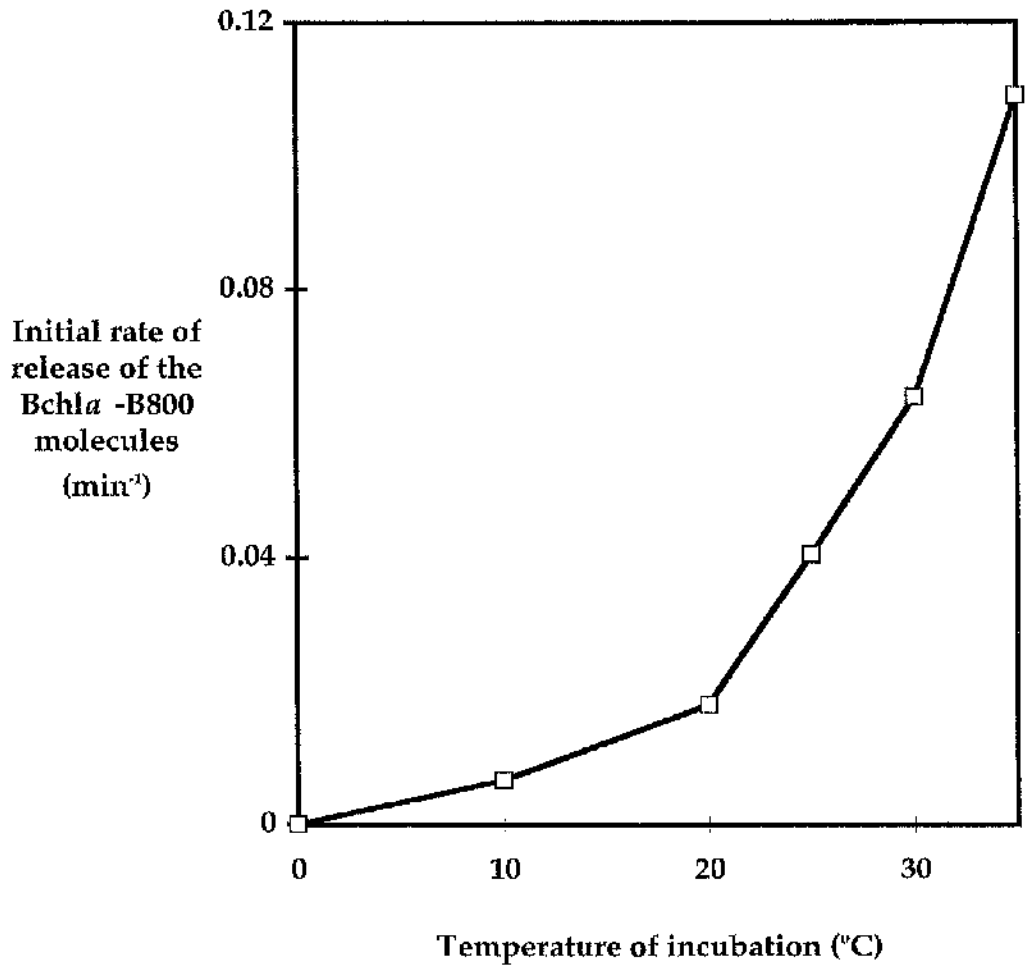

Figure 6d The effect of temperature of incubation on the initial rate of release of the Bchl*a*-B800 molecules from their binding pockets. At each temperature of incubation, the initial rate of Bchl*a*-B800 release was determined as described in Section 4.1.1. The lengths of time necessary for complete release of the Bchl*a*-B800 molecules at each temperature of incubation are recorded in table 6iii. All samples had a protein concentration of 0.7 μM and were incubated at a pH of 4.75.

Table 6iii The effect of temperature of incubation on the time required for all of the Bchl*a*-B800 molecules to be completely released from their binding sites. The samples all had a protein concentration of 0.7 μM and were incubated at a pH of 4.75.

Temperature (°C)	Length of time for all Bchl*a*-B800 molecules to be released
0	no reaction
10	75% released after 6 h
20	5 h
25	90 min
30	45 min
35	25 min

Bchl*a*-B800 release is very sensitive to temperature. At temperatures less than 20°C, the Bchl*a*-B800 molecules are released very slowly from their binding pockets, if at all. In contrast, at temperatures greater than 20°C, rapid Bchl*a*-B800 release occurs. On increasing the temperature of incubation from 20 to 35°C, the initial rate of Bchl*a*-B800 release increases by a factor of 6 and the length of time for complete Bchla-B800 release decreases from 5 hours to 25 min.

The optimal temperature of incubation is 30°C. At this temperature, the Bchl*a*-B800 molecules are rapidly released from their binding sites without exposing the protein to excessively high temperatures.

6.3.4 The effect of choice of detergent on Bchl*a*-B800 release

The effect of choice of detergent on the release of the Bchl*a*-B800 molecules was investigated as described in Section 4.1.2. The lengths of time taken for complete release of the Bchl*a*-B800 molecules using the detergents Triton TBG10, Triton X100, βOG, LM and Brij 98. Using Triton TBG10, Triton X100 and βOG all of the Bchl*a*-B800 molecules were released within 1 h and using Brij 98 within 2 h. Using LM, only 75 % of the Bchl*a*-B800 molecules were released from their binding pockets within 6 h.

The detergent Triton TBG10 was chosen as the detergent for all future preparations.

6.3.5 Summary

All of the Bchl*a*-B800 molecules can be released from their binding sites by incubating a LH2 sample of concentration 0.7 μM in buffer containing Triton TBG10 at a pH of 4.75 at 30°C for 1 h. These conditions were routinely used in all subsequent preparations of B850-only complexes.

6.4 Purification of the B850-only complexes

After release of the Bchl*a*-B800 molecules from their binding sites, it was necessary to develop a method for removing the "free" Bchl*a* from the LH complexes. In their work, Bandilla *et al.* showed that B850-only complexes can be purified by binding the LH complex to a DE52 anion exchange column at pH 5.3, washing the column with buffer containing a low concentration of salt and detergent to remove the "free" Bchl*a* and then eluting the B850-only complexes with high salt (Bandilla *et al.*, 1998). On using this protocol with LH2 complexes from *Rps. acidophila* 10050, however, the LH2 complexes did not bind to the DE52 column. This suggested that LH2 complexes from *Rps. acidophila* 10050 have a net positive charge at pH 4.75. This was confirmed by the observation that the LH2 complexes bind to the negatively charged cation exchange medium phosphocellulose at pH 4.75. After binding the LH complexes to phosphocellulose, the "free" Bchl*a* was removed by washing the column extensively with buffer containing Triton TBG10. The removal of "free" Bchl*a* was monitored by recording the absorption spectrum of the eluant at regular time intervals. Once the eluant had an A_{770} <0.01, the B850-only

complexes were said to be "pure". At this stage, it was possible to elute B850-only complexes in TBG10 from the column using high salt. In later experiments, it was found that the optimal detergent for reconstitution is dodecyl-β-D–maltoside (LM) (see section 6.5.1). After removal of the "free" Bchl*a*, the B850-only sample was exchanged into LM by washing the column with buffer containing LM. Immediately after swapping detergents, the eluant contained both free carotenoid and Bchl*a* molecules. This suggested that detergent-exchange causes denaturation of a fraction of the B850-only complexes. The column was washed with buffer containing LM until the eluant had negligible absorbance at 770 nm. B850-only complexes were later eluted from the column using buffer containing high salt and LM as detergent. The absorption spectrum of the B850-only complexes was recorded and their absorption maxima noted (see figure 6e and table 6iv).

6.5 Optimising the conditions for reconstitution

In their work, Bandilla *et al.* (1998) were able to reconstitute the B800 site with Bchl*a* (an estimated occupancy of 50%), 3^1OH Bchl*a* (50%), 3^1vinyl Bchl*a* (7%) and acetyl Chl*a* (7%). Although Bandilla *et al.* were able to demonstrate that the B800 sites can be reconstituted with both bacteriochlorin and chlorin type molecules, the protocol has only limited potential to create LH2 complexes with a homogenous population of modified (B)Chl-B800 molecules suitable for spectroscopic analysis. Optimisation of the reconstitution reaction for LH complexes from *Rps. acidophila* 10050 involved studying the time course of the reconstitution

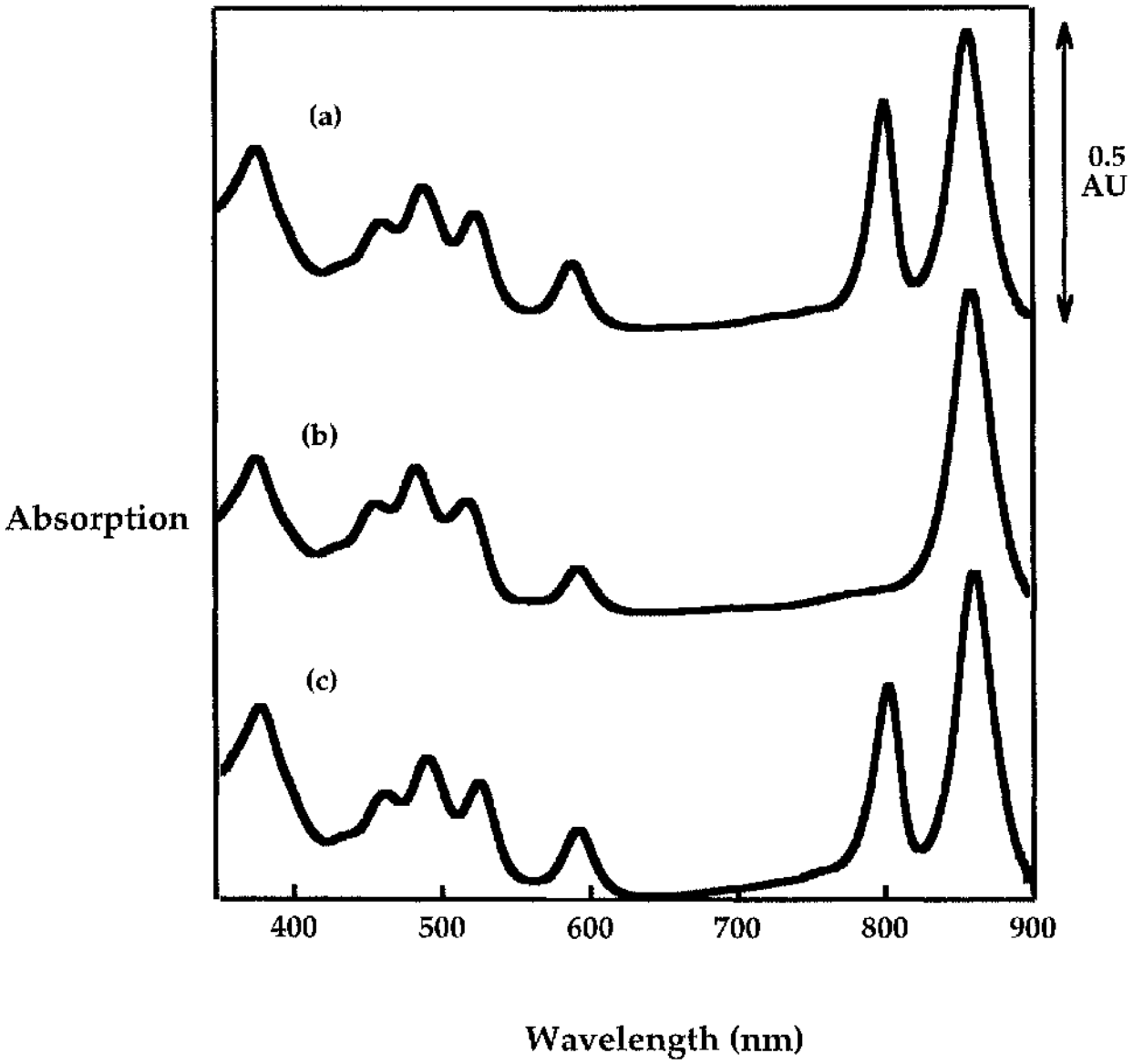

Figure 6e Absorption spectra of the (a) native LH2, (b) B850-only and (c) Bchl*a*-B800 reconstituted complexes. The B850-only and Bchl*a*-B800 reconstituted complexes were prepared as described in Section 4.4. The absorption spectra were recorded on a Shimadzu UV-2101PC. All of the samples had an OD_{859} of 0.5 cm^{-1}. The wavelengths of the absorption maxima in each of the complexes are recorded in table 6iv.

Table 6iv The wavelengths of the absorption maxima in the native, B850-only and Bchl*a*-B800 reconstituted complexes. The B850-only and Bchl*a*-B800 reconstituted complexes were prepared as described in Section 4.4. The absorption spectra were recorded using a Shimadzu UV-2101PC. All samples had an OD_{859} of 0.5 cm^{-1}.

	Wavelength of maximum absorption (nm)		
	LH2	B850-only	Bchl*a*-B800 reconstituted complex
Bchl*a*-B850 Q_y	858	859	859
Bchl*a*-B800 Q_y	802	n/a	802
Bchl*a* Q_x	590	594	591
carotenoid	524, 490, 461	520, 485, 458	524, 490, 461
Bchl*a* Soret	377	377	377

reaction and investigating the effects of detergent, the concentration of exogenous Bchl*a* in the reconstitution mixture and the temperature of incubation on the final occupancy of the B800 site.

6.5.1 LM as the preferred detergent for reconstitution

In their experiments, Bandilla *et al.* used either Triton TBG10 or LDAO as the detergent for reconstitution. Bandilla *et al.* showed that the B800 sites can be partially reconstituted using TBG10 as detergent. Efforts to reconstitute the B800 sites using LDAO as detergent resulted in denaturation of some of the LH complexes. The Bchl*a* which was released on denaturation was incorporated into the B800 sites of neighbouring intact complexes. These effects were also noted in preliminary reconstitution reactions with B850-only complexes from *Rps. acidophila* 10050. Reconstitution reactions were performed using a series of detergents including Chaps, Brij 98, βOG and LM as described in Section 4.3. After the incubation period was complete, the reconstituted complexes were purified by ion-exchange chromatography before their absorption spectra were recorded (results not shown). The detergents Brij 98 and Chaps were incompatible with the DE52 column which was used to purify the reconstituted complexes as the complexes were irreversibly adsorbed to the column. This meant that neither Brij 98 or Chaps could be used as the detergent for reconstitution. The occupancy of the B800 sites in those reconstituted complexes with LM and βOG were both ~ 80%. This is significantly better then the 50% reconstitution which was reported by

Bandilla *et al.* when they used TBG10. LM was used in all subsequent reconstitution experiments.

6.5.2 Time course of reconstitution

The time course of reconstitution was studied in a fluorescence emission experiment (see Section 4.2). Occupancy of the B800 site was determined every 10 s during a 2 h period by measuring fluorescence emission from the Bchl*a*-B850 molecules after direct excitation of the Q_y absorption band of the Bchl*a* molecules bound in the B800 sites (see figure 6f). At t=0, significant fluorescence (14000 cps) from the Bchl*a*-B850 molecules was observed. This basal level of fluorescence is due to direct excitation of the Bchl*a*-B850 molecules themselves. Fluorescence from the Bchl*a*-B850 molecules increases rapidly during the first hour (3600 s) before increasing more gradually during the next hour. Maximal fluorescence occurs at times greater than 2 h. This shows that the reconstitution reaction is complete after an incubation period of 2 h.

6.5.3 The effect of Bchl*a* concentration on the occupancy of the B800 site

The effect of the concentration of exogenous Bchl*a* in the reconstitution mixture on the occupancy of the B800 sites was investigated as described in Section 4.3. For each concentration of Bchl*a*, a reconstitution experiment was performed and the occupancy of the B800 site determined (see figure 6g). Initially, the occupancy of the B800 sites rises sharply with increasing

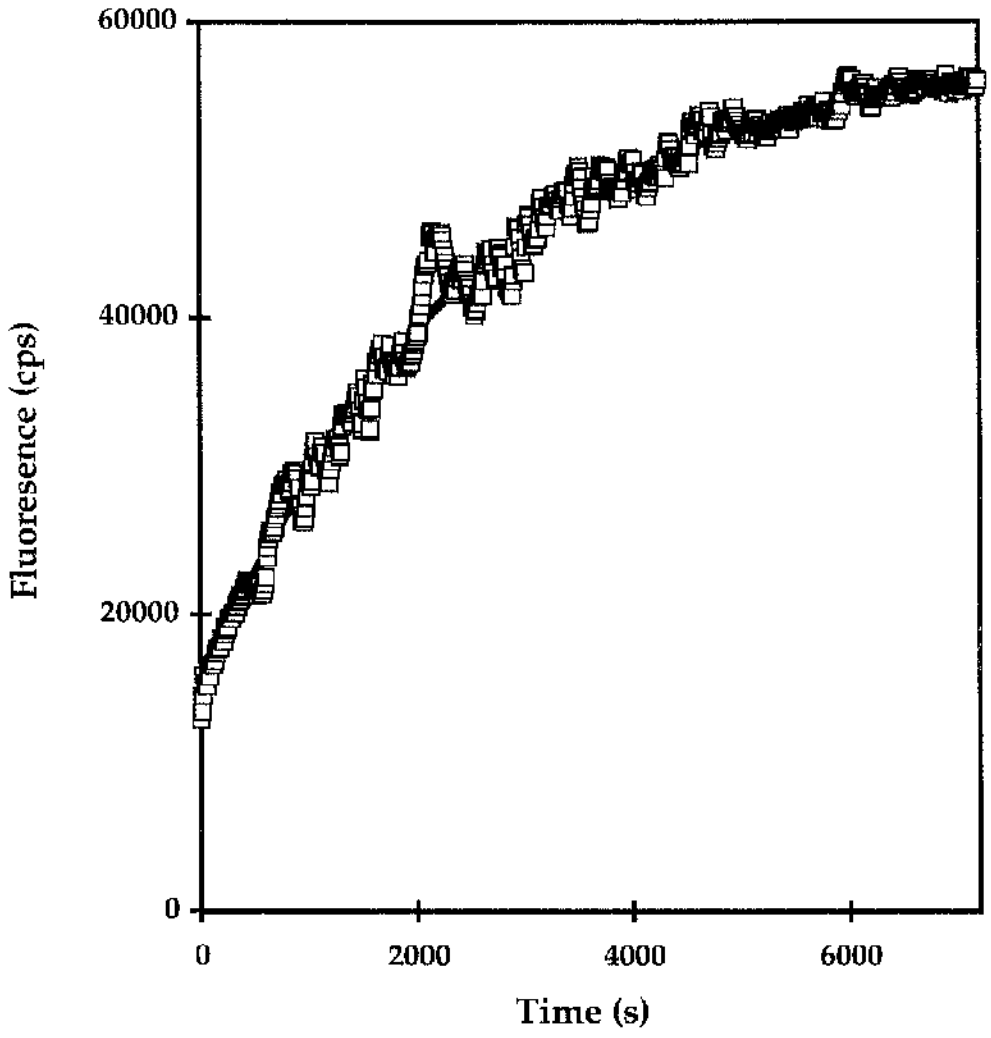

Figure 6f The time course of the reconstitution reaction. The occupancy of the B800 sites was determined at 10 s intervals during a two hour period by measuring fluorescence emission from the Bchl*a*-B850 molecules after direct excitation of the Q_y absorption band of the Bchl*a* molecules bound in the B800 sites. The excitation and emission wavelengths used were 800 and 875 nm respectively.

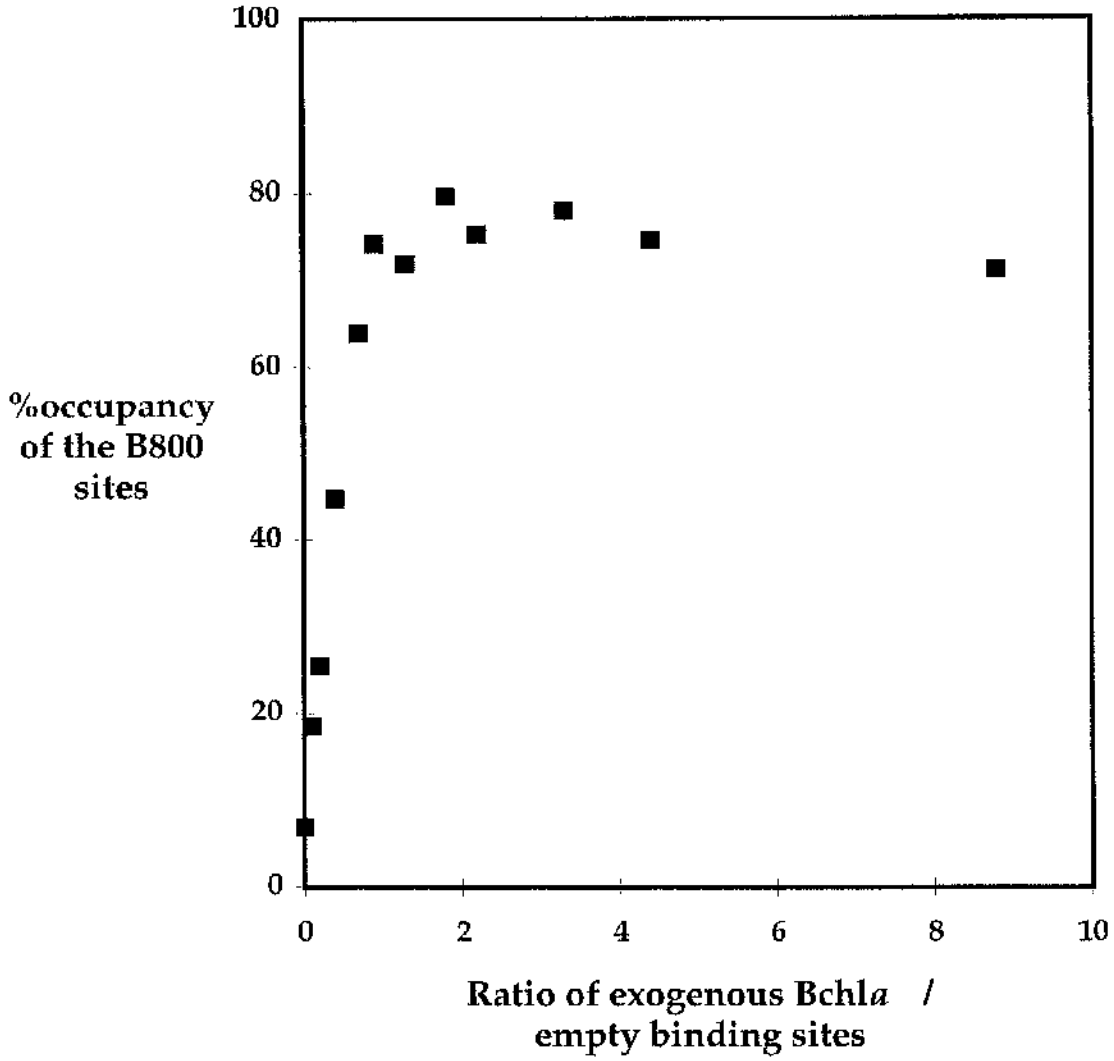

Figure 6g The effect of the concentration of exogenous Bchl*a* in the incubation mixture on the final occupancy of the B800 sites in the reconstituted complex. For each concentration of Bchl*a*, a reconstitution reaction was performed and the occupancy of the B800 sites determined as described in Section 4.3. A maximum B800 site occupancy of 80% occurs when the incubation mixture contains a 3x fold excess of Bchl*a*.

concentrations of exogenous Bchl*a*. A maximum occupancy of 80% occurs when the incubation mixture contains a 3x fold excess of Bchl*a*. At higher concentrations of Bchl*a*, the occupancy of the B800 sites decreases slightly. The optimal concentration of Bchl*a* for reconstitution is a 3x fold excess and was used in all subsequent experiments.

6.5.4 The effect of temperature of incubation on the occupancy of the B800 sites

The effect of the temperature of incubation on the reconstitution reaction was investigated as described in Section 4.3. Reconstitution cocktails containing either a 3x fold excess of Bchl*a* or no Bchl*a* were incubated for 2 h at 30°C. After incubation, the complexes were purified and their absorption spectra recorded (results not shown). The B850-only sample reconstituted with a 3x fold excess of Bchl*a* had a B800 site occupancy of 80% similar to those complexes which were incubated at room temperature. The absorption spectrum of the control, B850-only sample was the same at the end of the incubation period as it was at the start. This showed that incubating at 30°C did not cause any of the LH complexes to be denatured. As incubating the sample at 30°C did not affect the final occupancy of the B800 sites, all subsequent reconstitution reactions were performed at room temperature.

6.5.5 Summary

The B800 binding sites can be optimally reconstituted by incubating a B850-only sample with a 3-fold excess of Bchl*a* for 2 at a pH of 8 and at room temperature.

6.6 Comparison of the absorption spectra of native LH2 and Bchl*a*-B800 reconstituted complexes

In the B850-only complex, the Bchl*a* Q_x absorption maximum is red-shifted by 4 nm and the carotenoid absorption maxima and minima are blue-shifted by 4 nm compared to that in the native complex. The effectiveness of the reconstitution reaction was checked by determining whether or not these band-shifts were reversed in the reconstituted complex. The absorption spectrum of the Bchl*a*-B800 reconstituted complex was recorded (see figure 6e) and the wavelengths of its absorption maxima noted (see table 6iv). In the Bchl*a*-B800 reconstituted complex, both spectral shifts are fully reversed. This suggests that the reconstituted pigments are bound correctly.

7.1 Introduction

In chapter 6, a protocol was described which allows the selective release and removal of the Bchl*a*-B800 molecules from the LH2 complex. This method also allows the reconstitution of empty B800 binding sites with Bchl*a*. Before reconstitution was tried using a range of modified pigments, it was first necessary to fully characterise the Bchl*a*-B800 reconstituted complex to determine how similar it is to the native complex. This characterisation comprised of a series of experiments which were designed to investigate the occupancy of the B800 sites, the overall structure of the reconstituted complex and the binding and energy transfer properties of the reconstituted pigments. The pigment compositions of the native LH2, B850-only and Bchl*a*-B800 reconstituted complexes were determined by HPLC (see Section 7.2). The global structures of the LH2, B850-only and Bchl*a*-B800 reconstituted complexes were investigated using circular dichroism (CD) spectroscopy (see Section 7.3). The interactions between the protein and the reconstituted pigments were studied by resonance Raman (RR) spectroscopy (see Section 7.4). The ability of the reconstituted pigments to function in energy transfer was investigated by fluorescence emission spectroscopy (see Section 7.5).

7.2 Determination of the pigment composition of the native LH2, B850-only and Bchl*a*-B800 reconstituted complexes by HPLC

7.2.1 Introduction

A pigment extract of LH2 complexes from *Rps. acidophila* 10050 contains a mixture of Bchl*a*, rhodopin glucoside and rhodopin (Gardiner *et al.*, 1993). The ratio of Bchl*a* to carotenoid molecules in such an extract can be determined by HPLC. In the HPLC experiments performed in this study, an aliquot of the extracted pigments was injected onto a silica column. Silica is very hydrophillic and allows the pigments to be separated according to their hydrophobicity. The absorption spectrum of the eluant was recorded every 2 s using a multi-wavelength diode-array-detector (DAD). Elution of a pigment from the column was denoted by a peak in the elution profile. The absorbance area of each peak was determined by integration. The concentration of each pigment in the injected sample was determined by dividing the peak area by the millimolar extinction coefficient of the pigment in the solvent mixture used for elution. By scaling the relative concentrations of each pigment, it was possible to determine the ratio of Bchl*a* to carotenoid molecules in the initial extract. In this Section, the pigment compositions of the native, B850-only and Bchl*a*-B800 reconstituted complexes were determined. The results from the pigment analysis experiments are described in Section 7.2.2. The experimental methods are detailed in Section 5.5.

7.2.2 The pigment composition of the native LH2, B850-only and Bchl*a*-B800 reconstituted complexes

A typical trace showing the elution profile of the pigments isolated from the native complex is shown in figure 7a. The trace has 3 main peaks. The individual peaks were identified from their absorption spectra. Rhodopin and Bchl*a* were eluted from the column using a hexane/isopropanol (85/15) mixture with retention times of 3.3 and 3.8 min respectively. After 10 minutes, the percentage of isopropanol was increased to 40%. This caused rhodopin glucoside to be eluted from the column as a sharp peak with a retention time of 14.5 min. The chromatographs of the pigments isolated from the B850-only and Bchl*a*-B800 reconstituted complexes are similar (results not shown). For each complex, the area under the major peaks was measured and the Bchl*a* : carotenoid ratio determined (see table 7i). In the native complex, the Bchl*a* : carotenoid ratio is 3.0 ± 0.1 : 1. This means that the number of rhodopin glucoside molecules/αβ pair is 1. The number of carotenoid molecules/monomeric sub-unit in the LH2 complex from *Rps. acidophila* 10050 is a contentious issue. In the original structure only one carotenoid per αβ pair was observed (McDermott *et al.*, 1995). In a subsequent crystal structure using LDAO as detergent, poorly resolved electron density, which had previously been attributed to a molecule of the detergent β-octyl glucoside, was suggested to belong to a second rhodopin glucoside molecule (Freer *et al.*, 1996). The results from this biochemical study, however, show that there is only one carotenoid/αβ pair. In the B850-only complex, the Bchl*a* : carotenoid ratio is 2.0 ± 0.1 : 1. This shows that the

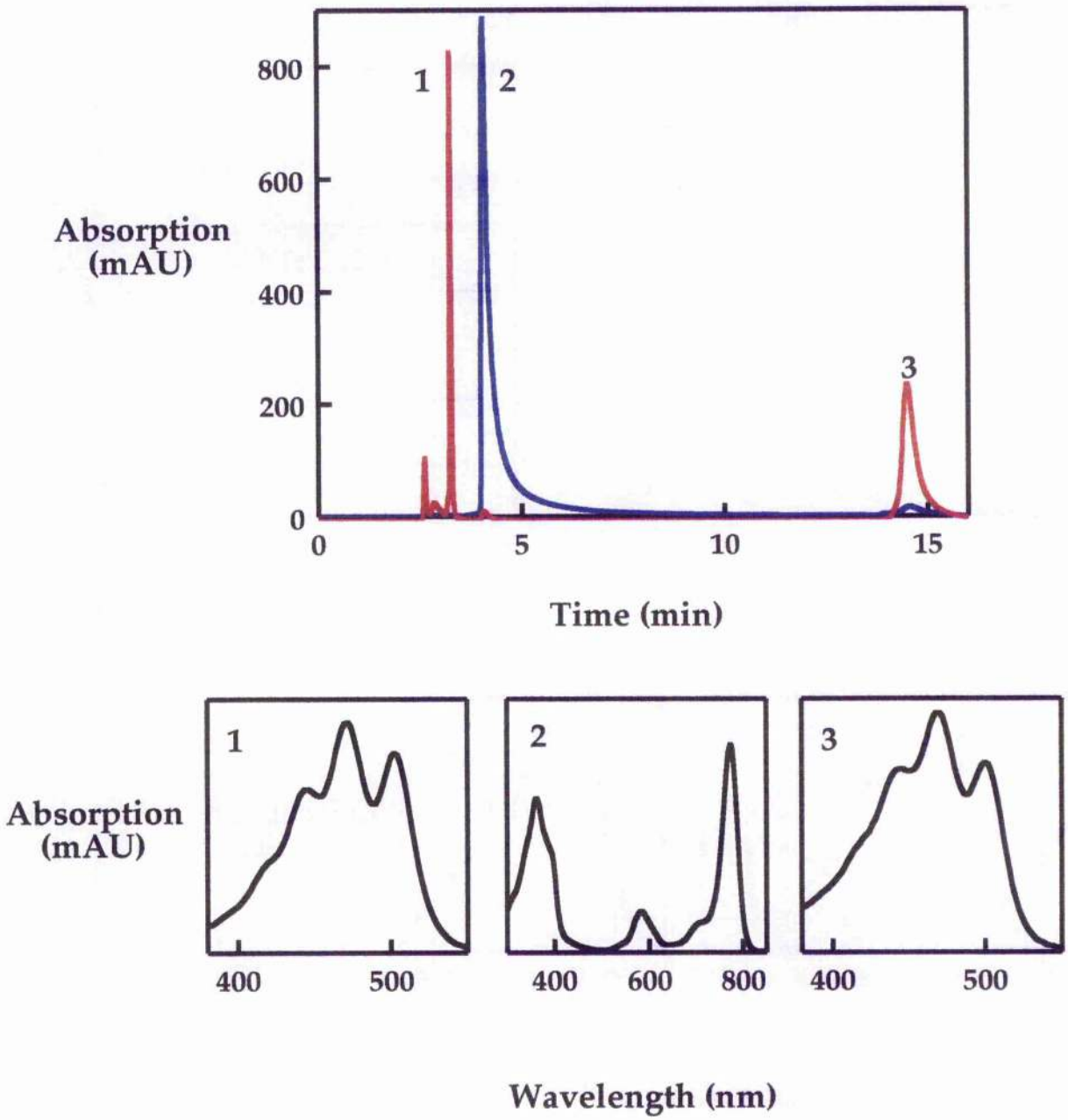

Figure 7a The elution profile of a pigment extract from the native complex. The pigments were separated on a silica column by HPLC. Elution of the Bchl*a* and carotenoid molecules from the column were detected at 773 (blue) and 470 (red) nm respectively. The peaks labelled 1, 2 and 3 are rhodopin, Bchl*a* and rhodopin glucoside respectively. The area under each peak was measured and the Bchl*a* : carotenoid ratio determined as described in Section 7.2.1. The Bchl*a* : carotenoid ratio in the native complex is 3.0 : 1.

Table 7i The pigment ratios in the native, B850-only and Bchl*a*-B800 reconstituted complexes as determined by HPLC. The pigments were extracted from the respective complexes as described in Section 5.4.1. The pigments were separated on a silica column and quantitated as described in Section 7.2.1. A typical elution profile is shown in figure 7a.

Complex	Bchl*a* : carotenoid ratio
LH2	$3.0 \pm 0.1 : 1$
B850-only	$2.0 \pm 0.1 : 1$
Bchl*a*-B800 reconstituted	$2.8 \pm 0.1 : 1$

B800 pockets in the B850-only complex are completely depleted. In the Bchl*a*-B800 reconstituted complex, the Bchl*a* : carotenoid ratio is 2.8 ± 0.1 : 1. This shows that the average occupancy of the B800 sites in the reconstituted sample is approximately 80%. Using their protocol, Bandilla *et al.* (1998) were able to reconstitute approximately 50% of the empty B800 binding sites with Bchl*a* . The method described in Chapter 6, therefore, is a significant improvement upon the previously described procedure but still does not allow reconstitution of all of the B800 sites. This can be explained in one of two ways. Firstly, the conditions used for reconstitution are not optimal. Alternatively, damage to the B800 sites during the pigment release and removal process may prevent subsequent reconstitution of these sites. The value for the average occupancy of the B800 sites in the reconstituted sample can be interpreted in one of two ways. This value may reflect a situation in which the B800 sites in 80% of the reconstituted complexes are fully occupied and in the other 20% are completely empty. Alternatively, the reconstituted sample may contain a series of complexes in which the B800 sites are partially occupied. In the work reported here, it was not possible to discriminate between these two possibilities, though it is thought that the latter situation is more likely.

7.3 Structural analysis of the native LH2, B850-only and Bchl*a*-B800 reconstituted complexes by circular dichroism spectroscopy

7.3.1 Introduction

Circular dichroism (CD) is a property of certain molecules which differentially absorb left and right circularly polarised light (Price, 1997). Molecules which exhibit CD, therefore, must either have intrinsic chirality or an asymmetric environment. In free solution, Bchl*a* monomers have a weak negative CD signal associated with their Q_y absorption transition whereas carotenoids, such as rhodopin glucoside, do not have a CD signal at all. The explanation for this is quite simple. Bchl*a* molecules have asymmetry. Carotenoid molecules do not. In the LH2 complex, however, both the Bchl*a* and carotenoid molecules have very pronounced, distinct CD spectra. These are due to the conformation adopted by and the arrangement of the pigments in the complex. CD is very sensitive to the orientation of the pigments within the complex and to interactions between proximal chromatophores. For example, the ring of Bchl*a*-B850 molecules have a very distinctive CD signal consisting of a positive band followed by a negative band. This signal was originally interpreted as excitonic coupling of the Bchl*a*-B850 molecules (Cogdell & Scheer, 1985). This has since been confirmed in the crystal structure of the LH2 complex from *Rps. acidophila* 10050.

In this Section, putative changes in the arrangement and position of the chromatophores in the B850-only and Bchl*a*-B800 reconstituted complexes were assessed by comparing the CD spectra of the B850-only and Bchl*a*-B800

reconstituted complexes in the NIR and visible regions with those of the native complex. The results are presented in Sections 7.3.2 and 7.3.3. The experimental method is described in Section 5.3.

7.3.2 CD spectra of the LH2, B850-only and Bchl*a*-B800 reconstituted complexes in the NIR

The CD spectra of the LH2, B850-only and Bchl*a*-B800 reconstituted complexes in the NIR are shown in figure 7b. The CD signal associated with the Bchl*a*-B850 molecules (region 820-920nm) has the same shape in all three complexes. In the native complex, the signal consists of a positive band with a maximum at 858 nm and a negative band with a minimum at 880 nm. In the B850-only complex, this signal is red-shifted by 6 nm. In the Bchl*a* reconstituted complex, this red-shift is reversed by 2 nm. As the signal has the same shape in all three complexes, it suggests that the removal and reconstitution of Bchl*a* molecules into the B800 binding pockets does not affect the structure of the ring of Bchl*a*-B850 molecules. In the native complex, the negative CD signal with a minimum value at 798 nm is due to the Bchl*a*-B800 molecules. In the B850-only complex, this large, negative signal is absent. Instead, a very weak, broad negative CD signal which has a minimum value at 777 nm is observed. A similar signal has recently been reported by Koolhass *et al.* (1998) in a low temperature CD study of a B850-only mutant from *Rb. sphaeroides*. This signal was attributed to the upper excitonic absorption component associated with the Bchl*a*-B850 molecules. In the Bchl*a*-B800 reconstituted complex, the negative CD signal at 798 nm is restored. The return of this CD signal

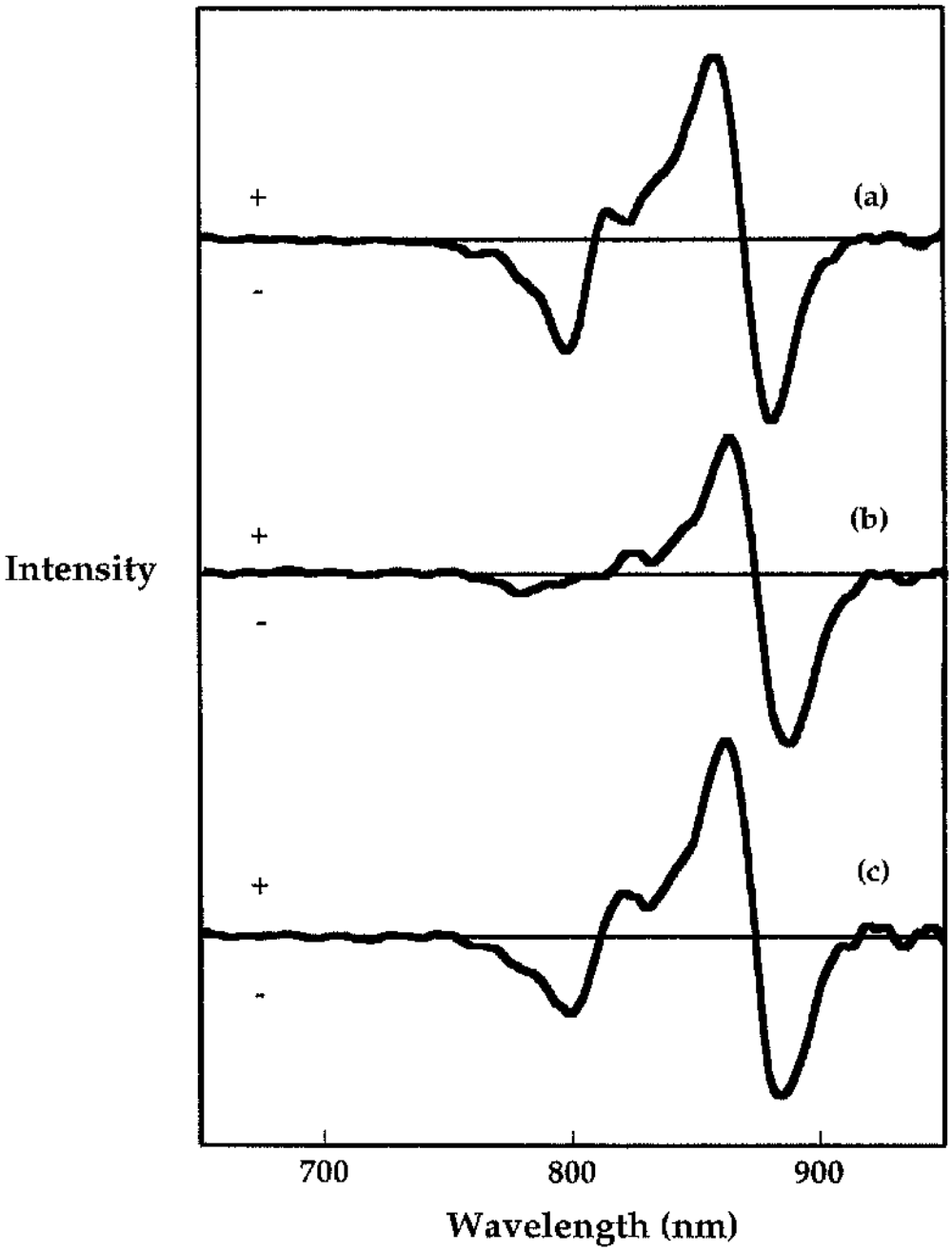

Figure 7b CD spectra of the (a) LH2, (b) B850-only and (c) Bchl*a*-B800 reconstituted complexes in the NIR. The spectra were recorded as described in Section 5.3. All samples had an OD_{859} = 0.6 cm^{-1}. The CD signal associated with the Bchl*a*-B850 molecules (region 820-920nm) has the same shape in all three complexes. This shows that the removal and reconstitution of Bchl*a* molecules into the B800 binding sites does not affect the structure of the ring of Bchl*a*-B850 molecules. The negative CD signal which is associated with the Bchl*a*-B800 molecules (region 760 - 810 nm) is absent in the B850-only complex but is restored in the Bchl*a*-B800 reconstituted complex. This suggests that the Bchl*a*-B800 molecules in the reconstituted complex have a similar orientation and arrangement as those in the native complex.

suggests that the orientation and arrangement of the Bchl*a*-B800 molecules in the reconstituted complex is similar to those in native LH2.

7.3.3 CD spectra of the LH2, B850-only and Bchl*a*-B800 reconstituted complexes in the visible region

The CD spectra of the LH2, B850-only and Bchl*a*-B800 reconstituted complexes in the visible region are presented in figure 7c. The CD signal associated with the carotenoid molecules (region 450-550 nm) has the same shape in all three complexes. In the native complex, this signal has maxima at 470, 498 and 531 nm and minima at 480 and 514 nm. In the B850-only complex, these maxima and minima are blue shifted by 4 nm. In the Bchl*a*-B800 reconstituted complex, this blue-shift is completely reversed. The shape of the induced CD signal associated with the carotenoid molecules depends strictly upon the asymmetric conformation of the carotenoids within the complex. As the carotenoid CD signal has the same shape in all three complexes, it suggests that the carotenoid molecules all have the same conformation. The carotenoid molecules are integral to the structure of the LH2 complex and adopt an extended conformation across the whole complex. As the conformations of the carotenoids are the same in all of the complexes, it is also likely that the native, B850-only and Bchl*a*-B800 reconstituted complexes have the same overall structure.

In the native complex, the CD signal associated with the Bchl*a* Q_x transition is positive in value and has a maximum intensity at 590 nm (see figure 7c). This signal has the same shape in the B850-only and Bchl*a*-B800 reconstituted complexes. In the B850-only complex, however, this

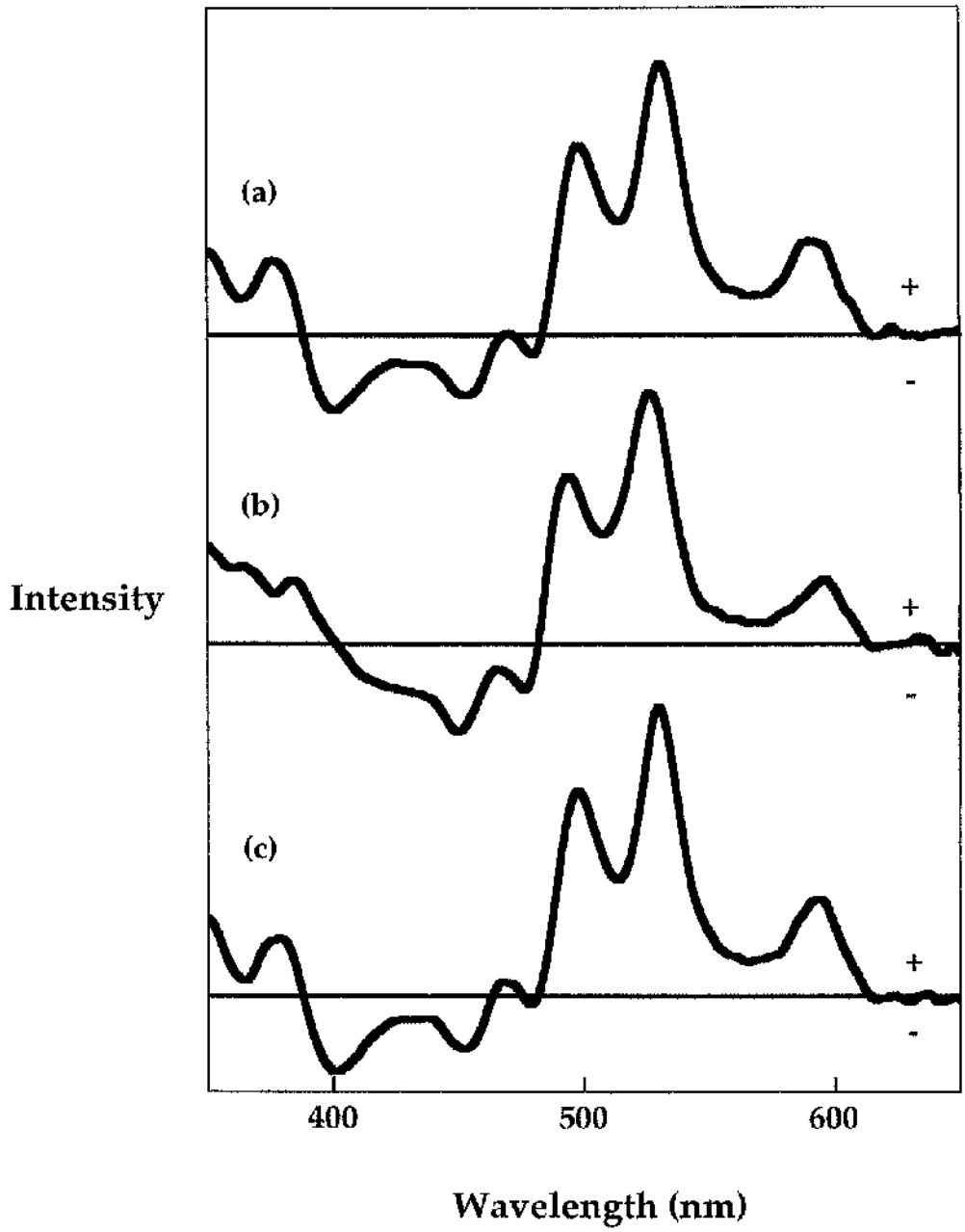

Figure 7c CD spectra of the (a) LH2, (b) B850-only and (c) Bchl*a*-B800 reconstituted complexes in the visible region. The spectra were recorded as described in Section 5.3. The samples all had an $OD_{859} = 0.6$ cm^{-1}. The CD signal associated with the carotenoid molecules (region 450-550 nm) has the same shape in all three complexes. This suggests that the carotenoid molecules have the same asymmetric conformation in the native, B850-only and Bchl*a*-B800 reconstituted complexes.

maximum is red-shifted by 6 nm. This red-shift is reversed by 3 nm in the reconstituted complex. In native LH2, the CD signal associated with the Bchl*a* Soret transition (region 300-450 nm) has a well defined character with maxima at 350, 376 and 432 nm and minima at 364 and 400 nm (see figure 7c). In the B850-only complex, the Soret CD signal has a poorly defined shape (see figure 7c). In the Bchl*a*-B800 reconstituted complex, the CD signal is essentially the same as that in native LH2 with maxima at 350, 378 and 432 nm and minima at 364 and 400 nm. The restoration of the CD signal associated with the Bchl*a* Soret transition in the reconstituted complex is further evidence which suggests that the orientation and arrangement of the Bchl*a*-B800 molecules in it is similar to those in the native complex.

7.4 A study of the protein-Bchl*a* interactions in the native, B850-only and Bchl*a*-B800 reconstituted complexes by resonance Raman spectroscopy

7.4.1 Introduction

All molecules vibrate. The particular frequencies at which a given molecule will vibrate depends upon two factors. These are the chemical structure of and the environment surrounding the molecule. Molecular vibrational modes can be investigated using a technique called resonance Raman (RR) spectroscopy. In RR spectroscopy, a sample of interest is illuminated with monochromatic light from a laser source. Some of the excitation light is scattered by the molecules in the sample. The majority of the scattered light has the same frequency as the excitation beam. The frequency of some of the

scattered light, however, is altered. These changes in frequency are caused by interactions between the photons of light energy and the molecule of interest. Depending upon the type of interaction which occurs the scattered light can have either a slightly lower or a slightly higher frequency. In the majority of interactions, the molecule accepts energy from the photon. The light which is scattered, therefore, has a lower frequency. If the molecule is in its excited state, however, energy is transferred from the molecule to the photon. This type of interaction causes the scattered light to have a higher frequency. In both types of interaction, only discrete changes in energy can occur. These correspond with transitions between vibrational energy levels within the irradiated molecule. In RR measurements, the changes in the frequency of the scattered light are measured.

Bchl*a* molecules have a very distinctive RR spectrum. The frequency of the vibrational modes of the Bchl*a* molecules in the LH2 complex are affected by interactions with the protein. For example, the C3 acetyl carbonyl groups of both the Bchl*a*-B800 and -B850 molecules are H-bonded. This causes a down-shift in the frequency at which these carbonyl groups vibrate (Fowler *et al.*, 1994; Sturgis *et al.*, 1995b; Gall *et al.*, 1997). As the frequency of the vibrational modes of the Bchl*a* molecules are sensitive to interactions with the protein, RR can be used to probe local pigment-protein interactions. To test whether or not the Bchl*a*-B800 molecules are correctly bound within the reconstituted complex, the vibrational modes of the Bchl*a* molecules in the native and Bchl*a*-B800 reconstituted complexes were compared especially in

the carbonyl stretching region. The results are presented in Sections 7.4.2 and 7.4.3. The experimental method is described in Section 5.4.

7.4.2 The carbonyl stretching modes of Bchl*a* in native, B850-only and Bchl*a*-B800 reconstituted complexes

The carbonyl stretching modes of the Bchl*a* molecules in the LH2, B850-only and Bchl*a*-B800 reconstituted complexes were compared by measuring the induced RR spectrum in the frequency range 1580 to 1740 cm^{-1} after selective excitation of the Bchl*a* molecules in their Soret transition (see figure 7d). All of the Raman spectra are dominated by a strong signal at 1610 cm^{-1}. This is due to the vibrations of the Bchl*a* methine bridges. In comparison, the contributions from the Bchl*a* carbonyl stretching modes are weak and are partially hidden by this intense band. The RR spectrum of the LH2 complex has a shoulder at 1623 cm^{-1} and two weak, broad bands at 1671 and at 1696 cm^{-1}. The shoulder at 1623 cm^{-1} is due to the hydrogen bonded C3 acetyl carbonyl groups. The bands at 1671 and 1696 cm^{-1} are due to the hydrogen bonded and free keto groups at position C13 on the Bchl*a* rings (Robert & Lutz, 1988a; Sturgis *et al.*, 1995a). In the RR spectrum of the B850-only complex, the signal associated with the C3 acetyl carbonyl group has a defined maximum at 1626 cm^{-1}. The weak signal at 1671 cm^{-1} is still observed but the signal at 1696 cm^{-1} is missing. This shows that the C13 keto group of both the α and β apoprotein associated Bchl*a*-B850 molecules are weakly H-bonded. The RR spectrum of the Bchl*a*-B800 molecules was obtained by subtracting the RR spectrum of the B850-only complex from that of native

Figure 7d The high frequency carbonyl stretching modes of the Bchl*a* molecules in the (a) native, (b) B850-only and (c) Bchl*a*-B800 reconstituted complexes. The RR spectrum of the Bchl*a*-B800 molecules (d) was obtained by subtracting the RR spectrum for the B850–only complex from that for native LH2. All spectra were recorded at 10 K. The Bchl*a* molecules were excited in their Soret transition at 364 nm.

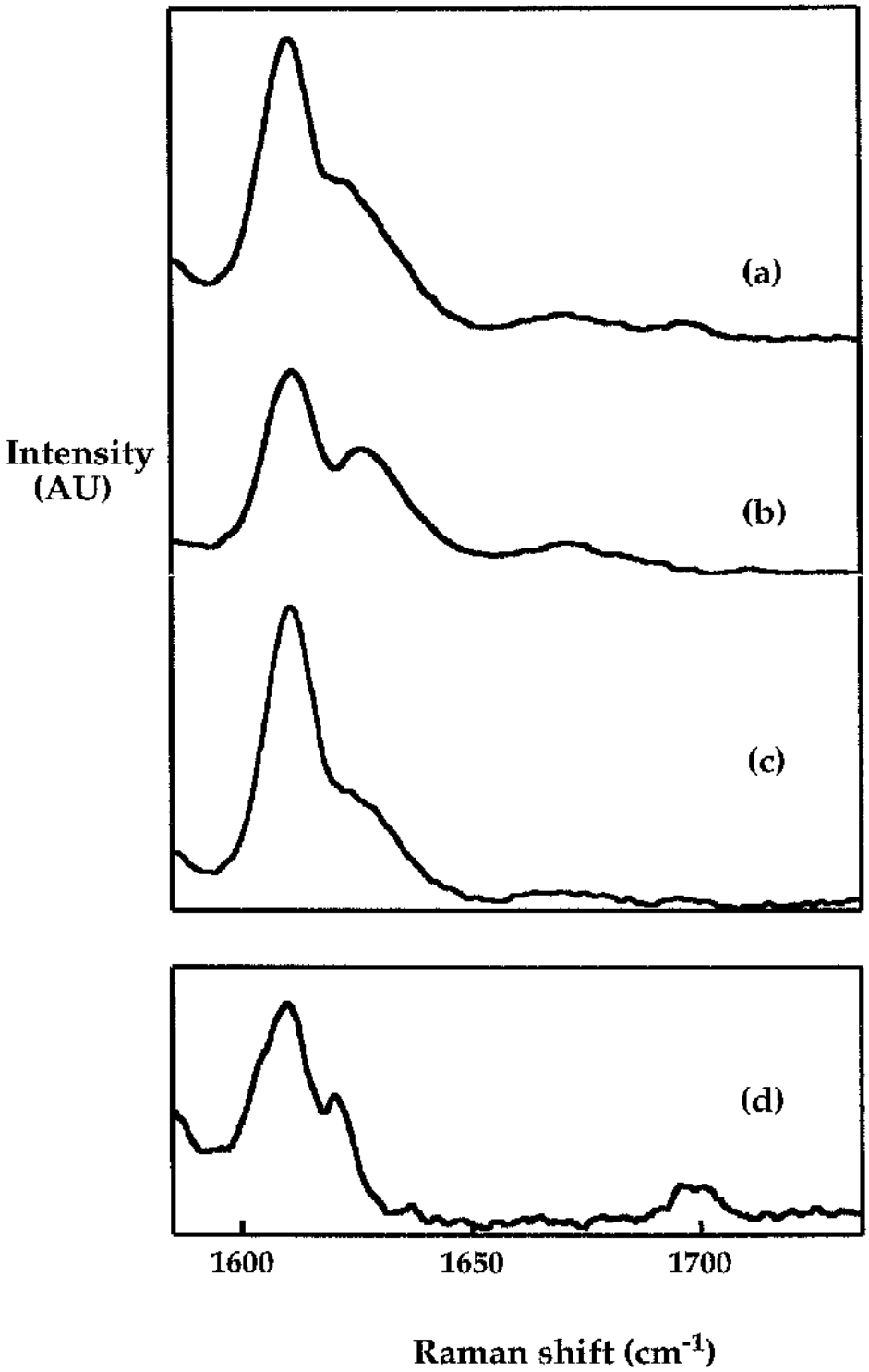
Intensity (AU)
(a)
(b)
(c)
(d)
1600
1650
1700
Raman shift (cm-1)

LH2 (see figure 7d). In this difference spectrum, two interesting spectral features can be observed. The signal associated with the C3 acetyl carbonyl group is very narrow and has a maximum value at 1620 cm^{-1}. In contrast, the corresponding signal in the RR spectrum of the B850-only complex is much broader and has a maximum value at 1626 cm^{-1}. These results suggest that the H-bond between the protein and C3 acetyl carbonyl group of the Bchl*a*-B800 molecules is stronger than that which is made to the Bchl*a*-B850 molecules. In addition, the RR spectrum of the Bchl*a*-B800 molecules has a signal at 1699 cm^{-1} but not at 1669 cm^{-1}. This shows that the C13 keto groups of the Bchl*a*-B800 molecules are free.

The RR spectrum of the Bchl*a*-B800 reconstituted complex is essentially the same as that for native LH2 with a shoulder at 1623 and weak bands at 1669 and 1696 cm^{-1}. The intensity of these signals, however, is weaker than that which occurs in the native complex (see figure 7d). This may be due to incomplete occupancy of the B800 sites. The reappearance of the shoulder at 1623 cm^{-1} would suggest that the C3 acetyl carbonyl group of the Bchl*a*-B800 molecules in the reconstituted complex are hydrogen bonded.

7.4.3 A comparison of all of the Bchl*a* vibrational modes in native and Bchl*a*-B800 reconstituted complexes

All of the vibrational modes of the Bchl*a* molecules in the native and Bchl*a*-B800 reconstituted complexes were compared by measuring the induced Raman shift over an extended frequency region after selective excitation of the Bchl*a* molecules in their Soret transition (see figure 7e). A

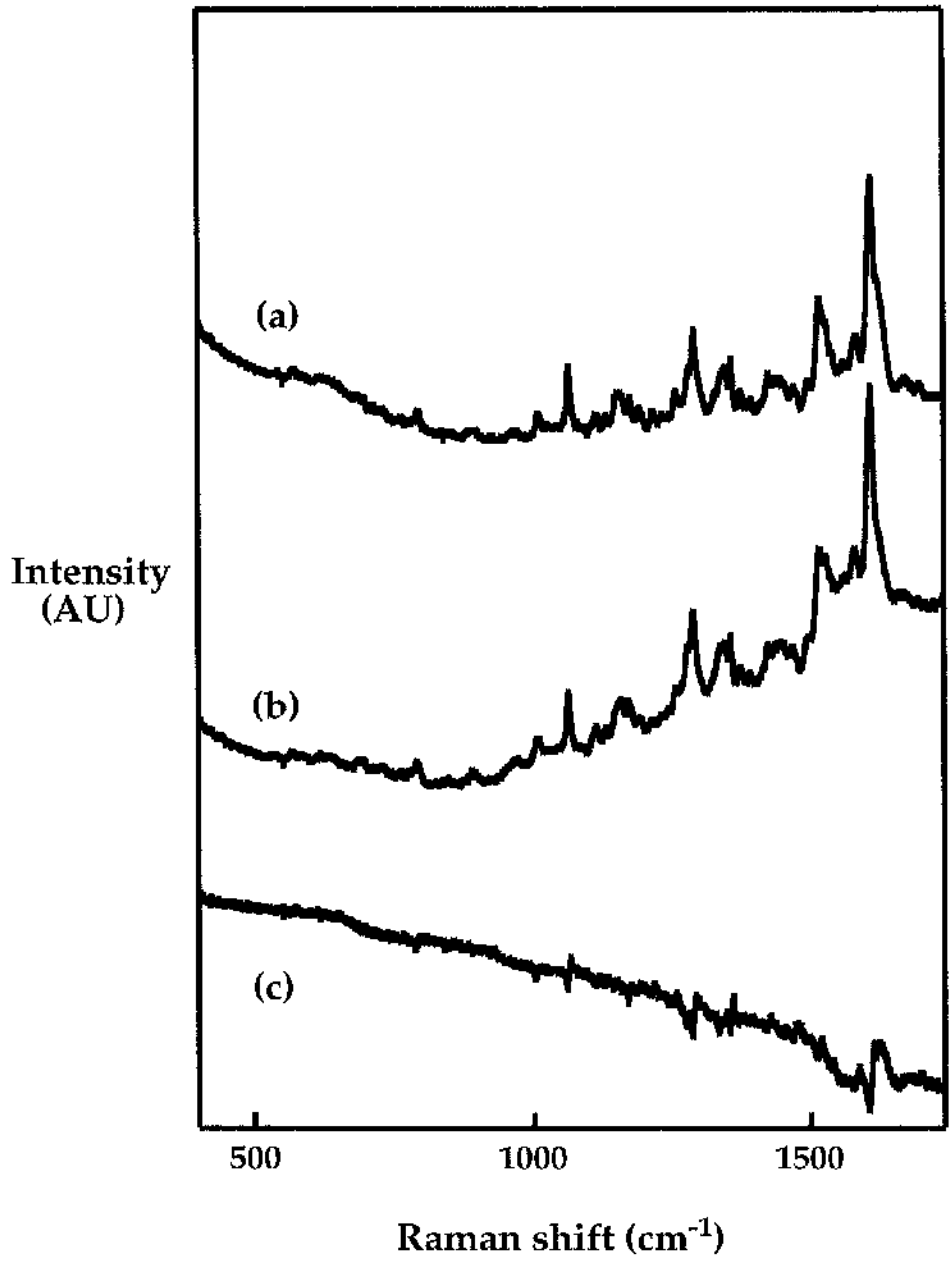

Figure 7c Comparison of the vibrational modes of the Bchl*a* molecules in the (a) native and (b) Bchl*a*-B800 reconstituted complexes over an extended frequency range (400 to 1740 cm^{-1}). The difference spectrum (c) was obtained by subtracting the spectrum for the Bchl*a*-B800 reconstituted complex from that for native LH2. Both spectra were recorded at 10 K. The Bchl*a* molecules were excited in their Soret transition at 364 nm.

reconstituted complex from that for native LH2 (see figure 7e). The difference spectrum is essentially a smooth line which decreases in value as the frequency of the Raman shift increases. If the frequency of each of the Bchl*a* vibrational modes was different in the two complexes, the difference spectrum would contain many spikes. As the difference spectrum is essentially smooth, the frequency of each of the vibrational modes of the Bchl*a* molecules in both the native and reconstituted complexes must be the same. This would suggest that the interactions between the protein and the Bchl*a* molecules in the reconstituted complex are the same as those in the native complex. The difference spectrum decreases in value as the frequency of the Raman shift increases. This is because the Bchl*a*-B800 reconstituted complex has an increased level of background fluorescence at high frequencies compared to the native complex (see figure 7e). This suggests that the reconstituted sample contains a small amount of non-specifically bound Bchl*a*.

7.5 Fluorescence emission experiments as a simple probe of B800 to B850 energy transfer

7.5.1 Introduction

Previously, it has been demonstrated empty B800 binding sites can be reconstituted with Bchl*a* (see Section 6.5) and that the reconstituted pigments are properly liganded within the complex (see Section 7.4). In this Section, a simple fluorescence emission experiment was designed to investigate whether or not the reconstituted pigments can function in

energy transfer. In this experiment, the Bchl*a*-B800 molecules were excited in their Q_y absorption band. After excitation, fluorescence could be emitted from the Q_y absorption band of either the Bchl*a*-B800 or -B850 molecules. If the Bchl*a*-B800 molecules were unable to transfer their excitation energy to the Bchl*a*-B850 molecules, fluorescence would be observed directly from the Bchl*a*-B800 molecules. If the Bchl*a*-B800 molecules were able to efficiently transfer their excitation energy to the Bchl*a*-B850 molecules, predominantly all of the fluorescence would come from the Bchl*a*-B850 molecules. By noting the relative contributions of fluorescence emission from the Bchl*a*-B800 and -B850 molecules, it was possible to conclude whether or not the reconstituted pigments participate in efficient B800→B850 energy transfer. The fluorescence emission spectra of the native and Bchl*a*-B800 reconstituted complexes are presented in Section 7.5.2. The experimental procedure is described in Section 5.2.

7.5.2 B800 to B850 energy transfer in native LH2 and Bchl*a*-B800 reconstituted complexes

The Bchl*a*-B800 molecules in the native complex were excited on the blue side of their Q_y absorption band and a fluorescence emission spectrum recorded in the region 800 to 950 nm (see figure 7f). The spectrum has a small fluorescence emission band at 805 nm and a large fluorescence emission band at 875 nm. These peaks correspond to fluorescence from the Bchl*a*-B800 and -B850 molecules respectively. This shows that predominantly all of the excitation energy which is absorbed by the Bchl*a*-

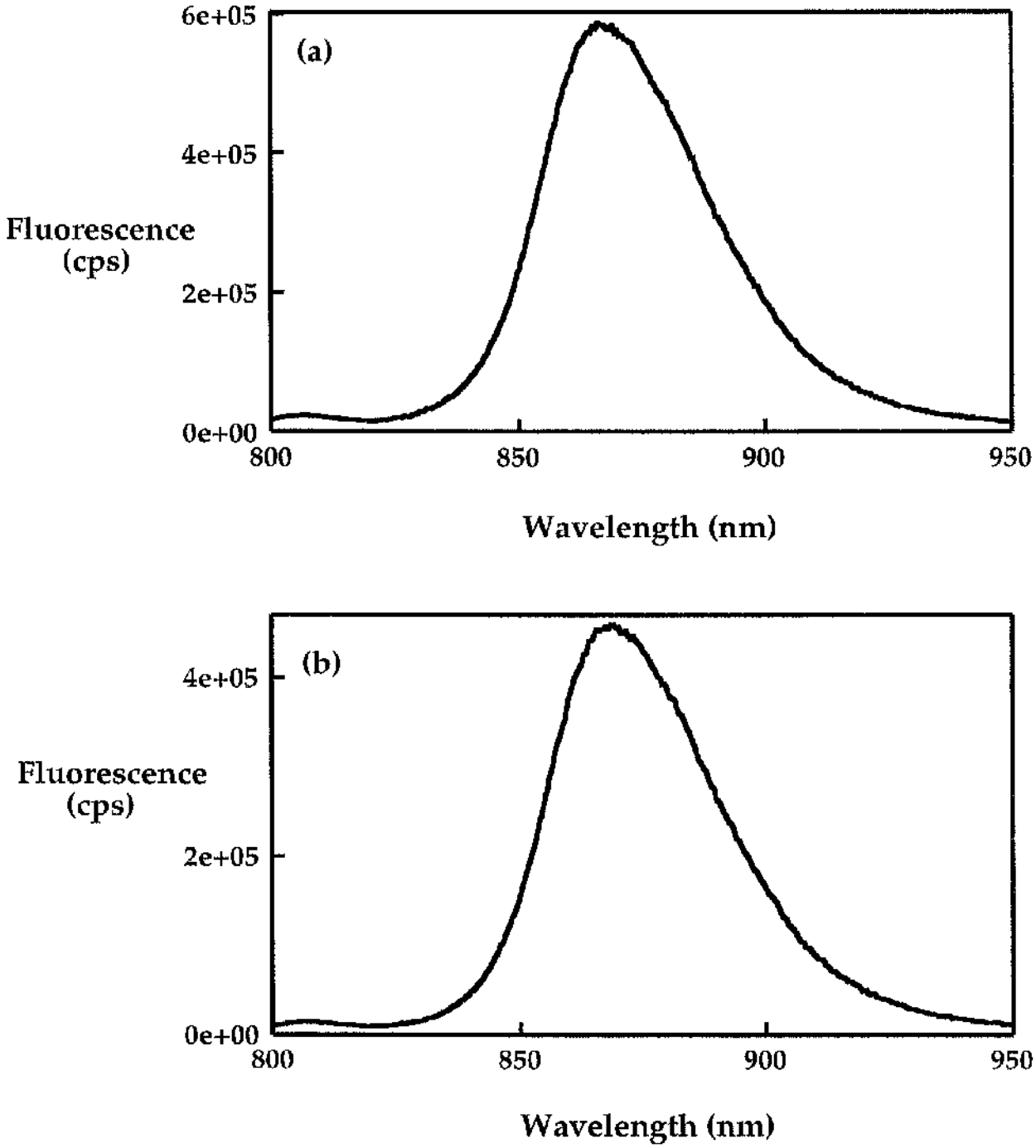

Figure 7f The fluorescence emission spectra of the (a) native and (b) Bchl*a*-B800 reconstituted complexes. In both complexes, the Bchl*a*-B800 molecules were excited on the blue side of their Q_y absorption band at 788 nm. Both emission spectra have a small peak at 805 nm and a large peak at 875 nm. These are due to fluorescence from the Bchl*a*-B800 and the -B850 molecules respectively. The efficiency of B800→B850 energy transfer in both complexes is very high.

B800 molecules is emitted as fluorescence by the Bchl*a*-B850 molecules. It can be concluded that the efficiency of B800→B850 energy transfer in nativeLH2 is very high. This experiment was repeated for the Bchl*a*-B800 reconstituted complex (see figure 7f). The fluorescence emission spectrum of the reconstituted complex is essentially the same as that of the native complex. The majority of the fluorescence emission comes from the Bchl*a*-B850 molecules (peak at 875 nm) though a small fraction of the fluorescence emission occurs directly from the Bchl*a*-B800 molecules (peak at 805 nm). This shows that the Bchl*a*-B800 molecules in the reconstituted complex can also transfer excitation energy to the Bchl*a*-B850 molecules with a very high efficiency.

7.6 Summary

In summary, the average occupancy of the B800 sites in the Bchl*a*-B800 reconstituted complex is approximately 80%. The reconstituted pigments are correctly bound within the complex and participate in efficient B800→B850 energy transfer. The overall structure of the LH complex is not affected by the pigment-exchange process.

8.1 Introduction

In chapter 6, a method was presented which allows the reconstitution of empty B800 binding sites with Bchl*a*. This chapter describes the use of this procedure with modified pigments to create complexes with altered spectral properties. The structural and energetic properties of the modified complexes were then characterised. The range of reconstituted complexes which can be made are described in Section 8.2. The occupancy of the B800 sites in selected reconstituted complexes was investigated by HPLC (see Section 8.3). Binding of the modified pigments in the reconstituted complexes was investigated by CD spectroscopy (see Section 8.4). The ability of the (B)Chl-B800 molecules to transfer excitation energy to the Bchl*a*-B850 molecules in each of the complexes was assessed by fluorescence emission spectroscopy (see Section 8.5).

8.2 Creating spectrally modified complexes

Reconstitution reactions were performed using geranylgeraniol Bchl*a*, 13^2OH Bchl*a*, pyro-Bchl*a*, 3^1vinyl Bchl*a*, 3^1OH Bchl*a*, acetyl Chl*a*, Chl*a*, Zn-Bph*e*, Cu-Bph*e* and Ni-Bph*e*. [The structures and spectral properties of these modified pigments are described in Section 2.4]. The conditions for the reconstitution reactions were the same as that for Bchl*a* (see Section 6.5.5). That is to say, B850-only complexes were incubated with a three fold excess of modified pigment at pH 8 for two hours at room temperature. The geranylgeraniol Bchl*a*, 13^2OH Bchl*a*, 3^1vinyl Bchl*a*, 3^1OH Bchl*a*, Zn-Bph*e*, acetyl Chl*a* and Chl*a* pigments undergo reconstitution whereas pyro-Bchl*a*,

Cu-Bphe and Ni-Bphe do not. The wavelengths of the "B800" Q_y absorption maxima in the reconstituted complexes are recorded in table 8i. The absorption spectra of selected reconstituted complexes are shown in figure 8a. The absorption spectra of the geranylgeraniol Bchl*a*- and 13^2OH Bchl*a*-B800 reconstituted complexes are the same as that for the Bchl*a*-B800 reconstituted complex (results not shown). The wavelengths of the "B800" Q_y maxima in the Zn-Bphe-, 3^1vinyl Bchl*a*-, 3^1OH Bchl*a*-, acetyl Chl*a*- and Chl*a*-B800 reconstituted complexes are 795, 765, 751, 693 and 669 nm respectively. The absence of an absorption shoulder at 800 nm in the 3^1vinyl Bchl*a*-, 3^1OH Bchl*a*-, acetyl Chl*a*- and Chl*a*-B800 reconstituted complexes shows that the B800 binding pockets do not contain any residual Bchl*a*. The absorption spectrum of the 3^1OH Bchl*a*-B800 reconstituted complex has a small shoulder at 680 nm. This is due to absorption by a 3^1OH Bchl*a* oxidation product. Both 3^1vinyl Bchl*a* and 3^1OH Bchl*a* are very prone to oxidation. As a consequence, it is very difficult to make these reconstituted complexes without them containing any oxidation products. The "B800" Q_y absorption peaks in the 3^1vinyl Bchl*a*-, 3^1OH Bchl*a*-, acetyl Chl*a*- and Chl*a*-B800 reconstituted complexes are smaller than that in the Bchl*a*-B800 reconstituted complex. This could be due to one of several different factors. The molar extinction coefficients of these pigments are less than that for Bchl*a* (see table 3i). This would explain, at least in part, the smaller peak heights. Alternatively, the average occupancy of the B800 sites in these reconstituted complexes may be less than that in the Bchl*a*-B800 reconstituted complex. The best way of determining the occupancy of the

Table 8i The "B800" Q_y maxima for reconstituted complexes containing modified pigments.

Complex	Wavelength of "B800" Q_y absorption maximum (nm)
native LH2	802
Reconstituted	
Bchl*a*-B800	802
geranylgeraniol Bchl*a*-B800	802
13^2OH Bchl*a*-B800	802
Zn-Bph*e*-B800	795
3^1vinyl Bchl*a*-B800	765
3^1OH Bchl*a*-B800	751
acetyl Chl*a*-B800	693
Chl*a*-B800	669

Figure 8a Absorption spectra of the A) native LH2, B) Zn-Bphe-, C) 3^{1}vinyl Bchl*a*-, D) 3^{1}OH Bchl*a*-, E) acetyl Chl*a*- and F) Chl*a*-B800 reconstituted complexes. The absorption spectra were recorded on a Shimadzu UV-2101PC. All of the samples had an OD_{859} of 0.5 cm^{-1}. The wavelengths of the "B800" Q_y absorption maxima are recorded in table 8i.

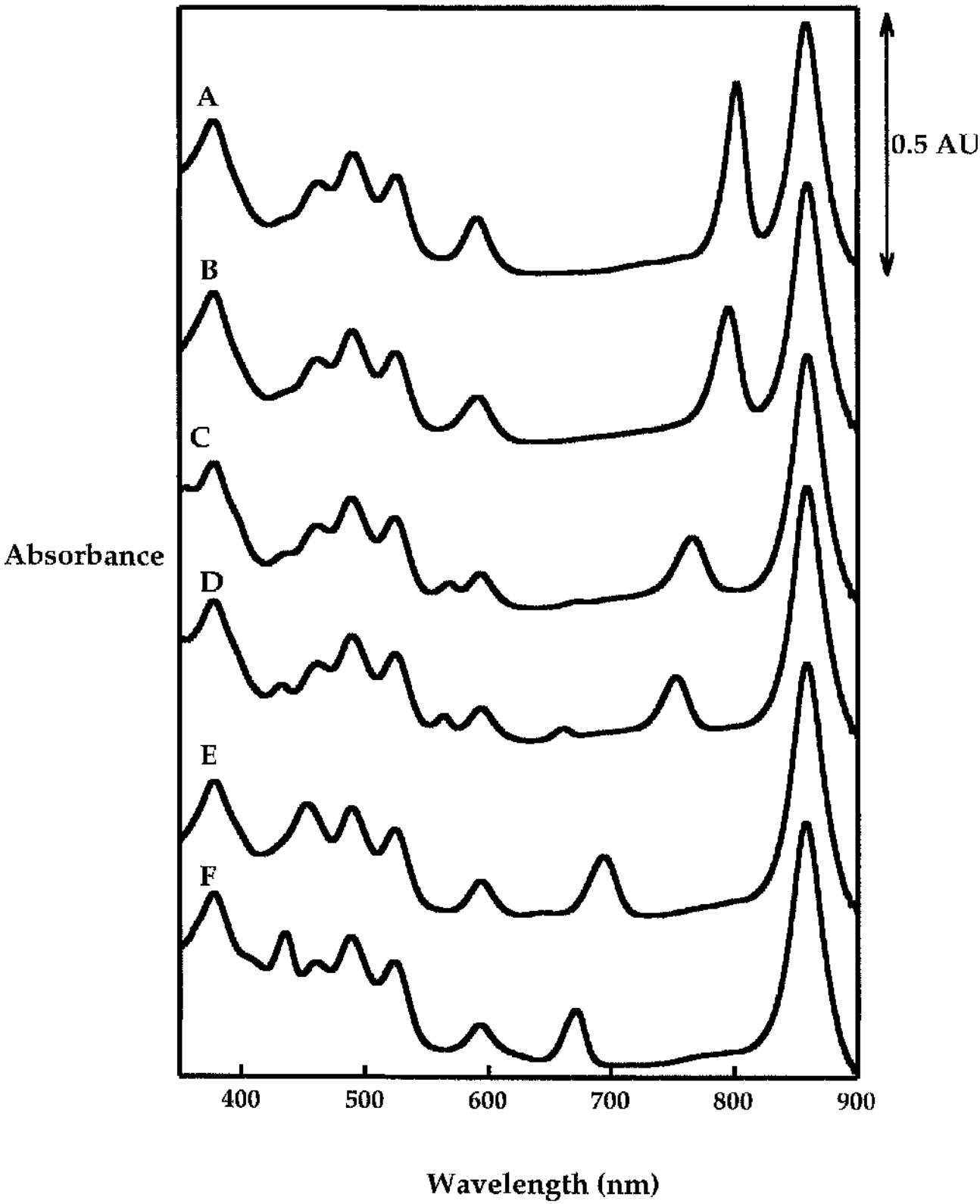
A
B
C
D
E
F
0.5 AU
Absorbance
400
500
600
700
800
900
Wavelength (nm)

B800 sites in these complexes is to extract the pigments from the complex and quantitate them by HPLC (see Section 8.3). The wavelengths of maximum absorption of the Soret and Q_x transitions of the (B)Chl-B800 molecules in the 3^1vinyl Bchl*a*-B800 reconstituted complex are 356 and 568 nm and in the 3^1OH Bchl*a*-B800 reconstituted complex are 350 and 563 nm (see figure 8a). In the acetyl Chl*a*- and Chl*a*-B800 reconstituted complexes, the Soret transitions of the acetyl Chl*a* and Chl*a* molecules can be clearly seen at 452 nm and 435 nm respectively.

It was not possible to reconstitute the B800 binding sites with either pyro-Bchl*a*, Cu-Bph*e* or Ni-Bph*e*. This can be explained in one of two ways. Firstly, the incubation conditions used are not optimal for reconstitution with these pigments or, secondly, that these pigments are unable to bind in the B800 pockets. In pyro-Bchl*a*, the methoxycarbonyl group at position $C13^2$ is removed. As pyro-Bchl*a* can not be reconstituted, it may suggest that the methoxycarbonyl group is essential for pigment binding. Pyro-Bchl*a* can not be reconstituted in either LH1 or RC complexes (Scheer & Struck 1993; Davis *et al.*, 1996). This is further evidence which suggests that the methoxycarbonyl group has an universally important role in pigment binding. The Cu^{2+} ion can only form four valent ligands. As it has no capacity to form a fifth bond with the protein, it is not surprising that it does not undergo reconstitution. Ni-Bph*e* can be incorporated into both RC and LH1 complexes by using a 10x fold rather than a 3x fold excess in the reconstitution mixture (Hartwich *et al.*, 1995b; Davis *et al.*, 1996). In an attempt to incorporate Ni-Bph*e* into the B800 sites, a reconstitution reaction

was performed using a 10 fold excess on Ni-Bphe. Even at this high concentration, it was not possible to reconstitute any of the B800 sites.

8.3 Determination of the occupancy of the B800 sites in each of the modified complexes by HPLC

8.3.1 Introduction

Before the modified reconstituted complexes could be characterised spectroscopically, it was first necessary to determine the occupancy of the B800 sites in each of the complexes. The absorption spectra of the geranylgeraniol Bchl*a*- and 13^2OH Bchl*a*-B800 reconstituted complexes are essentially the same as that of the Bchl*a*-B800 reconstituted complex. This suggests that the occupancy of the B800 binding pockets in these complexes is approximately 80%. The occupancy of the B800 sites in the 3^1vinyl Bchl*a*-, 3^1OH Bchl*a*-, acetyl Chl*a*- and Chl*a*-B800 reconstituted complexes can not be estimated from their absorption spectra (see discussion in Section 8.2). Rather, it was necessary to extract the pigments from the complex and quantitate them by HPLC. In this Section, efforts were made to determine the occupancy of the B800 sites in the 3^1vinyl Bchl*a*-, 3^1OH Bchl*a*-, acetyl Chl*a*- and Chl*a*-B800 reconstituted complexes by HPLC. The results are described in Section 8.3.2. The experimental method is detailed in Section 5.5.

8.3.2 Results

These experiments were performed towards the end of my thesis. By this stage, I only had a small quantity of each of the reconstituted samples left. This meant that it was not possible to conduct as thorough a HPLC study as was originally desired. On extraction from their respective reconstituted complexes, the 3^1vinyl Bchl*a* and 3^1OH Bchl*a* molecules were oxidised very easily. This prevented an accurate determination of the occupancy of the B800 sites in these complexes. Attempts to determine the pigment composition of the acetyl Chl*a* and Chl*a*-B800 reconstituted complexes were only slightly more successful. The elution profile of the pigments isolated from the Chl*a*-B800 reconstituted complex is shown in figure 8b. Using a hexane / isopropanol 85 : 15 (v/v) mixture, rhodopin, Chl*a* and Bchl*a* were eluted from the column with retention times of 3.6, 3.8 and 5.1 min respectively. On increasing the percentage of isopropanol to 40 %, rhodopin glucoside was eluted from the column with a retention time of 18.0 min. Acetyl Chl*a* and Bchl*a* extracted from the acetyl Chl*a*-B800 reconstituted complex were separated using a hexane / isopropanol 19 : 1 (v/v) mixture (results not shown). This is no small achievement because acetyl Chl*a* and Bchl*a* only differ in structure by a single double bond. For both complexes, the areas under the peaks were measured. The ratios of carotenoid : Bchl*a* : modified pigment in the acetyl Chl*a*- and Chl*a*-B800 reconstituted complexes are $1 : 0.7 \pm 0.1 : 0.6 \pm 0.1$ and $1 : 2.2 \pm 0.1 : 1.3 \pm 0.1$. In both complexes, the ratio of Bchl*a* : carotenoid should be 2 : 1. In the acetyl Chl*a*-B800 reconstituted complex, the measured ratio is 0.7 : 1. This suggests that,

Figure 8b Elution profile of the pigments extracted from the Chl*a*-B800 reconstituted complex. The pigments were separated on a silica column by HPLC. The Bchl*a*, Chl*a* and carotenoid molecules were detected at 773 (blue), 660 (yellow) and 470 (red) nm respectively. The peaks labelled 1, 2, 3 and 4 are rhodopin, Chl*a*, Bchl*a* and rhodopin glucoside respectively.

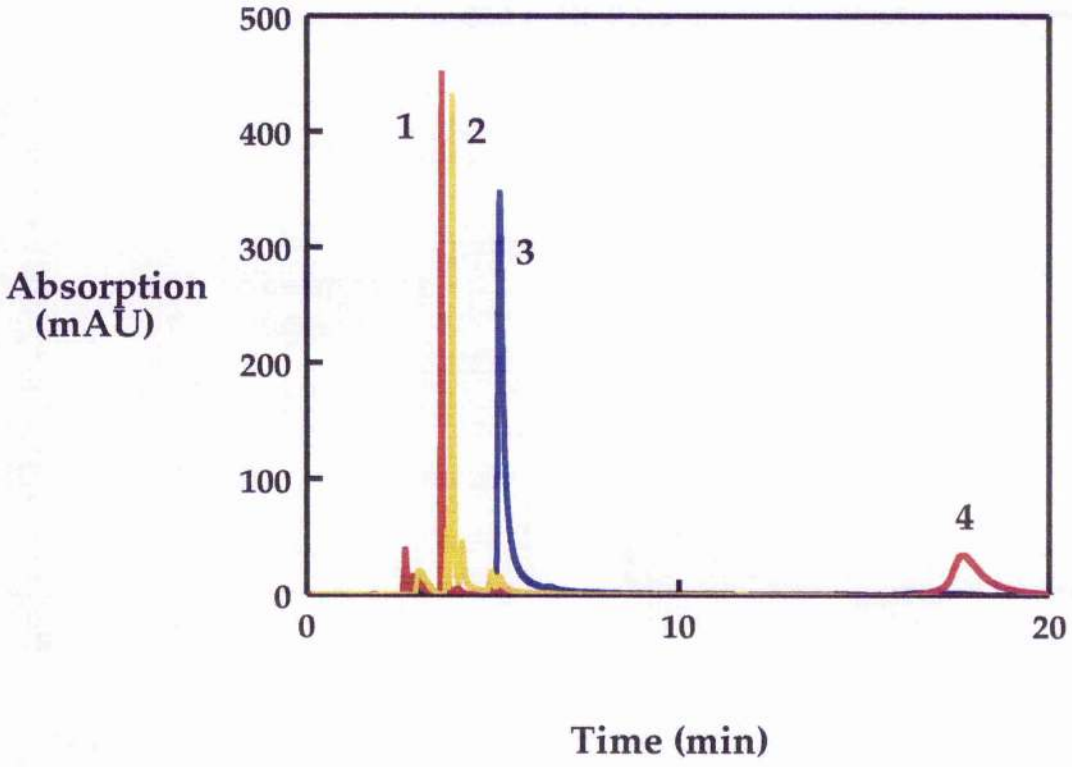
500
400
300
200
100
0
Absorption
(mAU)
1
2
3
4
0
10
20
Time (min)

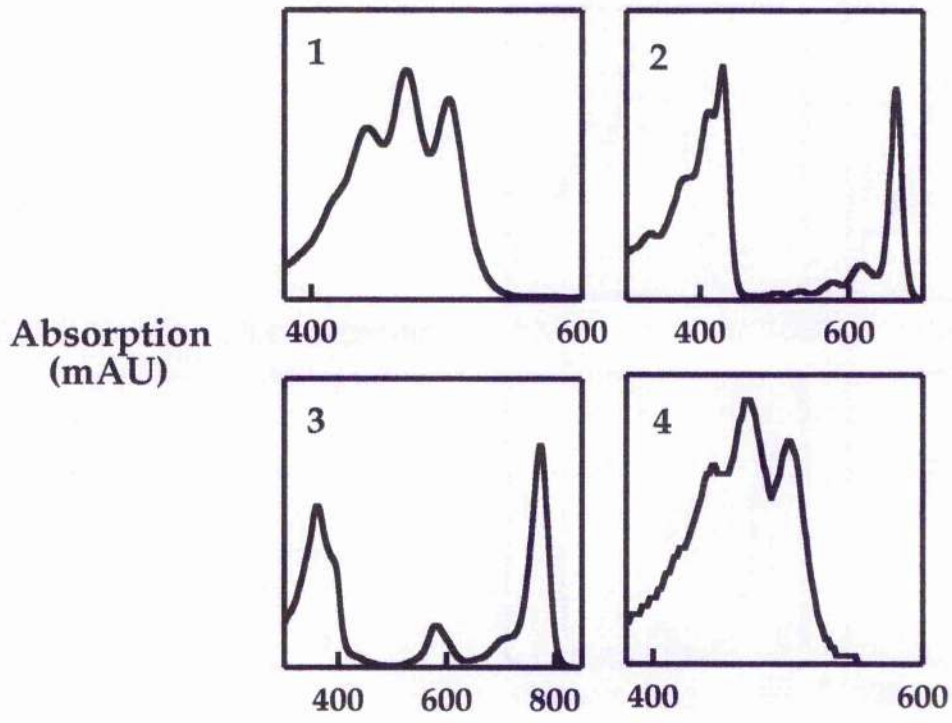
Absorption
(mAU)
1
2
3
4
400
600
400
600
400
600
800
400
600
Wavelength (nm)

for some unknown reason, the Bchl*a* has not been properly extracted from the reconstituted complex. As a consequence, the relative value for the acetyl Chl*a* molecules is not reliable. In the Chl*a*-B800 reconstituted complex, the measured ratio is 2.2 : 1. This is, within the upper limits of experimental error, that which is expected. Consequently, the relative value for the Chl*a* population (1.3) is also quite accurate. As the relative value is bigger than 1, it suggests that the reconstituted sample contains non-specifically bound chlorin molecules.

The results obtained in this Section are clearly not yet satisfactory. It has been shown that the system which was developed for determining the pigment ratios in the native complex also allows the separation of structurally similar pigments. That said, however, this method will require further development before the occupancies of the B800 sites in the 3^1vinyl Bchl*a*-, 3^1OH Bchl*a*-, acetyl Chl*a*- and Chl*a*-B800 reconstituted complexes can be accurately determined.

8.4 CD as a probe of the overall structure and binding of the (B)Chl-B800 pigments in the modified, reconstituted complexes

8.4.1 Introduction

In Section 7.3, the structure of the Bchl*a*-B800 reconstituted complex was investigated using CD. It was shown that the conformation adopted by and the arrangement of the Bchl*a*-B850 and carotenoid molecules in the Bchl*a*-B800 reconstituted complex is the same as that in native LH2. In addition,

the negative CD band associated with the Bchl*a*-B800 molecules, absent in the B850-only complex, is restored on reconstitution of the B800 binding pockets with Bchl*a*. This was interpreted as correct binding of the Bchl*a* molecules within the complex. In this Section, CD was used to investigate both the overall structure and pigment binding in each of the modified complexes. The results are presented in Section 8.4.2. The experimental method is detailed in Section 5.3.

8.4.2 CD spectra of the reconstituted complexes containing modified pigments

A typical CD spectrum of a reconstituted complex is shown in figure 8c. The CD spectra of the reconstituted complexes have certain features in common with that for native LH2. These are the shape of the CD signals associated with the Bchl*a*-B850 Q_y absorption transition and the carotenoid molecules (see figures 8c and 7d). That is to say, the CD signal associated with the Bchl*a*-B850 molecules (region 820 - 920 nm) consists of a positive band followed by a negative band. The CD signal associated with the carotenoid molecules (region 450 - 550 nm) has a three finger like shape consisting of three maxima separated by two minima. This suggests that the conformations adopted by and the organisation of the Bchl*a*-B850 and carotenoid molecules in the reconstituted complexes are the same as that in native LH2.

In all of the reconstituted complexes, a negative CD signal was observed at the wavelength of the "B800" Q_y absorption maximum (see figure 8c). By analogy with the Bchl*a*-B800 reconstituted complex, this suggests that the

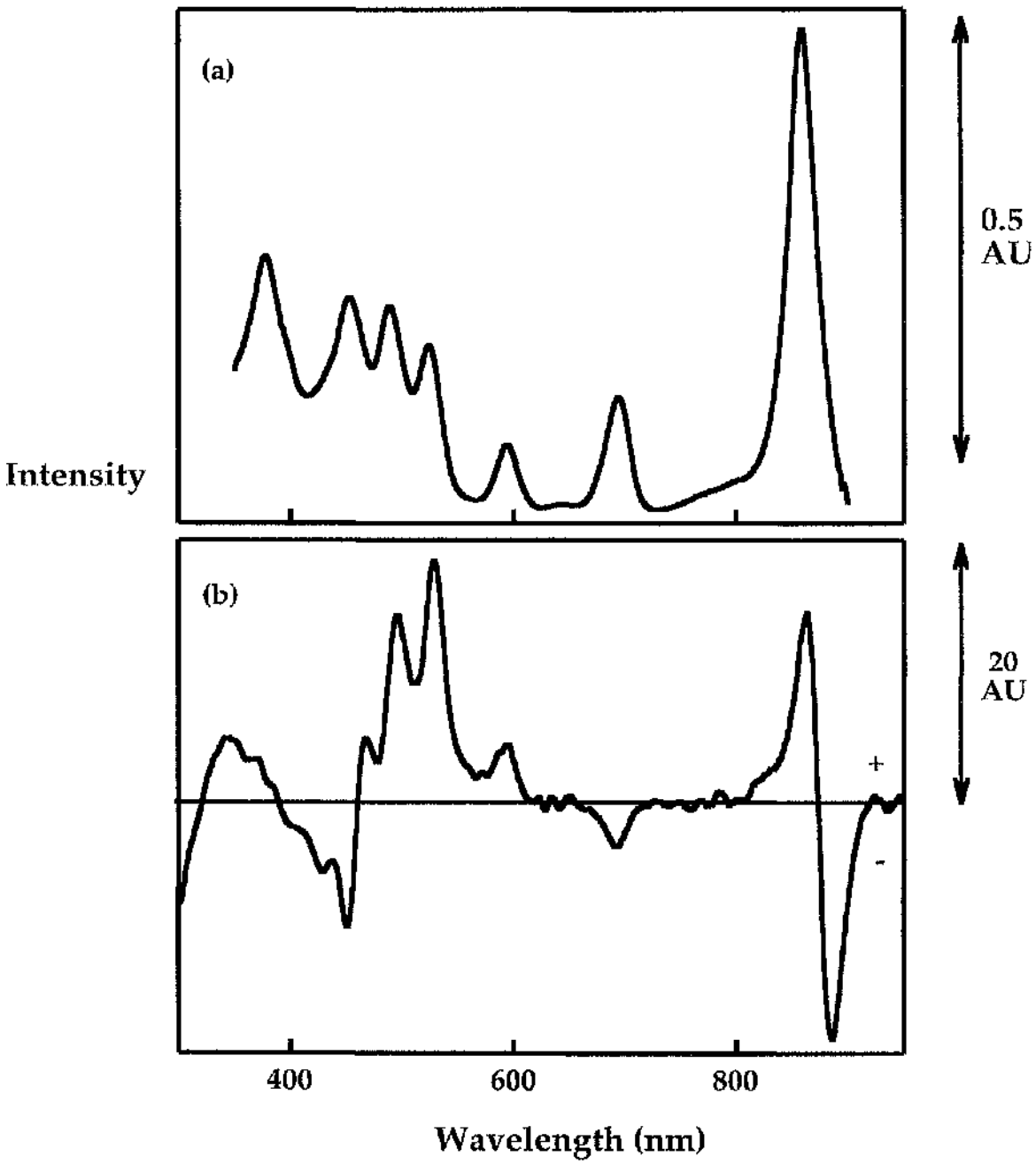

Figure 8c The (a) absorption and (b) CD spectra of the acetyl Chl*a*-B800 reconstituted complexes. The sample for absorption measurements had an OD_{859} of 0.5 cm^{-1} and for circular dichroism measurements had an OD_{859} of 0.6 cm^{-1}. The CD spectrum has a negative band at 692 nm. This is the same wavelength as the "B800" Q_y absorption maximum. This shows that the reconstituted molecules are correctly bound within the B800 pockets.

modified pigments are correctly bound within the B800 binding pockets. The CD signals associated with the Q_x and Soret transitions of the reconstituted pigments are different in the various reconstituted complexes. The CD signals associated with the Soret and Q_x transitions of the Bchl*a* molecules in the geranylgeraniol Bchl*a*- and 13^2OH Bchl*a*-B800 reconstituted complexes are the same as that for native LH2 (see figure 7c). The CD signal associated with the Bchl*a* Q_x absorption transition in the 3^1vinyl Bchl*a*- and 3^1OH Bchl*a*-B800 reconstituted complexes has an extra maximum at 565 and 562 nm respectively compared to the native complex. These maxima have the same wavelengths as those in their absorption spectra (see figure 8a). In both the 3^1vinyl Bchl*a*- and 3^1OH Bchl*a*-B800 reconstituted complexes, the CD signals associated with the Soret absorption transition of the Bchl*a* molecules are the same as those in the native complex. In the acetyl Chl*a*- and Chl*a*-B800 reconstituted complexes, however, the CD signal associated with the Soret absorption transition of the reconstituted pigments can be clearly seen as a maximum at 468 and 415 nm in the respective complexes (see figure 8c). These maxima have the same wavelengths as those in their absorption spectrum. In these complexes, the CD signal associated with the Soret transition of the Bchl*a*-B850 molecules (region 300- 400 nm) is the same as that which is observed in the B850-only complex (compare figures 8c and 7c).

8.5 Investigating B800 to B850 energy transfer in the modified, reconstituted complexes by fluorescence emission spectroscopy

8.5.1 Introduction

The efficiency of B800→B850 energy transfer can be investigated by fluorescence emission spectroscopy (see Section 7.6.1). In this Section, the ability of the (B)Chl-B800 molecules in each of the reconstituted complexes to transfer excitation energy to the Bchl*a*-B850 molecules was studied. The results are presented in Section 8.5.2. The experimental methods are described in Section 5.2.2.

8.5.2 Fluorescence emission spectra of the reconstituted complexes

The fluorescence emission spectra of the reconstituted complexes can be divided into two main groups. A typical spectrum of both groups are shown in figure 8d.

The fluorescence emission spectra of the geranylgeraniol Bchl*a*-, 13^2OH Bchl*a*-, Zn-Bph*e*-and 3^1OH Bchl*a*-B800 reconstituted complexes are similar to that for the reconstituted complex containing 3^1vinyl Bchl*a* (see figure 8d). This type of spectrum has two emission bands - a small peak (which corresponds to fluorescence from the (B)Chl-B800 molecules) and a large peak at 875 nm (which corresponds to fluorescence from the Bchl*a*-B850 molecules). The wavelength of maximum fluorescence from the (B)Chl-B800 molecules is different in the various reconstituted complexes and is approximately 5 nm to the red of its (B)Chl-B800 Q_y absorption maxima. In

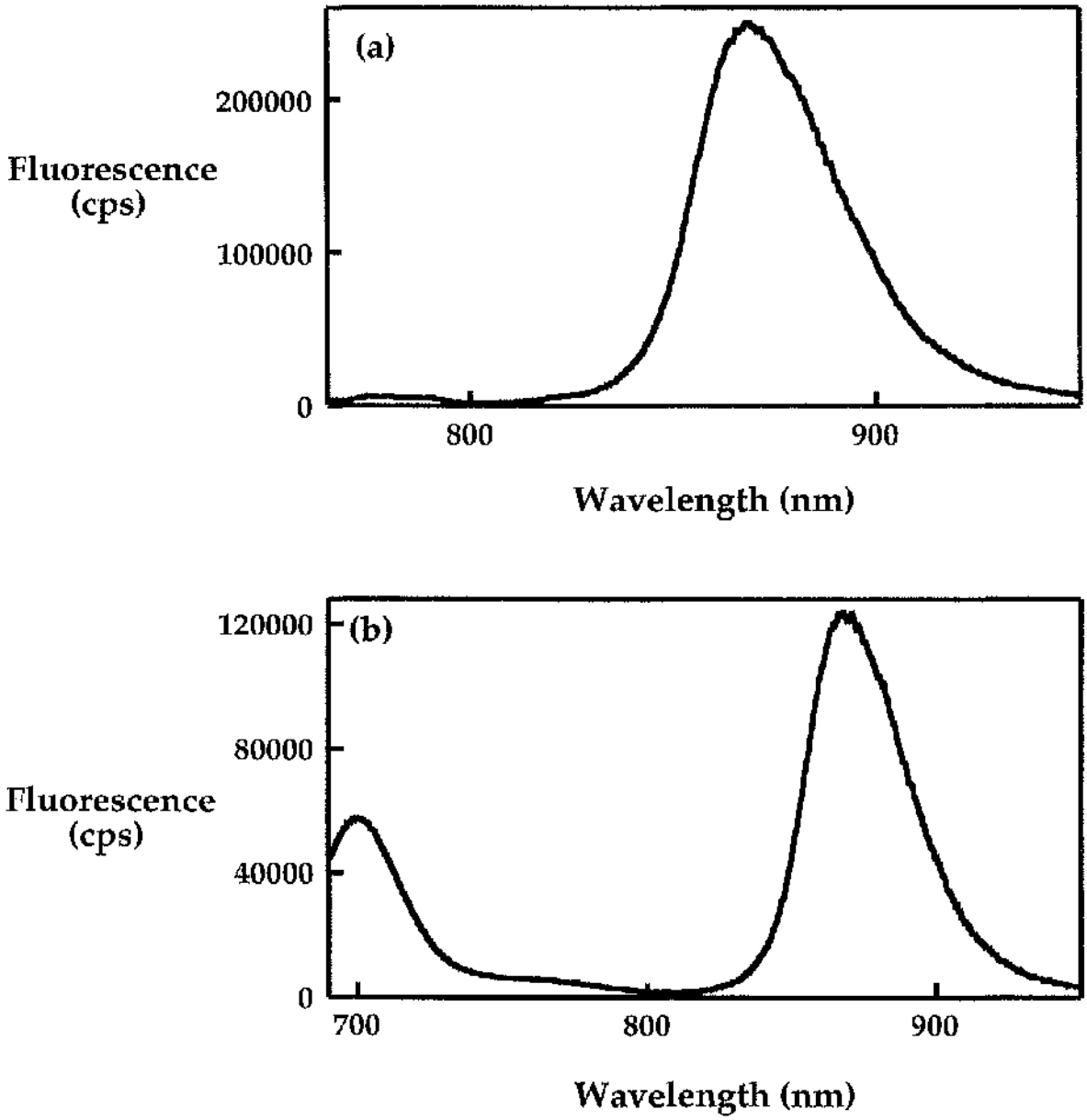

Figure 8d Fluorescence emission spectra of (a) 3^1 vinyl Bchl*a*- and (b) acetyl Chl*a*-B800 reconstituted complexes. Both samples had an OD_{859} of 0.1 cm^{-1}. In a), predominantly all of the fluorescence emission occurs from the Bchl*a*-B850 molecules. This shows that the (B)Chl-B800 molecules efficiently transfer excitation energy to the Bchl*a*-B850 molecules. In b), the majority of the fluorescence comes from the Bchl*a*-B850 molecules. This shows that those (B)Chl-B800 molecules which are correctly bound in the reconstituted complex participate in efficient B800→B850 energy transfer. Appreciable fluorescence from the (B)Chl-B800 molecules is also observed. This is probably due to fluorescence from non-specifically bound chlorin molecules.

these reconstituted complexes, it can be concluded that predominantly all of the excitation energy absorbed by the (B)Chl-B800 molecules is efficiently transferred to the Bchl*a*-B850 molecules.

The fluorescence emission spectra of the acetyl Chl*a*- and Chl*a*-B800 reconstituted complexes also have two emission peaks. Different from the first type of spectrum, however, is the relative heights of the two emission peaks. The bigger of the two emission bands is the one with a maximum value at 875 nm and is due to fluorescence from the Bchl*a*-B850 molecules. This shows that those (B)Chl-B800 molecules which are correctly bound within these reconstituted complexes efficiently transfer their excitation energy to the Bchl*a*-B850 molecules. In these complexes, however, appreciable fluorescence from the (B)Chl-B800 molecules also occurs. The most likely explanation for this observation is that the samples contains a small amount of non-specifically attached chlorin molecules which are unable to transfer their energy to the Bchl*a*-B850 molecules. If this were true, an obvious improvement for future preparations of these complexes would be to include another purification step to remove these non-specifically bound pigments.

8.6 Summary

The B800 binding sites can be reconstituted with a wide range of modified (bacterio)chlorin molecules including geranylgeraniol Bchl*a*, 13^2OH Bchl*a*, Zn-Bph*e*, 3^1vinyl Bchl*a*, 3^1OH Bchl*a*, acetyl Chl*a* and Chl*a*. In the 3^1vinyl Bchl*a*-, 3^1OH Bchl*a*-, acetyl Chl*a*- and Chl*a*-B800 reconstituted complexes, the

"B800" Q_y absorption bands have maxima at 765, 751, 693 and 669 nm respectively. As judged by CD spectroscopy, the reconstituted pigments are correctly bound within the complex. As shown by fluorescence emission experiments, those (B)Chl-B800 molecules which are correctly bound in all of the reconstituted complexes efficiently transfer their excitation energy to the Bchl*a*-B850 molecules.

9.1 Introduction

One important parameter in determining the rate of energy transfer between two molecules is the spectral overlap between the emission spectrum of the donor molecule and the absorption spectrum of the acceptor molecule. The various reconstituted complexes which are described in Chapter 8, in particular the 3^1vinyl Bchl*a*-, 3^1OH Bchl*a*-, acetyl Chl*a*- and Chl*a* –B800 reconstituted complexes, have altered spectral overlap functions compared to native LH2. In this Chapter, the effect of spectral overlap on the rate of B800→B850 energy transfer was investigated by measuring the rates of energy transfer in the reconstituted complexes (see Section 9.2). The predicted transfer time for each complex was modelled according to Förster's dipole-dipole, weak interaction mechanism (see Section 9.3). Comparison of the actual and predicted transfer times allowed the appropriateness of Förster's theory to fully describe B800→B850 energy transfer to be assessed. In addition, the effect of spectral overlap on the efficiency of B800→B850 energy transfer was studied (see Section 9.4).

9.2 The kinetics of B800→B850 energy transfer

9.2.1 Introduction

The kinetics of B800→B850 energy transfer can be studied in two different ways. Energy transfer can be followed by measuring either the decay of the Bchl*a*-B800 excited state population (Bchl*a*-B800*) or the arrival of the excitation energy at the Bchl*a*-B850 molecules with time. In this Chapter, fs transient absorption techniques were used to measure both the decay of the

Bchl*a*-B800 and the rise in the -B850 excited state populations with time. The principles of transient absorption spectroscopy are outlined in Section 9.2.2. The actual kinetic data which was obtained for the native and reconstituted complexes is recorded in Sections 9.2.3 and 9.2.4. The experimental methods are fully described in Section 5.5.

9.2.2 Transient absorption spectroscopy

In transient absorption measurements, the sample is excited with a pump pulse. At various time delays, the excited region is probed with a second weak pulse of light of known wavelength. The ability of the excited region to absorb probe light is compared to that of an unexcited region. The difference in absorption between the excited and unexcited regions, ΔA, gives a direct measure of the capacity of the molecules in the excited region to absorb further excitation energy relative to that in the unexcited region. All of the transient absorption experiments which were performed in this study were two colour experiments. That is to say, the sample was pumped with light of one wavelength and was probed with light of a different wavelength. The samples were always pumped on the blue edge of their "B800" Q_y absorption band. In those measurements where the decay of the excitation energy from the (B)Chl-B800 molecules was being followed, the probe and reference pulses were set to an appropriate wavelength on the red side of the "B800" Q_y absorption band. In those measurements where the arrival of excitation energy at the Bchl*a*-B850 molecules was being followed, the probe and reference pulses were set to the wavelength of maximum

bleaching of the Q_y absorption band of the Bchl*a*-B850 molecules. Dependent upon the wavelength of the probe pulses, it was possible to determine the time dependent bleaching of either the "B800" or the B850 Q_y absorption bands. By fitting these kinetics, it was possible to determine the time constant for B800→B850 energy transfer in each complex.

9.2.3 Isotropic kinetics in the (B)Chl-B800 Q_y band

The kinetics of the bleaching and recovery of the "B800" Q_y absorption band were studied in native LH2 and Bchl*a*-, 3^1vinyl Bchl*a*-, 3^1OH Bchl*a*-, acetyl Chl*a*- and Chl*a*-B800 reconstituted complexes. A typical kinetic trace is shown in figure 9a. All of the kinetic traces had the same general pattern. On excitation of the Q_y absorption band of the (B)Chl-B800 molecules, a rapid bleaching occurred. With time, the bleach decayed with ΔA returning towards zero. In most of the complexes, after energy transfer to the Bchl*a*-B850 molecules was complete, ΔA had positive values. These positive ΔA values are due to excited-state absorption (ESA) by the Bchl*a*-B850 molecules. In the acetyl Chl*a*- and Chl*a*-B800 reconstituted complexes, however, ΔA did not have a positive value at any time delay (results not shown). This is because the contribution of B850 ESA to the ΔA signal at the probe wavelengths of 680 and 705 nm used in these measurements was negligible. For each complex, the contribution from B850 ESA was subtracted from the raw data before the kinetics were fitted (see figure 9b). In each complex, the rise in bleaching of the "B800" Q_y absorption band was found to have two components - an instantaneous component and a

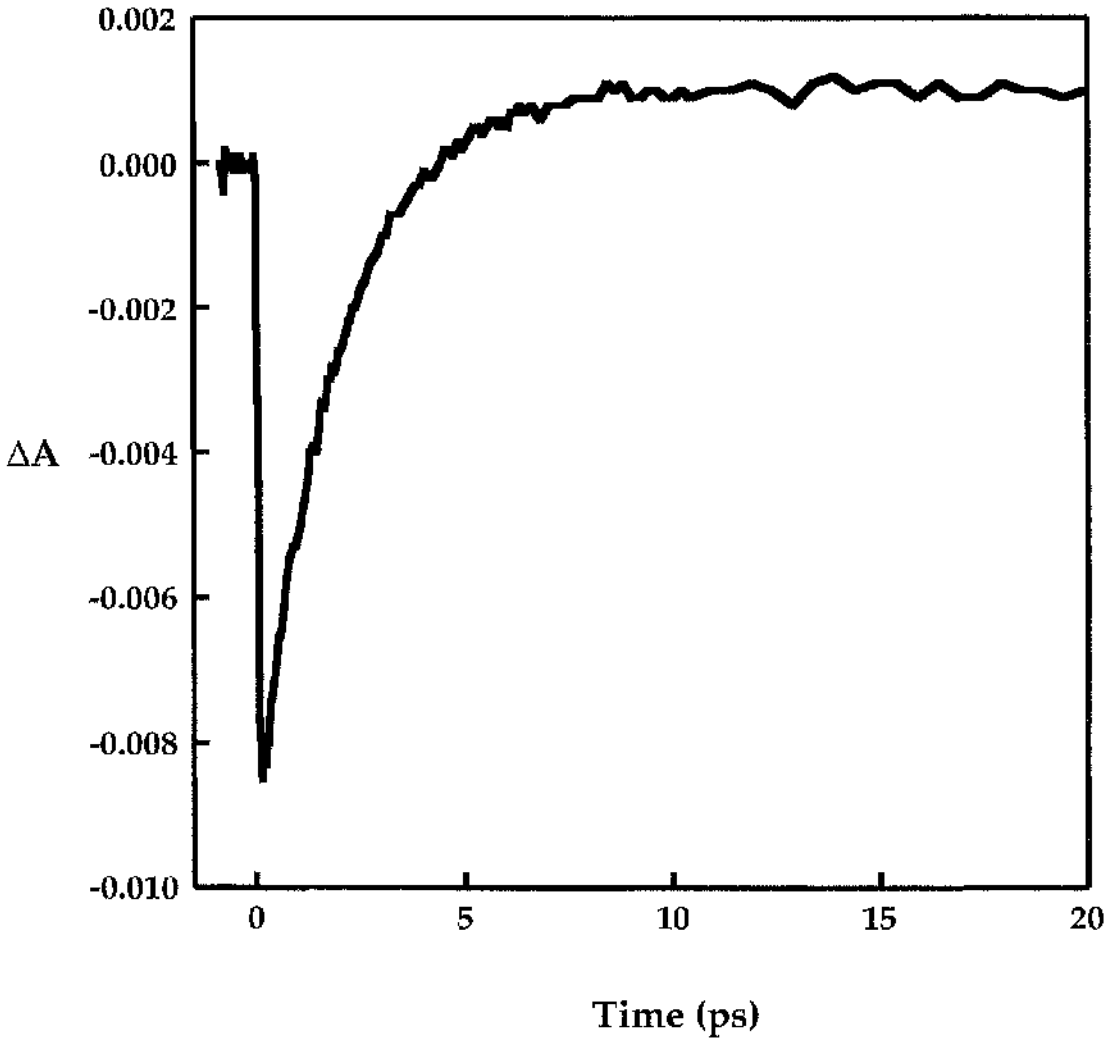

Figure 9a Isotropic kinetic data showing the time-dependent bleaching and recovery of the "B800" Q_y absorption band in LH2 complexes reconstituted with 3^1OH Bchl*a*. On excitation of the Q_y transition of the 3^1OH Bchl*a*-B800 molecules, a rapid bleaching of the band occurred. Within approximately 5 ps, the bleach had completely decayed. At times greater than 5 ps , ΔA had a positive value. These positive ΔA values are due to excited state absorption (ESA) by the Bchl*a*-B850 molecules.

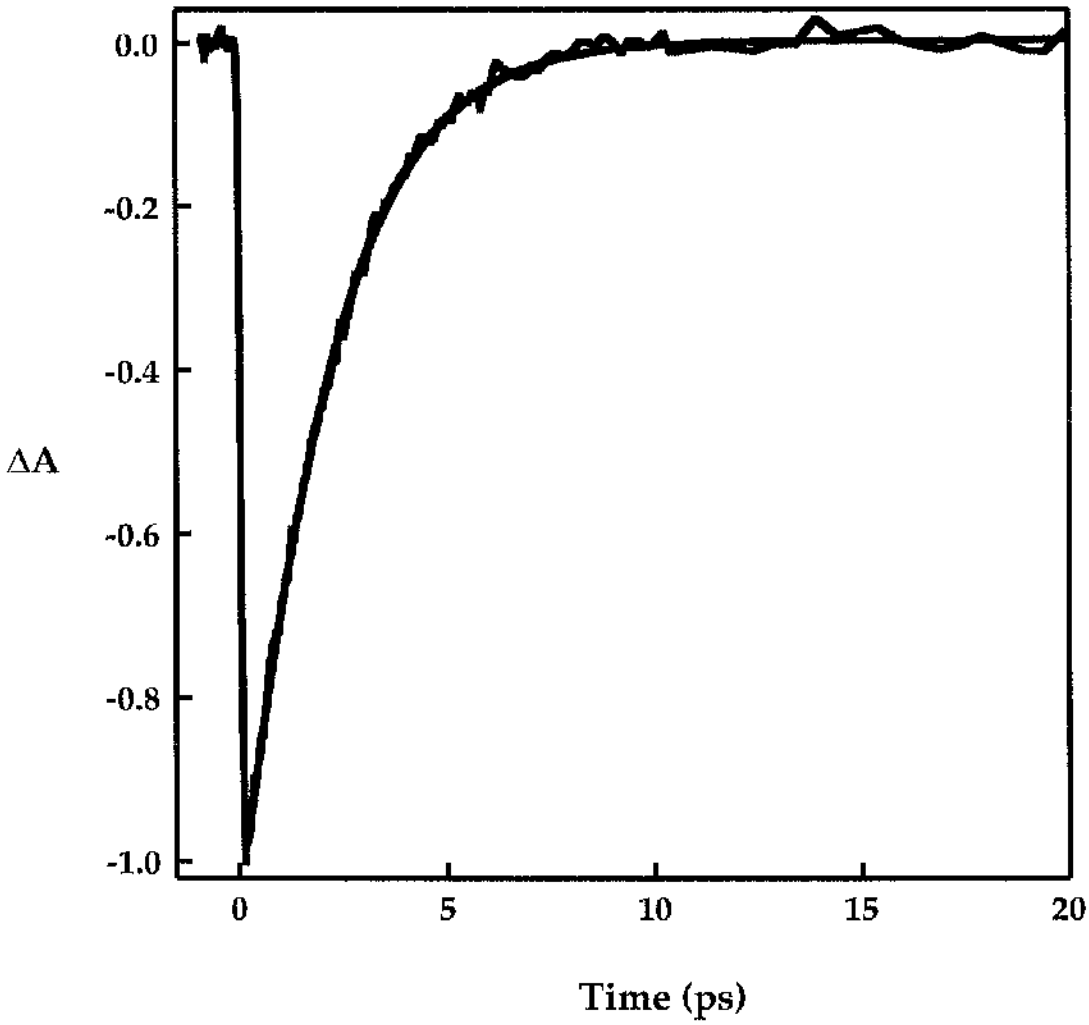

Figure 9b Calculated isotropic kinetics for the bleaching and recovery of the "B800" Q_y absorption band in 3^1OH Bchl*a*-B800 reconstituted complexes from which the contribution of B850 ESA has been subtracted. The wavelengths of the pump and probe beams were 742 and 760 nm respectively. The sample had an OD_{742} =1 cm^{-1}. On excitation of the "B800" Q_y absorption transition, 59% of the band bleached instantly. The remaining 41% bleached with a time constant of 1.2 ps. This is due to energy equilibration within the inhomogenously broadened "B800" Q_y absorption band. The decay of the bleaching was fitted with a single exponential and the time constant for B800→B850 energy transfer determined to be 1.8 ps (see table 9i).

variable, slower component. The lifetime of this slow component varied from 0.4 ps in the native complex to a maximum of 3.3 ps in the Chl*a*-B800 reconstituted complex (see table 9i). This slow rise component is most probably due to energy equilibration within the inhomogeneously broadened "B800" Q_y absorption band and likely represents energy transfer from those pigments on the blue side of the transition to those on the red side (Monshouwer & van Grondelle, 1996).

For each kinetic trace, the decay of the "B800" Q_y absorption band bleach was fitted with a single exponential and the time constant for B800→B850 energy transfer determined as described in chapter 5.5 (see table 9i). In both the native and Bchl*a*-B800 reconstituted complexes, B800→B850 energy transfer takes approximately 0.9 ps. This suggests that the Bchl*a*-B800 pigments in the reconstituted complex adopt a functionally active conformation similar to those in native LH2. In the 3^1vinyl Bchl*a*-, 3^1OH Bchl*a*-, acetyl Chl*a*- and Chl*a*-B800 reconstituted complexes, the rate of B800→B850 energy transfer was found to decrease as the spectral separation between the "B800" and the B850 Q_y absorption bands increased (see table 9i). The effect on the rate of B800→B850 excitation transfer was surprisingly small, however, given the apparent large decrease in spectral overlap. In the furthest blue-shifted, Chl*a*-B800 reconstituted complex, the time constant for B800→B850 energy transfer is 8.4 ps. This only corresponds to a 10 fold decrease in the rate of energy transfer compared to that which occurs in the native complex.

Table 9i Calculated isotropic kinetic data for the bleaching and recovery of the "B800" Q_y absorption band in native LH2 and selected reconstituted complexes. All samples were excited on the blue side and probed on the red side of their "B800" Q_y absorption band. The kinetic data was corrected for B850 ESA prior to fitting. The rise in bleaching of the (B)Chl-B800 molecules has two components - an instantaneous component and a slower, variable component (see figure 9b). For each complex, the decay of the bleach was fitted with a single exponential and the time constant for B800→B850 energy transfer determined (see figure 9b).

Complex	Pump and probe wavelengths (nm)	Slow rise component in the "B800" Q_y band bleach τ_{rise} (ps) (% contribution)	Time constant for B800 to B850 energy transfer, τ (ps)
LH2	785, 810	0.4 +/- 0.1 (57%)	0.9 ± 0.1
Bchl*a*-B800	785, 810	0.7 +/- 0.1 (75%)	0.9 ± 0.1
3^1vinyl Bchl*a*-B800	754, 775	100% instantaneous	1.5 ± 0.2
3^1OH Bchl*a*-B800	742, 760	1.2 +/- 0.1 (41%)	1.8 ± 0.2
acetyl Chl*a*-B800	685, 705	2.3 +/- 0.2 (43%)	4.6 ± 0.5
Chl*a*-B800	660, 680	3.3 +/- 0.3 (27%)	8.4 ± 0.5

Table 9ii The time constants for B800→B850 energy transfer in native and reconstituted complexes as determined from the time-dependent rise in the bleaching of the B850 Q_y absorption band after excitation of their (B)Chl-B800 molecules. The samples were all excited on the blue edge of their "B800" Q_y absorption bands. Bleaching of the B850 Q_y absorption band was probed at 870 nm. The rise kinetics were all fitted with a single exponential and the time constants for B800→B850 energy transfer determined (see figure 9c).

Complex	Excitation wavelength (nm)	Time constant for B800 to B850 energy transfer τ (ps)
LH2	785	0.9 ± 0.1
Bchl*a*-B800	785	0.9 ± 0.1
gg Bchl*a*-B800	785	0.8 ± 0.1
13^2OH Bchl*a*-B800	785	0.8 ± 0.1
Zn-Bph*e*-B800	785	0.8 ± 0.1
3^1vinyl Bchl*a*-B800	754	1.4 ± 0.2
3^1OH Bchl*a*-B800	742	1.8 ± 0.2
acetyl Chl*a*-B800	685	4.4 ± 0.5
Chl*a*-B800	663	8.5 ± 0.5

9.2.4 B850 rise kinetics

Typical kinetic traces for the rise in bleaching of the B850 Q_y absorption band with time are shown in figure 9c. In all of the complexes, the rise kinetics have two components - a small, instantaneous component and a slower, variable component. The origin of the instantaneous component was investigated in a series of control experiments using B850-only complexes. The B850-only complexes were used as a control as they allowed the rise kinetics of the bleaching of the B850 Q_y absorption band to be studied in the absence of any absorption by the (B)Chl-B800 molecules. The B850-only sample was excited at the same wavelengths as were used in the measurements on the reconstituted complexes (see table 9ii). At each excitation wavelength, the B850 Q_y absorption band was found to bleach on a timescale quicker than could be accurately time resolved (results not shown). This suggested that the instantaneous component in the rise kinetics of B850 Q_y absorption band bleaching in the reconstituted complexes is due to direct excitation of the Bchl*a*-B850 molecules (which have a low broad absorption throughout the spectral region 650 to 800nm). The variable, slower component in the rise kinetics is due to the arrival of excitation energy from the (B)Chl-B800 molecules. For each data set, the non-instantaneous rise kinetics were fitted with a single exponential and the time constant for B800→B850 energy transfer determined as described in chapter 5.5 (see table 9ii).

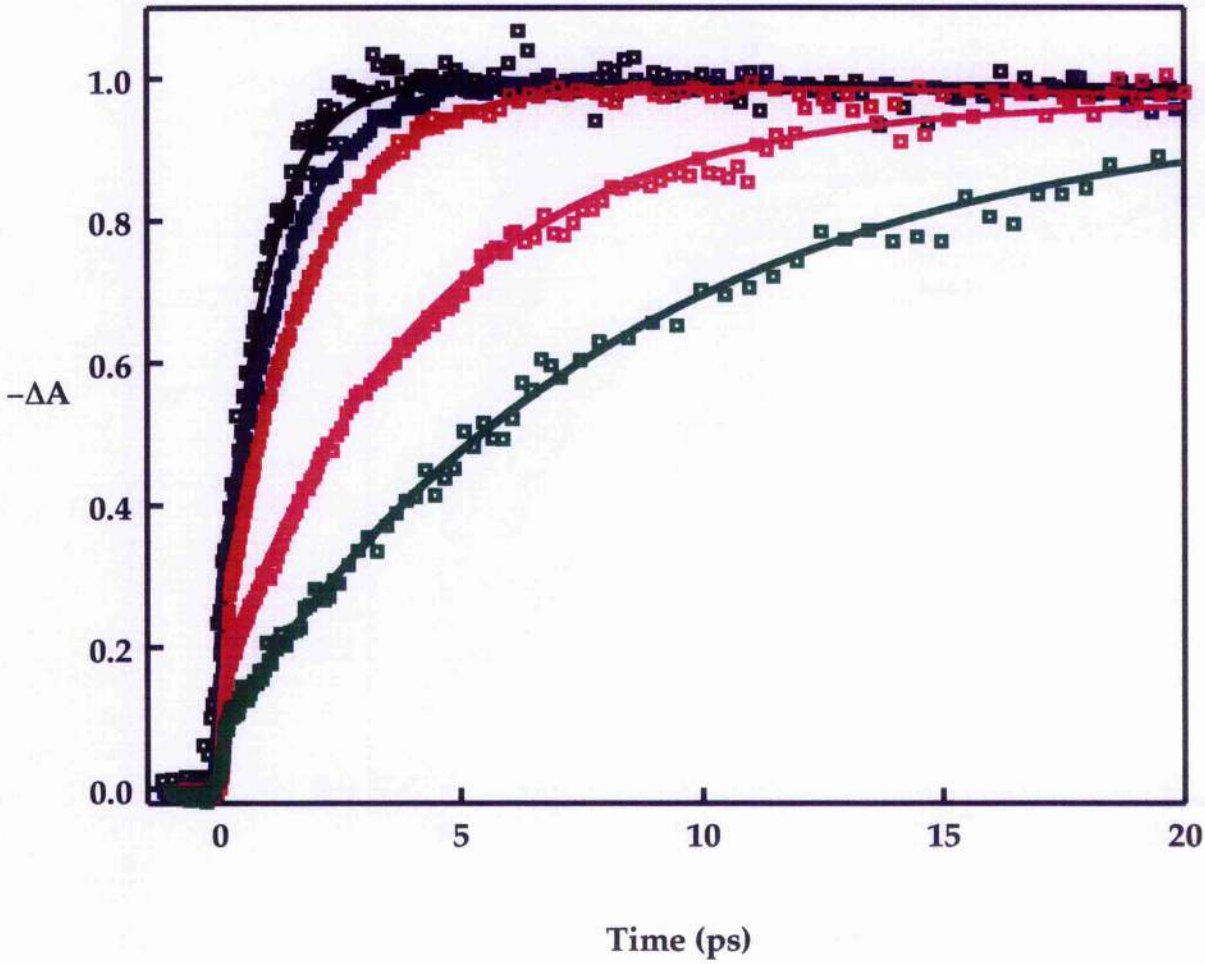

Figure 9c The rise in bleaching of the Q_y absorption band of the Bchl*a*-B850 molecules with time in native LH2 and selected reconstituted complexes after Q_y excitation of their (B)Chl-B800 molecules. The excitation wavelengths are recorded in table 9ii. The arrival of energy at the Bchl*a*-B850 molecules was followed by measuring their bleaching at 870 nm. The rise kinetics were all fitted with single exponentials. The time constants for B800→B850 energy transfer are recorded in table 9ii.

Key Black LH2, Blue 3^1vinyl Bchl*a*-, Red 3^1OH Bchl*a*-, Pink acetyl Chl*a*-, and Green Chl*a*-B800 reconstituted complexes.

In the native LH2 and Bchl*a*-, geranylgeraniol Bchl*a*-, 13^2OH Bchl*a*- and Zn-Bph*e*-B800 reconstituted complexes, B800→B850 energy transfer takes approximately 0.9 ps. This is not surprising as the spectral overlap function in these complexes is roughly the same. In the 3^1vinyl Bchl*a*-, 3^1OH Bchl*a*-, acetyl Chl*a*- and Chl*a*-B800 reconstituted complexes the time constants for B800→B850 energy transfer are 1.4, 1.8, 4.4 and 8.5 ps respectively. These values are, within the limits of experimental error, the same as those determined by measuring the decay of the bleach of the "B800" Q_y absorption bands (see tables 9i and 9ii). These results show that the rate of B800→B850 energy transfer decreases as the spectral overlap between the "B800" and B850 Q_y bands is reduced.

9.3 Modelling the rate of B800→B850 energy transfer in native and selected reconstituted complexes by Förster theory

According to Förster theory, the rate of energy transfer rate between two molecules is proportional to the overlap integral between the emission spectrum of the donor, $f_D(v)$, and the absorption spectrum of the acceptor molecules, $\varepsilon_A(v)$ according to the equation

$$K_{et} = C \int f_D(v)\, \varepsilon_A(v)\, dv$$

where K_{et} is the rate of energy transfer and C is a constant. Strictly speaking, C is not independent of v, but in these qualitative calculations its weak wavelength dependence was ignored. In each complex, the spectral overlap between the fluorescence emission spectrum of the (B)Chl-B800 molecules and the Q_y absorption transition of the Bchl*a*-B850 molecules was

determined. This can be done in one of two ways - either by direct measurement or by modelling the fluorescence emission spectrum of the (B)Chl-B800 and the absorption spectrum of the Bchl*a*-B850 pigments. The excited state lifetimes of the (B)Chl-B800 molecules in the various complexes are very short. As a consequence, it is very difficult to detect fluorescence emission from these pigments. Even if it were possible to accurately measure their emission spectra, they would be inhomogeneously broadened. This is not desirable because each spectrum would consist of a series of emission spectra arising from a heterogenous population of pigment molecules which have different site energies. Rather, it is preferable to know the homogeneously broadened spectra of both the donor and acceptor pigments. For these reasons, the overlap integral in each of the complexes was determined by calculating the fluorescence and absorption spectra of the donor and acceptor pigments as described by Hess *et al.* (1994) [N.B. These calculations were performed by Dr. Tonu Pullerits from the Dept. of Chemical Physics at the University of Lund, Sweden]. These calculations do not give absolute values for the rate of B800→B850 energy transfer in the modified complexes. Rather, they allow the effect of spectral overlap on the measured and calculated rates of B800→B850 energy transfer to be compared. The calculated transfer rates were normalised with the measured rate in the native complex (see figure 9d). In the native, Zn-Bph*e*-, 3^1vinyl Bchl*a*- and 3^1OH Bchl*a*-B800 reconstituted complexes, the measured rates are, within the limits of experimental error, the same as that predicted by Förster. In the acetyl Chl*a*- and Chl*a*-B800 reconstituted

Figure 9d Dependence of the rate of B800→B850 energy transfer on the spectral separation between the (B)Chl-B800 and B850 Q_y absorption bands (energy gap). Squares represent the experimentally determined time constants. The solid line is the calculated dependence as predicted by Förster theory. The calculated dependence was normalised with the measured rate in native LH2. In the native, Zn-Bphe-, 3^1vinyl Bchl*a*- and 3^1OH Bchl*a*-B800 reconstituted complexes, the measured rates are, within the limits of experimental error, the same as that predicted by Förster. In the acetyl Chl*a*- and Chl*a*-B800 reconstituted complexes, the measured rates are much faster than Förster would predict. Here, it can be concluded that B800→B850 energy transfer is not adequately described by Förster's theory assuming that the only B850 acceptor state which is involved in the transfer process is the Q_y state.

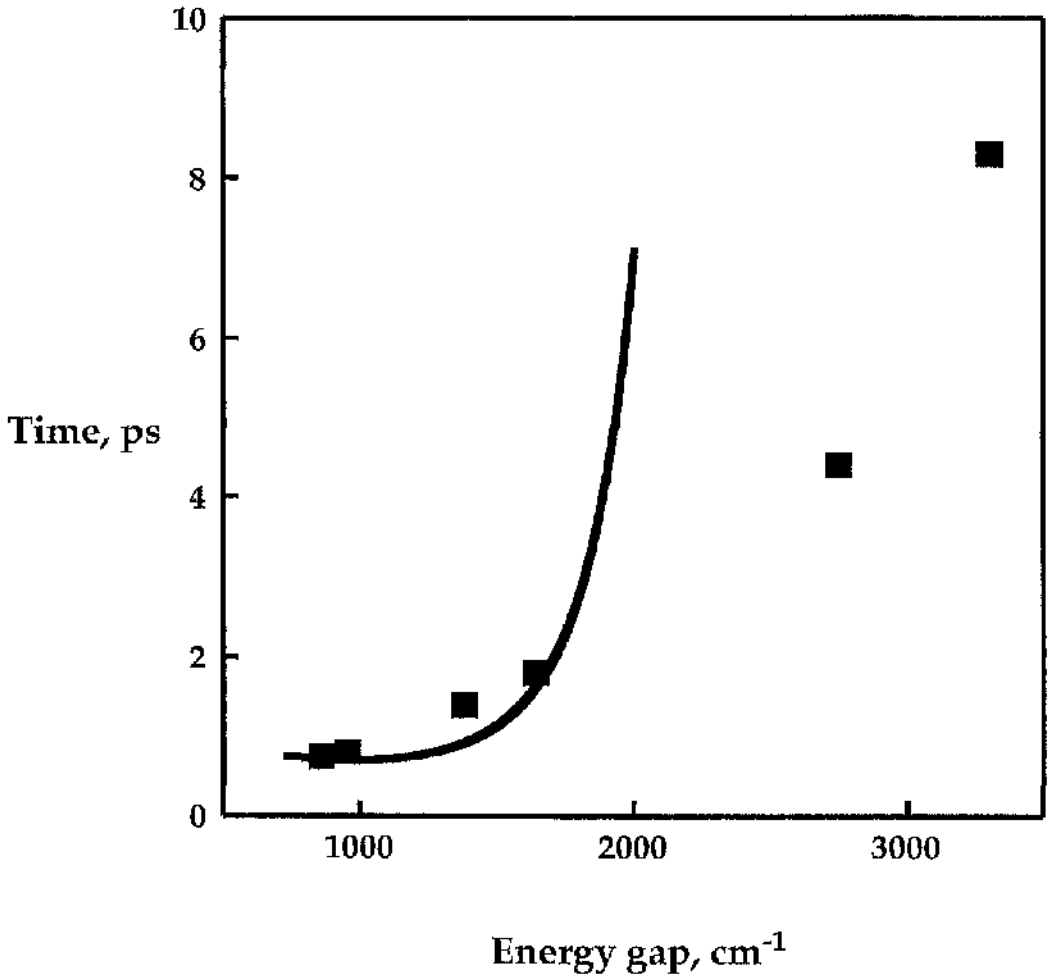
10
8
6
4
2
0
Time, ps
1000
2000
3000
Energy gap, cm-1

complexes, the measured rates are much faster than Förster would predict. In these complexes, it can be concluded that B800→B850 energy transfer is not adequately described by Förster's theory assuming that the only Bchl*a*-B850 acceptor state which is involved in the transfer process is the Q_y state

9.4 The effect of spectral overlap on the efficiency of B800→B850 energy transfer

The effect of spectral overlap on the efficiency of B800→B850 energy transfer was investigated by comparing the calculated efficiency of energy transfer in the native complex (good spectral overlap) with that in the Chl*a*-B800 reconstituted complex (poor spectral overlap). The efficiency of energy transfer between two molecules, Φ, is given by the formula

$$\Phi = 1 - \frac{K_{fl}}{K_{et}}$$

where K_{fl} - rate of fluorescence decay of donor molecule's first excited singlet state
K_{et} - rate of energy transfer between the donor and acceptor molecules

The time constants for B800→B850 energy transfer in the native and Chl*a*-B800 reconstituted complexes are 0.9 and 8.4 ps respectively (see Section 9.2). The fluorescence lifetimes of Bchl*a* and Chl*a* are 2.9 and 5.8 ns respectively (see Appendix A). On substitution of these values into the above equation, the efficiencies of B800→B850 energy transfer in the native and Chl*a*-B800 reconstituted complexes were calculated to be 100.0 and 99.9 % respectively. Although the spectral overlap function in the LH2 complexes is

significantly greater than that in the Chl*a*-B800 reconstituted complexes, the calculated efficiencies of energy transfer are essentially the same. This shows that spectral overlap has a negligible effect on the efficiency of B800→B850 energy transfer.

Attempts were made to measure the efficiencies of B800→B850 energy transfer in both the native and reconstituted complexes. This can be determined by measuring the intensity of fluorescence from the Bchl*a*-B850 molecules after excitation of the (B)Chl-B800 molecules and is given by the ratio of the fluorescence excitation spectrum to the fractional absorption spectrum in the region of the "B800" Q_y absorption maximum. For accurate determinations of the efficiency of energy transfer, it is essential that the fluorescence excitation spectrum is properly corrected for instrument function. Despite much effort, it was not possible to calibrate the fluorimeter for fluorescence excitation spectra in the NIR region (see Appendix B). This meant it was not possible to accurately measure the efficiency of B800→B850 energy transfer in any of the reconstituted complexes.

10.1 Introduction

B800→B800 energy transfer takes place on a sub-picosecond timescale (Hess *et al.*, 1993, 1995; Monshouwer & van Grondelle, 1996; Jiminez *et al.*, 1996) and is thought to occur by Förster's dipole-dipole weak interaction mechanism (see Section 2.3.3 for an in-depth discussion). In the LH2 complex, the nine Bchl*a*-B800 molecules are arranged in a ring. The angle between the Q_y transition dipoles of neighbouring pigments is 40°. After Q_y excitation of a given Bchl*a*-B800 molecule, energy transfer to a neighbouring Bchl*a*-B800 molecule will result in a decrease in the anisotropy of its excited state bleach. By time-resolving this decay in anisotropy, the rate of energy transfer between them can be determined. In this Chapter, the rate of B800→B800 energy transfer was studied in native and Bchl*a*-, 3^1vinyl Bchl*a*-, 3^1OH Bchl*a*-, acetyl Chl*a* and Chl*a*-B800 reconstituted complexes. The time constants for depolarisation of the bleaching of the (B)Chl-B800 Q_y absorption band and B800→B800 hopping were determined as described in Section 10.2. The results are recorded in Section 10.3. The experimental procedure is detailed in Section 5.6.

10.2 Calculating anisotropy values and B800→B800 hopping times from isotropic kinetic data

Values for anisotropy in the (B)Chl-B800 Q_y absorption band can be calculated from the decay kinetics of (B)Chl-B800 Q_y absorption band bleaching probed with both parallel and perpendicular polarised light according to the formula

$$r(t) = \frac{I_{VV}(t) - I_{VH}(t)}{I_{VV}(t) + 2I_{VH}(t)}$$

(Hess, 1997)

where r(t) - anisotropy at time t

$I_{VV}(t)$ - absorption intensity at time t after exciting with linear polarised light and probing with pulsed light which has a parallel polarisation

$I_{VH}(t)$ - absorption intensity at time t after exciting with linear polarised light and probing with pulsed light which has a perpendicular polarisation.

The decay in anisotropy with time can be fitted with a single exponential and the time constant for depolarisation of the bleaching of the (B)Chl-B800 Q_y absorption band determined. From this, the time constant for hopping between neighbouring Bchl*a*-B800 molecules can be determined according to the formula

$$\tau_{depolarization} = \frac{\tau_{hop}}{4(1 - \cos 2\theta)}$$

(Jiminez *et al.*, 1996)

$\tau_{depolarisation}$ - time constant for depolarisation of the Bchl*a*-B800 Q_y absorption band

τ_{hop} - time constant for B800→B800 energy transfer

θ - angle between the Q_y dipole moments of neighbouring Bchl*a*-B800 pigments (which in *Rps. acidophila* 10050 is 40°)

10.3 B800→B800 energy transfer in native LH2 and selected reconstituted complexes

Typical traces showing the decay in anisotropy of the (B)Chl-B800 Q_y absorption band with time are shown in figures 10a and 10b. In the native complex, the anisotropy has an initial value of approximately 0.3. The theoretically expected value for excitations localised on monomers is 0.4 (Hess, 1997). In experimental situations, however, this is rarely observed. Within 2 ps, the anisotropy has decayed to a value of 0.1. At times greater than 2 ps, the anisotropy values have a completely random distribution. This can be explained as follows. By 2 ps the population of Bchl*a*-B800 molecules in their first excited singlet state is so low that the calculated anisotropy values are no longer reliable. The decrease in anisotropy which occurs during the first 2 ps also has a rather poor signal to noise ratio. This is due to the rapid decay of the Bchl*a*-B800 excited state population which is due to energy transfer to the Bchl*a*-B850 molecules. The decay in anisotropy was fitted with a single exponential. The time constants for depolarisation of the Bchl*a*-B800 Q_y absorption band and B800→B800 hopping are 0.4 and 0.7 ps respectively.

In contrast, the anisotropy data and the kinetic fit for the Chl*a*-B800 reconstituted complex is significantly more accurate than that for native LH2 (see figure 10b). Similar to that which occurs in the native complex, the anisotropy has an initial value of approximately 0.3. Within approximately 10 ps, the anisotropy has decayed to a value of 0.1. This anisotropic decay has a much better signal to noise ratio than that for native LH2. This can be

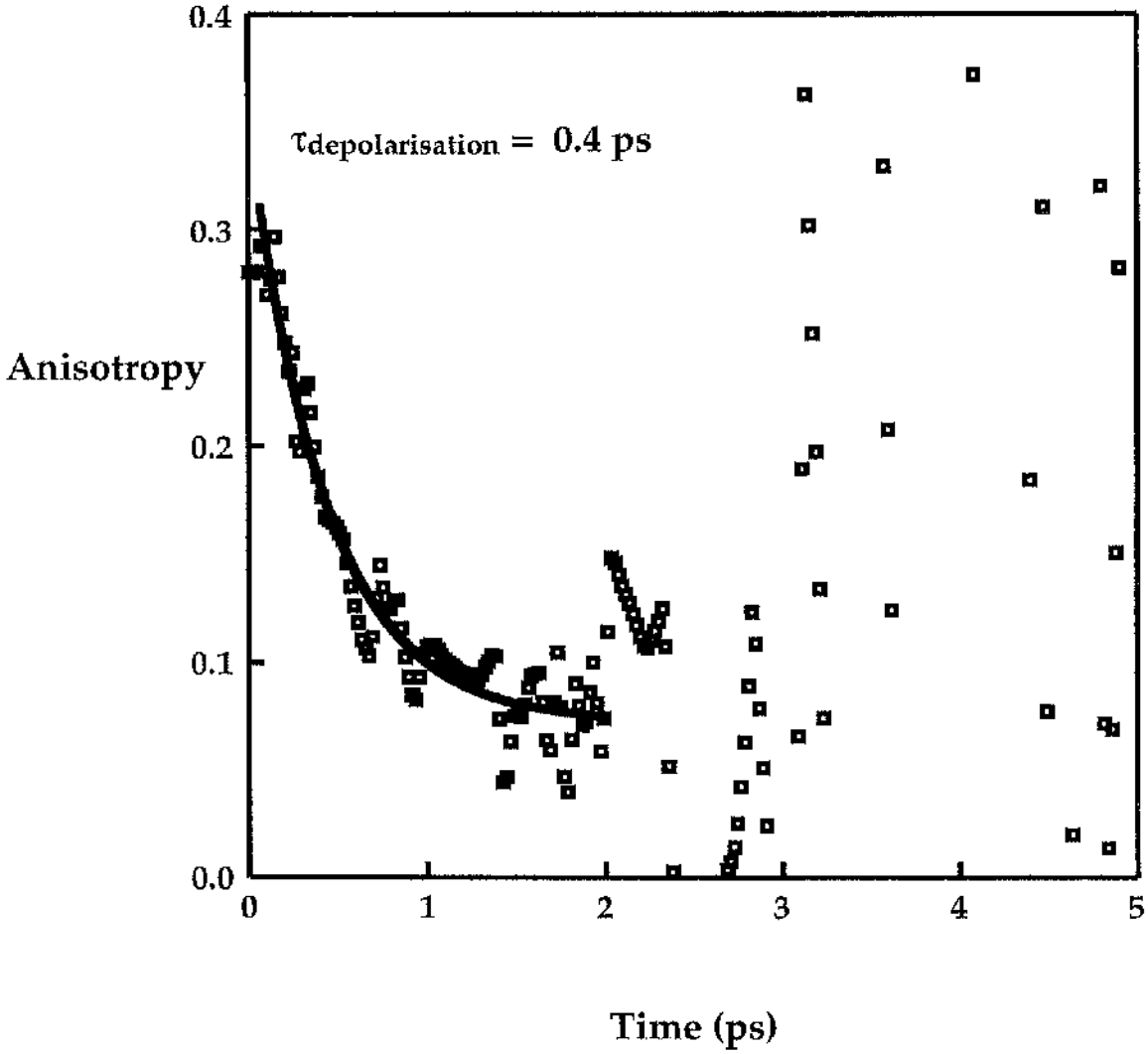

Figure 10a The depolarisation of the Bchl*a*-B800 Q_y absorption band in native LH2 with time. The anisotropy values were calculated from isotropic kinetic data as described in Section 10.2. The wavelengths of the pump and probe pulses were 785 and 810 nm respectively. The decay in anisotropy was fitted with a single exponential. The time constants of depolarisation and B800→B800 energy transfer are 0.4 and 0.7 ps respectively. At times > 2ps, the population of Bchl*a*-B800 molecules in their first excited singlet state is so low that the calculated anisotropy values are not reliable.

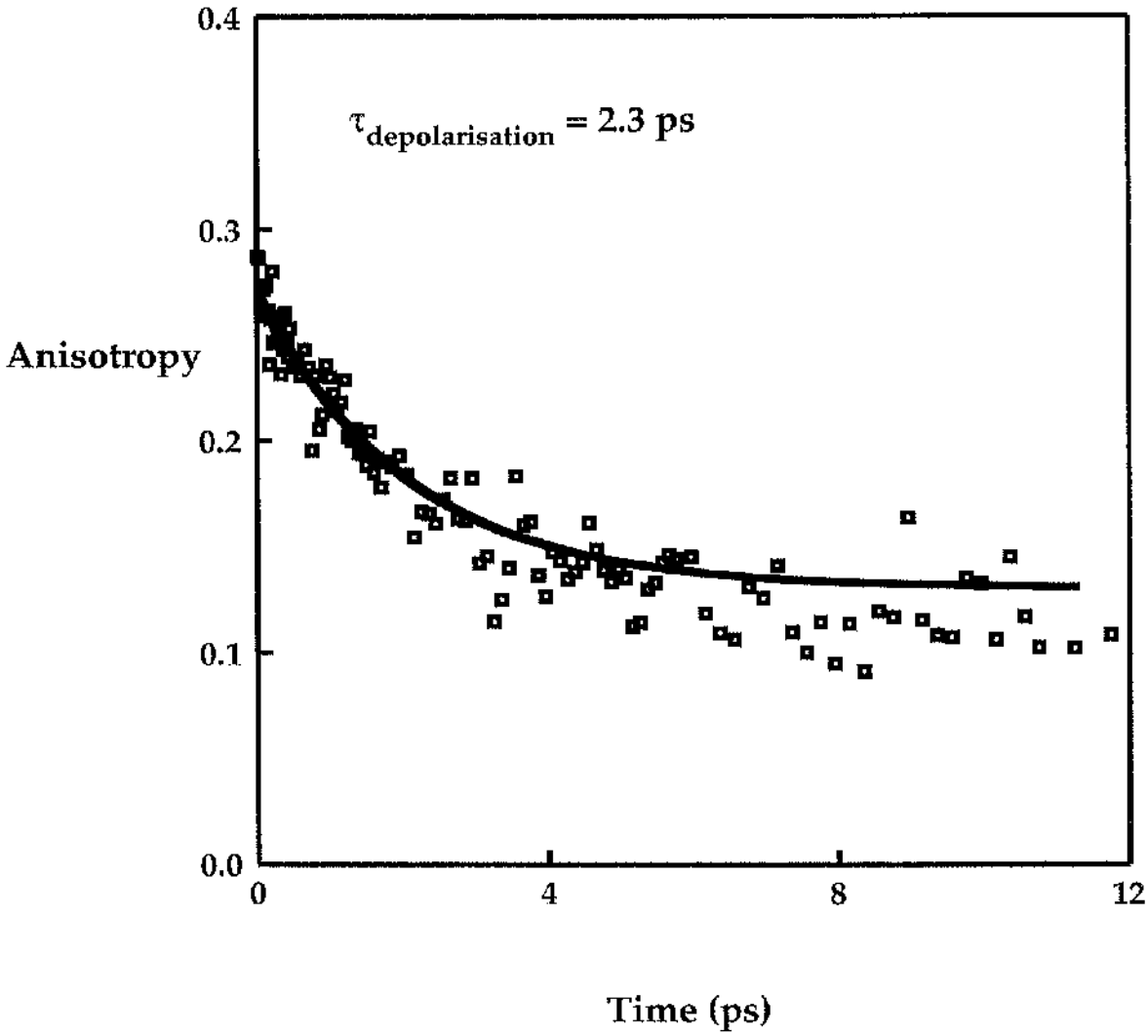

Figure 10b The kinetics of depolarisation of the "B800" Q_y absorption band in LH2 complexes reconstituted with Chl*a*. The anisotropy values were calculated as described in Section 10.2. The wavelengths of the pump and probe pulses were 660 and 680 nm respectively. The decay in anisotropy was fitted with a single exponential. The time constants for depolarisation and B800→B800 energy transfer are 2.3 and 3.8 ps respectively.

explained as follows. As the rate of B800→B850 energy transfer in the Chl*a*-B800 reconstituted complex is approximately ten times slower than that in the native complex, the Chl*a*-B800 excited state population decays more slowly. This means that the anisotropy values can be calculated more accurately. A consequence of this improved signal to noise ratio is that the fit to the kinetic data is more accurate. At t > 12 ps, once the majority of the excitation energy has been transferred to the Bchl*a*-B850 molecules, the calculated anisotropy values have a random distribution. The time constants for depolarisation of the Chl*a*-B800 Q_y absorption band and B800→B800 hopping are 2.3 and 3.8 ps respectively.

The time constants for (B)Chl-B800 Q_y absorption band depolarisation and B800→B800 hopping in the native and selected reconstituted complexes are recorded in table 10i. The time constants for B800→B800 energy transfer in native and Bchl*a*-B800 reconstituted complexes are both 0.7 ps. The average occupancy of the B800 binding sites in the Bchl*a*-B800 reconstituted complex is approximately 80% (see chapter 7.2). Together, these results show that the transfer time for B800→B800 energy transfer is not significantly affected by incomplete occupancy of the B800 binding sites. In the 3^1vinyl Bchl*a*-, 3^1OH Bchl*a*-, acetyl Chl*a*- and Chl*a*-B800 reconstituted complexes, the time constants for B800→B800 energy transfer are 1.7, 2.0, 2.8 and 3.8 ps respectively. These time constants are in qualitative agreement with the trend which occurs in the rise kinetics of the bleaching of the (B)Chl-B800 Q_y absorption band (see chapter 9.2.3). The slow rise component in the (B)Chl-B800 bleach is due to B800→B800 energy transfer. This component

Table 10i The time constants for depolarization of the (B)Chl-B800 Q_y absorption band and B800→B800 energy transfer in native LH2 and selected reconstituted complexes. The time constants for depolarization and B800→B800 hopping were determined as described in Section 10.2. All of the samples were pumped on the blue side and probed on the red side of their (B)Chl-B800 Q_y absorption bands.

Complex	Wavelengths of pump, probe (nm)	Time constant for depolarization $\tau_{depolarization}$ (ps)	Time constant for B800→B800 hopping τ_{hop} (ps)
LH2	785, 810	0.4	0.7
Reconstituted			
Bchl*a*-B800	785, 810	0.4	0.7
3^1vinyl Bchl*a*-B800	754, 775	1.0	1.7
3^1OH Bchl*a*-B800	742, 760	1.2	2.0
acetyl Chl*a*-B800	685, 705	1.7	2.8
Chl*a*-B800	660, 680	2.3	3.8

has a lifetime of 1.2, 2.3 and 3.3 ps in the 3^1OH Bchl*a*-, acetyl Chl*a*- and Chl*a*-B800 reconstituted complexes respectively. These two sets of results clearly show that the rate of B800→B800 energy transfer decreases as the (B)Chl-B800 Q_y absorption band is blue-shifted. The underlying mechanism which gives rise to this trend is not fully understood.

Factors which can affect the rate of B800→B800 energy transfer include the distance and angle between neighbouring Bchl*a*-B800 molecules and the spectral overlap function between the individual donor and acceptor pigments. In the reconstituted complexes, the B800 binding sites are not fully occupied. In these complexes, there are potentially two types of B800→B800 hopping event which can occur - those between Bchl*a*-B800 molecules in adjacent binding sites and those between Bchl*a*-B800 molecules separated by an empty binding site. In the Bchl*a*-B800 reconstituted complex, there is, on average, only one or two empty binding sites per complex. This means that most of the Bchl*a*-B800 molecules will have at least one neighbouring Bchl*a*-B800 molecule to which they can transfer excitation energy. This likely explains why the measured rate of B800→B800 energy transfer in the native complex (completely filled B800 sites) is the same as that in the Bchl*a*-B800 reconstituted complex (incompletely filled B800 sites). If the occupancy of the B800 sites was such that most of the individual molecules had no nearest neighbour, then the transfer time for B800→B800 hopping is predicted to slow dramatically. This can be explained as follows. In the native complex, the distance separating neighbouring Bchl*a*-B800 molecules is 21 Å (Freer *et al.*, 1996). If the Bchl*a*-

B800 molecules are separated by an empty binding site, this distance becomes approximately 40 Å. According to Förster, the rate of energy transfer between two molecules is proportional to $1/r^6$ (where r is the distance between the molecules). As B800→B800 energy transfer is thought to occur by Förster's mechanism, doubling the distance between the Bchl*a*-B800 molecules is predicted to slow the rate of B800→B800 energy transfer by a factor of 64. In addition, the angle between the Q_y transition dipoles of the donor and acceptor molecules would be much less favourable for energy transfer. This would cause a further slowing effect. In short, poor occupancy of the B800 sites is predicted to slow the rate of B800→B800 energy transfer by at least two orders of magnitude. In the 3^1vinyl Bchl*a*-, 3^1OH Bchl*a*-, acetyl Chl*a*- and Chl*a*-B800 reconstituted complexes, the time constants for B800→B800 hopping are 1.7, 2.0, 2.8 and 3.8 ps respectively. Although the transfer times in these complexes are slower than that in native LH2 (0.7 ps), these differences are very small compared to that which would be expected if the B800 binding pockets had a poor occupancy. Rather, it is thought that these differences are due to some other parameter.

A second possible explanation for the slower B800→B800 hopping events which occur in these modified complexes is that the spectral overlap function between the individual donor and acceptor (B)Chl-B800 molecules is different in the different complexes. To assess this possibility, the widths of the (B)Chl-B800 Q_y absorption bands in the various reconstituted complexes were compared. The full-width, half-maximum (fwhm) values of the (B)Chl-B800 Q_y absorption band in the native and Bchl*a*-, 3^1vinyl

Bchl*a*-, 3^1OH Bchl*a*-, acetyl Chl*a*- and Chl*a*-B800 reconstituted complexes are 20, 20, 25, 25, 25 and 31 nm respectively. As the width of an absorption band increases, the spectral overlap between the donor pigments on the blue side and the acceptor pigments on the red side of the band decreases. As the (B)Chl-B800 Q_y absorption bands in the 3^1vinyl Bchl*a*-, 3^1OH Bchl*a*-, acetyl Chl*a*- and Chl*a*-B800 reconstituted complexes are broader than those in the native and Bchl*a*-B800 reconstituted complexes, this may, at least in part, explain the slower rates of B800→B800 energy transfer which occur in these complexes.

Alternatively, these kinetic results maybe indicative of a parameter which affects the rate of B800→B800 energy transfer but which we, as yet, do not understand.

11.1 Introduction

Carotenoids have two low-lying excited states which are important for singlet-singlet energy transfer. These are the S_2 and S_1 states (see Section 2.3.5.1 for an in-depth discussion). In the LH2 complex, the S_2 and S_1 states can both potentially participate as donors for energy transfer to the Bchl*a* molecules. The Q_x and Q_y electronic transitions of both the Bchl*a*-B800 and the -B850 molecules can potentially accept excitation energy from the carotenoids. The possible energy pathways between the carotenoid S_2 state and the Q_y transition of the Bchl*a*-B850 molecules are numerous. The actual pathways in any given LH2 complex depends upon the following factors. These are the distance between the carotenoid and Bchl*a* molecules, the relative orientation of their transition dipole moments, the lifetimes of the carotenoid S_2 and S_1 states and the relative energies of the electronic states of the carotenoid and Bchl*a* molecules.

In this Chapter, the energy transfer processes between the rhodopin glucoside and the Bchl*a*-B850 molecules in the LH2 complex were characterised. This was achieved by performing four types of experiment. Firstly, the lifetimes of the S_2 and S_1 states of rhodopin glucoside in the native and B850-only complexes were compared with that in benzyl alcohol. This allowed the effect of competing energy transfer processes in the LH complexes on the lifetime of both excited states to be assessed (see Section 11.2). Secondly, the kinetics of carotenoid→B850 energy transfer in the native and B850-only complexes were studied. From this, it was possible to determine the number of energy transfer pathways which occur in each of

the complexes (see Section 11.3). Thirdly, the efficiency of carotenoid→B850 energy transfer in the native complex was compared with that in the B850-only complex. From this, it was possible to determine the extent of carotenoid→B850 energy transfer which takes place via the Bchl*a*-B800 molecules (see Section 11.4). Finally, the energies of the Q_x and Q_y acceptor states of the (B)Chl-B800 molecules in the 3^1vinyl Bchl*a*-, 3^1OH Bchl*a*-, acetyl Chl*a*- and Chl*a*-B800 reconstituted complexes are different from those in native LH2. The effect of these altered acceptor energy levels on the efficiency of carotenoid→B850 energy transfer was investigated (see Section 11.5).

11.2 A comparison of the S_2 and S_1 lifetimes of rhodopin glucoside in native LH2 and B850-only complexes with those in benzyl alcohol

11.2.1 Introduction

The fluorescence lifetimes of the S_2 and S_1 states of certain carotenoids have been determined *in vitro*. Typically, carotenoids have a S_2 lifetime in the range of a few hundred fs (Shreve *et al.*, 1991a; Andersson *et al.*, 1995; Ricci *et al.*, 1996; MacPherson & Gillbro, 1998) and a S_1 lifetime in the order of about 10 ps (Wasielewski & Kispert, 1986; Gillbro & Cogdell, 1989; Kuki *et al.*, 1990; Frank *et al.*, 1993a). In the LH2 complex, energy transfer from the carotenoid's excited states competes with its intrinsic fluorescence and internal conversion processes. Energy transfer from an excited electronic state reduces the lifetime of that state. The greater is the extent of energy transfer from an excited state, the shorter is its lifetime. In this Section, the

lifetimes of the S_2 and S_1 states of rhodopin glucoside in benzyl alcohol were compared with those in the native and B850-only complexes. This comparison allowed the extent of energy transfer which occurs from the S_2 and S_1 states in the respective complexes to be determined. Benzyl alcohol was chosen as the solvent for the *in vitro* measurements because the absorption maxima of rhodopin glucoside in this solvent is essentially the same as that in the native complex. The S_2 lifetimes were determined by fluorescence up-conversion (see Section 11.2.2) whereas the S_1 lifetimes were determined by transient absorption spectroscopy (see Section 9.2.1). The principal investigators in these experiments were Dr. Alasdair N. McPherson (University of Umea) and Dr. Juan B. Arellano (University of Glasgow). My contribution to this study was to provide the B850-only samples. The results are presented in Section 11.2.3. The experimental method is described in Section 5.7.

11.2.2 Fluorescence up-conversion

A schematic diagram of the apparatus used in the fluorescence up-conversion measurements is shown in figure 11a. The principle of fluorescence up-conversion is as follows. A series of pulses from a laser source is split into two beams. The weaker of the two beams is used to excite the sample. The fluorescence from the sample is focused onto the surface of a non-linear crystal. The other beam is used as a series of "gating" pulses. The gating pulses are sent through an optical delay line before they are focused onto the same area of the crystal. If the two sets of pulses are in

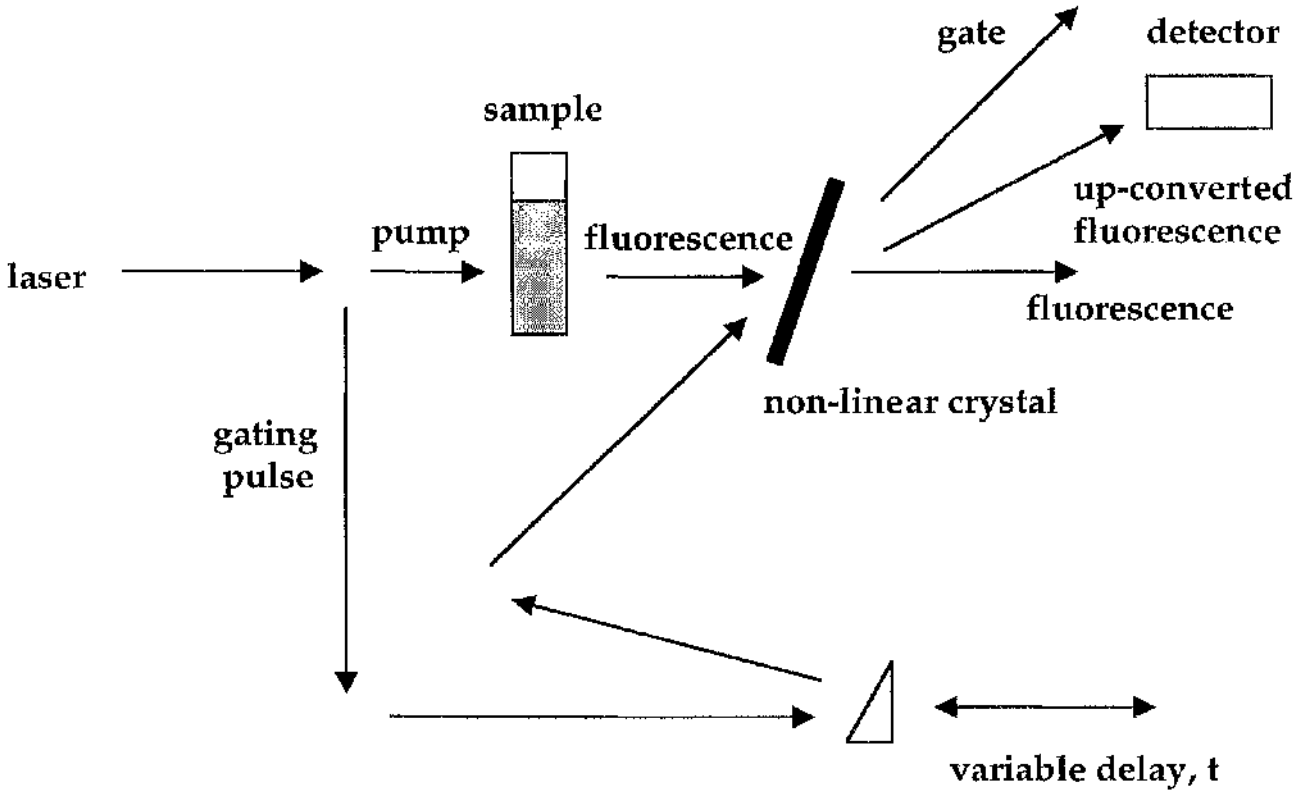

Figure 11a Fluorescence up-conversion. A series of pulses from a laser source is split into two beams. The weaker of the two beams is used to excite the sample. The fluorescence from the sample is focussed onto the surface of a non-linear crystal. The gating pulses are sent through an optical delay line before they are focused on the same area of the non-linear crystal. The non-linear character of the crystal produces a series of up-converted pulses in the UV region at a frequency equal to the sum of the frequencies of the gate and fluorescence pulses and at an angle between the transmitted gate and fluorescence pulses. The up-converted signal is detected using a photon counting photomultiplier.

phase, some of the light which exits from the crystal has a frequency equal to the sum of the frequency of the gate and fluorescence pulses. This up-converted signal is detected using a photomultiplier tube connected to a photon counter. Time-dependent changes in fluorescence can be determined by gradually increasing the optical delay of the gating pulse. The wavelength of fluorescence from the sample which is up-converted is determined by the orientation of the crystal surface relative to the direction of the fluorescence pulses from the sample. The time resolution of this system is determined by the instrument response function (IRF). The IRF is approximately given by the cross-correlation of the excitation pulse with the gate pulse.

11.2.3 S_2 and S_1 lifetime data

Fluorescence emission from the S_2 state of rhodopin glucoside is very weak and has a maximum value in the region of 570 nm (Alasdair MacPherson, personal communication). The lifetimes of the S_2 state of rhodopin glucoside in benzyl alcohol and in the native and B850-only complexes were determined by exciting the carotenoids at 489 nm and then measuring the time-dependent decay in fluorescence at 578 nm (see figure 11b). The lifetimes of the S_2 state in the LH2 and B850-only complexes and in benzyl alcohol are approximately 61, 76 and 132 fs respectively. The S_2 lifetime in the B850-only complex is significantly shorter than that in benzyl alcohol. This shows that energy is transferred from the S_2 state of the carotenoid to the Bchl*a*-B850 molecules. The S_2 lifetime in the LH2 complex is even

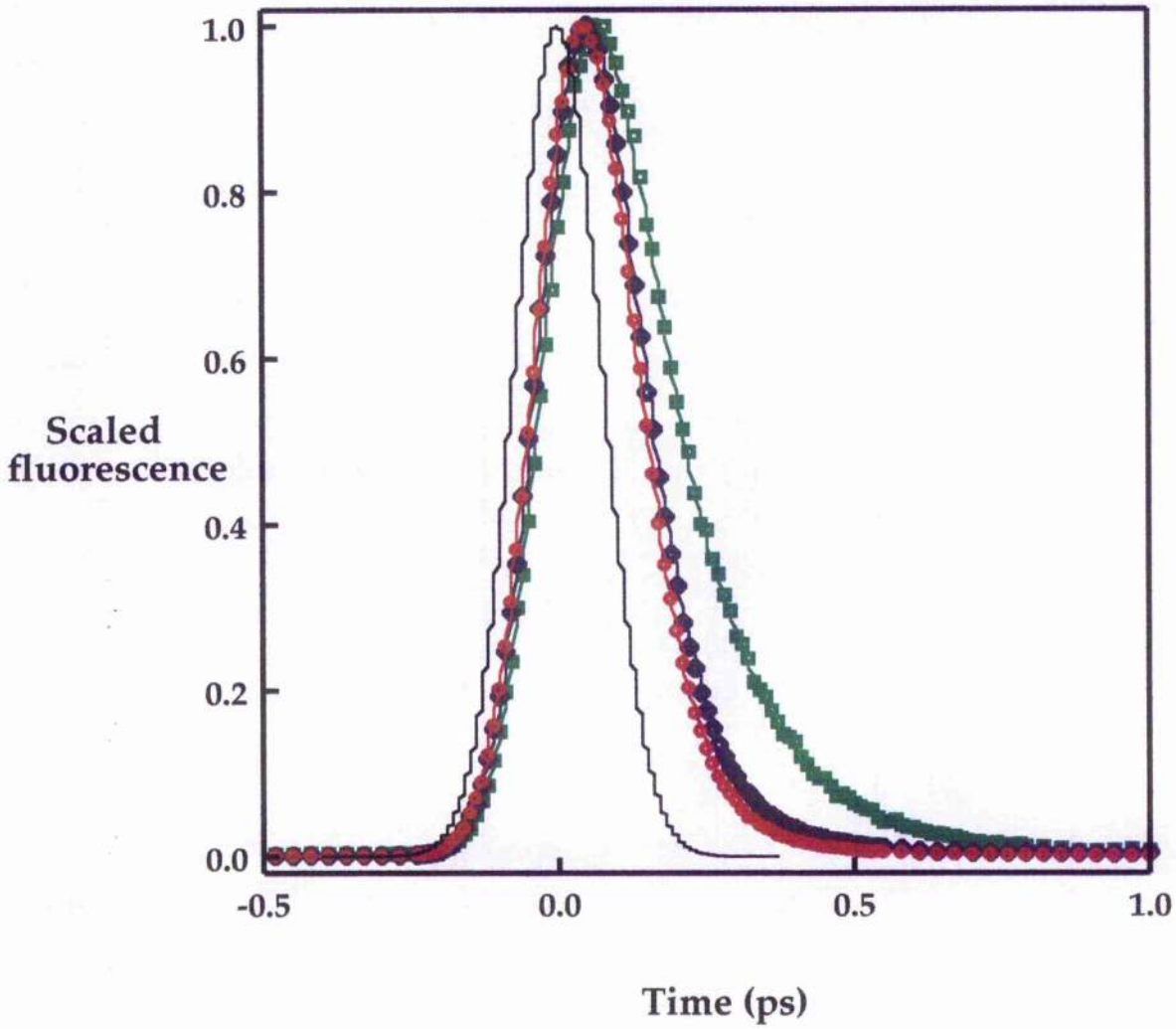

Figure 11b A comparison of the decay kinetics of fluorescence emission from the rhodopin glucoside S_2 state in benzyl alcohol with that in the native LH2 and B850-only complexes. The carotenoid molecules were excited at 489 nm. Emission from the S_2 state was probed at 578 nm. The decay kinetics were all fitted with single exponentials. The lifetimes of the S_2 state in the native and B850-only complexes and in benzyl alcohol are 61, 76 and 132 fs respectively. The reduced S_2 lifetimes in the LH2 and B850-only complexes shows that energy is transferred from the carotenoid S_2 state to both the Bchl*a*-B800 and -B850 molecules. [**Key** Red LH2, Purple B850-only, Green benzyl alcohol, Black instrument response function (IRF)].

shorter. This shows that energy is also transferred from the carotenoid S_2 state to the Bchl*a*-B800 molecules. To determine the role of the S_1 state in singlet-singlet energy transfer, the decay kinetics of the carotenoid S_1 state ESA were measured (results not shown). The lifetime of the S_1 state in benzyl alcohol is 4.5 ps. In the LH2 and B850-only complexes, the S_1 lifetimes are 3.6 and 4.1 ps respectively. These shortened lifetimes suggests that limited energy transfer occurs from the carotenoid S_1 state. The S_1 lifetime in the native complex is shorter than that in the B850-only complex. This shows that of the excitation energy which is transferred from the S_1 state, most is transferred to the Bchl*a*-B800 molecules.

11.3 A comparison of the kinetics of carotenoid→B850 energy transfer in native and B850-only complexes

11.3.1 Introduction

The principal carotenoid donor state in the LH2 complex is the S_2 state (see Section 11.2). Excitation energy can be transferred to the Bchl*a*-B850 molecules either directly or indirectly via the Bchl*a*-B800 molecules. In this Section, the kinetics of carotenoid→B850 energy transfer in native and B850-only complexes were studied by fluorescence up-conversion. The results are presented in Section 11.3.2. The experimental method is described in Section 5.7.

11.3.2 The kinetics of carotenoid→B850 energy transfer in the LH2 and B850-only complexes

In both the LH2 and B850-only complexes, the carotenoid molecules were excited at 499 nm. Initially, the rise in fluorescence emission of the Bchl*a*-B850 molecules was measured at 872 nm. The kinetic traces of both complexes are shown in figures 11c and 11d. In native LH2, the rise kinetics are bi-exponential. The two rise components have lifetimes of approximately 130 (contribution to overall kinetics 70%) and 820 fs (30%). In the B850-only complex, the kinetics can be fitted with a single exponential which has a lifetime of approximately 130 fs. In both complexes, the fast rise component is due to energy transfer from the S_2 state of the carotenoid to the Bchl*a*-B850 molecules. In contrast, the lifetime of the carotenoid S_2 state in the LH2 complex is 61 fs (see Section 11.2.3). The apparent discrepancy between these two values can be explained as follows. The lifetime of the fast rise component of the Bchl*a*-B850 fluorescence emission is wavelength-dependent and varies between 63 fs at 850 nm and 180 fs at 900 nm (results not shown). The lifetime of the rise component at the blue-edge of the Bchl*a*-B850 emission spectrum is, within the limits of experimental error, the same as that of the carotenoid S_2 lifetime. As the probe wavelength is red-shifted, the lifetime of this rise component increases. This is due to relaxation of the excitation energy amongst the Bchl*a*-B850 molecules. The additional, slow rise component observed in the LH2 complex is due to energy transfer via the Bchl*a*-B800 molecules. This pathway consists of two separate steps. Excitation energy is first transferred from the carotenoid to the Bchl*a*-B800 molecules and then to the -B850 molecules. The time

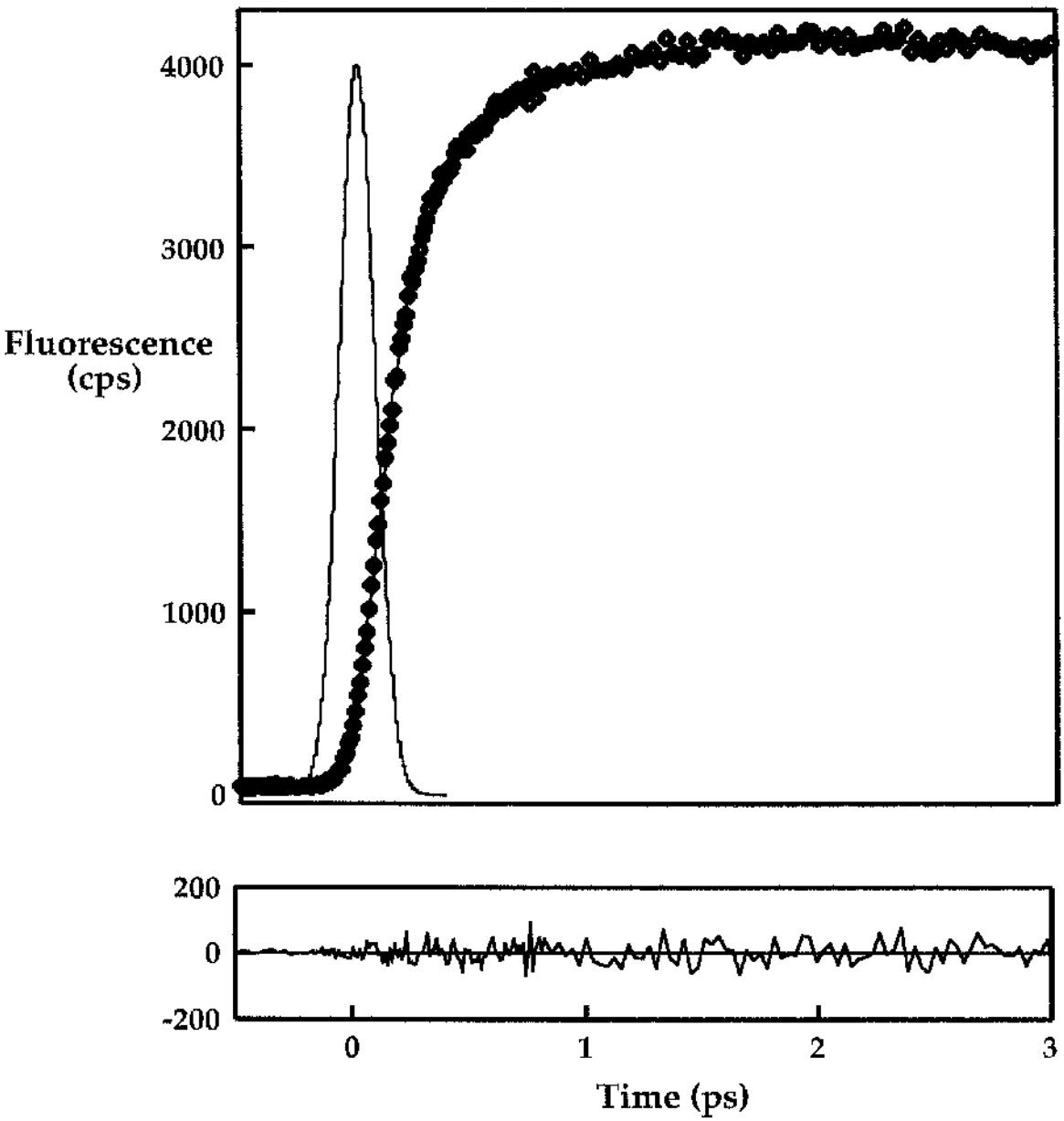

Figure 11c The time-dependent rise in fluorescence emission of the Bchl*a*-B850 molecules in the native LH2 complex after excitation of the rhodopin glucoside molecules at 499 nm. Fluorescence emission was probed at 872 nm. The rise kinetics were fitted with a bi-exponential. The lifetimes of the two rise components are 130 fs (contribution to overall fit 70 %) and 820 fs (30 %). This shows that there is two routes by which excitation energy is transferred from the carotenoid to the Bchl*a*-B850 molecules in the native complex - either directly with a time constant of 130 fs or via the Bchl*a*-B800 molecules with a time constant of 820 fs. The goodness of the fit is also shown.

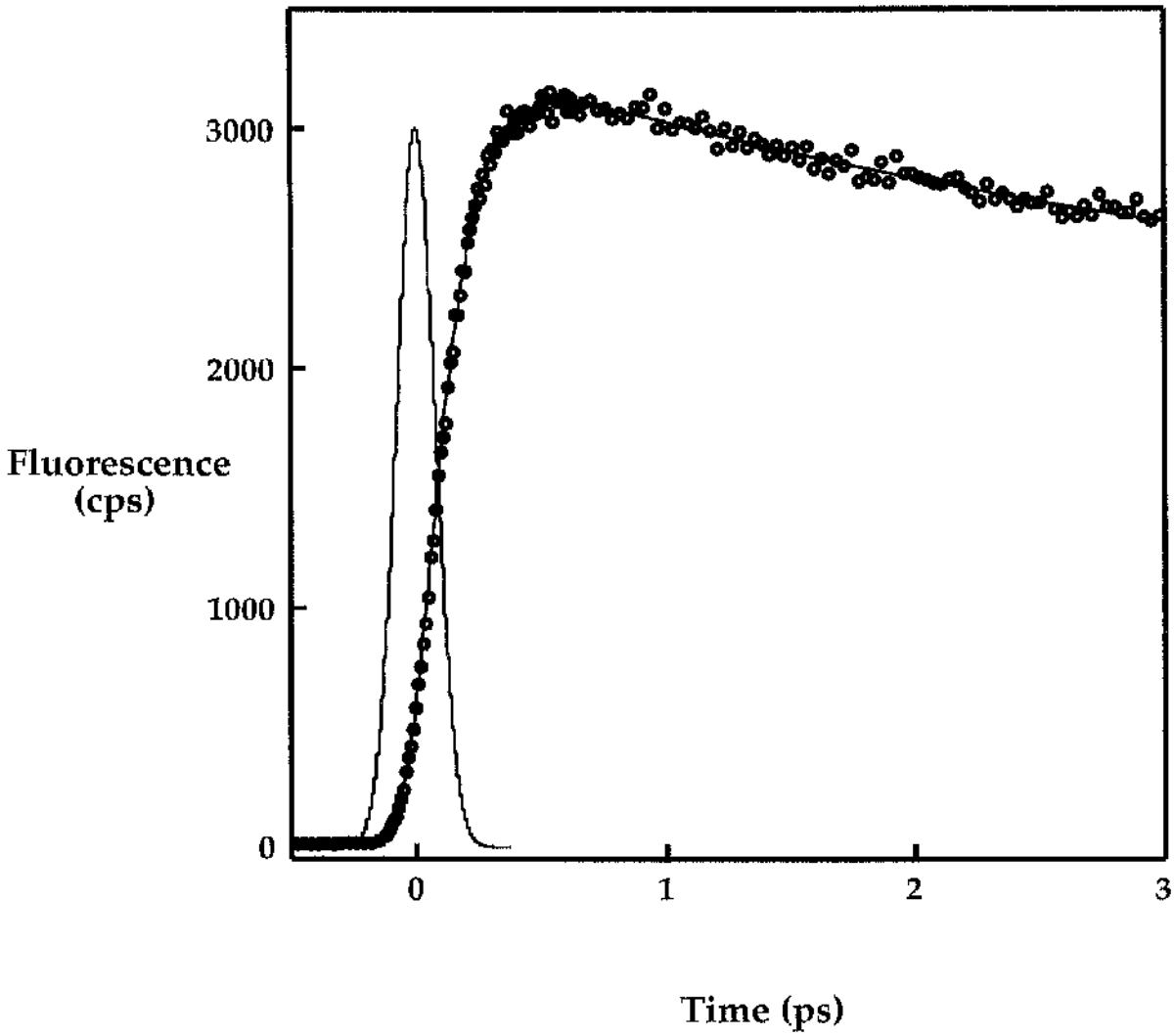

Figure 11d The time-dependent rise in fluorescence emission of the Bchl*a*-B850 molecules with time in the B850-only complex after excitation of the rhodopin glucoside molecules at 499 nm. Fluorescence emission was probed at 872 nm. The rise kinetics were fitted with a single exponential with a lifetime of 130 fs. The emission has a bi-exponential decay with lifetimes of 3.7 ps (contribution to decay 39%) and 470 ps (61%). The Bchl*a*-B850 molecules normally have a fluorescence lifetime of 1 ns. The shortened decay lifetimes observed here are due to singlet-singlet and singlet-triplet annihilation (van Grondelle, 1985).

constant for B800→B850 energy transfer in the native complex is 0.9 ps (see Section 9.2). This suggests that the lifetime of the slow rise component is shorter than that which might be expected. More importantly, carotenoid→ B800 energy transfer must occur on a time-scale of approximately 100 fs. The relative contributions of the fast and slow rise components in the native complex is 70 : 30. This shows that approximately 70% of all of the carotenoid→B850 energy transfer occurs directly. The remaining 30% occurs via the Bchl*a*-B800 molecules. In both complexes, the fluorescence has a bi-exponential decay. In the LH2 complex, these time constants are 8.3 ps (contribution to overall kinetics 37%) and 420 ps (63%) and in the B850-only complex are 3.7 ps (39%) and 470 ps (61%). In the absence of any quenching, the fluorescence lifetime of the Bchl*a*-B850 molecules is approximately 1 ns. The reduced fluorescence lifetimes which are observed here are likely to result from singlet-singlet and singlet-triplet annihilation caused by the use of high excitation densities (van Grondelle, 1985; Bradforth *et al.*, 1995).

11.4 A comparison of the efficiencies of carotenoid→B850 energy transfer in native and B850-only complexes

11.4.1 Introduction

In this Section, the extent of carotenoid→B850 energy transfer which occurs via the Bchl*a*-B800 molecules was determined by comparing the efficiency of carotenoid→B850 energy transfer in native LH2 with that in the B850-only complex. The efficiency of energy transfer in each complex was determined

from its action spectrum (see Appendix B). The results are presented in Section 11.4.2. The experimental method is described in Section 5.2

11.4.2 Results

The efficiencies of carotenoid→B850 energy transfer in the native and B850-only complexes are 57 and 40 % respectively (see table 11i). These results suggest that of the energy transfer which occurs between the carotenoid and the Bchl*a*-B850 molecules in the native complex, only 30% is transferred via the Bchl*a*-B800 molecules. This conclusion can be made only if the pathways of energy transfer from the carotenoid to the Bchl*a*-B800 and -B850 molecules do not compete.

To establish whether or not this is the case, further work would have to performed. A possible method would be to compare the efficiency of carotenoid→B850 energy transfer in a complex in which the Bchl*a*-B800 molecules were able to accept excitation energy from the carotenoids but were unable to pass it on to the Bchl*a*-B850 molecules, with that in the B850-only complex. Such a complex could be created by reconstituting the B800 binding pockets with Ni-Bph*e*. Ni-Bph*e* has a very short lifetime and effectively quenches all of the excitation energy which it receives (Teuchner *et al.*, 1997). If the Bchl*a*-B800 and -B850 molecules do compete for excitation energy, the efficiency of carotenoid→B850 energy transfer in the B850-only complex would be greater than that in the Ni-Bph*e*-B800 reconstituted complex. The reason for this is quite simple. Competition between the Bchla-B800 and -B850 molecules in the Ni-Bph*e*-B800 reconstituted complex

Table 11i The efficiencies of carotenoid→B850 energy transfer in native, B850-only and selected reconstituted complexes. The efficiency of energy transfer in each complex was determined from its action spectrum in the region 350 to 600 nm (see Appendix B).

Type of complex	Efficiency of carotenoid→ B850 energy transfer (%)
LH2	57 ± 1
B850-only	40 ± 1
Reconstituted complexes	
Bchl*a*-B800	57 ± 1
3^1vinyl Bchl*a*-B800	52 ± 1
3^1OH Bchl*a*-B800	49 ± 1
acetyl Chl*a*-B800	53 ± 1
Chl*a*-B800	55 ± 1

would mean that less excitation energy would be transferred to the Bchl*a*-B850 molecules compared to that in the B850-only complex. The energy which is transferred to the Ni-Bph*e*-B800 molecules would not be transferred to the Bchl*a*-B850 molecules. Rather it would be dissipated. This will result in a overall decrease in the efficiency of carotenoid→B850 energy transfer compared to that in the B850-only complex. If the efficiency of carotenoid→B850 energy transfer was the same in the B850-only and Ni-Bph*e*-B800 reconstituted complexes, however, it would suggest that the energy transfer pathways do not compete.

11.5 A comparison of the efficiency of carotenoid→B850 energy transfer in selected reconstituted complexes

11.5.1 Introduction

The principal donor state of the rhodopin glucoside molecules in the LH2 complex is the S_2 state (see Section 11.2). In the LH2 complex, fluorescence emission from the S_2 state of rhodopin glucoside occurs in the region of 570 nm. The Q_x transition of the Bchl*a* molecules in the LH2 complex has a maximum absorption at 590 nm. As there is good spectral overlap between these two transitions, it may suggest that the most likely Bchl*a* acceptor state is the Q_x state. In the 3^1vinyl Bchl*a*-, 3^1OH Bchl*a*-, acetyl Chl*a*- and Chl*a*-B800 reconstituted complexes, the energies of the Q_x and Q_y electronic states of the (B)Chl-B800 molecules are different from those in the native complex. In this Section, the effect of these altered energy levels on the efficiency of

carotenoid→B850 energy transfer was investigated. The results are presented in Section 11.5.2. The experimental method is described in Section 5.2.

11.5.2 Results

The efficiencies of carotenoid→B850 energy transfer in the Bchl*a*-, 3^1vinyl Bchl*a*-, 3^1OH Bchl*a*-, acetyl Chl*a*- and Chl*a*-B800 reconstituted complexes are recorded in table 11i. The efficiency of energy transfer in the Bchl*a*-B800 reconstituted complex is 57%. This is the same as that in native LH2 (see table 11i). It can be concluded, therefore, that maximal carotenoid→B850 energy transfer can be restored by reconstitution of the B800 binding pockets with Bchl*a*. The efficiencies of carotenoid→B850 energy transfer in the 3^1vinyl Bchl*a*-, 3^1OH Bchl*a*-, acetyl Chl*a*- and Chl*a*-B800 reconstituted complexes are 52, 49, 53 and 55% respectively. The efficiency of B800→B850 energy transfer in these complexes is 100% (see Section 9.4). This means that the different efficiencies of carotenoid→B850 energy transfer which occur in the various reconstituted complexes are real and are not due to the efficiencies of B800→B850 energy transfer being different in the different complexes. Figure 11e shows the % restoration of carotenoid→B850 energy transfer in the 3^1vinyl Bchl*a*-, 3^1OH Bchl*a*-, acetyl Chl*a*- and Chl*a*-B800 reconstituted complexes. The difference between the efficiency of carotenoid →B850 energy transfer in the LH2 and B850-only complexes was defined to be 100%. The % restoration value for each of the reconstituted complexes was expressed relative to this value.

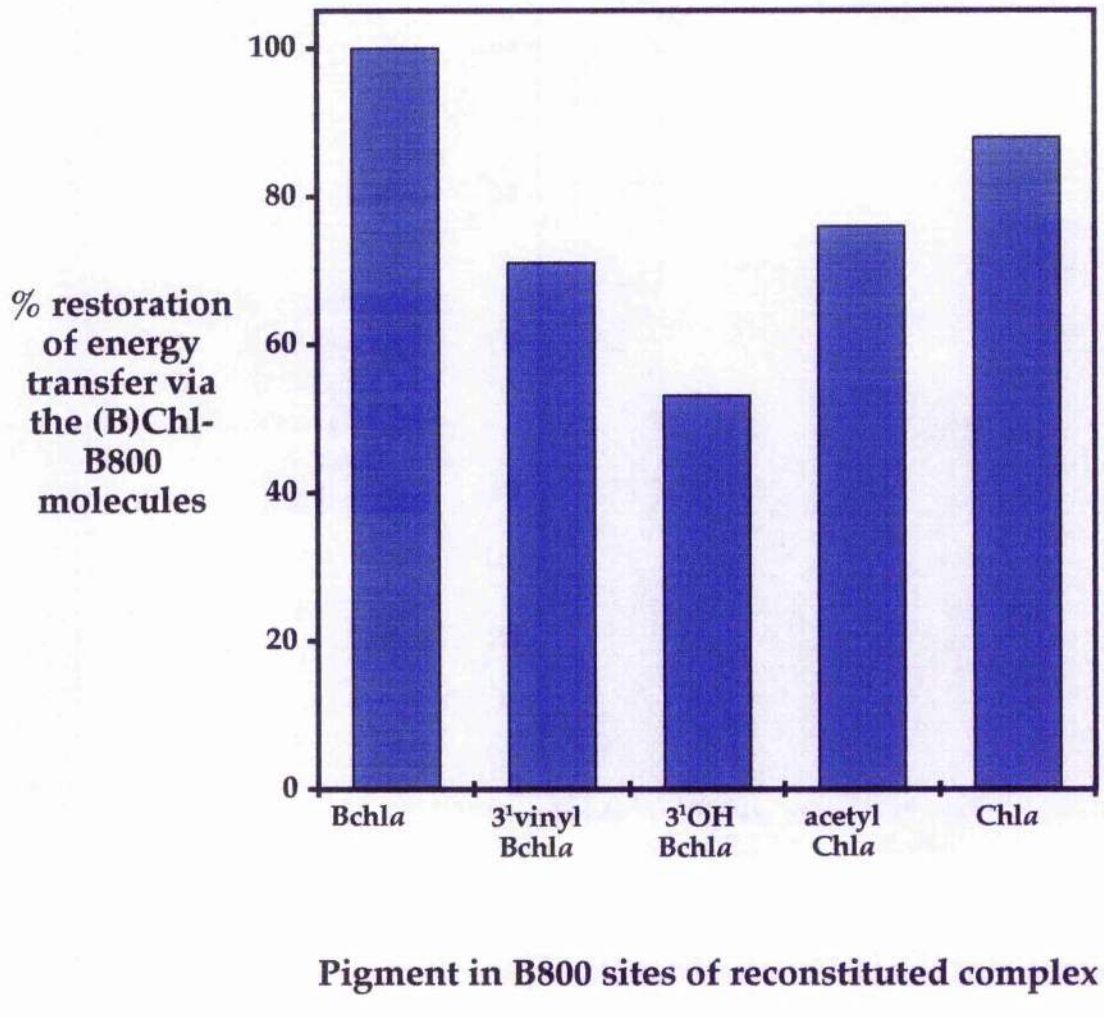

Figure 11e The % restoration of carotenoid→B850 energy transfer via the (B)Chl-B800 molecules in the Bchl*a*-, 3¹vinyl Bchl*a*-, 3¹OH Bchl*a*-, acetyl Chl*a*- and Chl*a*-B800 reconstituted complexes. The difference in the efficiency of carotenoid→B850 energy transfer between the LH2 and B850-only complexes was defined to be 100%. The % restoration value for each of the reconstituted complexes was expressed relative to this value. In the Bchl*a*-B800 reconstituted complex, the % restoration is 100%. This shows that maximal efficiency of carotenoid→B850 energy transfer can be restored by reconstitution of the B800 binding pockets with Bchl*a*. The restorations of carotenoid→B850 energy transfer in the modified complexes depends upon the spectral properties of the reconstituted pigments.

The restoration of carotenoid→B850 energy transfer in the 3¹vinyl Bchl*a*-, 3¹OH Bchl*a*-, acetyl Chl*a*- and Chl*a*-B800 reconstituted complexes depends upon the spectral properties of the reconstituted pigments. The graph shows that for the bacteriochlorin molecules the % restoration values decrease in the order Bchl*a* > 3¹vinyl Bchl*a* > 3¹OH Bchl*a* and for the chlorin molecules is Chl*a* > acetyl Chl*a*. These results can be explained in terms of the spectral overlap between the fluorescence emission spectrum of the carotenoid molecules and the absorption spectrum of the reconstituted pigments. A spectrum showing the fluorescence emission profile of both the S_2 and S_1 states of the carotenoid and the absorption profiles of the Q_x acceptor transitions of the 3¹vinyl Bchl*a* and 3¹OH Bchl*a* and the Q_y transitions of the acetyl Chl*a* and Chl*a* molecules was generated (see figure 11f).

From this, it can be seen that the spectral overlap function between the S_2 fluorescence emission profile of the carotenoid and the Q_x absorption transition of the Bchl*a*-B800 molecules decreases in the series Bchl*a* > 3¹vinyl Bchl*a* > 3¹OH Bchl*a* as the Q_x transition is blue-shifted. The reduced spectral overlap function in the 3¹vinyl Bchl*a* and 3¹OH Bchl*a* reconstituted complexes is predicted to slow the rate of energy transfer between the carotenoid and (B)Chl-B800 molecules. The lifetime of the S_2 state is so short that any reduction in the rate of carotenoid→B800 energy transfer is likely to affect the efficiency of energy transfer also. On completion of my thesis, this theory will be tested by measuring the rate of carotenoid→B800 energy transfer in the Bchl*a*-, 3¹vinyl Bchl*a*- and 3¹OH Bchl*a*-B800

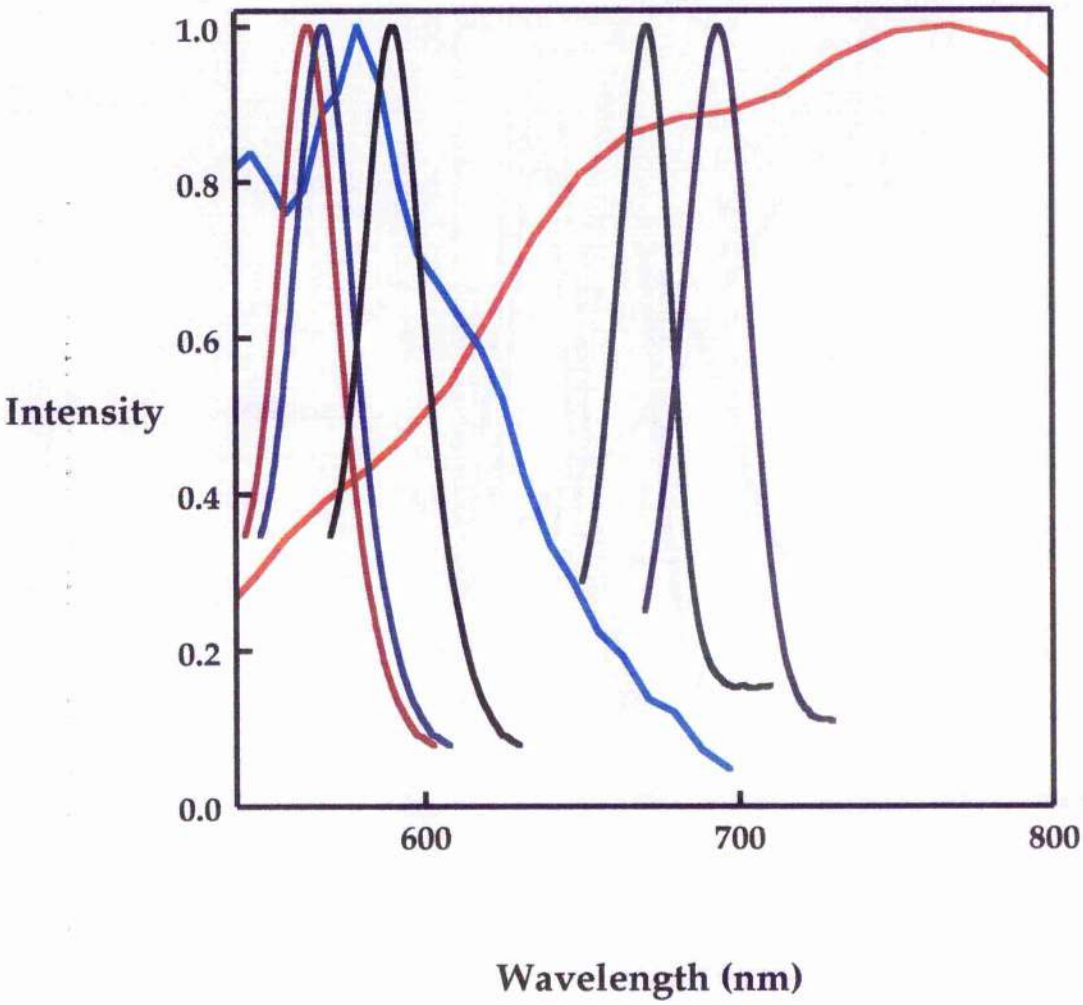

Figure 11f Spectral overlap between the hypothetical fluorescence emission spectra of the S_2 and S_1 states of rhodopin glucoside and the Q_x transition of the (B)Chl-B800 molecules in the 3^1vinyl Bchl*a*- and 3^1OH Bchl*a*-B800 reconstituted complexes and the Q_y transition of those in the acetyl Chl*a*- and Chl*a*-B800 reconstituted complexes. All spectra were scaled such that they had a maximum value of 1. The S_2 emission spectrum of rhodopin glucoside was generated by shifting the actual fluorescence emission spectrum of 5′,6′-dihydro-7′,8′-didehydrospheroidene (11 conjugated double bonds) to its spectral origin at 580 nm (Alasdair MacPherson, personal communication). Similarly, the S_1 emission profile was generated by shifting the fluorescence emission spectrum of 3,4,7,8 tetrahydrospheroidene to its spectral origin at 768 nm (Frank *et al.*, 1997). [**Key** Q_x absorption 3^1OH Bchl*a* Red, 3^1vinyl Bchl*a* Blue, Bchl*a* Black : Q_y absorption Chl*a* Green, acetyl Chl*a* Purple : rhodopin glucoside S_2 emission cyan, S_1 emission orange].

reconstituted complexes in a series of fluorescence up-conversion experiments at the University of Umea, Sweden.

The % restorations values in the acetyl Chl*a*- and Chl*a*-B800 reconstituted complexes are 76 and 88 % respectively. These values are surprisingly high given that the chlorin molecules lack a suitable absorption transition capable of absorbing energy from the carotenoid S_2 state. Rather, it is thought that carotenoid→B800 energy transfer in these complexes occurs between the broad S_1 fluorescence emission band of the carotenoids and the Q_y absorption band of the chlorin molecules (see figure 11f). This theory could be tested by measuring the lifetime of the S_1 state in the acetyl Chl*a*- and Chl*a*-B800 reconstituted complexes. A reduction of the S_1 lifetime in the reconstituted complexes compared to that in benzyl alcohol would be indicative of energy transfer from the S_1 state. On completion of my thesis, this idea will be tested in a series of fluorescence up-conversion experiments at the University of Umea, Sweden.

Discussion

Discussion

The recently determined crystal structure of the LH2 complex from *Rps. acidophila* 10050 has revealed the relative positions of the pigments within that complex (McDermott *et al.*, 1995). From the structure, considerable insights have been gained concerning the energy transfer processes which occur within the complex. For example, it is now known that the Bchl*a*-B850 molecules are arranged in a tightly-coupled circular aggregate. The proximity of these molecules facilitates the delocalization of excitons over at least part if not all of the ring (see Section 2.3.4 for a full discussion). The actual delocalization length has important implications for the energy transfer mechanism which applies. If the exciton is delocalized over the entire ring, nearest neighbour energy transfer will occur via relaxation between different excited states. As the coherence length decreases, energy transfer around the B850 ring will have a more Förster-like, "hopping" character. In addition, the distances between and the relative orientations of the transition dipoles of the Bchl*a*-B800 and -B850 molecules suggests that both B800→B800 and B800→B850 energy transfer occur by Förster's dipole-dipole, weak interaction mechanism (Freer *et al.*, 1996). Such insights into the mechanisms of energy transfer from the structure alone are at best speculative. That said, however, the structure can be used to design critical experiments with the purpose of investigating the mechanisms of energy transfer within the complex.

Previously, the mechanisms of energy transfer within the LH2 complex have been investigated using genetic techniques. For example, site-directed

mutagenesis has been used to create LH2 complexes in which the spectral overlap between the fluorescence emission spectrum of the Bchl*a*-B800 and the Q_y absorption profile of the Bchl*a*-B850 molecules is altered (Fowler *et al.*, 1992, 1995). In these mutants, the changes in the rates of energy transfer were in qualitative agreement with that predicted by Förster (Hess *et al.*, 1994; Fowler *et al.*, 1997). Using this technique, however, it was not possible to conduct a more thorough investigation of the effect of spectral overlap on the rate of B800→B850 energy transfer. The reason for this is quite simple. The environment of the pigment in the protein can only be changed so much by mutating proximal residues. As a consequence, the spectral shifts in the Bchl*a*-B800 and -B850 Q_y absorption maxima are limited also.

In addition, LH2 complexes containing plant-type carotenoids have been created by splicing the carotenoid biosynthetic genes of *Er. herbicola* into the host genome of *Rb. sphaeroides* (Hunter *et al.*, 1994). The energetic properties of these complexes have not yet been fully characterised. It is envisaged, however, that these complexes will give interesting insights into the effects of altered S_2 and S_1 state energies on the efficiency and rate of carotenoid to Bchl*a* energy transfer. The range of carotenoids which can be incorporated into LH2 complexes by genetic manipulation are limited by that which the bacteria has the enzymatic machinery to produce. A much more diverse series of carotenoids made by chemical synthesis can be reconstituted into the B850-only complex from *Rb. sphaeroides* strain R26.1 using a biochemical approach (Davidson & Cogdell, 1981; Frank *et al.*, 1993b). The main advantage that this system has over the genetic approach

is that it allows the creation of a series of LH2 complexes containing carotenoids in which their properties have been systematically altered. This approach has been used to study the effect of the length of the carotenoid conjugated system on the efficiency of carotenoid→B850 energy transfer (Frank *et al.*, 1993; Desamero *et al.*, 1998).

Reconstitution techniques have also been developed which allow the creation of RC and LH complexes with altered spectroscopic properties by selective exchange of the native tetrapyrrole pigments with other modified pigments (see Section 2.4 for a full discussion). A diverse range of RC with modified spectral properties can be created (Struck *et al.*, 1990a,b; Hartwich, 1994; Meyer & Scheer, 1995). These complexes have given insights into the singlet-singlet (Hartwich *et al.*, 1995b), triplet-triplet (Hartwich *et al.*, 1995a; Frank *et al.*, 1996) and electron transfer (Finkele *et al.*, 1992) processes which occur in the RC. In contrast, only a limited range of modified pigments can be incorporated into stable LH1 complexes (Parkes-Loach *et al.*, 1990; Davis *et al.*, 1996). Unfortunately, those pigments which do undergo exchange have the same spectroscopic properties as the native pigments. The spectral similarity of the reconstituted and native complexes has precluded the use of these modified complexes as a tool to further our understanding of the energy transfer processes which occur within the LH1 complex.

Recently, Bandilla *et al.* (1998) have reported a technique which allows the Bchl*a*-B800 molecules to be removed from their binding sites and later replaced with a limited range of modified pigments in LH2 complexes from *Rb. sphaeroides*. In my work, the approach of Bandilla *et al.* was adopted

and optimised for LH2 complexes from *Rps. acidophila* 10050. The procedure developed in this thesis allows 80 % of the B800 sites to be reconstituted with Bchl*a* compared with only 50 % using the method of Bandilla *et al.*. This increase can be attributed to using the detergent LM in the reconstitution mixture rather than Triton TBG10. In addition, the protocol developed here allows the B800 binding sites to be reconstituted with a wide variety of modified pigments including geranylgaraniol Bchl*a*, 13^2OH Bchl*a*, Zn-Bph*e*, 3^1vinyl Bchl*a*, 3^1OH Bchl*a*, acetyl Chl*a* and Chl*a*. Significantly, this system is the first one which allows the incorporation of both Chl*a* and acetyl Chl*a* into either a bacterial RC or LH complex. The 3^1vinyl Bchl*a*-, 3^1OH Bchl*a*-, acetyl Chl*a*- and Chl*a*-B800 reconstituted complexes are of particular interest as they have strongly blue-shifted "B800" Q_y absorptions with maxima at 765, 751, 693 and 669 nm respectively. The kinetics of B800→B850 energy transfer in native and selected reconstituted complexes were studied by fs transient absorption spectroscopy (see Section 9.2). In both the native and Bchl*a*-B800 reconstituted complex, B800→B850 energy transfer takes approximately 0.9 ps. The time constants for B800→B850 energy transfer in the 3^1vinyl Bchl*a*-, 3^1OH Bchl*a*-, acetyl Chl*a*- and Chl*a*-B800 reconstituted complexes are 1.4, 1.8, 4.4 and 8.5 ps respectively. This shows that the rate of B800→B850 energy transfer decreases as the spectral separation between the (B)Chl-B800 and B850 Q_y absorption bands increases. This effect is rather small, however, given the apparent large decrease in spectral overlap. Model calculations show that the rate of B800→B850 energy transfer in these complexes, in particular the

acetyl Chl*a*- and Chl*a*-B800 reconstituted complexes, is much quicker than that predicted by simple Förster theory alone. In these calculations, it was assumed that the only B850 acceptor state which is involved in the transfer process is the Q_y state. This may or may not be true. The exact spectroscopic properties of the excitonically coupled B850 aggregate are a controversial issue (see Section 2.3.4 for a full discussion). One of the main areas of debate is concerned with the location of the high energy exciton component of the B850 absorption The exact location of this transition is primarily influenced by the strength of the interaction between neighbouring pigments. The stronger the interaction, the further to the blue the upper absorption component will lie. This excitonic component has been tentatively identified at ~ 780 nm in a CD study of a B850 only mutant of *Rb. sphaeroides* (Koolhass *et al.*, 1998). If this band has a similar energy in LH2 complexes from *Rps. acidophila* 10050, this could not explain the extremely quick B800→B850 transfer rates which occur in the acetyl Chl*a*- and Chl*a*-B800 reconstituted complexes. Alternatively, these enhanced transfer rates may be explained if B800→B850 energy transfer occurs via the carotenoid molecules in a charge-transfer type mechanism (Pullerits *et al.*, 1997; Scholes *et al.*, 1997; Damjanovic *et al.*, 1998; Krueger *et al.*, 1998). This theory could be tested by measuring the rate of B800→B850 energy transfer in carotenoid-deficient complexes containing modified (B)Chl-B800 molecules. Carotenoid-deficient complexes could be created either by "knock-out" mutagenesis or by selective solvent extraction.

The rate of B800→B800 energy transfer in native LH2 and selected reconstituted complexes was determined by following the decay of anisotropy in the (B)Chl-B800 Q_y absorption band with time (see Section 10.3). The transfer time for B800→B800 energy transfer in both the native and Bchl*a*-B800 reconstituted complexes is 0.7 ps. The B800→B800 hopping times in the 3^1vinyl Bchl*a*-, 3^1OH Bchl*a*-, acetyl Chl*a*- and Chl*a*-B800 reconstituted complexes are 1.7, 2.0, 2.8 and 3.8 ps respectively. This shows that the rate of B800→B800 energy transfer decreases as the (B)Chl-B800 Q_y absorption band is blue-shifted. The underlying mechanism which gives rise to this trend is not fully understood.

The energy transfer processes which occur between the S_2 state of the carotenoid and the Q_y transition of the Bchl*a*-B850 molecules were characterised using both steady-state and rapid kinetic techniques (see Chapter 11). It was shown that extensive energy transfer occurs from the carotenoid S_2 state. Approximately two-thirds of carotenoid→B850 energy transfer occurs directly. The other third occurs indirectly via the (B)Chl-B800 molecules. In the native complex, the efficiency of carotenoid→B850 energy transfer is approximately 60 %. This means that the complex is unable to harvest 40 % of the light absorbed by the carotenoids. In native LH2, only limited energy transfer occurs from the S_1 state (see Section11.2.3). This is probably due to poor spectral overlap between the fluorescence emission spectrum of the carotenoid S_1 state and the absorption profiles of the Bchl*a* molecules. Steady-state efficiency measurements suggested that energy transfer may occur from the carotenoid S_1 state to the Q_y transition of the

(B)Chl-B800 molecules in the acetyl Chl*a*- and Chl*a*-B800 reconstituted complexes (see Section 11.5.2). The role of the S_1 state in singlet-singlet energy transfer in these complexes will be investigated by comparing the S_1 lifetime in the reconstituted complexes with that in benzyl alcohol. A reduction in the S_1 lifetime of the rhodopin glucoside molecules will be indicative of energy transfer from that state. These measurements will be made in the group of Thomas Gillbro at the University of Umea, Sweden. Finally, the protocol developed here allows the incorporation of ^{15}N, ^{13}C labelled Bchl*a* into the B800 binding sites. The interactions between the labelled pigments and the protein can then be studied by 2D-NMR. This work has been started in collaboration with Peter Gast's group in Leiden and will be pursued in the next 6 months.

Appendix

A.1 Introduction

In this Appendix, the fluorescence lifetimes of the modified pigments were determined by time-resolved single photon counting. This technique is briefly described in Section A.2. The results are recorded in Section A.3. The experimental methods are detailed in Section 5.8.

A.2 Time-resolved single photon counting

A schematic diagram of the apparatus used in the time-resolved single photon counting measurements is shown in figure A1. Time-resolved single photon counting can be summarised as follows. Pulses of light from a laser source are split into two beams. The weaker series of pulses are sent to a photodiode. On arrival of the first photon of light energy, an electronic signal is sent from the photodiode to the time-to-amplitude converter (TAC). This signal defines time zero. The stronger of the two beams is used to excite the sample. Photons emitted by the sample are detected through an appropriate interference filter using a photomultiplier tube (PMT). On arrival of the first photon at the PMT, a second electronic signal is sent to the TAC. The TAC then produces a voltage which is proportional in size to the time delay between the two electronic pulses. This voltage is converted to and recorded as a time delay by a multi-channel analyser (MCA). After several thousand excitation events, a histogram showing the detection frequency at each time delay is produced. The fluorescence lifetime of the sample can then be determined by kinetic analysis of the histogram.

Figure A1 Time-resolved single photon counting. Pulses of light from a laser source are split into two beams. The weaker series of pulses are sent to a photodiode. On excitation by the laser, an electronic signal is sent from the photodiode to a time-to-amplitude converter (TAC). This signal defines time zero. The stronger of the two beams is used to excite the sample. Photons emitted by the sample are detected through an appropriate interference filter using a photomultiplier tube (PMT). On arrival of the first photon at the PMT, a second electronic signal is sent to the TAC. The TAC then produces a voltage which is proportional in size to the time delay between the two electronic pulses. This voltage is converted to and recorded as a time delay by a multi-channel analyser (MCA). After several thousand excitation events, a histogram showing the detection frequency at each time-delay is produced. The fluorescence lifetime of the sample can then be determined by kinetic analysis of the histogram.

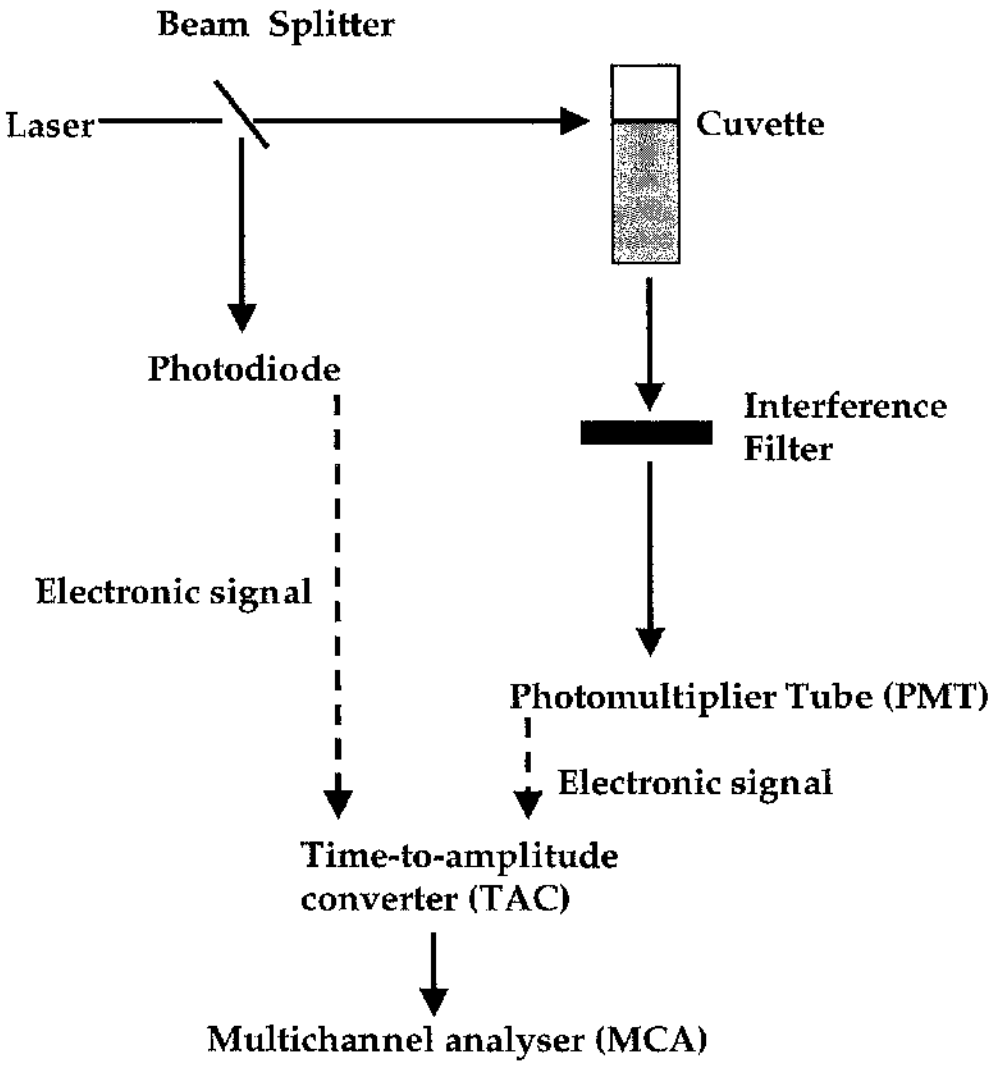
Beam Splitter
Laser
Cuvette
Photodiode
Interference Filter
Electronic signal
Photomultiplier Tube (PMT)
Electronic signal
Time-to-amplitude converter (TAC)
Multichannel analyser (MCA)

A.3 The fluorescence lifetimes of the modified pigments

A typical kinetic trace is shown in figure A2. The kinetic traces all have the same general pattern. On excitation of the pigment molecules, there is a rapid rise in fluorescence from the sample. With time, the fluorescence decays to zero. For each pigment, this decay was fitted with a single exponential and its fluorescence lifetime determined (see table Ai). The fluorescence lifetimes of the Bchl*a*, Zn-Bphe, 3^1vinyl Bchl*a*, 3^1OH Bchl*a*, acetyl Chl*a* and Chl*a* pigments have been determined previously (Teuchner *et al.*, 1994, 1997) (see table Ai). Comparison of the measured lifetimes with the literature values shows that, within the limits of experimental error, our measurements are indistinguishable from those previously reported. The fluorescence lifetimes of geranylgeraniol Bchl*a* and 13^2OH Bchl*a* have not been previously reported. They are 2.4 and 2.8 ns respectively. The modified pigments can be divided into two main groups according to their fluorescence lifetime. Bchl*a*, geranylgeraniol Bchl*a*, 13^2OH Bchl*a*, Zn-Bphe, 3^1vinyl Bchl*a* and 3^1OH Bchl*a* have fluorescence lifetimes in the range 2.4 to 3.0 ns. In contrast, acetyl Chl*a* and Chl*a* have fluorescence lifetimes of approximately 5.7 ns.

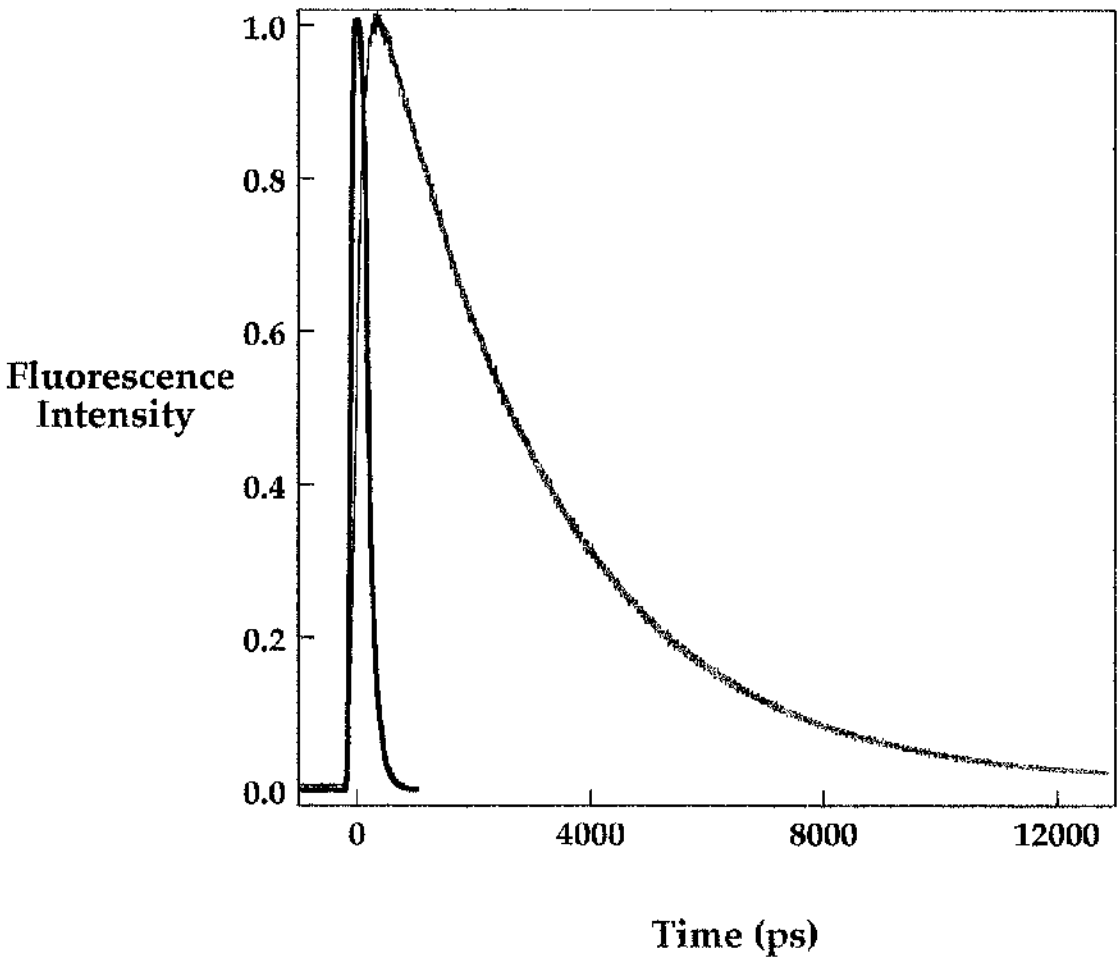

Figure A2 The time-dependent rise and decay in fluorescence emission of Bchl*a* molecules after excitation in their Soret absorption transition at 375 nm. On excitation of the pigment molecules, there is a rapid rise in fluorescence from the sample. With time, this fluorescence decays to zero. The decay was fitted with a single exponential and the fluorescence lifetime of Bchl*a* determined. It is 2.9 ns (see table Ai). [**Key** Black instrument response function, Blue fluorescence emission from the Bchl*a* molecules].

Table Ai The fluorescence lifetimes of the modified (bacterio)chlorin molecules as determined by time-resolved single photon counting. All pigments were excited in their Soret absorption band at 375 nm. The wavelength of fluorescence emission was selected using an appropriate interference filter. For each kinetic trace, the decay in fluorescence was fitted with a single exponential and the fluorescence lifetime of the pigment determined. The fluorescence lifetimes of certain of the modified pigments have been previously determined (Teuchner *et al.*, 1994, 1997). They are recorded for comparison where they exist.

Pigment	Wavelength of maximum transmission by interference filter (nm)	Experimentally determined lifetime (ns)	Literature value (ns)
Bchl*a*	775	2.9 ± 0.1	3.0 ± 0.2
geranylgeraniol Bchl*a*	775	2.8 ± 0.1	n/a
13^2OH Bchl*a*	775	2.4 ± 0.1	n/a
Zn-Bphe	775	2.6 ± 0.1	2.6 ± 0.2
3^1vinyl Bchl*a*	750	3.0 ± 0.1	3.0 ± 0.2
3^1OH Bchl*a*	722	3.1 ± 0.1	3.1 ± 0.2
acetyl Chl*a*	675	5.7 ± 0.1	5.9 ± 0.2
Chl*a*	660	5.7 ± 0.1	6.0 ± 0.2

Appendix B Approaches to calibrating the fluorimeter for fluorescence excitation spectra

B1 Introduction

Accurate determination of the efficiency of energy transfer between two molecules is no small task. In the LH2 complex, the efficiencies of B800→B850 and carotenoid→B850 energy transfer can be determined by measuring the intensity of fluorescence from the Bchl*a*-B850 molecules after excitation of either the Bchl*a*-B800 or the carotenoid molecules respectively. The efficiency of energy transfer can be determined from an action spectrum and is the ratio of the fluorescence excitation spectrum to the fractional absorption spectrum. For accurate determinations of the efficiency of energy transfer, therefore, it is imperative that the fluorescence excitation spectrum is properly corrected for instrument function.

In this thesis, all of the fluorescence excitation spectra were recorded using a Spex Fluorolog 2. A schematic diagram of the fluorimeter is shown in figure B1. Excitation light from either a xenon or a halogen source is selected using a monochromator. The monochromatic light is then split into reference and excitation beams using a dichroic mirror. The dichroic mirror reflects approximately 5% of the light. This light is focused onto the SD in the reference (R) position using a lens. The remainder of the light is transmitted by the dichroic mirror and is aligned using mirrors prior to sample excitation. The wavelength of fluorescence emission is selected using a second monochromator. Emitted photons are detected using a cooled photomultiplier tube (S).

Figure B1 Schematic diagram of the Spex Fluorolog2 fluorimeter. Excitation light from either a xenon or a halogen source is selected using a monochromator. The monochromatic light is then split into reference and excitation beams using a dichroic mirror. The dichroic mirror reflects approximately 5% of the light. This light is focused onto the SD in the reference (R) position using a lens. The remainder of the light is transmitted and is aligned using mirrors prior to sample excitation. The wavelength of fluorescence emission is selected using a second monochromator. Emitted photons are detected using a cooled photomultiplier tube (S).

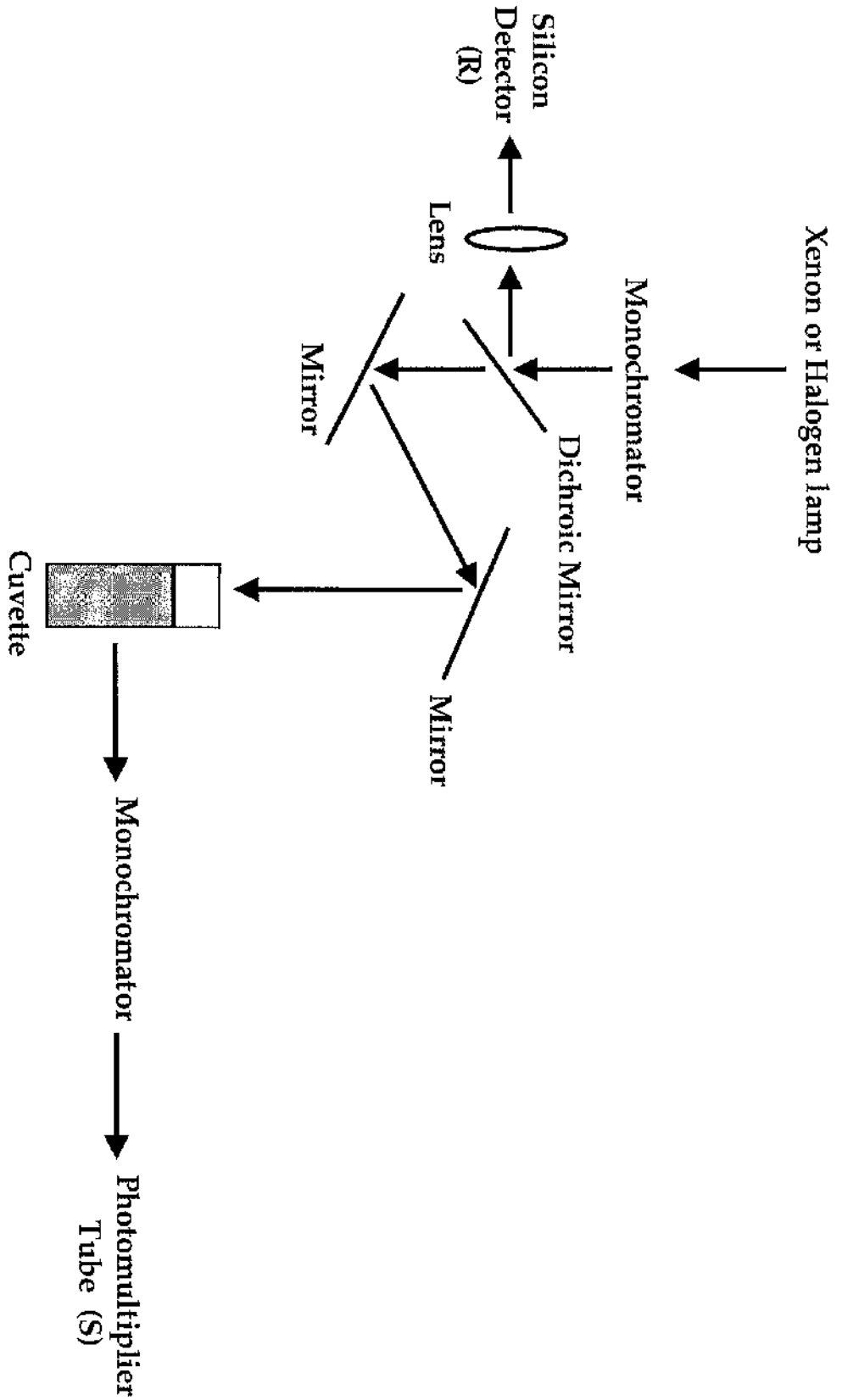
Xenon or Halogen lamp
Monochromator
Dichroic Mirror
Mirror
Lens
Silicon Detector (R)
Mirror
Cuvette
Monochromator
Photomultiplier Tube (S)

In a fluorescence excitation experiment, S and R are measured at each excitation wavelength. The ratio S/R gives a value for fluorescence emission from the sample corrected for differences in excitation intensity. The measured S/R ratio is not the true value for fluorescence excitation because there are two wavelength dependent errors associated with the optics of the instrument. Firstly, the quantum efficiency of the SD is different across the spectrum. This means that there is an error in measuring R. Secondly, the mirrors between the SD in the reference position and the cuvette in the sample position are wavelength dependent. This means that there is an error associated with the light path also. To obtain correct fluorescence excitation spectra, it is necessary to correct the measured S/R value for both of these errors. In this Appendix, approaches to calibrating the fluorimeter for fluorescence excitation measurements are described.

B.2 Correction of fluorescence excitation spectra in the visible region using rhodamine 6B as a quantum counter

A popular approach to solving this calibration problem has been to use laser dyes as quantum counters. For use as a quantum counter, the dye must have two properties. Firstly, it must be able to absorb all of the excitation energy in the wavelength range in which the dye is being used to calibrate the machine. This necessitates the use of dye solutions with concentrations in the range g l^{-1}. Secondly, even at these high concentrations, the dye must have a fluorescence quantum yield of 1 at all wavelengths. This means that for each photon of light which is absorbed by the dye, irrespective of its

energy, a photon is emitted. The laser dye rhodamine 6B satisfies both of these criteria and can be used to correct fluorescence excitation spectra in the wavelength range 350-600 nm (Chen, 1967; Taylor & Demas, 1979). A correction file was collected as described in Section 5.2.1 (see figure B2). This file was then used to correct the fluorescence excitation spectrum of B850-only complexes in the same wavelength range. The corresponding action spectrum is shown in figure B3. The fractional absorption and corrected fluorescence excitation spectra were normalised on the Bchl*a*-B850 Q_x absorption band. Both spectra overlap on the Bchl*a*-B850 Soret maximum also. This shows that the fluorimeter is properly calibrated in the visible region. The reason for this is as follows. The rate of internal conversion from the Soret (B_x and B_y) and Q_x states to the Q_y state of the Bchl*a*-B850 molecules is so short compared to their fluorescence lifetime that the efficiency of energy transfer between these energy states is 100 %. The efficiency of carotenoid→B850 energy transfer was determined by measuring the ratio of the fluorescence excitation to the fractional absorption spectra in the wavelength range 520 to 530 nm.

B.3 Approaches to correcting fluorescence excitation spectra in the NIR region

Calibrating the fluorimeter in the NIR region is much more difficult. In this work, two main strategies were adopted. The first approach involved using the dye HITC as a quantum counter (Nothnagel, 1987). The second approach involved calibrating the SD with a thermopile and then using the calibrated SD to correct for errors in the light path.

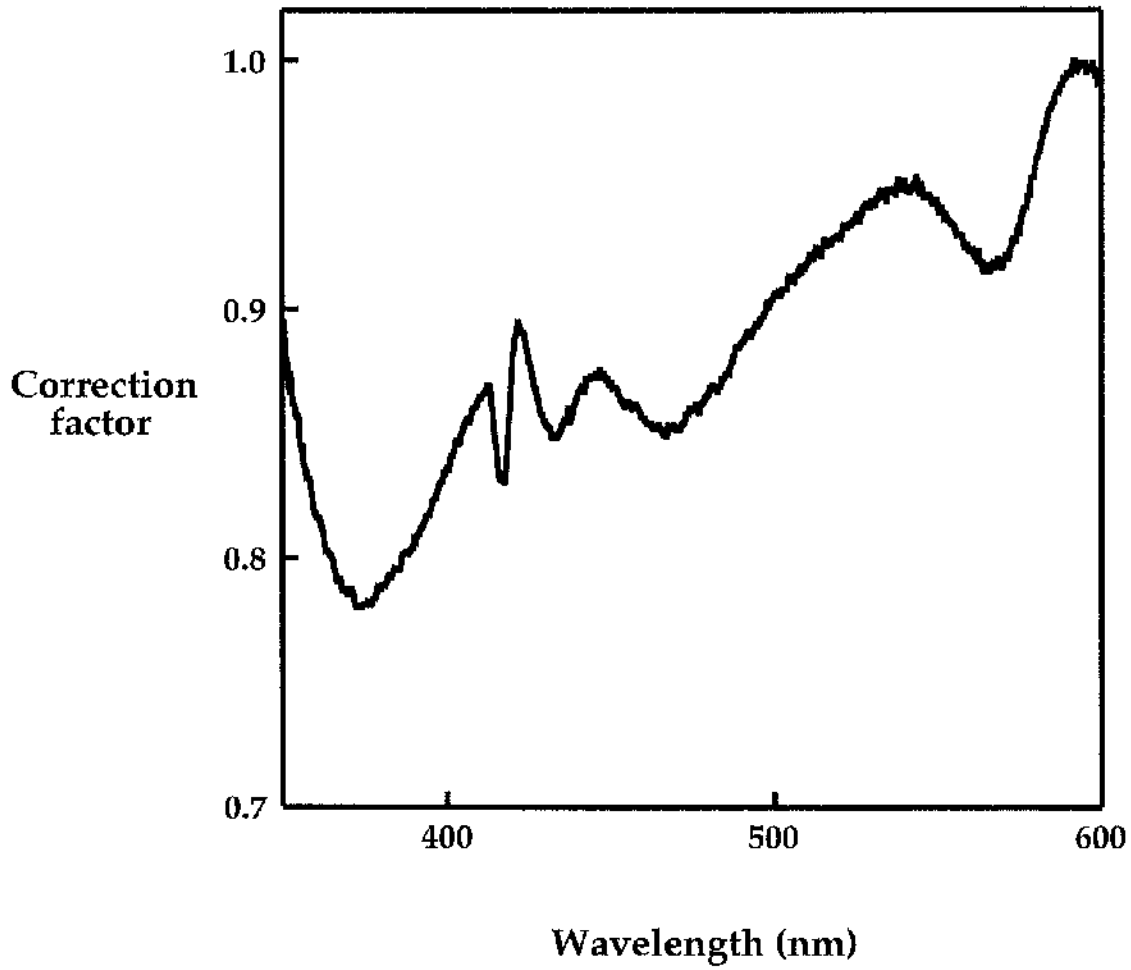

Figure B2 Correction file for fluorescence excitation spectra in the visible region using rhodamine 6B as a quantum counter. The correction file was generated as described in Section B2. The experimental method is detailed in Section 5.2.1.

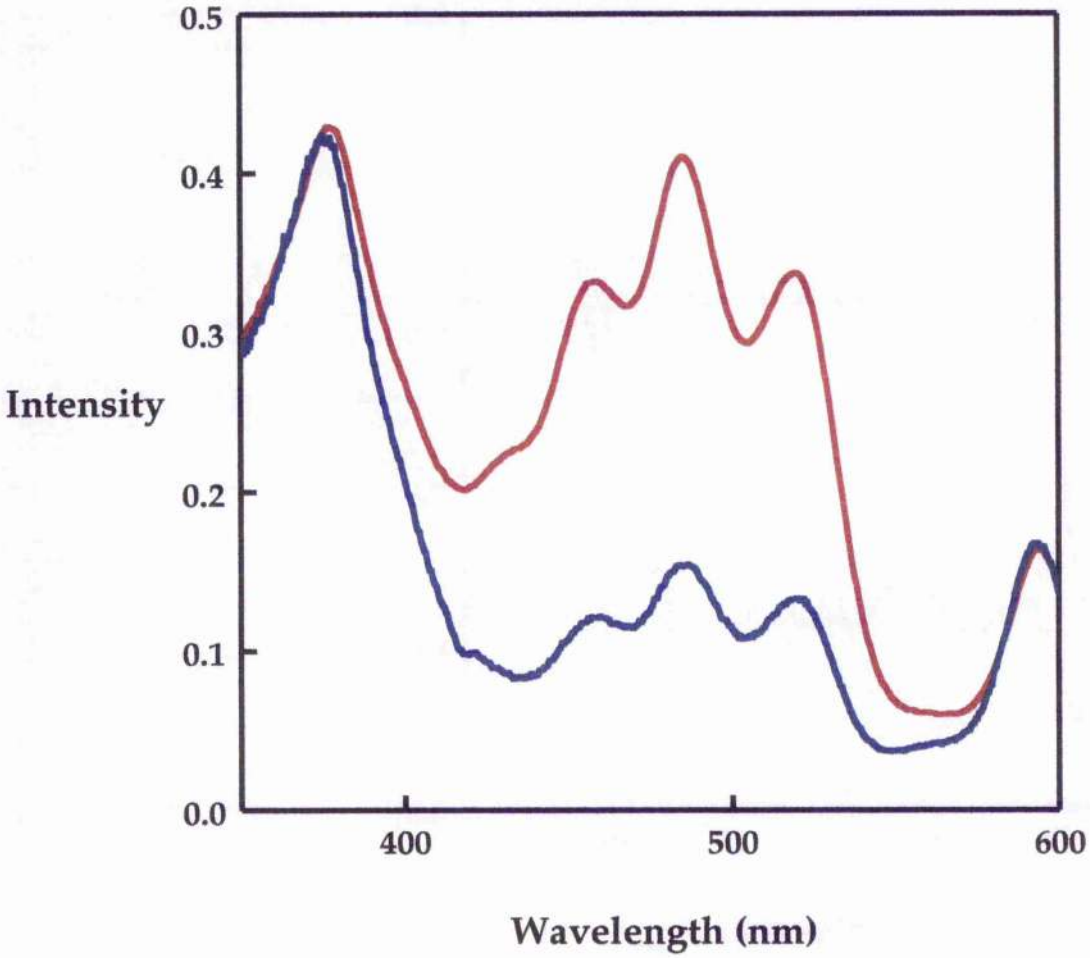

Figure B3 Action spectrum for B850-only complexes in the visible region. The fluorescence excitation spectrum was corrected using the file displayed in figure B2. The fractional absorption and the fluorescence excitation spectra were normalised on the Bchl*a*-B850 Q_x transition. The two spectra overlap in the Soret region also. The efficiency of carotenoid→ B850 energy transfer was determined by measuring the ratio of the fluorescence excitation to fractional absorption values in the range of 520-530 nm. [**Key** Red fractional absorption Blue fluorescence excitation].

B.3.1 Quantum counter approach

Previously, it has been shown that HITC can be used as a quantum counter in the region 300 to 800 nm (Nothnagel, 1987). In the experimental set-up used by Nothnagel, fluorescence was measured from the rear-face of the cuvette. In contrast, the fluorimeter used in this work only allows fluorescence to be measured from the side and front faces of the cuvette. At the concentration of HITC required for use as a quantum counter, it was not possible to detect any fluorescence at right angles from the cuvette. The explanation for this is quite simple. At this high concentration of HITC, fluorescence emitted by any individual molecule is reabsorbed by neighbouring molecules. This effectively prevents excitation light absorbed at the front-face of the cuvette being emitted from the side-face of the cuvette. It was possible, however, to measure fluorescence from the front-face of the cuvette. A correction file in the range 580 to 810 nm was collected (see figure B4). This file was then used to correct the fluorescence excitation spectrum of LH2 complexes in the same wavelength range. The corresponding action spectrum is shown in figure B5. The fractional absorption and fluorescence excitation spectra were normalised on the Bchl*a* Q_x absorption band. In the region 580 to 780 nm, the fractional absorption and fluorescence excitation spectra are essentially the same. In the region 780 to 810 nm, however, the values for fluorescence excitation are significantly greater than those for fractional absorption. More light can not be emitted as fluorescence than that which was originally absorbed. This shows that HITC is not a quantum counter in the range 780 to 810 nm.

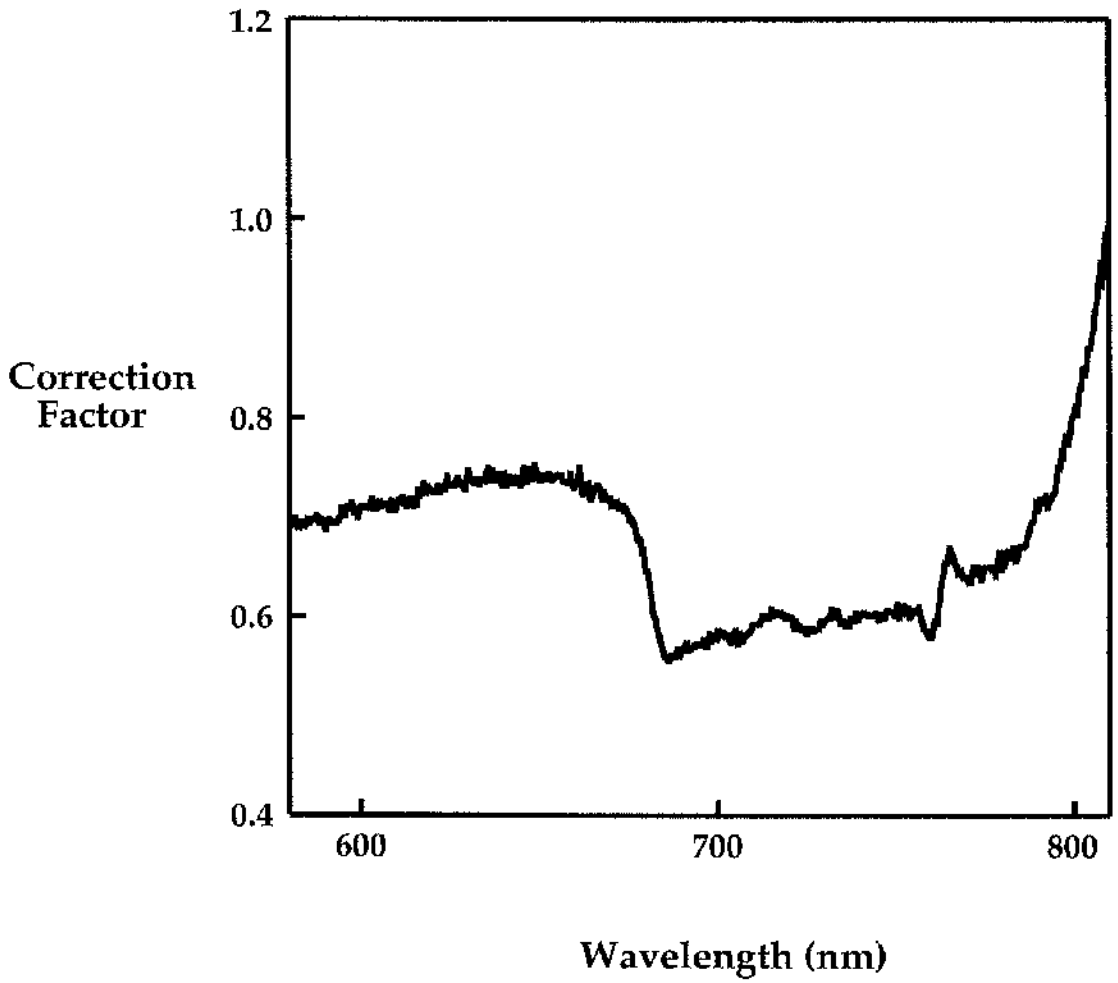

Figure B4 Correction file for fluorescence excitation spectra in the NIR region using HITC as a quantum counter. The correction file was generated as described in Section B3.1.

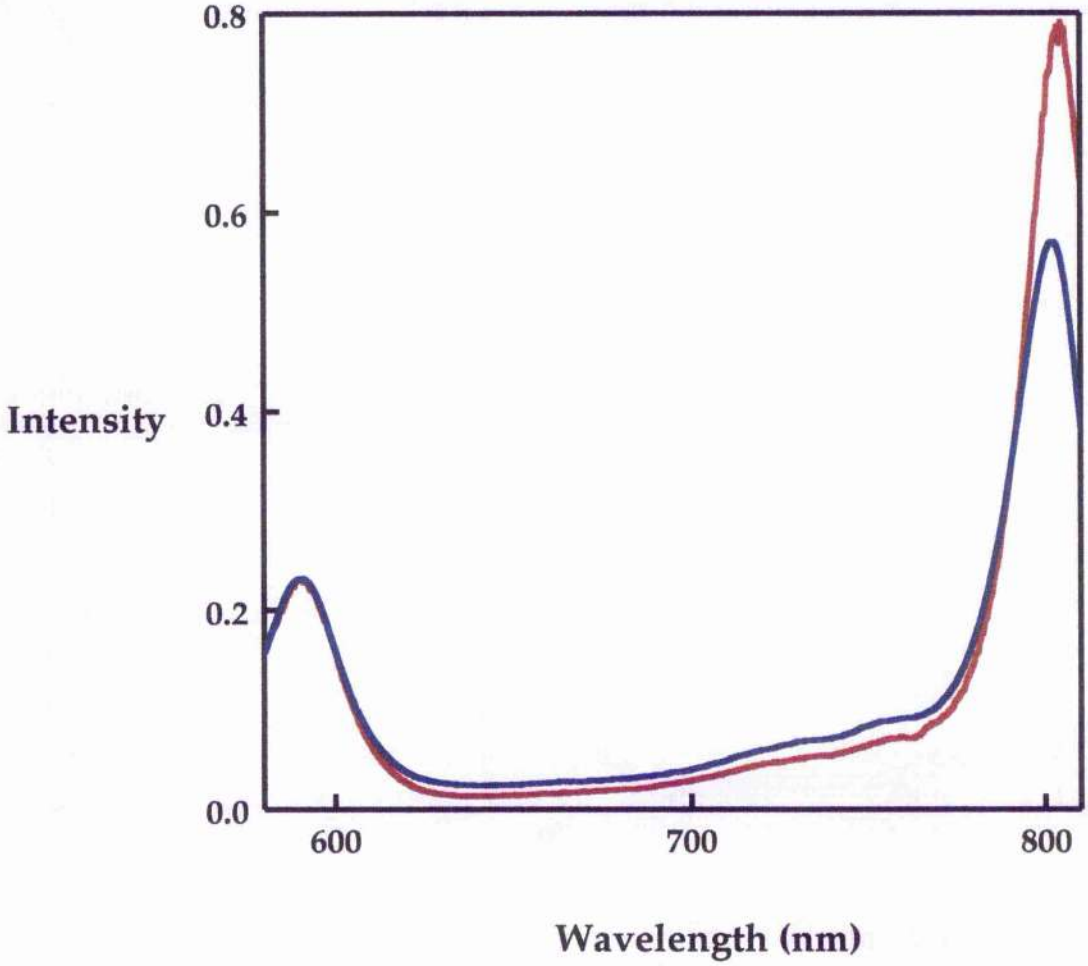

Figure B5 Action spectrum for LH2 complexes in the NIR region. The fluorescence excitation spectra was corrected using the file in figure B4. The fractional absorption and the fluorescence excitation spectra were normalised on the Bchl*a* Q_x transition. In the wavelength range 580 - 780 nm, the two spectra are essentially the same. In the region 780 to 810 nm, the values for fluorescence excitation are appreciably bigger than those for the fractional absorption. This shows that HITC can not be used to calibrate the fluorimeter in the range 780 to 810 nm. [**Key** Blue - fractional absorption, Red - fluorescence excitation].

B.3.2 Direct approach

As it was not possible to calibrate the fluorimeter by a quantum counter approach in the NIR region, another strategy was pursued. This strategy involved calibrating the SD with a thermopile and then using the calibrated SD to correct for errors in the light path.

The SD was calibrated in the region 350-1000 nm as follows. The profile of the xenon lamp in the sample position was recorded using the SD, SD_{sam}. To prevent bleaching of the SD, the excitation light was attenuated using a 10% neutral density filter. The absolute profile of the xenon lamp in the sample position, T_{sam}, was recorded manually using a thermopile connected to a micro-voltmeter. The response function of the SD is the ratio SD_{sam}/T_{sam} (see figure B6). The response curve was fitted with a seventh order polynomial (see figure B6). The fitted response curve was scaled such that it had a maximum value of 1. The correction file for the SD response curve, CF_{SD}, was then generated by taking the reciprocal of the scaled, fitted response curve.

The correction file for the light path in the region 580-1000 nm was determined as follows. A spectrum of the halogen lamp in the reference position was recorded using the SD, $SD_{halogen\text{-}ref}$. The SD and lens were then moved to the sample position where a further spectrum was recorded, $SD_{halogen\text{-}sam}$. The spectra $SD_{halogen\text{-}ref}$ and $SD_{halogen\text{-}sam}$ were both scaled to 1 at their maximum value. The correction file for the light path ,$CF_{lightpath}$, was given by the ratio of scaled $SD_{halogen\text{-}ref}$/scaled $SD_{halogen\text{-}sam}$ (see figure B7).

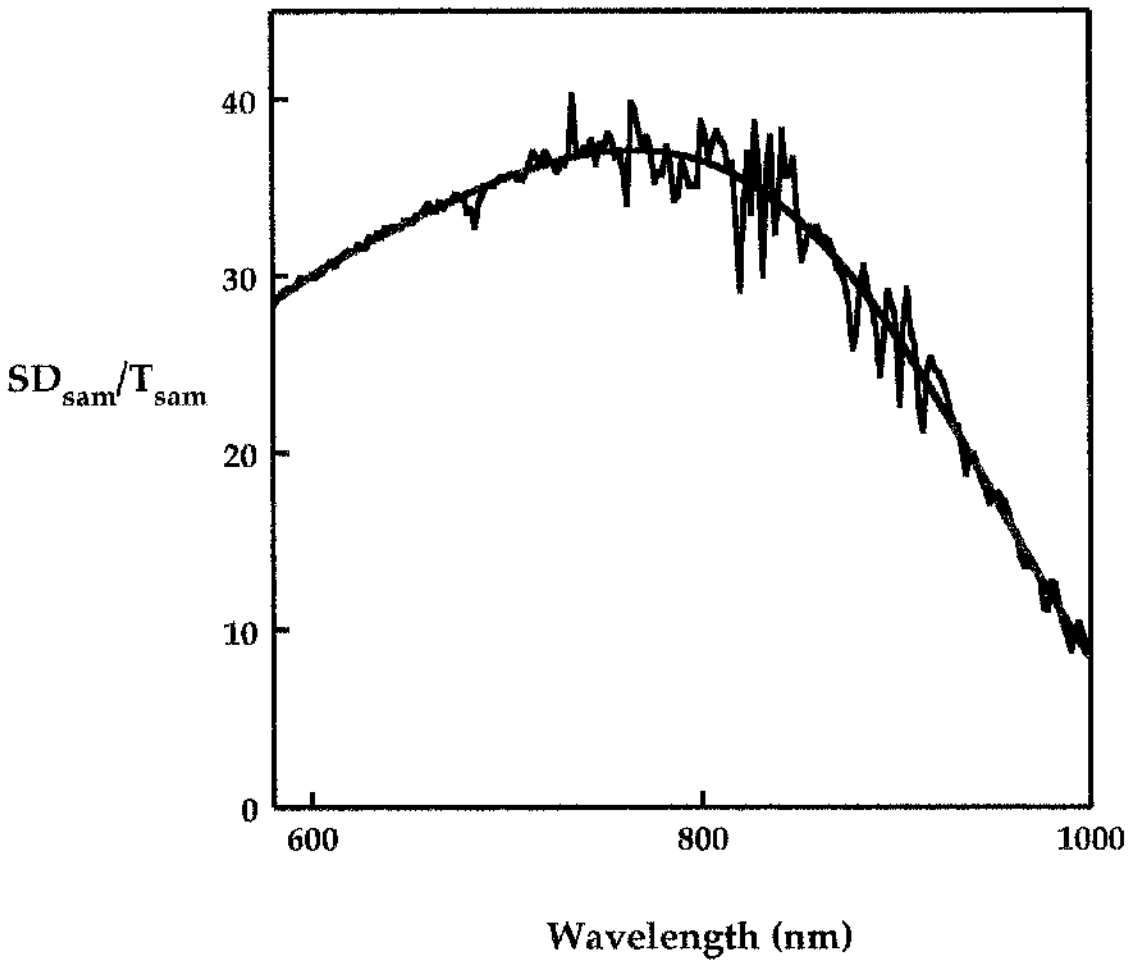

Figure B6 The response curve of the SD as determined using a thermopile. The calibration procedure is fully described in Section B3.2. The response curve was fitted with a seventh order polynomial.

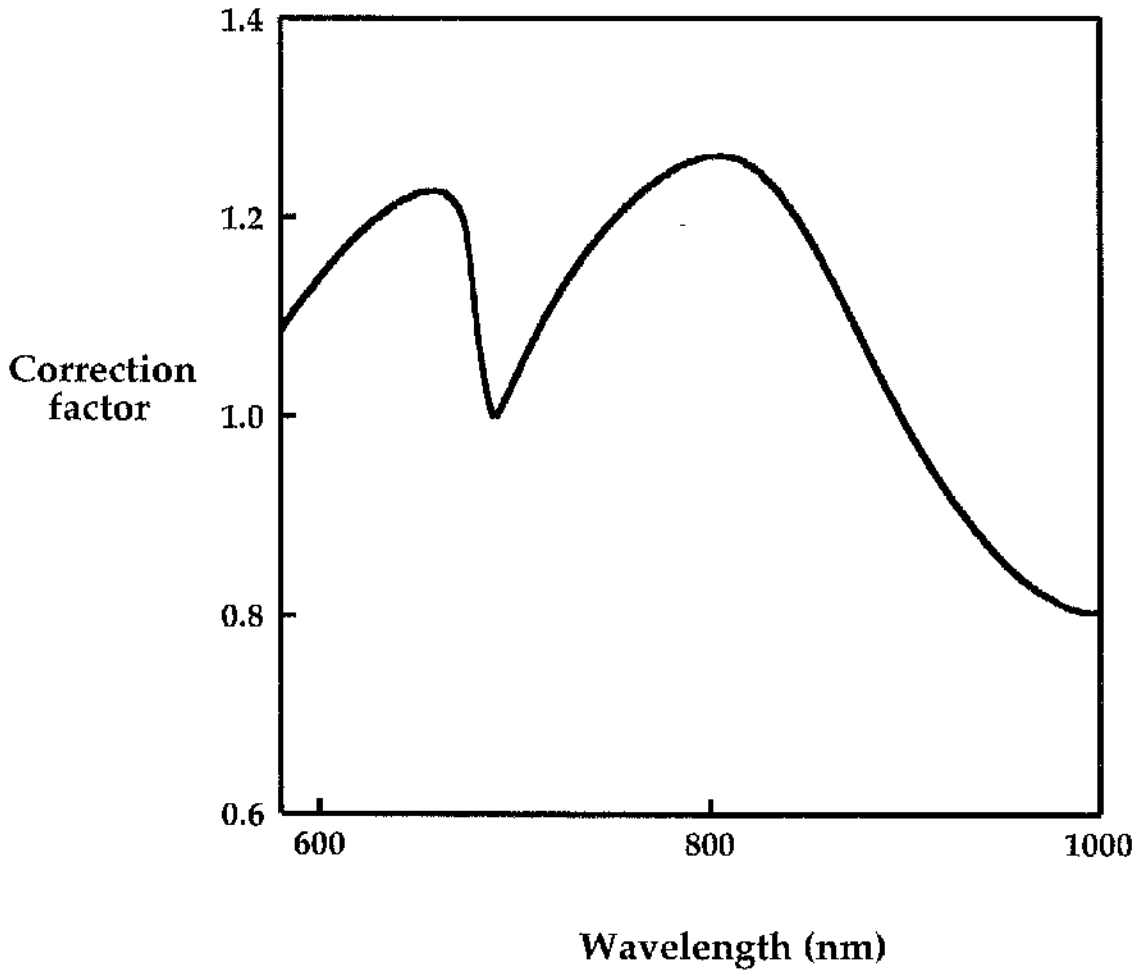

Figure B7 Correction file for the light path in the region 580 to 1000 nm. The correction file was generated as described in Section B3.2.

Finally, it was necessary to correct for the fact that the energy of a photon is wavelength dependent. The ratio S/R gives a value for fluorescence emission/unit of excitation energy. Dependent upon the excitation wavelength, however, this energy unit will correspond to a different number of photons. To compensate for this, a correction file, $CF_{photons}$, was generated.

The complete correction file $CF_{complete}$ is given by the equation

$$CF_{complete} = CF_{lightpath} \times CF_{photons} \; / \; CF_{SD}$$

This correction file was used to correct the fluorescence excitation spectrum of LH2 complexes in the wavelength range 580 to 865 nm. The corresponding action spectrum is shown in figure B8. The fractional absorption and fluorescence excitation spectra were normalised on the Bchl*a* Q_x transition. In the range 580 to 840 nm, allowing for a 10% error, the spectra are the same. In the wavelength region, 840 to 865 nm, the values for fluorescence excitation are approximately 25 % greater than those for the fractional absorption. This shows that the calibration file in the region 840 to 865 nm is not particularly accurate.

Despite much effort, it was not possible to calibrate the fluorimeter sufficiently accurately in the NIR region to allow correct determination of the efficiencies of B800→B850 energy transfer in the native and reconstituted complexes.

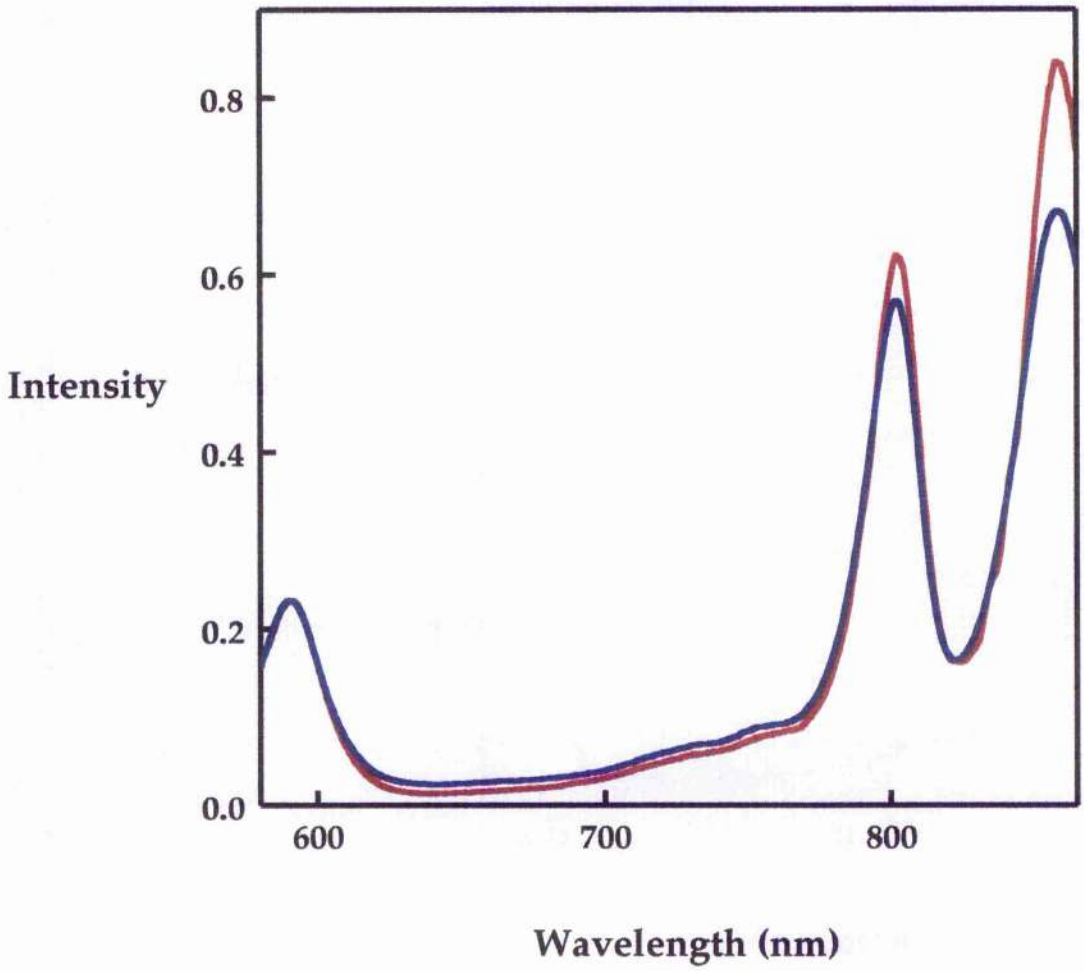

Figure B8 Action spectrum for LH2 complexes in the NIR region. The fluorescence excitation spectrum was corrected as described in Section B3.2. The fractional absorption and fluorescence excitation spectra were normalised on the Bchl*a* Q_x transition. Allowing for a 10% error, the two spectra are essentially the same in the range 580 to 840 nm. Between 840 and 865 nm, however, the values for fluorescence excitation are approximately 25% bigger than those for the fractional absorption. [**Key** Blue - fractional absorption, Red - fluorescence excitation].

References

Aagaard, J. & Sistrom, W.R. (1972) *Photochem. Photobiol.* **15** 209-225.

Alden, R.G., Johnson, E., Nagarajan, V., Parson, W.W., Law, C.J. & Cogdell, R.J. (1997) *J. Phys. Chem. B* **101** 4667-4680.

Allen, J.P., Feher, G., Yeates, T.O., Komiya, H. & Rees, D.C. (1987a) *Proc. Nat. Acad. Sci. USA* **84** 5730-5734.

Allen, J.P., Feher, G., Yeates, T.O., Komiya, H. & Rees, D.C. (1987b) *Proc. Nat. Acad. Sci. USA* **84** 6162-6166.

Andersson, P.O., Bachilo, S.M., Chen, R.-L. & Gillbro, T. (1995) *J. Phys. Chem.* **99** 16199-16209.

Andersson, P.O., Cogdell, R.J. & Gillbro, T. (1996) *Chem. Phys.* **210** 195-217.

Armstrong, G.A., Albertini, M., Leach, F. & Hearst, J.E. (1989) *Mol. Gen. Genet.* **216** 254-268.

Arnoux, B., Ducruix, A., Reiss-Husson, F., Luz, M., Norris, J., Schiffer, M. & Chang, C.H. (1989) *FEBS Letts.* **58** 47-50.

Bachofen, R. & Wiemken, V. (1986) "Topology of the chromatophore membranes of purple bacteria" In: Staehelin, L.A. & Arntzen, C.J. (eds) Photosynthesis III, Springer Publ., Berlin, 620 -631.

Bandilla, M., Ücker, B., Ram, M., Simonin, I., Gelhaye, E., McDermott, G., Cogdell, R.J. & Scheer, H. (1998) *Biochim. Biophys. Acta* **1364** 390-402.

Barz, W.P. & Oesterhelt, D. (1994) *Biochemistry* **33** 9741-9752.

Barz, W.P., Francia, F., Venturoli, G., Melandri, B.A., Vermeglio, A. & Oesterhelt, D. (1995a) *Biochemistry* **34** 15235-15247.

Barz, W.P., Vermeglio, A.,Francia, F., Venturoli, G., Melandri, B.A. & Oesterhelt, D. (1995b) *Biochemistry* **34** 15248-15258.

Bavendamm, W. (1924) Die farblosen und roten Schwefelbakterien des Sub-und Salzwassers. Fischer Verlag, Jena.

Boonstra, A.F., Lothar, G. & Boekema, E.J. (1994) *Biochim. Biophys. Acta* **1184** 227-234.

Bose, S.K. (1963) "Media for aerobic growth of photosynthetic bacteria" In : Bacterial Photosynthesis Gest, H., San Pietro, A. & Vernon, L.F. (eds), Antioch Press, Yellow Springs, Ohio, 501-510.

Bowyer, J.R., Hunter, C.N., Ohnishi, T. & Niederman, R.A. (1985) *J. Biol. Chem.* **260** 3295-3304.

Bradforth, S.E., Jimenez, R., van Mourik, F., van Grondelle, R. & Fleming, G.R. (1995) *J. Phys. Chem.* **99** 16179-16191.

Breton, J., Martin, J.L., Migus, A., Antonetti, A. & Orszag, A. (1986) *Proc. Nat. Acad. Sci. USA* **83** 5121-5125.

Chachisvilis, M., Kühn, O., Pullerits, T. & Sundström, V. (1997) *J. Phys. Chem. B* **101** 7275-7283.

Chadwick, B.W., Zhang, C., Cogdell, R.J. & Frank, H.A. (1987) *Biochim. Biophys. Acta* **893** 444-451.

Chang, M.C., Meyer, L. & Loach, P.A. (1990) *Photochem. Photobiol.* **52** 873-881.

Chen, R.F. (1967) *Anal. Biochem.* **20** 339-357.

Clayton, R.K. (1966) *Photochem. Photobiol.* **5** 669.

Clayton, R.K. & Clayton, B.J. (1981) *Proc. Nat. Acad. Sci. USA* **78** 5583-5587.

Cogdell, R.J. & Scheer, H. (1985) *Photochem. Photobiol.* **42** 669-689.

Crofts, A.R. & Wraight, C.A. (1983) *Biochim. Biophys. Acta* **726** 149-185.

Damjanovic, A., Ritz, T. & Schulten, K. (1998) *Biophys. J.* **74**

Davidson, E. & Cogdell, R.J. (1981) *Biochim. Biophys. Acta* **635** 295-303.

Davies, B.H. (1965) "Analysis of carotenoid pigments" In : Goodwin, T.W. (Ed) Chemistry and Biochemistry of Plant Pigments, Academic Press, London and New York, 489-532.

Davis, C.M., Bustamante, P.L. & Loach, P.A. (1995) *J. Biol. Chem.* **270** 5793-5804.

Davis, C.M., Parkes-Loach, P.S., Cook, C.K., Meadows, K.A., Bandilla, M., Scheer, H. & Loach, P.A. (1996) *Biochemistry* **35** 3072-3084.

Davydov, A.S. (1962) "Theory of molecular excitons" (translated by Kasha, M. & Oenheimer, M. Jr.), McGraw-Hill, New York.

Dawkins, D.J., Ferguson, L.A. & Cogdell, R.J. (1988) "The structure of the purple bacteria photosynthetic unit" In Photosynthetic Light-Harvesting Systems, Scheer, H. & Schneider, S. (Eds)., Walter de Gruyler, Berlin, 115-127.

Debus, R.J., Feher, G. & Okamura, M.Y. (1986) *Biochemistry* **25** 2276-2287.

Deisenhofer, J., E, O., Miki, K., Huber, R. & Michel, H. (1985) *Nature* **318** 618-624.

Deisenhofer, J., E, O., Sinning, I. & Michel, H. (1995) *J. Mol. Biol.* **246** 429-457.

Desamero, R.Z.B., Chynwat, V., van der Hoef, I., Jansen, F.J., Lugtenburg, J., Gosztola, D., Wasielewski, M.R., Cua, A., Bocian, D.F. & Frank, H.A. (1998) *J. Phys. Chem. B* **102** 8151-8162.

Dexter, D.L. (1953) *J. Chem. Phys.* **21** 836-850.

Dracheva, S.M., Drachev, L.A., Konstantinov, A.A., Semenov, A.Y. & Skuvalev, V.P. (1988) *Eur. J. Biochem.* **171** 253-264.

Drews, G. & Imhoff, J.F. (1991) In Variations in autotrophic life, Shively, J.M. & Barton, L.L. (Eds), Academic Press, London, 51-97.

Ducruix, A. & Reiss-Husson, F. (1987) *J. Mol. Biol.* **193** 419-421.

Dutton, P.L. (1986) "Energy transduction in anoxygenic photosynthesis" In Photosynthesis III Stehlin, L.A. & Arntzen, C.J. (Eds.) Encyclopedia of plant physiology Vol. 19 Springer-Verlay, Netherlands, 197-237.

El-Kabbani, O., Chang, C.H., Tiede, D., Norris, J. & Schiffer, M. (1991) *Biochemistry* **30** 5361-5369.

Emerson, R. & Arnold, W.A. (1932) *J. Gen. Physiol.* **16** 191-205.

Ermler, V., Fritzsch, G., Buchanan, S.K. & Michel, H. (1994) *Structure* **2** 925-936.

Farchaus, J.W., Barz, W.P., Grunberg, H. & Oesterhelt, D. (1992) *EMBO J.* **11** 2779-2788.

Feher, G. (1971) *Photochem. & Photobiol.* **14** 373-387.

Feher, G., Allen, J.P., Okamura, M.Y. & Rees, D.C. (1989) *Nature* **339** 111-116.

Finkele, U., Lauterwasser, C., Struck, A., Scheer, H. & Zinth, W. (1992) *Proc. Nat. Acad. Sci. USA* **89** 9514-9518.

Fleming, G.R., Martin, J.-L. & Breton, J. (1988) *Nature* **333** 190-192.

Fleming, G.R. & van Grondelle, R. (1994) *Physics Today* **47** 48-55.

Förster, Th. (1948) *Annu. Rev. Phsiol.* **2** 55-75.

Fowler, G.J.S., Visschers, R.W., Grief, G.G., van Grondelle, R. & Hunter, C.N. (1992) *Nature* **355** 848-850.

Fowler, G.J.S., Sockalingum, G.D., Robert, B. & Hunter, C.N. (1994) *Biochem. J.* **299** 695-700.

Fowler, G.J.S., Hess, S., Pullerits, T., Sündstrom, V. & Hunter, C.N. (1997) *Biochemistry* **36** 11282-11291.

Francke, C. & Amesz, J. (1995) *Photosynth. Res.* **46** 347-352.

Frank, H.A., Farhoosh, R., Gebhard, R., Lugtenburg, J., Gosztola, D. & Wasielewski, M.R. (1993a) *Chem. Phys. Lett.* **207** 88-92.

Frank, H.A., Farhoosh, R., Aldeno, M.L., Decoster, B., Christensen, R.L., Gebhard, R. & Lugtenburg, J. (1993b) *Photochem. Photobiol.* **57** 49-55.

Frank, H.A., Chynwat, V., Posteraro, A., Hartwich, G., Simonin, I. & Scheer, H. (1996) *Photochem. Photobiol.* **64** 823-831.

Frank, H.A., Chynwat, V., Desamero, R.Z.B., Farhoosh, R., Erickson, J. & Bautista, J. (1997) *Pure & Al. Chem.* **10** 2117-2124.

Freer, A.A., Prince, S.M., Sauer, K., Papiz, M.Z., Hawthornthwaite-Lawless, A.M., McDermott, G., Cogdell, R.J. & Isaacs, N.W. (1996) *Structure* **4** 449-462.

Gabbelini, N., Bowyer, J.R., Hurt, E., Melandri, B.A. & Hauska, G. (1982) *Eur. J. Biochem.* **126** 105-111.

Gall, A. (1995) PhD thesis, University of Glasgow, UK.

Gall, A., Fowler, G.J.S., Hunter, C.N. & Robert, B. (1997) *Biochemistry* **36** 16282-16287.

Gardiner, A.T., Cogdell, R.J. & Takaichi, S. (1993) *Photosynth. Res.* **38** 159-167.

Gest, H. (1993) *FEMS Microbiol. Letts.* **112** 1-6.

Ghosh, R., Hoenger, A., Hardmeyer, A., Mihailescu, D., Bachofen, R., Engel, A. & Rosenbusch, J.P. (1993) *J. Mol. Biol.* **231** 501-504.

Gillbro, T. & Cogdell, R.J. (1989) *Chem. Phys. Lett.* **158** 312-316.

Hartwich, G. (1994) Dissertation, Technische Universität München.

Hartwich, G., Scheer, H., Aust, V. & Angerhofer, A. (1995a) *Biochem. Biophys. Acta* 97-113.

Hartwich, G., Friese, M., Scheer, H., Ogrodnik, A. & Michelbeyerle, M.E. (1995b) *Chem. Phys.* **197** 423-434.

Heller, B.A. & Loach, P.A. (1990) *Photochem. Photobiol.* **51** 621-627.

Heller, B.A. (1992) Ph.D Thesis, Northwestern University, USA.

Hess, S., Feldchtein, F., Babin, A., Nurgaleev, I., Pullerits, T., Sergeev, A. & Sundström, V. (1993) *Chem. Phys. Lett.* **216** 247-257.

Hess, S., Visscher, K.J., Pullerits, T., Sundström, V., Fowler, G.J.S. & Hunter, C.N. (1994) *Biochemistry* **33** 8300-8305.

Hess, S., Åkesson, E., Cogdell, R.J., Pullerits, T. & Sundström, V. (1995) *Biophys. J.* **69** 2211-2225.

Hess, S. (1997) PhD Thesis, University of Lund, Sweden.

Hickmann, D.D. & Frenkel, A.W. (1965) *J. Cell Biol.* **25** 279-291.

Hundle, B., Beyer, P., Kliening, H., Englert, G. & Hearst, J.E. (1994) *Mol. Gen. Genet.*

Hunter, C.N., Hundle, B.S., Hearst, J.E., Lang, H.P., Gardiner, A.T., Takaichi, S. & Cogdell, R.J. (1994) *J. Bacteriol.* **176** 3692-3697.

Imhoff, J.F. (1984) *Intl. J. Syst. Bacteriol.* **34** 338-339.

Imhoff, J.F. and Truper, H.G. (1989) "The purple non-sulphur bacteria" In Staley, J.T., Bryant, M.P., Pfennig, N. And Holt, J.C. (eds) Bergey's Manual of Systematic Bacteriology, Vol. 3 1658-1661, Williams and Wilkins, Baltimore.

Jay, F., Lambillotte, M., Stark, W. & Muhlethaler, K. (1984) *EMBO J.* **3** 773-776.

Jimenez, R., Dikshit, S.N., Bradforth, S.E. & Fleming, G.R. (1996) *J. Phys. Chem.* **100** 6825-6834.

Joo, T., Jia, Y., Yu, J.-Y., Lang, M.J. & Fleming, G.R. (1996) *J. Phys. Chem.* **100** 6089-6108.

Karrasch, S., Bullough, P.A. & Ghosh, R. (1995) *EMBO J.* **14** 631-638.

Kehoe, J.W., Meadows, K.A., Parkes-Loach, P.S. & Loach, P.A. (1998) *Biochemistry* **37** 3418-3428.

Kennis, J.T.M., Streltsov, A.M., Vulto, S.T.E., Aartsma, T.J., Nozowa, T. & Amesz, J. (1997) *J. Phys. Chem. B* **101** 7827-7834.

Kirmaier, C. & Holten, D. (1987) *Photosynth. Res.* **13** 225-260.

Kleinfeld, D., Okamura, M.Y. & Feher, G. (1984) *Biochim. Biophys. Acta* **766** 126-140.

Koepke, J., Hu, X., Muenke, C., Schulten, K. & Michel, H. (1996) *Structure* **4** 581-597.

Koolhaas, M.H.C., van der Zwan, G., Frese, R.N. & van Grondelle, R. (1997) *J. Phys. Chem. B* **101** 7262-7270.

Koolhass, M.H.C., Frese, R.N., Fowler, G.J.S., Bibby, T.S., Georgakopoulou, S., van der Zwan, G., Hunter, C.N. & van Grondelle, R. (1998) *Biochemistry* **37** 4693-4698.

Kramer, H.J.M., Pennoyer, J.D., van Grondelle, R., Westerhuis, W.H.J., Niederman, R.A. & Amesz, J. (1984) *Biochim. Biophys. Acta.* **767** 335-344.

Krueger, B.P., Scholes, G.D. & Fleming, G.R. (1998) *J. Phys. Chem. B* **102** 5378-5386.

Kuki, M., Hashimoto, H. & Koyama, Y. (1990) *Chem. Phys. Lett.* **165** 417-422.

Lang, H.P., Cogdell, R.J., Takaichi, S. & Hunter, C.N. (1993) *J. Bacteriol.* **177** 2064-2073.

Lee, J.K., Dehoff, B.S., Donohue, T.J., Gumport, R.I. & Kaplan, S. (1989) *J. Biol. Chem.* **264** 19354-19365.

Loach, P.A., Parkes-Loach, P.S., Davis, C.M. & Heller, B.A. (1994) *Photosynth. Res.* **40** 231-245.

MacPherson, A.N. & Gillbro, T. (1998) *J. Phys. Chem. B* **102** 5049-5058.

McAuley-Hecht, K.E., Fyfe, P.K., Ridge, J.P., Prince, S.M., Hunter, C.N., Isaacs, N.W., Cogdell, R.J. & Jones, M.R. (1998) *Biochemistry* **37** 4740-4750.

McDermott, G., Prince, S.M., Freer, A.A., Hawthornthwaite-Lawless, A.M., Papiz, M.Z., Cogdell, R.J. & Isaacs, N.W. (1995) *Nature* **374** 517-521.

McGlynn, P., Hunter, C.N. & Jones, M.R. (1994) *FEBS Letts.* **349** 349-353.

McGlynn, P., Westerhuis, W.H.J., Jones, M.R. & Hunter, C.N. (1996) *J. Biol. Chem.* **271** 3285-3292.

Ma, Y.-Z., Cogdell, R.J. & Gillbro, T. (1997) *J. Phys. Chem. B* **101** 1087-1095.

Martin, J.-L., Breton, J., Hoff, A., Migus, A. & Antonetti, A. (1986) *Proc. Nat. Acad. Amer. Sci. USA* **83** 957-961.

Meadows, K.A., Iida, K., Tsuda, K., Recchia, P.A., Heller, B.A., Antonio, B., Nango, M. & Loach, P.A. (1995) *Biochemistry* **34** 1559-1574.

Meadows, K.A., Parkes-Loach, P.S., Kehoe, J.W. & Loach, P.A. (1998) *Biochemistry* **37** 3411-3417.

Meckenstock, R.U., Brunisholz, R.A. & Zuber, H. (1992a) *FEBS Letts.* **311** 128-134.

Meckenstock, R.U., Krusche, K., Brunisholz, R.A. & Zuber, H. (1992b) *FEBS Letts.* **311** 35-138.

Meier, T., Chernyak, V. & Mukamel, S. (1997) *J. Phys. Chem. B* **101** 7332-7342.

Meyer, M. & Scheer, H. (1995) *Photosynth. Res.* **44** 55-65.

Meyer, M., Scheer, H. & Breton, J. (1996) *FEBS Letts.* **393** 131-134.

Miller, J.F., Hinchigeri, S.B., Parkes-Loach, P.S., Callahan, P.M., Sprinkle, J.R., Riccobono, J.R. & Loach, P.A. (1987) *Biochemistry* **26** 5055-5062.

Miller, K.R. (1982) *Nature* **300** 53-55.

Molisch, H. (1907) Die Purpurbakterien nach neuen Untersuchungen, G.Fischer, Jena.

Monshouwer, R., de Zarate, I.O., van Mourik, F. & van Grondelle, R. (1995) *Chem. Phys. Lett.* **246** 341-346.

Monshouwer, R. & van Grondelle, R. (1996) *Biochim. Biophys. Acta* **1275** 70-75.

Monshouwer, R., Abrahamsson, M., van Mourik, F. & van Grondelle, R. (1997) *J. Phys. Chem. B* **101** 7241-7248.

Nagae, H., Kikitani, T. & Mimuro, M. (1993) *J. Chem. Phys.* **98** 8012-8023.

Nothnagel, E.A. (1987) *Anal. Biochem.* **163** 224-237.

Oelze, J. & Drews, J.F. (1972) *Biochim. Biophys. A cta* **265** 209-239.

Omata, T. & Murata, N. (1983) *Plant & Cell Physiol.* **24** 1093-1100.

Papiz, M.Z., Prince, S.M., Hawthornthwaite-Lawless, A. M., McDermott, G., Freer, A.A., Isaacs, N.W. & Cogdell, R.J. (1996) *TIPS* **1** 198-206.

Parkes-Loach, P.S., Sprinkle, J.R. & Loach, P.A. (1988) *Biochemistry* **27** 2718-2727.

Parkes-Loach, P.S., Michalski, T.J., Bass, W.J., Smith, U. & Loach, P.A. (1990) *Biochemistry* **29** 2951-2960.

Parkes-Loach, P.S., Jones, S.M. & Loach, P.A. (1994) *Photosynth. Res.* **40** 247-261.

Parson, W.W. & Warshel, A. (1987) *J. Am. Chem. Soc.* **109** 6152-6163.

Pfenning, N. (1969) *J. Bacteriol.* **99** 597-602.

Pfenning, N. & Truper, H.G. (1971) *Intl J. Syst. Bacteriol.* **21** 17-18.

Pfenning, N. & Truper, H.G. (1974) "The phototropic bacteria" In: Buchanan R.E. and Gibbons, N.E. (eds)Bergey's Manual of Determinative Bacteriology, Williams and Wilkins, Baltimore 24-64.

Price, N.C. (1997) "Protein analysis by circular dichroism" In : Meyers, R.A. (ed) Encylcopedia of Molecular Biology and Biotechnology, VCH Press, Weinheim.

Prince, S.M., Papiz, M.Z., Freer, A.A., McDermott, G., Hawthornthwaite-Lawless, A.M., Cogdell, R.J. & Isaacs, N.W. (1997) *J. Mol. Biol.* **268** 412-423.

Pullerits, T., Chachisvilis, M. & Sündstrom, V. (1996) *J. Phys. Chem.* **100** 10787-10792.

Pullerits, T., Hess, S., Herek, J.L. & Sundström, V. (1997) *J. Phys. Chem. B* **101** 10560-10567.

Reed, D.W. & Clayton, R.K. (1968) *J. Biol. Chem.* **244** 4396-4941.

Ricci, M., Bradforth, S.E., Jiminez, R. & Fleming, G.R. (1996) *Chem. Phys. Letts.* **259** 381-390.

Robert, B. & Lutz, M. (1988a) In : Spiro, T.G. (ed) Biological alications of Raman spectroscopy Vol. 3., John Wiley & Sons, Inc., New York, 347-411.

Robert, B. & Frank, H. (1988b) "Effect of lithium dodecyl sulphate on B800-B850 antenna complexes from *Rps. acidophila* : a resonance Raman study" In : Scheer, H. & Schneider (eds) Photosynthetic Light-Harvesting Systems : Organization and Function

Sauer, K., Cogdell, R.J., Prince, S.M., Freer, A.A., Isaacs, N.W. & Scheer, H. (1996) *Photochem. Photobiol.* **64** 564-576.

Savage, H., Cyrklaff, M., Montoya, G., Kühlbrandt, W. & Sinning, I. (1996) *Structure* **4** 243-251.

Scheer, H. & Hartwich, G. (1995) "Bacterial reaction centres with modified tetrapyrrole chromophores" In : Blakenship, R.E., Madigan, M.T. & Bauer, C.E. (eds) Anoxygenic Photosynthetic Bacteria, Kluwer Academic Publishers, Netherlands 649-663.

Scheer, H. & Struck, A. (1993) "Bacterial reaction centres with modified tetrapyrrole chromophores" In : Deisenhofer, J. & Norris, J.R. (eds) The Photosynthetic Reaction Centre Volume I, Academic Press Inc., San Diego, USA 157-192.

Scholes, G.D., Harcourt, R.D. & Fleming, G.R. (1997) *J. Phys. Chem. B* **101** 7302-7312.

Shreve, A.P., Trautman, J.K., Owens, T.G. & Albrecht, A.C. (1991a) *Chem. Phys. Letts.* **178** 89-96.

Shreve, A.P., Trautman, J.K., Frank, H.A., Owens, T.G. & Albrecht, A.C. (1991b) *Biochem. Biophys. Acta* **1058** 280-288.

Sprague, S.G. & Varga, A.R. (1986) "Membrane architecture of anoxygenic photosynthetic bacteria" In: Stachlin, L.A. & Arntzen, C.J. (eds) Photosynthesis III, Springer Publ., Berlin, 603-619.

Stark, W., Kuhlbrnadt, W., Wildhaber, I., Wehrli, E. & Muhlethaler, K. (1984) *EMBO J.* 3 777-783.

Stowell, M.H.B., McPhillips, T.M., Rees, D.C., Soltis, S.M., Abresch, E. & Feher, G. (1997) *Science* **276** 812-816.

Struck, A., Cmiel, E., Katheder, I. & Scheer, H. (1990a) *FEBS Letts.* 268 180-184.

Struck, A. & Scheer, H. (1990b) *FEBS Letts.* 261 385-388.

Sturgis, J.N., Jirsakova, V., Reiss-Husson, F., Cogdell, R.J. & Robert, B. (1995a) *Biochemistry* **34** 517-523.

Sturgis, J.N., Hageman, G., Tadros, M.H. & Robert, B. (1995b) *Biochemistry* **34** 10519-10524.

Sündstrom, V., van Grondelle, R., Bergström, H., Åkesson, E. & Gillbro, T. (1986) *Biochim. Biophys. Acta* **851** 431-446.

Taylor, D.G & Demas, J.N. (1979) *Anal. Chem.* **51** 712-717.

Teuchner, K., Stiel, H., Leupold, D., Katheder, I. & Scheer, H. (1994) *J. Luminescence* **60-61** 520-522.

Teuchner, K., Stiel, H., Leupold, D., Scherz, A., Noy, D., Simonin, I., Hartwich, G. & Scheer, H. (1997) *J. Luminescence* **72-74** 612-614.

van Grondelle, R. (1985) *Biochim. Biophys. Acta* **811** 147-195.

Walz, T. & Ghosh, R. (1997) *J. Mol. Biol.* **265** 107-111.

Wasielewski, M.R. & Kispert, L.D. (1986) *Chem. Phys. Lett.* **128** 238-243.

Westerhuis, W.H.J., Farchaus, J.W. & Niederman, R.A. (1993) *Photochem. Photobiol.* **58** 460-463.

Wraight, C.A. (1979) *Biochim. Biophys. Acta* **548** 309-327.

Zinth, W., Kna, E.W., Fischer, S.F., Kaiser, W., Deisenhofer, J. & Michel, H. (1985) *Chem. Phys. Lett.* **119** 1-4.